



National Library of Canada

Cataloguing Branch
Canadian Theses Division

Ottawa, Canada
K1A 0N4

Bibliothèque nationale du Canada

Direction du catalogage
Division des thèses canadiennes

NOTICE

The quality of this microfiche is heavily dependent upon the quality of the original thesis submitted for microfilming. Every effort has been made to ensure the highest quality of reproduction possible.

If pages are missing, contact the university which granted the degree.

Some pages may have indistinct print especially if the original pages were typed with a poor typewriter ribbon or if the university sent us a poor photocopy.

Previously copyrighted materials (journal articles, published tests, etc.) are not filmed.

Reproduction in full or in part of this film is governed by the Canadian Copyright Act, R.S.C. 1970, c. C-30. Please read the authorization forms which accompany this thesis.

**THIS DISSERTATION
HAS BEEN MICROFILMED
EXACTLY AS RECEIVED**

AVIS

La qualité de cette microfiche dépend grandement de la qualité de la thèse soumise au microfilmage. Nous avons tout fait pour assurer une qualité supérieure de reproduction.

S'il manque des pages, veuillez communiquer avec l'université qui a conféré le grade.

La qualité d'impression de certaines pages peut laisser à désirer, surtout si les pages originales ont été dactylographiées à l'aide d'un ruban usé ou si l'université nous a fait parvenir une photocopie de mauvaise qualité.

Les documents qui font déjà l'objet d'un droit d'auteur (articles de revue, examens publiés, etc.) ne sont pas microfilmés.

La reproduction, même partielle, de ce microfilm est soumise à la Loi canadienne sur le droit d'auteur, SRC 1970, c. C-30. Veuillez prendre connaissance des formules d'autorisation qui accompagnent cette thèse.

**LA THÈSE A ÉTÉ
MICROFILMÉE TELLE QUE
NOUS L'AVONS REÇUE**

ANALYSIS OF PERFORATED WALLS AND TUBE-TYPE
TALL BUILDING STRUCTURES

Osama El-Sayed El-Moselhi

A Thesis

in

The Faculty

of

Engineering

Presented in Partial Fulfillment of the Requirements
for the degree of Doctor of Engineering

Centre for Building Studies
Concordia University
Montreal, Quebec, Canada

June 1978

© Osama El-Sayed El-Moselhi, 1978

ABSTRACT

ABSTRACT

ANALYSIS OF PERFORATED WALLS AND TUBE-TYPE
TALL BUILDING STRUCTURES

Osama El-Sayed El-Moselhi, D.Eng.,
Concordia University, 1978

An efficient technique for the analysis of perforated walls and tube-type tall building structures is presented. The method is based on replacing the discrete beam-column system and any band of lintel beams by an elastically equivalent orthotropic membrane. The equivalent structure is then analyzed for the displacements and stresses. From the condition of elastic equivalence, the displacements directly represent those of the actual structure and the member internal forces are obtained by integrating the corresponding stress components.

Refined expressions for the elastic properties of the equivalent membrane are developed taking into account bending and shear deformations of members, axial deformations in columns, flexibility of finite size joints, and the reduction of member stiffness due to axial loads.

Two specially orthotropic finite elements are developed for the efficient modelling of the equivalent membrane by making use of the assumption of infinite in-plane rigidity of floors. The element may span over

several bays and stories of uniform properties.

A computer program is written, incorporating the theoretical developments presented in this thesis, with the capability for the analysis of most of the existing two and three-dimensional structural systems for tall buildings.

Closed-form solutions are also developed for planar uniformly perforated walls under the action of uniform lateral loads. The solutions enable not only the development of design curves and a complete reduction technique, but also the determination of the characteristic parameters controlling the behavior of such structures. These parameters are of particular importance to an efficient implementation of the present method.

A number of representative two and three-dimensional structures consisting of frames, walls, and coupled shear walls are analyzed. The results are in very close agreement with those obtained by the "exact" and other simplified methods. The present method, however, requires only a fraction of the computer time and storage required by the others. In view of the accuracy, efficiency, simplicity and flexibility offered by the present technique, it is believed that the method is not only suitable for routine office design but also gives a new viewpoint where the artificial classification of structural systems for tall buildings can be removed.

ACKNOWLEDGEMENTS

ACKNOWLEDGEMENTS

I would like to express my sincere appreciation to Professors P.P. Fazio and H.K. Ha, for their guidance, encouragement and critical supervision throughout the course of this research.

I am indebted to Professor Z.A. Zielinski for his encouragement and helpful comments in the early stage of the study and to Professor M.S. Troitsky for his interest and helpful suggestions.

The financial support of the National Research Council of Canada in the form of post-graduate scholarship and Research Grant No. A4770 is gratefully acknowledged. Thanks are due to the Computer Centre staff of Concordia University for their technical advice, and to Miss M. Stredder, for her concerned work in typing the manuscript.

With love and respect, I would like to express my deep gratitude to my dedicated parents who are living to give and my understanding wife who is shafing to add.



TABLE OF CONTENTS

TABLE OF CONTENTS

	PAGE
ABSTRACT	i
ACKNOWLEDGEMENTS	iii
LIST OF FIGURES	vii
LIST OF TABLES	xi
NOTATIONS	xii
I INTRODUCTION.	
1.1 General	1
1.2 Framed Tube System	3
1.3 Scope and Objectives	4
1.4 General Assumptions	6
1.5 Organization of the Thesis	6
II EQUIVALENT ORTHOTROPIC MEMBRANE	
2.1 Introduction	10
2.2 Orthotropic Membrane for Coupling Beams	14
2.3 Orthotropic Membrane for Planar Gridwork System	16
2.3.1 Moduli of elasticity, E_x and E_y	19
2.3.2 Shear modulus, G_{xy}	23
2.4 Consideration of Second-Order Effects	25
III BEHAVIORAL CHARACTERISTICS OF PERFORATED WALLS	
3.1 Introduction	39
3.2 Theoretical Analysis	41
3.2.1 Energy formulation	42
3.2.2 Equilibrium conditions	43
3.2.3 Stress components	44
3.2.4 Governing differential equation and its solution	46
3.2.5 Internal forces in the actual structure	47
3.2.6 Lateral deflection	49
3.3 Design Curves	50
3.4 Controlling Parameters	52
3.5 Numerical Example	54

PAGE

3.5.1 Structure properties 55

3.5.2 Elastic properties of the equivalent orthotropic membrane 55

3.5.3 Internal forces in the actual structure. 55

3.5.4 Lateral deflection 56

3.5.5 Comparison of results 56

3.6 Other Applications 57

3.7 Limitations 57

3.8 Discussions on Khan's Frame Reduction Technique 58

IV TWO-DIMENSIONAL FINITE ELEMENT ANALYSIS OF PERFORATED WALLS

4.1 Introduction 83

4.2 Analysis Procedure 87

4.3 Element Stiffness Matrix 89

4.4 Assembly of the Structure Stiffness Matrix and Load Vector 91

4.5 Boundary Conditions and Solution 91

4.6 Determination of Stresses 92

4.7 Computer Program 95

4.8 Numerical Example 95

4.9 Diaphragm Action of Floors 97

V SPECIALLY ORTHOTROPIC FINITE ELEMENT FOR TALL BUILDING ANALYSIS

5.1 Introduction 106

5.2 Procedure for Deriving Element Stiffness Matrix and Consistent Load Vector 106

5.3 Formulation of the Ordinary Element 108

5.4 Formulation of the Refined Element 114

5.5 Numerical Examples 120

5.5.1 Example 5-1 121

5.5.2 Example 5-2 122

5.5.3 Example 5-3 122

5.5.4 Example 5-4 124

5.5.5 Example 5-5 125

VI ANALYSIS OF TUBE-TYPE TALL BUILDING STRUCTURES

6.1 Introduction 143

6.2 Scope 151

6.3 Analysis Procedure 152

	PAGE
6.4 Structure Idealization	154
6.5 Assembly of Facade Stiffness Matrix in Local Axes	156
6.5.1 No Symmetry	157
6.5.2 Symmetry Type One	158
6.5.3 Symmetry Type Two	158
6.5.4 Symmetry Type Three	159
6.6 Condensation of Facade Internal Degrees of Freedom	160
6.7 Assembly of the Global Structure Stiffness Matrix	163
6.8 Transformation Matrices for Different Structural Symmetry Conditions	169
6.9 Solution for Displacements	171
6.10 Determination of Stresses	172
6.11 Computer Program	173
 VII APPLICATION TO THE ANALYSIS OF TUBE-TYPE TALL BUILDING STRUCTURES	
7.1 Introduction	178
7.2 Application to Framed Tube Structures	179
7.2.1 Example 7-1	179
7.2.2 Example 7-2	183
7.2.3 Example 7-3	185
7.3 Application to Core-Supported Structures	186
7.3.1 Structure Idealization	187
7.3.2 Comparison and Discussion of Results	187
 VIII CONCLUSIONS AND RECOMMENDATIONS	
8.1 Conclusions	214
8.2 Recommendations for Further Studies	217
REFERENCES	219
APPENDIX A - THE INTEGRALS USED IN EVALUATING THE TERMS OF THE ORDINARY ELEMENT STIFFNESS MATRIX	233
APPENDIX B - DERIVATION OF THE REFINED ELEMENT STIFF- NESS MATRIX	236
APPENDIX C - COMPUTER PROGRAM	249

LIST OF FIGURES

LIST OF FIGURES

FIGURE	DESCRIPTION	PAGE
1.1	Framed tube structure - Ref. [58].	9
2.1	Modelling of coupled shear walls - Beck [7].	32
2.2	Modelling of braced thin-walled elastic beam - Vlasov [119]	32
2.3	Modelling of gridwork shell - Flügge [40].	33
2.4	Modelling of framed tube structure - Coull and Bose [32]	33
2.5	Modelling of wall-frame structure - Khan and Stafford-Smith [61]	34
2.6	Present modelling of coupling beams	35
2.7	Model for evaluating the elastic modulus E_y	36
2.8	Model for evaluating the shear modulus G_{xy}	37
2.9	Modelling of second-order effects	38
3.1	Modelling of wall-frame structures	69
3.2	Shear lag effect on the distribution of the normal stress at the base	70
3.3	Definitions of symbols in equations (3.28) to (3.30)	71
3.4a	Shear lag functions ($R = 1$)	72
3.4b	Shear lag functions ($R = 2$)	73
3.4c	Shear lag functions ($R = 3$)	74
3.4d	Shear lag functions ($R = 4$)	75
3.4e	Shear lag functions ($R = 5$)	76
3.5	Stress coefficients	77

FIGURE	DESCRIPTION	PAGE
3.6	Example structure (3-1) - Khan and Stafford-Smith [61]	78
3.7	Design forces in columns and beams - Example 3-1	79
3.8	Lateral deflection - Example 3-1	80
3.9	Example 3-2	81
3.10	Example 3-3	82
4.1	Methods of analysis considered in the numerical example (4-1)	101
4.2	Specially orthotropic finite element of Ammar and Nilson [3]	102
4.3	Lateral deflection - Example 4-1	103
4.4	Column axial forces - Example 4-1	104
4.5	Variation of axial force in the exterior column - Example 4-1	105
5.1	The ordinary element	129
5.2	The refined element	130
5.3	20-storey wall-frame structure of Khan and Stafford-Smith [61] - Example 5-1	131
5.4	Structure idealization - Example 5-1	132
5.5	Lateral deflection - Example 5-1	133
5.6	Member internal forces at section a-a - Example 5-1	134
5.7	20-storey frame of DeClercq [34] - Example 5-3	135
5.8	Lateral deflection - Example 5-3 (variable properties)	136
5.9	Variation of shear in middle beam - Example 5-3 (variable properties)	137
5.10	Lateral deflection - Example 5-3 (constant properties)	138

FIGURE	DESCRIPTION	PAGE
5.11	Variation of axial force in the edge column of Example 5-3 (constant properties)	139
5.12	Structure idealization - Examples 5-4 and 5-5	140
5.13	Distribution of axial column forces at different floor levels - Example 5-4	141
5.14	Lateral deflection including P-Δ effect - Example 5-5	142
6.1	Structure idealization	174
6.2	Global degrees of freedom at the i^{th} level	175
6.3	Automated numbering systems of nodes and elements	176
6.4	Automated facade degrees of freedom system	177
7.1	16-storey framed tube of Chan [12] - (Example 7-1)	191
7.2	Lateral deflection - Example 7-1	192
7.3	Different meshes used in structure idealization - Example 7-1	193
7.4	Effect of mesh size on the distribution of column axial forces - Example 7-1	194
7.5	Convergence of maximum column axial force - Example 7-1	195
7.6	Variation of the axial force in the corner column - Example 7-1	196
7.7	Variation of the axial force in column 2 of normal frames - Example 7-1	197
7.8	Envelope of shear forces in beam 1 of parallel frames - Example 7-1	198
7.9	Envelope of shear forces in beam 1 of normal frames - Example 7-1	199
7.10	10-storey framed tube of DeClercq [34] - (Example 7-2)	200

FIGURE	DESCRIPTION	PAGE
7.11	Different meshes used in structure idealization - Example 7-2	201
7.12	Convergence of maximum column axial force - Example 7-2	202
7.13	Lateral deflection - Example 7-2	203
7.14	Member internal forces at first floor - Example 7-2	204
7.15	36-storey framed tube model of Chan [12] - (Example 7-3)	205
7.16	Lateral deflection of the model under $P = 10$ lb - Example 7-3	206
7.17	Variation of column axial stresses at mid-height of the 5 th storey of the model under $P = 10$ lb - Example 7-3	207
7.18	Lateral deflection of the model under uniform lateral load of 1 lb/in - Example 7-3	208
7.19	Variation of column axial stresses at mid-height of the 5 th storey of the model under uniform load of 1 lb/in - Example 7-3	209
7.20	Dimensions and loading of the core-supported structure - reference [109]	210
7.21	Structure idealization (core-supported structure)	211
7.22	Rotation (core-supported structure)	212
7.23	Normal stresses at the base of the core-supported structure	213

LIST OF TABLES

LIST OF TABLES

NUMBER	DESCRIPTION	PAGE
3.1	Values of F and F'	66
3.2	Column internal forces	67
3.3	Beam internal forces	68
4.1	Comparison of the number of unknowns and computer storage	99
4.2	Effect of the elastic modulus E_x on the analysis.	100
5.1	Comparison of the number of unknowns and computer storage	128
7.1	Effect of mesh size on the accuracy (Example 7-1)	189
7.2	Comparison of results obtained by different methods (core-supported structure)	190

NOTATIONS

NOTATIONS

a, b, c	Dimensions of the elements
A	Cross-sectional area
A_m, A_n, B_m, C_m, D_m	Coefficients used in determining the elastic properties of the equivalent membrane
A_r	Reduced (effective) area of beam cross-section
B	Bay width
C	Carry-over factor
C_x, C_{xy}, C_y	Coefficients used in determining the elastic properties of the equivalent membrane
d	Depth of lintel beam, half-width of perforated wall
$\{d\}$	Displacement vector
d_b	Depth of beam
d_c	Depth of column
D	The total width of a perforated wall, perpendicular distance between the z-axis and a facade
$[E]$	Elasticity matrix
E, G	Elastic moduli of the material of the actual structure
E_x, E_y, G_{xy}	Elastic moduli of the equivalent orthotropic membrane
F, F'	Shear lag functions
G_{xy}^*	Modified shear modulus of equivalent orthotropic membrane to account for second-order effects
H	Storey height

I	Moment of inertia
[K]	Stiffness matrix
K_n, K_m	Coefficients used in determining the elastic properties of the equivalent membrane
ℓ	length of a member, mapping function
L	height of building
M	Overturning moment
[N]	Shape function
P	Axial force in columns
{P}	Load vector
Prime	Denotes differentiation
Q	Applied shear
Q_1^*	Modified lateral load to account for P- Δ effect
r	Aspect ratio of an element
R	The aspect ratio of a wall-frame structure
[S]	Stiffness matrix of column-member subjected to axial compressive force
SL	Shear lag parameter
t	Thickness of the equivalent membrane
t_b	Thickness of the beam
t_c	Thickness of the column
{T}	In-plane surface tractions vector
[T]	Transformation matrix
u, v	Displacements in x- and y-directions respectively

U^*	Complementary strain energy
U	Strain energy
v	Lateral displacement in y-direction
V_b, V_c	Shear in column and beams
w	Intensity of uniform lateral load, vertical displacement at the corners of a tube type tall building
α	The angle between the x-axis and the positive direction of a facade
α, β	Coefficients used in the closed-form solutions
δ	Lateral deflection
$\Delta_1, \Delta_2, \Delta_3$	Deformations of Parts 1, 2 and 3 of the basic frame unit
Δ_m	Deformation of the equivalent membrane
$\{\epsilon\}$	Strain vector
$\epsilon_x, \epsilon_y, \gamma_{xy}$	Strain components in the equivalent orthotropic membrane
θ_i	The rotation at the i^{th} level in a tube-type tall building structure
λ	Coefficient used in the constitutive relation of orthotropic media
μ	Poisson's ratio of the material of the actual structure
μ_x, μ_y	Poisson's ratios of the equivalent orthotropic membrane
ξ, η	Coefficients, non-dimensional parameters = $x/a, y/b$ respectively
$\{\sigma\}$	Stress vector

$\sigma_x, \sigma_y, \tau_{xy}$ Stress components in the equivalent
membrane

$\Sigma R d$ Work done by the reactions

To the memories of the past ...
To the reality of the present ...
To the hope in the future ...

To you, my parents, my wife,
and my daughter

CHAPTER I
INTRODUCTION

CHAPTER I
INTRODUCTION

1.1 GENERAL

From time immemorial tall structures, as a symbol of greatness, have attracted and challenged the abilities of man. A good example is the great Egyptian pyramid of Cheops built by King Khufu in 2,900 B.C. at a height of 481 ft which is equivalent to a modern 50-storey building. The basic construction materials used in these early tall structures were masonry and timber, neither of which had qualities that were best suited to the construction of buildings having more than a few stories.

The socio-economic problems that came with industrialization of the 19th century and the insatiable need for space in the cities gave the big impetus towards high-rise construction. The invention of elevators, the use of high strength materials together with the introduction of the beam-column framing system by the Chicago School of Architecture brought the first major change to the scale of urban centres. The earlier six to eight storey buildings were replaced by 20 to 30 storey buildings, and this trend undoubtedly reached its peak with the construction of the Empire State Building.

After 1930, because of the depression years and later the Second World War, there was not much activity in the building construction. In the '50's, the fast growing indus-

trial development and the resulting economic prosperity produced new demands for more space in the urban centres. Land prices began climbing, dictating vertical rather than horizontal expansion. At this time the shear wall system was introduced allowing economic construction of concrete buildings up to 35 stories high.

Ever since the early sixties, the need for taller buildings has been steadily growing. This necessitated the development of new structural systems [38, 53, 63 to 66, 68, 69, 70, 72, 99] aimed at achieving ultimately what is referred to as "premium-free building" by keeping wind stresses below the allowable 33% overstress [69]. These systems utilize the interaction among the different planar systems (e.g., frame-shear wall system) or recognize the actual three-dimensional behavior of buildings (e.g. tube-type tall building structures.) In particular, the framed tube (also known as the perforated tube) introduced by Khan [67, 68] (for the design of the 43-storey Dewitt Chestnut Apartment Building in Chicago) in 1963 has proven to be a very efficient structural system [8, 58, 83, 90, 99]. Further studies [56, 66] revealed that the concept of perforated tube could effect economic gains not only for the tallest buildings but also for buildings with as few as twenty stories. A brief description of the system and its behavioral characteristics is outlined in the following section.

1.2 FRAMED TUBE SYSTEM

A typical framed tube system is shown in Fig. 1.1 where closely spaced columns are tied at each floor level by deep spandrel beams producing a number of frames with relatively deep members (perforated walls) around the periphery of the building which could be of arbitrary shape [34, 59] or rectangular as most often found. This structural arrangement is a logical extension of the shear wall frame system, since it is well known that the frame efficiency in resisting lateral loads results from deeper members and shorter spans.

The center-to-center spacing of columns of a framed tube generally varies from 4 ft to 10 ft although the structural efficiency is not significantly reduced for spacing up to 15 ft. Typical widths of columns or depths of spandrel beams vary from 2 ft to 5 ft depending on the structural requirements and the extent of the glazed area on the facades [58, 67]. The facades of the building act as bearing walls which, because of windows, appear as a perforated tube. This efficient form of facades (perforated walls) which are also known as wall-frame structures [61], combine the characteristic behavior of both frames and walls. Modelling of such structures for the purpose of analysis becomes complicated, since the use of an ordinary frame or a frame with rigid arms will result in underestimation and overestimation of the rigidity of the structure respectively. The finite element

method, on the other hand, requires a large number of unknowns to yield a reasonable degree of accuracy. An assembly of these perforated walls forming a tube-type tall building structure, obviously, precludes the use of the finite element technique for design.

Approximate methods of analysis [1, 12, 32, 59, 67] of framed tube systems are based on recognizing its behavior as a combination of the cantilever bending mode and the usual frame shear deformation mode. Considering, for example, the framed tube shown in Fig. 1.1, the overturning moment due to lateral forces is resisted by the entire three-dimensional tube form giving rise to compressive and tensile forces in the columns. In addition to this cantilever bending mode, the two facades parallel to the lateral loads undergo the shear mode deformation by bending of beams and columns. In contrast with the pure bending behavior of an ideal tube which exhibits linear variation of axial forces (Fig. 1.1b), the flexibility of spandrel beams results in the so-called "shear lag" in all facades which tends to increase the axial forces of columns near the corners and decrease those in the central region.

1.3 SCOPE AND OBJECTIVES

The primary objective of this thesis is to develop an efficient technique for the elastic analysis of framed tube structures. The technique is intended to be general and flexible enough for the analysis of most existing planar

and tubular structural systems for tall buildings. These systems may include multi-storey, multi-bay frames having a wide range of aspect ratios and stiffnesses, coupled shear walls, clad frames, planar and tubular structures consisting of frame and shear wall assemblies, and core-supported structures.

The analysis technique is based on replacing the discrete beam-column planar system and any band of lintel beams, by an elastically equivalent orthotropic membrane, which is then analyzed by the finite element method. Computational efficiency is achieved by a drastic reduction of the number of degrees of freedom expressing the deformations of the structure. Since each element in the idealized structure may span over several stories and bays of the actual structure, it is appropriate to term the present technique as "The Equivalent Orthotropic Macroelement Method."

The present work covers both the static and stability analyses of a large variety of planar and tubular structural systems for tall buildings; thus it seems to be appropriate to review the literature for each topic when it is first discussed. Nevertheless, it is noted that the work of DeClercq [34] is similar to the present study in that both approaches can be regarded as an extended version of the usual finite element method on a macro scale where a single element may span several beams and columns. However, the present method digresses from DeClercq's in several aspects

that will be discussed in detail at a later stage.

1.4 GENERAL ASSUMPTIONS

In addition to the specific assumptions which will be given later in connection with the specific topics treated in this work, the following are the main general assumptions in the present work.

- (1) The material is isotropic, homogeneous and linearly elastic.
- (2) The frame members form an orthogonal grid system, and the connections among the members are rigid.
- (3) The floor diaphragms are infinitely rigid in their own planes. This assumption is generally accepted for the "exact" analysis of tall building structures [110].
- (4) Out-of-plane deformations of frames and walls can be neglected. The effect of these deformationa has been shown to be negligible. [12, 36, 44, 110, 128].

1.5 ORGANIZATION OF THE THESIS

Chapter II of the thesis deals with the evaluation of the elastic properties of the equivalent membranes. The effect of bending and shear deformations, axial deformation in columns, and flexibility of finite size joints, are taken into account. These elastic properties are further modified

to allow for second-order (stability) analysis.

Because an understanding of the behavior of the entire structure is crucial to the application of the equivalent orthotropic macroelement method, Chapter III concentrates on the behavior of planar perforated walls and the identification of its characteristic parameters. Closed-form solutions of a simple planar system are derived and design curves are also developed. A typical 20-storey wall frame structure is analyzed and the results are compared to those obtained by a detailed finite element and other simplified methods. Applications to frame and shear wall structures are also presented.

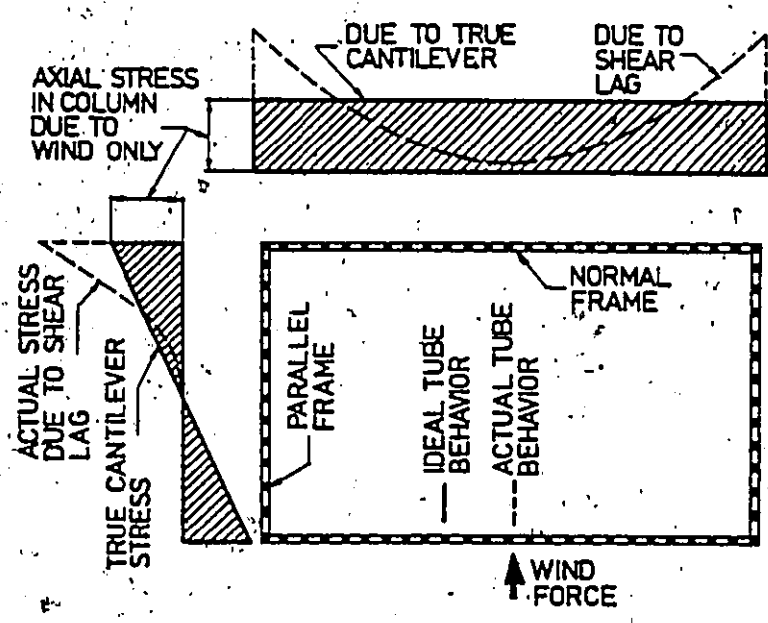
In Chapter IV, a finite element model for the analysis of planar systems is developed. Example analysis of a 52-storey frame is carried out and the results are compared to those obtained by the "exact" and other simplified methods. The validity of the assumption of infinite in-plane floor stiffness is also examined.

Chapter V presents two specially orthotropic rectangular finite elements specifically developed to incorporate the above assumption with a view to improving computational efficiency. The first is an ordinary element with four-corner nodes and six degrees of freedom. The second is an eight-node refined element with nine degrees of freedom. Various applications to planar systems are given to demonstrate the flexibility and efficiency of the method.

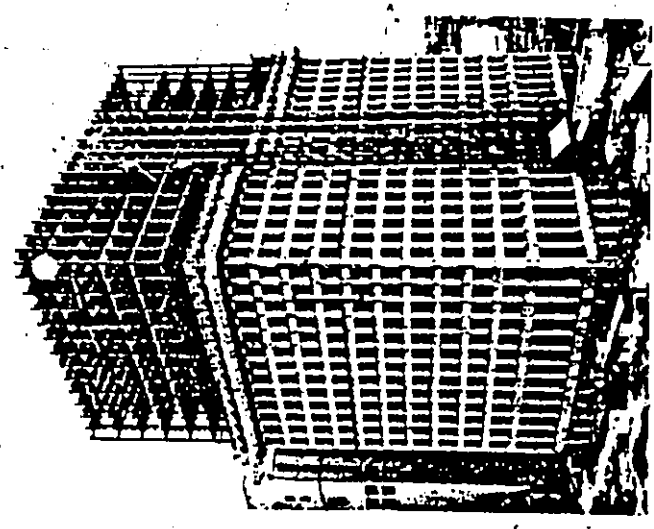
Formulation of the theory for application to three-dimensional structures is presented in Chapter VI.

Chapter VII is designed to demonstrate the practical applications of the present method and to illustrate its accuracy when applied for the analysis of tube-type tall building structures. A number of numerical examples representing both framed tube and core-supported structures are considered. The results are compared to those available in the literature.

Finally, the conclusions and recommendations for further studies in this area are presented in Chapter VIII.



(b) SHEAR LAG EFFECT



(a) ISOMETRIC VIEW

FIG. 1.1 FRAMED TUBE STRUCTURE - REF [58]

CHAPTER II
EQUIVALENT ORTHOTROPIC MEMBRANE

CHAPTER II

EQUIVALENT ORTHOTROPIC MEMBRANE

2.1 INTRODUCTION

The idea of replacing a complex, highly redundant, discrete system by an elastically equivalent continuum is not new. It was first applied for analysis of ship and aircraft structures [116]. Since then, it has been employed for the analysis of bridges [115], Shells [40], and space roof trusses [39]. In the early 1960's, the elastic equivalent concept has been employed for the analysis of coupled shear wall structures [7, 91] and recently to the analysis of tall building frame-type structures. [6, 32, 61].

Considering the application of this concept to coupled shear walls, it is commonly shown in the literature that the replacement of a band of lintel beams by an equivalent continuum (Fig. 2.1) is due to Beck [7] and Rosman [91 to 98]. However, the problem has been previously considered by Vlasov [119], in his theory on thin-walled elastic beams, where the closely-spaced strip braces of a thin-walled beam are replaced by an elastically equivalent orthotropic membrane (Fig. 2.2). In this case, the orthotropy manifests itself by the membrane being only able to sustain shear stresses and not tensile stresses.

The elastic equivalent concept was introduced at a later stage for the analysis of frame-type structures. In

1971, Bazant and Christensen [6] modelled planar multi-storey, multi-bay rigid frames by a special micropolar equivalent continuum. The resulting differential equations were solved by the finite difference method. Four years later, the equivalent orthotropic membrane technique was introduced by Coull and Bose [32] for the analysis of framed tube structures where closed-form solutions were derived for the orthotropic tube by employing an energy principle in conjunction with some assumed stress functions. But before any further elaboration on this technique, it seems more appropriate to consider first Flügge's model [40] for gridwork shells. The actual shell was replaced by an orthotropic solid one. Elastic properties of the equivalent continuum were evaluated considering line grid elements, as shown in Fig. 2.3, and only bending deformations were accounted for. This model was later adopted by Coull and Bose [32] for the analysis of framed tube structures. Infinitely rigid arms were introduced to model finite size joints, as shown in Fig. 2.4. Although framed tube structures consist of closely spaced columns connected by deep spandrel beams [8,58,67,83,90,99], shear deformations were neglected in evaluating the equivalent shear modulus and effect of finite size joints was completely ignored in evaluating the equivalent elastic modulus. Thus, the shear modulus was overestimated and the elastic modulus was underestimated [85].

In 1976, Khan and Stafford-Smith [61] presented a simplified method for the analysis of wall-frame structures

(also known as perforated walls). The actual structure was replaced by an equivalent isotropic solid wall. Stresses in the equivalent wall were evaluated by the engineering beam theory and internal forces in the actual structure were determined using specially defined stress concentration factors. The extensional and shear moduli of elasticity of the equivalent wall were derived from both the strength of materials approach and plane stress finite element idealization of the models shown in Fig. 2.5. In the strength of material approach, only shear deformations were considered in evaluating the shear modulus and, furthermore, the beam was assumed to elongate uniformly along its depth in evaluating the extensional elastic modulus. Therefore, both moduli, especially the shear modulus, were overestimated. On the other hand, the finite element models (Figs. 2.5.2(c) and 2.5.3(c)), due to their discretization and the imposed boundary conditions, are suitable only for relatively deep members. This may account for the appreciable loss of accuracy when the column depth/bay width and the beam depth/storey height ratios are each less than 0.25.

With respect to the P-Δ effect, the analysis of framed structures may be grouped into several categories: (1) approximate methods for the overall stability of the structure, generally based on an equivalent cantilever approach [41,57,73,98,126]; (2) simple modification of the results of first order analysis [8,15,42,55,75,76]; (3) negative bracing member method [87] in which a fictitious diagon-

al brace, of negative area, is introduced at each storey enabling a direct solution for the second-order deflections and moments by means of a standard first-order structural analysis program; (4) iterative P- Δ methods [2,74] and finally, (5) "Exact" methods based on the matrix formulation of the displacement method of analysis which could include the effects of the deflected shape of the structure and the reduction in member stiffness due to the axial loads-[48,120].

The methods in the second group are approximate but sufficiently accurate for all practical purposes as recently demonstrated by MacGregor [76] and Cheong-Siat-Moy [15] for concrete and steel framed structures, respectively. One may note that these methods ignore the fact that axial loads tend to reduce the column stiffness, which may in a severe case substantially increase moments in the columns and, decrease those in the beams. The equivalent micropolar continuum as advanced by Bazant and Christensen [6] allows for an iterative stability analysis of slender multi-bay, multi-storey planar frames. Despite the attractiveness of the underlying concept, the use of micropolar rather than the conventional elastic properties complicates the subsequent analysis to the extent that the complexity of the original problem is not likely to be significantly reduced [126].

Since the accuracy of the solutions based on the elastic equivalent concept depends to a great extent on the elastic properties of the equivalent continuum, the primary

concern in this chapter is to develop refined expressions of these elastic properties for two particular groups of structural systems:

- (1) Coupled shear walls and core-supported structures, where the lintel beams are to be represented by an equivalent orthotropic membrane.
- (2) Planar and tubular structures composed of orthogonal grid systems in which the members are not only representative of those in perforated walls but also those in multi-storey multi-bay slender frames at one extreme and completely solid walls at the other extreme. Expressions for the properties of the equivalent membrane are further extended to allow for the stability analyses of these structures including the loss of column stiffness due to high axial forces.

2.2 ORTHOTROPIC MEMBRANE FOR COUPLING LINTEL BEAMS

Lintel beams connecting planar or three-dimensional assembly of shear walls are replaced by an elastically equivalent orthotropic membrane as shown in Fig. 2.6. Both bending and shear deformations of the connecting beams are considered in evaluating the shear modulus of the membrane, thus allowing for modelling of a wide range of coupling elements (i.e.,

from slabs to relatively deep lintel beams.)

From the deflected shape of coupled shear walls under the action of lateral loads, points of contraflexure can be assumed to be in the mid-span of the coupling beams. This assumption is also employed in the continuous connection technique [5,7,9,10,19-27,29,30,31,51,59,91 to 98, 102,103, 105,117]. Considering now one half of the coupling beam as shown in Fig. 2.6(a), the maximum deflection due to both bending and shear deformations is

$$\Delta_b = \frac{Ql^3}{(24EI)} + \frac{Ql}{(2GA_r)} \quad (2.1)$$

in which

Q = applied shear

l = span of lintel beam

E, G = elastic moduli of the lintel beam material

I, A_r = moment of inertia and the reduced (effective) area of the beam cross-section

Equation (2.1) is obtained by a direct application of the method of virtual work. Equating the maximum deflection of half the beam, Eq. (2.1), to the shear deflection of the equivalent orthotropic membrane (Fig. 2.6(b)), i.e.,

$$\Delta_m = \frac{Q\ell}{(2tHG_{xy})} \quad (2.2)$$

in which

t = thickness of the membrane

H = storey height

G_{xy} = shear modulus of the equivalent orthotropic membrane

yields the following expression for the shear modulus

$$G_{xy} = \frac{\frac{E}{tH}}{\left[\frac{\ell^2}{12I} + \frac{1}{A_r} \left(\frac{E}{G} \right) \right]} \quad (2.3)$$

For a rectangular coupling beam having a thickness t and a depth d , the shear modulus G_{xy} can further be expressed as

$$G_{xy} = \frac{E \left(\frac{d}{H} \right)}{\left[\left(\frac{\ell}{d} \right)^2 + 1.2 \left(\frac{E}{G} \right) \right]} \quad (2.4)$$

2.3 ORTHOTROPIC MEMBRANE FOR PLANAR GRIDWORK SYSTEMS

In replacing the perforated wall or planar gridwork system by an elastically equivalent orthotropic membrane, it is necessary that the perforation ratios $\frac{B}{D}$ and $\frac{H}{L}$ of the structure be small [116],

where

B = bay width

H = storey height

D and L = width and height of the structure,
respectively.

Typical values for $\frac{B}{D}$ and $\frac{H}{L}$ in the existing structures [8, 67, 83, 90] are from $(\frac{1}{10}$ to $\frac{1}{20})$ and $(\frac{1}{20}$ to $\frac{1}{100})$ respectively which fall within the range for the applicability of the elastic equivalence concept as will be shown in later chapters.

In addition to the ~~above~~ restriction and the general assumptions in Section 1.4, it is further assumed, that member properties, storey heights, and bay widths are each constant either throughout the building or at least within a macroelement. This will soon become apparent in the formulation given later in Chapters III to V. This is not, as it may first appear, a severe limitation. For the reasons of economy, fast and easy construction, it is common in the design of tall buildings to repeat member sizes and properties over large parts of a structure [34, 67, 83, 90] which in typical concrete [90] and steel [83] framed tube structures, covers the whole structure. In other practical examples [67] member sizes and properties were kept constant over from 5 to 15 stories along the height of the structure. In general, this assumption characterizes macroelement tech-

niques [34].

Under the action of lateral (in-plane) forces, the members of an orthogonal grid system would bend in double curvature with the inflection points approximately at mid-spans of the members. This has also been assumed by Flügge [40], Coull and Bose [32], Khan [59], and Khan and Stafford-Smith [61] in evaluating the elastic properties of their different equivalent continuums. In most other simplified methods which are not based on the elastic equivalent concept [1,4,12,13,14,52,67,106] such an assumption is also introduced.

Consider a unit or a segment of the grid system bounded by four adjacent inflection points (Figs. 2.7(a) and 2.8(a)). It is proposed that such a unit be replaced by a solid orthotropic membrane spanning the same area. The elastic properties of the membrane are derived based on the condition that under statically equivalent external force systems, both the actual grid and membrane units develop the same characteristic deformations. Since the boundaries of the grid unit consist of four inflection points, the only forces applied are of axial and shear types as shown in Figs. 2.7 and 2.8. The corresponding characteristic deformations are then the axial and lateral displacements of the units. These two deformation models will furnish enough equations for the determination of the elastic properties of the equivalent membrane. For application to a wide range of

member sizes, these expressions would have to account for the flexibility of the finite size joints and axial deformation of columns in addition to the usual bending and shear deformations in the members [84, 85].

2.3.1 Moduli of Elasticity E_x and E_y

Considering the wall-frame unit (Fig. 2.7) under the action of an axial force P , the deformations in Parts 1 and 3 are:

$$\Delta_1 = \Delta_3 = \frac{P(H-d_b)}{(2t_c d_c E)} \quad (2.5)$$

in which

H = storey height

d_b = beam depth

d_c = column depth

t_c = column thickness

E = elastic modulus of the material of the actual structure

The deformation in Part 2 is not uniform as in Parts 1 and 3. Its average value along the column depth is obtained by integrating the strain in the y -direction as follows

$$\Delta_2 = \frac{1}{3} \sum_{n=1}^3 \frac{d_b}{2} \int_0^{d_b/2} \frac{(\sigma_y - \mu \sigma_x)_n}{E} dy \quad (2.6)$$

The stresses in Eq. (2.6) are given by Timoshenko [114] as:

$$\sigma_y = \frac{P}{t_b B} + \frac{4P}{\pi t_b d_c} \sum_{m=1}^{\infty} A_m [(B_m + C_m) \cosh 2\alpha y - D_m y \sinh 2\alpha y] A_n \quad (2.7)$$

$$\sigma_x = \frac{-4P}{-t_b d_c} \sum_{m=1}^{\infty} A_m [(B_m - C_m) \cosh 2\alpha y - D_m y \sinh 2\alpha y] A_n \quad (2.8)$$

in which

$$A_m = \frac{\sinh \alpha d_c}{m(\sinh 2\alpha d_b + 2\alpha d_b)}$$

$$B_m = \alpha d_b \cosh \alpha d_b$$

$$C_m = \sinh \alpha d_b \quad (2.9)$$

$$D_m = 2\alpha \sinh \alpha d_b; \text{ and } \alpha = m\pi/B$$

$$A_n = \cos \{ \alpha d_c (2-n)/2 \}$$

Equation (2.6) then gives

$$\Delta_2 = \frac{P d_b}{E B t_b} + \frac{8PB}{\pi^2 E t_b d_c} \frac{1}{3} \sum_{n=1}^3 \sum_{m=1}^{\infty} A_n \frac{A_m}{m} \sinh^2 \alpha d_b \quad (2.10)$$

By equating $\Delta_1 + \Delta_2 + \Delta_3$ to the deformation in the equivalent membrane (shown by the dotted line in Fig. 2.7(a))

$$\Delta_m = \frac{PH}{tBE_y} \quad (2.11)$$

in which

t = thickness of the membrane

the equivalent elastic modulus E_y is obtained as

$$E_y = \frac{Et_c d_c}{tBC_y} \quad (2.12)$$

in which

B = bay width

and C_y is defined by

$$C_y = 1 - \frac{d_b}{H} + \frac{t_c}{t_b} \left[\frac{d_b d_c}{BH} + \frac{8B}{\pi^2 H} \frac{1}{3} \sum_{n=1}^3 \sum_{m=1}^{\infty} A_n \frac{A_m}{m} \sinh^2 \alpha d_b \right]$$

(2.13)

It can be seen from Eq. (2.13) that for structures having slender members the factor C_y approaches unity, and for those having deep beams and wide columns the factor could be significantly less than one.

The elastic modulus E_x can be derived in a similar manner as

$$E_x = E \frac{t_b d_b}{t H C_x} \quad (2.14)$$

in which

t_b and d_b = thickness and depth of beam,
respectively

and C_x is defined by

$$C_x = 1 - \frac{d_c}{B} + \frac{t_b}{t_c} \left[\frac{d_c d_b}{B H} + \frac{8H}{\pi^2 B} \frac{1}{3} \sum_{n=1}^{\infty} \sum_{m=1}^{\infty} K_n \frac{K_m}{m} \sinh^2 \beta d_c \right] \quad (2.15)$$

in which

$$K_n = \cos \{ \beta d_b (2-n)/2 \}$$

$$K_m = \frac{\sinh \beta d_b}{m(\sinh 2\beta d_c + 2\beta d_c)} \quad (2.16)$$

$$\beta = m\pi/H$$

Except in the next chapter, where the effect of the elastic modulus E_x on the analysis is examined, E_x is assigned an infinite value throughout the theoretical developments presented in this thesis. The latter case corresponds to the acceptable assumption [110] of infinite in-plane rigidity of floors in tall building analysis. In such a case, Poisson's ratios μ_x and μ_y of the membrane which are

related to its elastic moduli E_x and E_y by [116]

$$\mu_y E_x = \mu_x E_y \quad (2.17)$$

are, therefore, assigned zero values.

2.3.2 Shear Modulus G_{xy}

The grid unit is now subjected to a lateral force Q as shown in Fig. 2.8. The lateral deflection may be computed as the sum of that due to bending, Δ_b , and due to shear Δ_v . The bending deflection can be obtained in the form

$$\Delta_b = \frac{QH}{E} \left[\frac{(H-d_b)^3}{12H I_c} + \frac{H(B-d_c)^3}{12 B^2 I_b} \right] \quad (2.18)$$

in which

I_b and I_c = the moments of inertia of the beam
and column, respectively

The deflection Δ_v is due to shear deformations in the members Δ_{vm} , and in the finite-size joint Δ_{vj} :

$$\Delta_{vm} = \frac{QH}{G} \left[\frac{H(B-d_c)}{B^2 A_{rb}} + \frac{H-d_b}{H A_{rc}} \right] \quad (2.19)$$

in which

A_{rb} , A_{rc} = the reduced or effective shear areas
of the beams and columns respectively; and

G = the shear modulus of the material of the actual structure

Equations (2.18) and (2.19) are derived by a straightforward application of the method of virtual work. Finally, the lateral deflection due to shear deformation of the joint, Δ_{vj} , can be evaluated using the same method in conjunction with a net shear force:

$$Q_n = Q - \frac{2M_b}{d_b} \quad (2.20)$$

acting at the top and bottom edges of the joint, in the same and the opposite direction of the lateral force Q , respectively

in which

M_b = maximum beam moment at the column face which from simple statics can be evaluated as

$$M_b = Q \frac{H}{B} \frac{(B-d_c)}{2} \quad (2.21)$$

In Eq. (2.20) the bending moment in the beam is assumed to be carried by the flanges or the extreme fibers of the beam cross-section. Applying the method of virtual work over the length of the joint, d_b , yields

$$\Delta_{vj} = \frac{H^2 Q}{G} \frac{\left(1 - \frac{d_c}{B} - \frac{d_b}{H}\right)^2}{A_{rj} d_b} \quad (2.22)$$

in which

A_{rj} = the cross-sectional area of the joint
parallel to the acting force Q

The total lateral deflection, the sum of Eqs. (2.18), (2.19) and (2.22), is now equated to the shear deflection of the equivalent membrane (shown by the dotted line in Fig. (2.8a)).

$$\Delta_m = \frac{QH}{G_{xy} tB} \quad (2.23)$$

and the equivalent shear modulus G_{xy} of the membrane is then

$$G_{xy} = \frac{E}{tB C_{xy}} \quad (2.24)$$

in which

$$C_{xy} = \frac{(H-d_b)^3}{12HI_c} + \frac{H(B-d_c)^3}{12B^2I_b} + \frac{E}{G} \left[\frac{H(B-d_c)}{B^2A_{rb}} + \frac{H-d_b}{H A_{rc}} + \frac{H}{A_{rj} d_b} \left(1 - \frac{d_c}{B} - \frac{d_b}{H} \right)^2 \right] \quad (2.25)$$

2.4 CONSIDERATION OF SECOND-ORDER EFFECTS

Frame-type structures when subjected to combined gravity and lateral loads are affected significantly by the $P-\Delta$ moment [74] resulting from gravity load action (P) through the sway displacement or drift (Δ). In the elastic range this moment tends to increase both stresses and

lateral deflection of the structure over those evaluated without the consideration of such effect. In tall building structures with a large height-to-width ratio the increase in these stresses and lateral deflection becomes relatively large [76].

The need for the consideration of the P- Δ effect has been steadily increasing with the use of high strength materials and the introduction of new highly efficient structural systems for tall buildings which resulted in a slender structure [38,57,74,76].

In this section, both the properties of the equivalent membrane developed in the previous section and the acting lateral load, Q , are modified to include both the reduction of member stiffness due to axial loads and the P- Δ effect, respectively.

Considering the frame segment or unit shown in Fig.2.9a under the combined action of axial (P) and lateral (Q_1) loads, the lateral deflection at the top can be evaluated by the displacement method of analysis. The stiffness matrix corresponding to the two rotational degrees of freedom at the ends i and j of a column member subjected to compressive force P is [120]

$$[S] = \begin{bmatrix} S_{ii} & S_{ij} \\ S_{ji} & S_{jj} \end{bmatrix} \quad (2.26)$$

in which

$$S_{ii} = S_{jj} = \frac{\alpha(\sin\alpha - \alpha\cos\alpha)}{(2 - 2\cos\alpha - \alpha\sin\alpha)} \frac{EI}{l} \quad (2.27)$$

$$S_{ij} = S_{ji} = \frac{\alpha(\alpha - \sin\alpha)}{(2 - 2\cos\alpha - \alpha\sin\alpha)} \frac{EI}{l} \quad (2.28)$$

where

l = member length

I = moment of inertia

and α is defined as

$$\alpha = l\sqrt{P/EI} \quad (2.29)$$

For small values of α , the expressions for S_{ii} and S_{ij} can be simplified [120] to

$$S_{ii} = \frac{4(1 - \alpha^2/10)}{(1 - \alpha^2/15)} \frac{EI}{l} \quad (2.30)$$

$$S_{ij} = \frac{2(1 - \alpha^2/20)}{(1 - \alpha^2/15)} \frac{EI}{l} \quad (2.31)$$

It can be seen that these stiffness coefficients approach their corresponding first-order values as α approaches

zero.

When the member is free to rotate at one end (Fig. 2.9b), the rotational stiffness at the other end is modified as

$$S_{ii}^* = S_{33} = S_{ii}(1-C^2) \quad (2.32)$$

in which

C = carry-over factor defined by the ratio

$$(S_{ij}/S_{ii}).$$

The other stiffness coefficients in this case are

$$S_{11} = -S_{21} = \left(\frac{S_{ii}^*}{l^2}\right) - \frac{P}{l} \quad (2.33)$$

$$S_{31} = \left(\frac{S_{ii}^*}{l}\right) \quad (2.34)$$

Using Eqs. (2.32) to (2.34) with the appropriate column properties, the force-displacement relation for the frame unit in Fig. (2.9c) can be derived as

$$\begin{Bmatrix} Q_1 \\ 0 \\ 0 \end{Bmatrix} = \begin{bmatrix} K_{11} & -K_{11} & K_{13} \\ -K_{11} & 2K_{11} & 0 \\ K_{31} & 0 & K_{33} \end{bmatrix} \begin{Bmatrix} D_1 \\ D_2 \\ D_3 \end{Bmatrix} \quad (2.35)$$

in which $K_{11} = S_{11}$, $K_{31} = S_{31}$, $K_{33} = 2S_{33} + (6EI_b/l_b)$, and $\{D\}$ and $\{Q\}$ are the displacement vector and its corresponding force vector, respectively. Solving the above set

of simultaneous equations yields the following expression for the lateral deflection D_1

$$D_1 = \frac{Q_1}{\left[\frac{1}{2} K_{11} - \left(\frac{K^2}{K_{33}} \right) \right]} \quad (2.36)$$

It should be noted that the deflection, D_1 , includes both the reduction of member stiffnesses due to axial loads and the additional P- Δ moments as directly reflected in Eq. (2.33). To account for these two effects in the case of the equivalent membrane, the shear modulus G_{xy} of the membrane is reduced to G_{xy}^* and the lateral load Q_1 is magnified to Q_1^* respectively. The latter is obtained by adding to the initial lateral load the following statically equivalent load

$$\Delta Q_1 = \frac{PD_1}{(2l_c)} \quad (2.37)$$

Eq. (2.37) is similar to the additional sway force recently presented by MacGregor and Hage [76]. The total magnified lateral load can then be expressed as

$$Q_1^* = Q_1 + \Delta Q_1 \quad (2.38)$$

Upon equating the lateral deflection, D_1 , of the frame unit to that, Δ_m , of the equivalent membrane

$$\Delta_m = \frac{Q_1^* \ell_c}{(G_{xy}^* t \ell_b)} \quad (2.39)$$

the following expression for the modified shear modulus (G_{xy}^*) of the equivalent orthotropic membrane is obtained:

$$G_{xy}^* = \left(\frac{\ell_c}{t \ell_b}\right) \left\{ \left[\frac{1}{2} k_{11} - \left(\frac{K_{31}^2}{K_{33}}\right) \right] + \frac{P}{2 \ell_c} \right\} \quad (2.40)$$

By substituting Eqs. (2.30) to (2.35) into Eq. (2.40) and rearranging the terms, the shear modulus of a second-order analysis, G_{xy}^* , can be expressed in terms of that of the first-order analysis, G_{xy} , as follows.

$$G_{xy}^* = G_{xy} \frac{1 + \eta}{\xi + \eta} \quad (2.41)$$

in which

$$\eta = \frac{I_c \ell_b}{(I_b \ell_c)}$$

and

$$\xi = \frac{(1 - \frac{\alpha^2}{15})(1 - \frac{\alpha^2}{10})}{(1 - \frac{\alpha^2}{12})(1 - \frac{3\alpha^2}{20})}$$

If α^4 can be ignored, then:

$$G_{xy}^* = G_{xy} \left\{ \frac{1 + \left(\frac{I_c}{I_b} \frac{\ell_b}{\ell_c}\right)}{\left(\frac{30 - 5\alpha^2}{30 - 7\alpha^2}\right) + \left(\frac{I_c}{I_b} \frac{\ell_b}{\ell_c}\right)} \right\} \quad (2.42)$$

Also, by substituting Eqs. (2.30) to (2.37) into Eq. (2.38), the modified lateral load, Q_1^* , can be expressed in terms of the shear modulus of the first-order analysis, G_{xy} , and the initial lateral load, Q_1 , as follows:

$$Q_1^* = Q_1 \left\{ \frac{1}{1 - \left(\frac{P}{t_B G_{xy}} \right)} \right\} \quad (2.43)$$

Again, Eq. (2.43) is similar to the amplification factors presented recently by MacGregor and Hage [76] and Cheong-Siat-Moy [15].

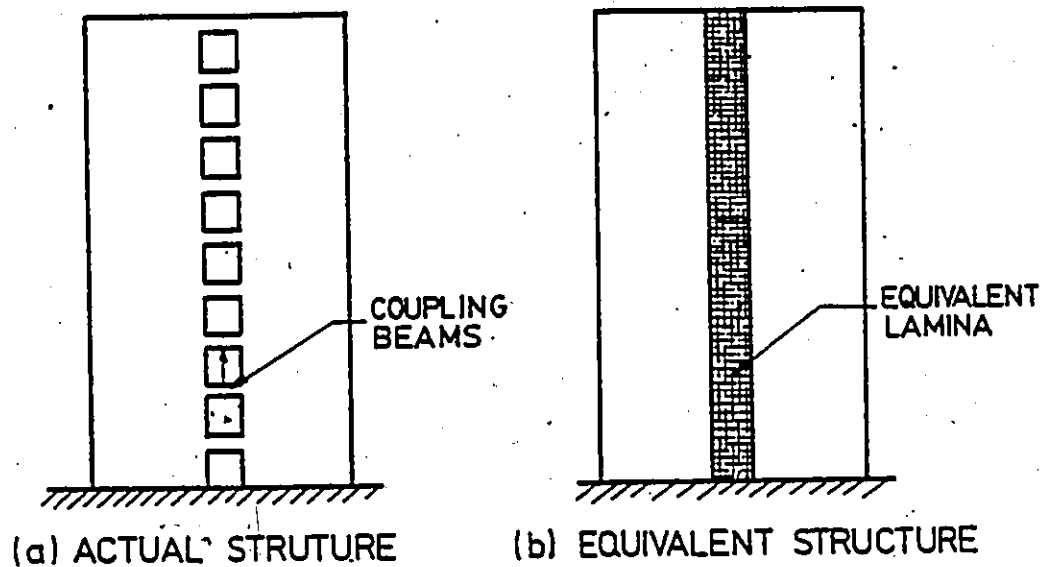


FIG. 2.1 MODELLING OF COUPLED SHEAR WALL-BECK [7]

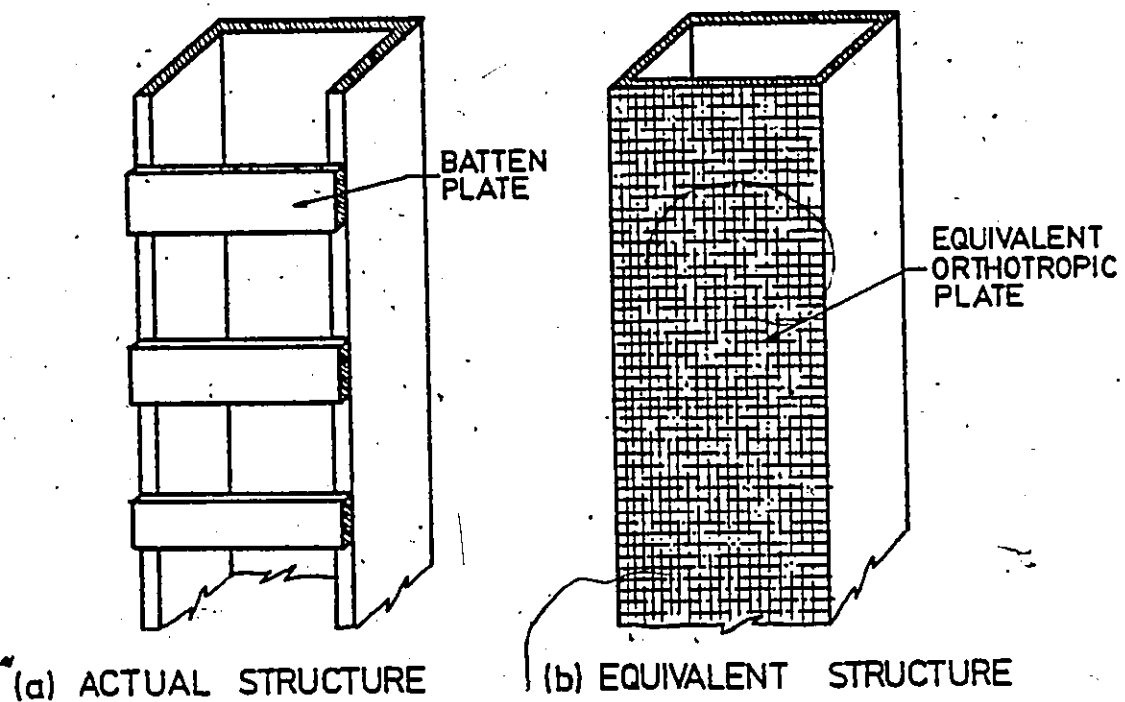


FIG. 2.2 MODELLING OF BRACED THIN-WALLED ELASTIC BEAM - VLASOV [119]

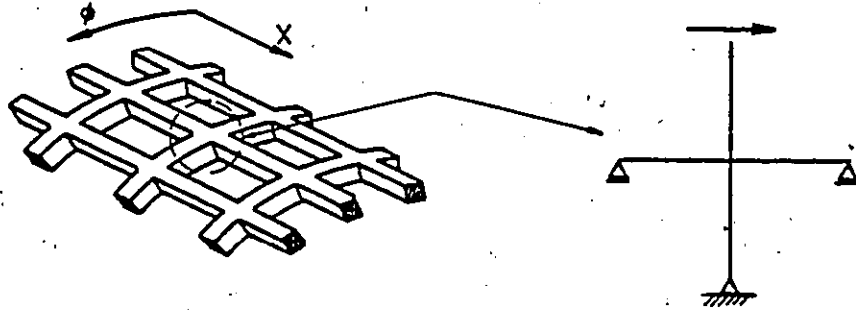


FIG. 2.3 MODELLING OF GRIDWORK SHELL - FLÜGGE [40]

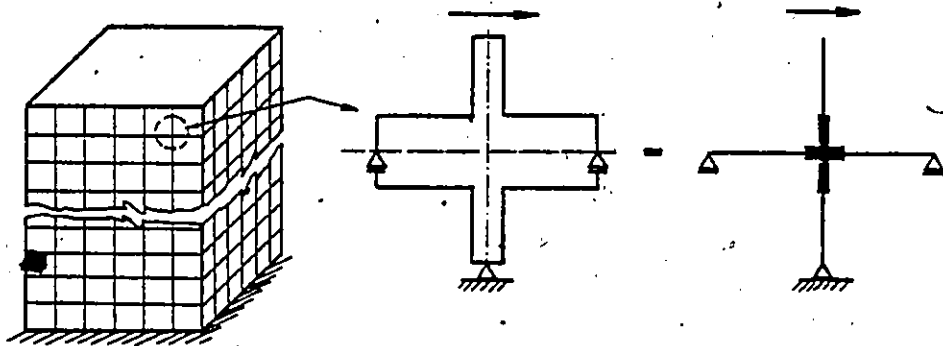


FIG. 2.4 MODELLING OF FRAMED TUBE STRUCTURE - COULL AND BOSE [32]

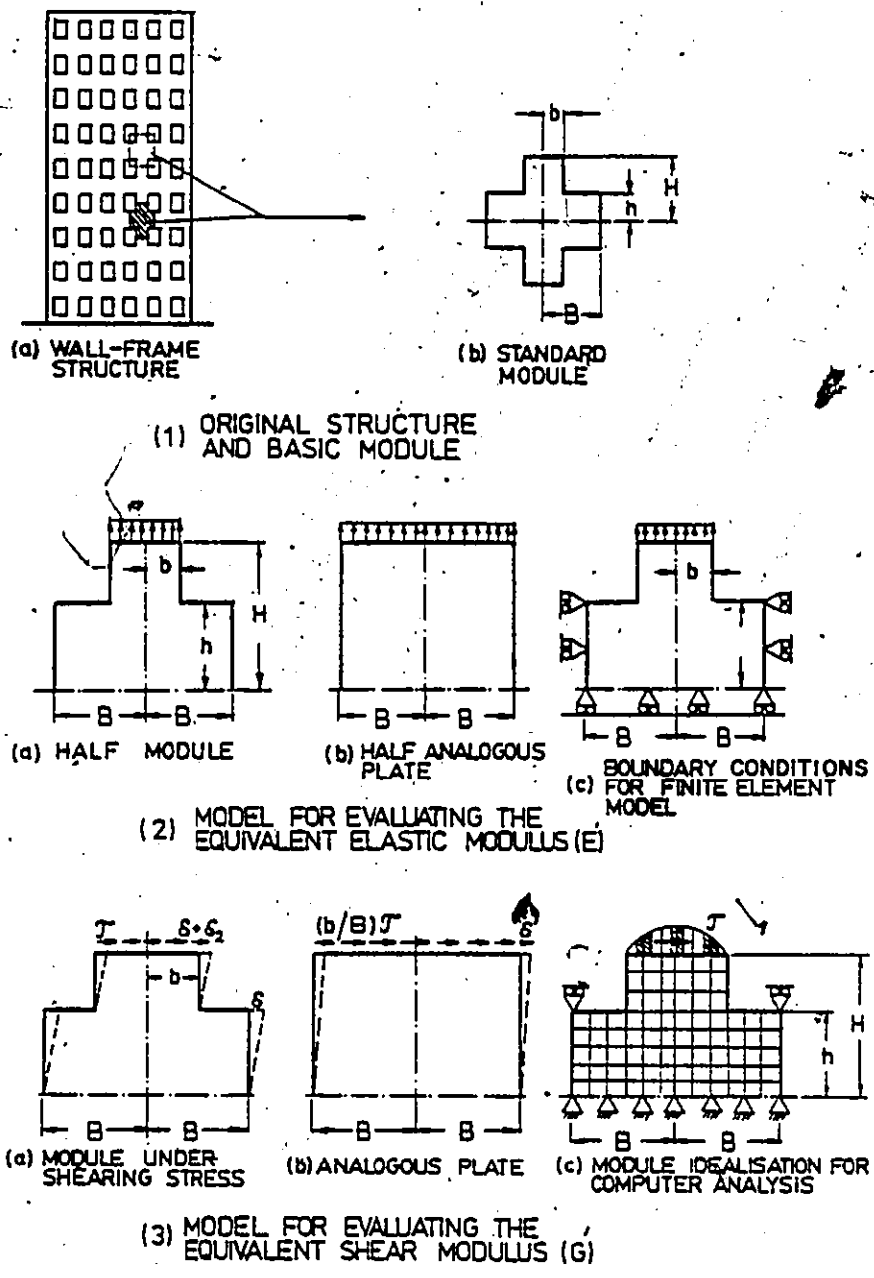
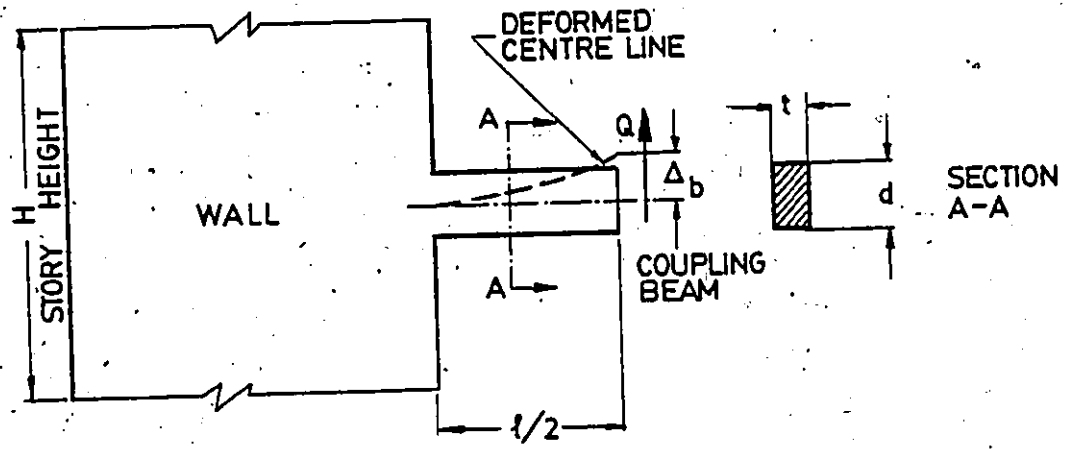
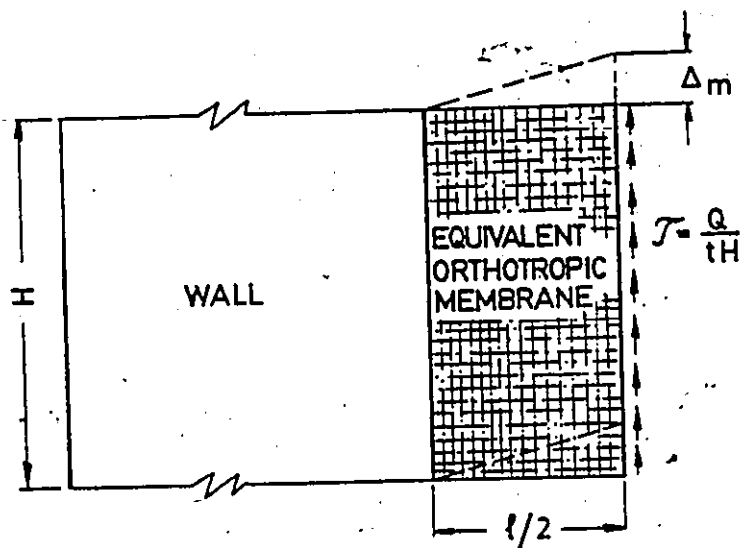


FIG. 2.5 MODELLING OF WALL-FRAME STRUCTURE - KHAN AND STAFFORD-SMITH [61]



(a) ACTUAL STRUCTURE



(b) EQUIVALENT STRUCTURE

FIG. 2.6 PRESENT MODELLING OF COUPLING BEAMS

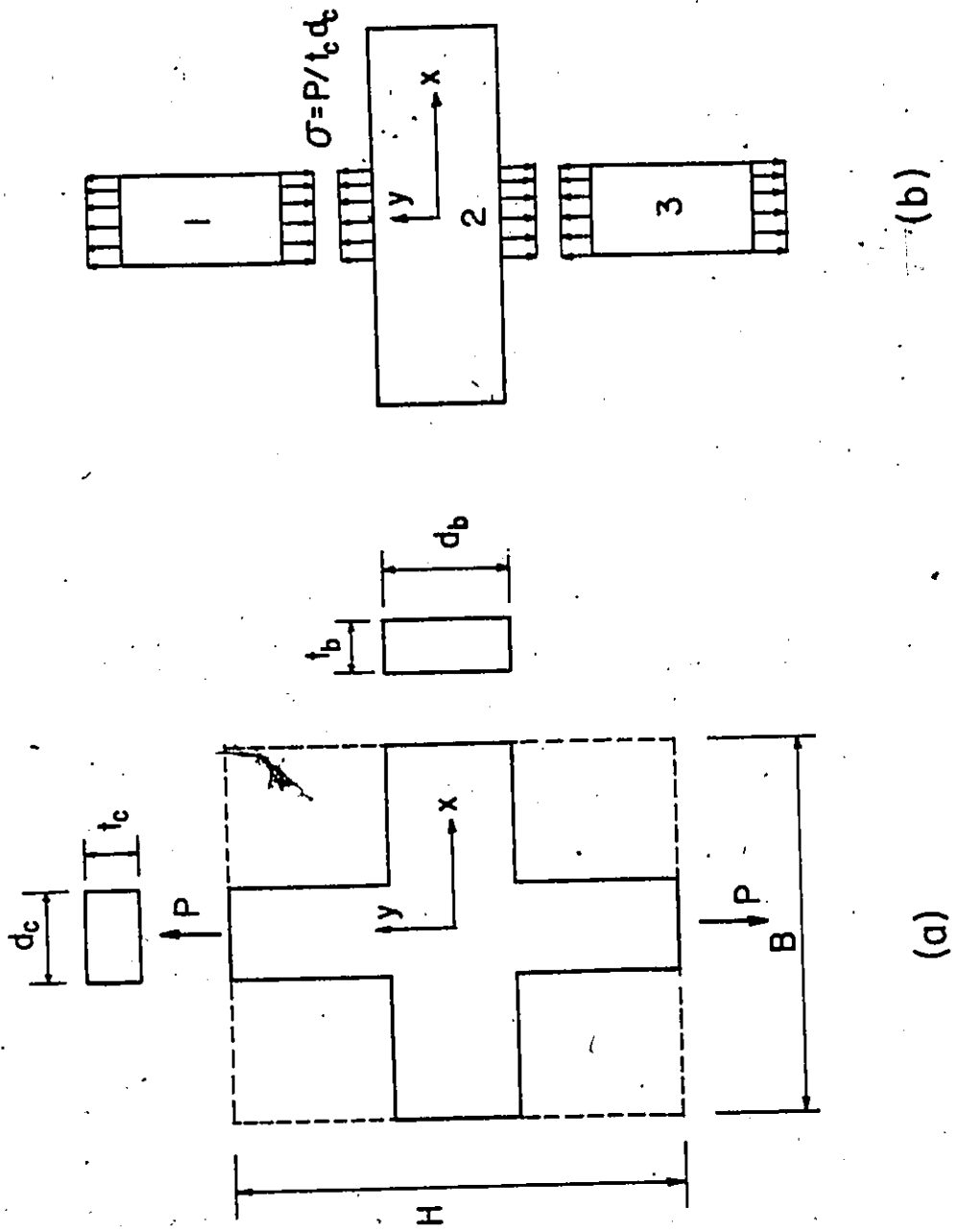


FIG. 2.7 MODEL FOR EVALUATING THE ELASTIC MODULUS E_y

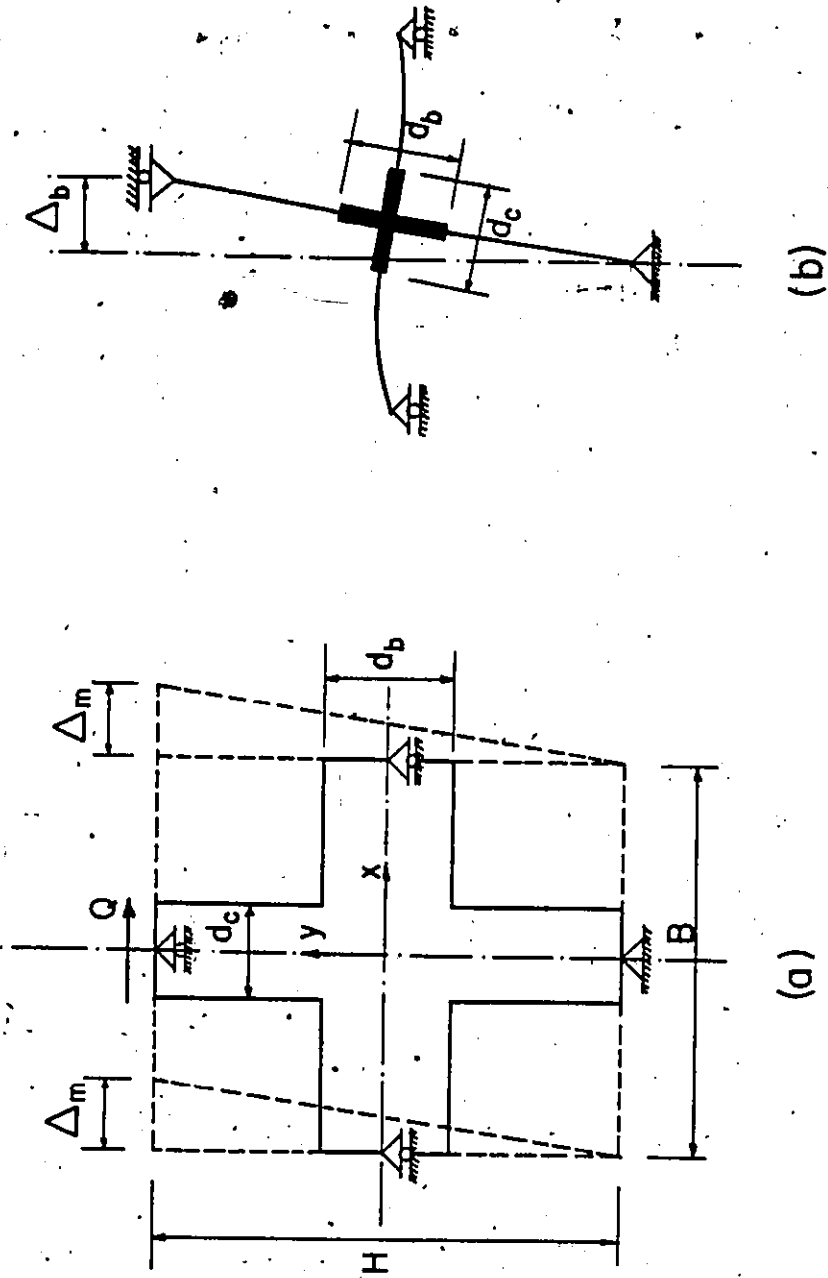


FIG. 2.8. MODEL FOR EVALUATING THE SHEAR MODULUS G_{xy}

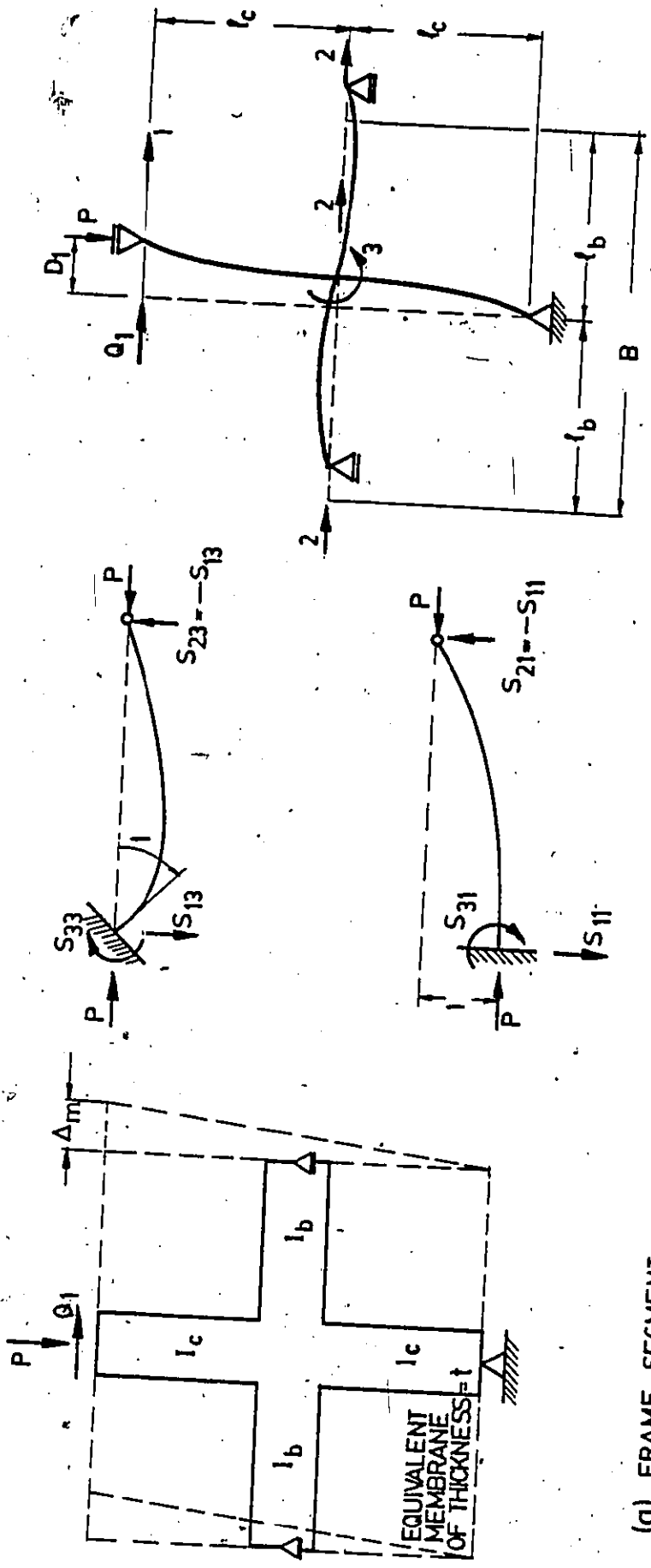


FIG. 2.9 MODELLING OF SECOND ORDER EFFECTS

CHAPTER III

BEHAVIORAL CHARACTERISTICS OF PERFORATED
WALLS

7

CHAPTER III
BEHAVIORAL CHARACTERISTICS OF PERFORATED
WALLS

3.1 INTRODUCTION

Since the work in this thesis is mainly confined to the analysis of planar perforated walls and their three-dimensional tubular assembly in tall building structures, this chapter is mostly dedicated to the establishment of the behavioral characteristics of planar perforated walls and the direct determination of the parameters which control their behavior. This, as will be shown later, provides a good required background for the efficient implementation of the equivalent orthotropic macroelement method (developed in the next three chapters) which depends crucially on the Engineer's perception of the behavior of the structure.

Perforated walls (Fig. 3.1(a)), also known as wall-frame structures [61] encompass, at one extreme, slender multi-storey, multi-bay frames and at the other, solid cantilever walls. Numerous techniques are available for the analysis of structures at either end of the spectrum, however structures in the intermediate range have received considerably less attention. It has been shown [61] that the analysis of these structures is complicated by their combining the characteristic behavior of both frames and walls.

While the exact analysis of this highly redundant structure in the intermediate range is practically impossible, the finite element method (FEM) is capable of providing a solution with as much accuracy as required. However, its use is not economically feasible, especially for preliminary design. Modelling of such structures, on the other hand, as plane frames with rigid arms simulating the finite size joints has proven to be excessively stiff [61].

Khan and Stafford-Smith [61] recently presented a simplified method for the analysis of these structures. It is based on replacing the actual structure by an equivalent isotropic solid wall, which is then analysed by the Engineering Beam theory. Internal forces in the actual structure are calculated using specially-defined stress concentration factors. But, as has been mentioned, the method is only suitable for structures with height/width ratio greater than two and is limited to structures with relatively small window openings in which both the ratios beam depth/storey height and column depth/bay width have to be greater than 0.25.

In this chapter, a simple hand-method for the analysis of planar perforated walls (wall-frame structures) under the action of in-plane lateral loads is presented. The perforated wall is modelled by an elastically equivalent orthotropic membrane (Fig. 3.1(b)) having the elastic properties defined in the previous chapter. The equivalent structure is then analysed by using the principle of minimum total

complementary potential energy. Internal forces in the actual structure are obtained by direct integration of the corresponding stress components in the equivalent structure. The present method is capable of analysing uniform wall-frame structures without any direct limitations on the sizes of window openings and the height/width ratio of the structure. i.e., it can be applied for the analysis of planar slender multi-storey multi-bay frames and solid walls with any height/width ratio, subjected to the limitations outlined at the end of this chapter.

Closed-form solutions and design charts are also developed which enable (i) the identification of the characteristic parameters controlling the behavior of planar perforated walls under the action of lateral loads, and (ii) the evaluation of the effect of these parameters on the response (deflection mode type, and distribution of member internal forces) of the structure.

3.2 THEORETICAL ANALYSIS

The wall-frame structure is first replaced by an equivalent orthotropic membrane with the elastic properties E_x , E_y , and G_{xy} (Fig. 3.1(b)) based on the expressions developed earlier in the previous chapter. In the subsequent analysis, the elastic modulus E_y is assigned an infinite value in correspondence with the acceptable [110] assumption of infinite in-plane rigidity of floors and consequently Poisson's ratios, μ_x and μ_y , are zero values as explained in the

previous chapter.

3.2.1 Energy Formulation

The principle of minimum total complementary potential energy [43] is represented by the equation

$$\delta(u^* + \Sigma R d) = 0 \quad (3.1)$$

in which

u^* = complementary strain energy

$\Sigma R d$ = work done by the reactions

For the cantilever structure shown in Fig. 3.1(b),

$$\Sigma R d = 0$$

Therefore, equation (3.1) becomes

$$\delta u^* = 0 \quad (3.2)$$

Although the complementary strain energy u^* is equal to the strain energy u for linearly elastic structures, the variation of the former should be with respect to the stresses.

The general expression for strain energy in the case of a plane problem is

$$U = \frac{1}{2} \iiint (\sigma_x \epsilon_x + \sigma_y \epsilon_y + \tau_{xy} \gamma_{xy}) dx dy dz \quad (3.3)$$

For orthotropic material, Hooke's Law is:

$$\left. \begin{aligned} \epsilon_x &= \frac{\sigma_x}{E_x} - \mu_y \frac{\sigma_y}{E_y} \\ \epsilon_y &= \frac{\sigma_y}{E_y} - \mu_x \frac{\sigma_x}{E_x} \\ \gamma_{xy} &= \frac{\tau_{xy}}{G_{xy}} \end{aligned} \right\} \quad (3.4)$$

Substituting Equation (3.4) into the strain energy expression, yields:

$$U = \frac{1}{2} \iiint \left[\frac{\sigma_x^2}{E_x} + \frac{\sigma_y^2}{E_y} - \left(\frac{\mu_x}{E_x} + \frac{\mu_y}{E_y} \right) \sigma_x \sigma_y + \frac{\tau_{xy}^2}{G_{xy}} \right] dx dy dz \quad (3.5)$$

For a plane stress state, the stresses are independent of z , therefore, Eq. (3.5) can be rewritten as:

$$U = \frac{t}{2} \iint \left[\frac{\sigma_x^2}{E_x} + \frac{\sigma_y^2}{E_y} - \left(\frac{\mu_x}{E_x} + \frac{\mu_y}{E_y} \right) \sigma_x \sigma_y + \frac{\tau_{xy}^2}{G_{xy}} \right] dx dy \quad (3.6)$$

3.2.2 Equilibrium Conditions

The equivalent orthotropic membrane (Fig. 3.1(b)), under the action of planar lateral loads is in plane stress state. Stress components $(\sigma_x, \sigma_y, \tau_{xy})$ in this case should satisfy

the following equilibrium conditions (neglecting body forces):

$$\frac{\partial \sigma_x}{\partial x} + \frac{\partial \tau_{xy}}{\partial y} = 0 \quad (3.7)$$

$$\frac{\partial \sigma_y}{\partial y} + \frac{\partial \tau_{xy}}{\partial x} = 0 \quad (3.8)$$

3.2.3 Stress Components

Because of the flexibility of the beams the axial forces tend to be higher in columns near the ends and lower in those in the middle region when compared to the simple linear variation (Fig.3.2). This phenomenon is termed "shear-lag" [12, 32, 34, 59, 67, 68].

Considering the above phenomenon and the anti-symmetrical distribution of the normal stress in the x-direction, one may assume σ_x in the form:

$$\sigma_x = F_1 \frac{M Y}{I} + F \left(\frac{Y}{d}\right)^3 \quad (3.9)$$

in which I is the moment of inertia of the equivalent membrane ($I = \frac{2td^3}{3}$); t and d are the thickness and one-half the depth of the membrane, respectively (Fig.3.1(b)); and F_1 and F are functions of the x-coordinate only, expressing the effect of the shear lag.

The normal stress σ_x has to satisfy, at any section of

constant x , the following condition of the overall moment equilibrium:

$$2t \int_0^d \sigma_x y dy = M \quad (3.10)$$

in which

M = overturning moment due to the external forces

Substituting (3.9) into (3.10), yields:

$$F_1 = 1 - \frac{F}{M} \frac{2t d^2}{5} \quad (3.11)$$

By substituting Eq. (3.11) into Eq. (3.9), σ_x can be expressed as

$$\sigma_x = \frac{My}{I} - \frac{3}{5} \left(\frac{y}{d}\right) F + \left(\frac{y}{d}\right)^3 F \quad (3.12)$$

The shear stress τ_{xy} may be obtained by integrating Eq. (3.7) and applying the boundary conditions

$$\tau_{xy} = 0 \text{ at } y = \pm d \quad (3.13)$$

The expression is

$$\begin{aligned} \tau_{xy} = & \frac{M' d^2}{2I} \left[1 - \left(\frac{y}{d}\right)^2 \right] + dF' \left[0.3 \left(\frac{y}{d}\right)^2 - \right. \\ & \left. - 0.25 \left(\frac{y}{d}\right)^4 - 0.05 \right] \quad (3.14) \end{aligned}$$

in which the prime denotes the first derivative with respect to x .

Similarly, by substituting (3.14) into (3.8), and considering the following boundary conditions

$$(\sigma_y)_{y=d} = -\frac{M''}{t} \quad (3.15)$$

$$(\sigma_y)_{y=-d} = 0 \quad (3.16)$$

in which the double prime denotes the second derivative with respect to x , the normal stress σ_y can be evaluated:

$$\sigma_y = \frac{M'' d^2}{2I} \left[\frac{1}{3} \left(\frac{y}{d}\right)^3 - \left(\frac{y}{d}\right) - \frac{2}{3} \right] + d^2 F'' \left[0.05 \left(\frac{y}{d}\right)^5 - 0.1 \left(\frac{y}{d}\right)^3 + 0.05 \left(\frac{y}{d}\right) \right] \quad (3.17)$$

3.2.4 Governing Differential Equation and Its Solution

Upon substituting Equations (3.12), (3.14), (3.17) and (3.6) into the strain energy expression, Eq. (3.2), and by means of calculus of variation [71], the following governing Euler-Lagrange equation is obtained.

$$F'' - \alpha^2 F = \beta M'' \quad (3.18)$$

in which

$$\alpha^2 = \frac{22.6336}{d^2} \left| \frac{G_{xy}}{E_x} \right| \quad (3.19)$$

$$\beta = 3.7787 \frac{d}{I} \quad (3.20)$$

The resulting natural boundary conditions are

$$\text{at } x = 0; \quad F = 0 \quad (3.21)$$

$$\text{at } x = l; \quad F' = \beta M' \quad (3.22)$$

The solution of Equation (3.18), subject to the boundary conditions of Equations (3.21) and (3.22), for the case of uniformly distributed lateral load (w) is:

$$F = \frac{\beta w}{\alpha^2} \left[\left(\frac{\alpha l}{\cosh \alpha l} - \tanh \alpha l \right) \sinh \alpha x + \cosh \alpha x - 1 \right] \quad (3.23)$$

and its first derivative with respect to x is:

$$F' = \frac{\beta w}{\alpha} \left[\left(\frac{\alpha l}{\cosh \alpha l} - \tanh \alpha l \right) \cosh \alpha x + \sinh \alpha x \right] \quad (3.24)$$

Similar solutions can be obtained for other loading configurations by considering the corresponding values of M'' and M' in the solution.

3.2.5 Internal Forces in the Actual Structure

Column axial forces and shear forces in beams and columns are evaluated first at their mid-length points by

integrating the corresponding stress component over a bay width B or a storey height H for columns or beams respectively, as follows:

$$P_{ij} = t \int_{y_j - B/2}^{y_j + B/2} (\sigma_x)_{x=x_i} dy \quad (3.25)$$

$$V_{cij} = t \int_{y_j - B/2}^{y_j + B/2} (\tau_{xy})_{x=x_i} dy \quad (3.26)$$

$$V_{bij} = t \int_{x_i - H/2}^{x_i + H/2} (\tau_{xy})_{y=y_j} dx \quad (3.27)$$

in which

P_{ij} and V_{cij} = the axial and shear forces respectively in the ij column

V_{bij} = the shear force in the ij beam

and

x_i and y_j = the coordinates of the appropriate mid-length point, as shown in Fig. 3.3.

By assuming a linear variation of the stress components σ_x and τ_{xy} within the limits of these integrations with an average value at the location of the appropriate mid-length points, Eqs. (3.25 to 3.27) can further be simpli-

fied to:

$$P_{ij} = t.B. (\sigma_x)_{x=x_i, y=y_j} \quad (3.28)$$

$$V_{cij} = t.B (\tau_{xy})_{x=x_i, y=y_j} \quad (3.29)$$

$$V_{bij} = t.H (\tau_{xy})_{x=x_{ib}, y=y_{jb}} \quad (3.30)$$

Bending moments in any section at a distance s from these mid-points along the length of the beam or the column are directly obtained by multiplying the appropriate shear force, V_{bij} or V_{cij} respectively, by the distance s .

3.2.6 Lateral Deflection

Since the condition of elastic equivalence is that both the perforated wall and the equivalent orthotropic membrane should have the same rigidities, the lateral deflection of the actual structure is equal to that of the equivalent structure. By using the method of virtual work, the following expression is obtained for the lateral deflection due to a uniformly distributed load, w , along the height:

$$\delta = \frac{wl^4}{8 E_x I_x} \left[1 - \frac{4}{3}\xi + \frac{1}{3}\xi^4 \right] + \frac{1.2 wl^2}{2 G_{xy} A} [1 - \xi^2] \quad (3.31)$$

in which

A = cross-sectional area of the equivalent cantilever (2td), and ξ is a nondimensional parameter = x/l (Fig.3.2).

The maximum deflection is at the top ($\xi = 0$);

$$\delta_{\max} = \frac{wl^4}{8 E_x I} + \frac{1.2 wl^2}{2 G_{xy} A} \quad (3.32)$$

3.3 DESIGN CURVES

By introducing the following two characteristic nondimensional parameters:

(1) The aspect ratio, $R = L/D$.

(2) The shear lag parameter, $SL = G_{xy}/E_x$

and using the nondimensional coordinates $\xi = x/l$ and $\eta = y/d$, the functions $(\frac{t}{w})F$ and $(\frac{t}{w})dF'$ can be expressed in nondimensional form, as follows:

$$\left(\frac{t}{w}\right)F = 0.25 (C \sinh \alpha l \xi + \cosh \alpha l \xi - 1.0) / SL \quad (3.33)$$

$$\left(\frac{t}{w}\right)dF' = 1.1914 (C \cosh \alpha l \xi + \sinh \alpha l \xi) / \sqrt{SL} \quad (3.34)$$

in which

$$C = (\alpha l / \cosh \alpha l) - \tanh \alpha l$$

$$\alpha l = 9.515 \sqrt{SL} R$$

The curves for the rapid evaluation of the two functions are shown in Figs. 3.4(a) to 3.4(e).

The stress components σ_x and τ_{xy} can also be expressed as

$$\sigma_x = \frac{W}{t} \left[\frac{3}{4} C_1 \left(\frac{x}{d} \right)^2 + C_2 \left(\frac{t}{W} \right) F \right] \quad (3.35)$$

$$\tau_{xy} = \frac{W}{t} \left[\frac{3}{4} C_3 \left(\frac{x}{d} \right) + C_4 \left(\frac{t}{W} \right) dF' \right] \quad (3.36)$$

in which C_1 to C_4 are functions of the coordinate y :

$$C_1 = \eta$$

$$C_2 = \eta^3 - 0.6\eta$$

$$C_3 = 1 - \eta^2$$

$$C_4 = 0.3\eta^2 - 0.25\eta^4 - 0.05; \quad \eta = \frac{y}{d}$$

Curves for the evaluation of these functions are shown in Fig. 3.5.

To determine the axial force in columns and the shear forces in beams and columns, the functions C_1 to C_4 should be evaluated at the locations of the mid-length points as mentioned previously.

3.4 CONTROLLING PARAMETERS

To identify the parameters controlling the behavior of slender planar frames, De Clercq [34] carried out a series of exact analyses of a ten-storey, twelve (and eight) bay hypothetical frame. The bending stiffness of the beams and columns, as well as the axial stiffness of the columns were varied. It was concluded in this study that:

- (i) the most important factor is the shear lag parameter which is defined as the ratio of the joint rotational stiffness to the column axial stiffness;
- (ii) the number of bays insignificantly affect the behavior of the structure;
- (iii) the reduction stiffness factor, introduced by Khan and Amin [67] for the purpose of reducing any framed tube structure to a 10-storey equivalent one, is generally valid at least for the planar frames which were investigated.

The above findings by De Clercq [34] will further be discussed in this section.

The closed form solutions presented in this chapter enable the direct determination of the characteristic parameters which control the response of planar perforated walls to lateral loads. It can be seen from the previous formulation (Eqs. 3.31 and 3.33 to 3.36 and Figs. 3.4(a) to 3.4(e)), that the shear lag and the aspect ratios are the main parameters influencing the distribution of both the deflection and stresses. The shear lag parameter reflects the importance of the bending and shear stiffnesses of

beams and columns with respect to the axial stiffness of columns. It also reflects the effect of finite size joints, as indicated by Eqs. (2.12) and (2.24). Thus, it is clear that the shear lag parameter presently defined is, in fact, a refined version of De Clercq's [34].

Introducing the aspect ratio R and the shear lag parameter SL of Section 3.3 into Eq. (3.31), yields:

$$\delta = \frac{3}{2} \frac{wl}{tG_{xy}} [R^3 SL(1 - \frac{4}{3}\xi + \frac{1}{3}\xi^4) + 0.4R(1 - \xi^2)] \quad (3.37)$$

Equations (3.31) and (3.37) show that the lateral deflection is composed of two components. On the one hand, it consists of a cantilever bending mode as represented by the first term of Eq. (3.37), and, on the other hand, the usual shear mode of frames which primarily depends on the aspect ratio and the rotational stiffness of the joints (represented by G_{xy}).

The bending mode of deformation increases with the increase in the aspect ratio and the decrease in the column axial stiffness. The appearance of R^3 in the first term of Eq. (3.37) emphasizes the importance of considering the axial deformation of the columns in tall building analysis [12, 34, 59, 67, 83, 90, 117, 121]. The shear mode is directly proportional to the aspect ratio and inversely proportional to the rotational stiffness of joints (represented by G_{xy}). This discussion clearly shows that in contradiction

to what is found by De Clercq [34], the aspect ratio R has a significant effect on the shear mode of deformation as well as the bending mode.

With regard to the distribution of member internal forces, the shear lag parameter and the aspect ratio also play dominant roles. This can readily be seen from Eqs. (3.12) and (3.14) which express the stress variation in terms of the functions F and F' (Eqs. (3.33) and (3.34), and Figs. (3.4(a) to (3.4(e))). The most interesting distribution is that of the column axial forces. From Figs. (3.4(a) to (3.4(e)) it can be seen that a decrease in the shear lag parameter would increase the shear lag function F , which, in turn, increases the nonlinearity of the axial force distribution (Eq. 3.12). A similar effect on the axial force distribution is due to the increase in the aspect ratio R .

3.5 NUMERICAL EXAMPLE

In order to demonstrate the use of the present method, and to illustrate its accuracy, the 20-storey concrete shear wall-frame structure analysed by Khan and Stafford-Smith [61] is considered herein. The structure has the dimensions shown in Fig. 3.6.

3.5.1 Structure Properties

Storey height, $H = 12'$ (3.66 m)

Bay width, $B = 10'$ (3.05 m)

Structure height, $L = 240'$ (73.15 m)

Structure width, $D = 2d = 60'$ (18.29 m)

Clear column height, $h = 7.2'$ (2.19 m)

Clear beam span $b = 6.0'$ (1.83 m)

Depth of beam, $d_b = 4.8'$ (1.46 m)

Depth of column, $d_c = 4.0'$ (1.22 m)

Lateral load intensity, $w = 1$ k/ft (14.593 KN/m)

Young's modulus, $E = 4.32 \times 10^5$ ksf (3208.5 KN/m²)

Poisson's ratio, $\mu = 0.15$

3.5.2 Elastic Properties of the Equivalent Orthotropic Membrane

By using Eqs. (2.12), (2.13) and (2.24), (2.25), E_x and G_{xy} are evaluated respectively as

$$E_x = 2.01 \times 10^5 \text{ ksf}$$

$$G_{xy} = 0.273 \times 10^5 \text{ ksf}$$

3.5.3 Internal Forces in the Actual Structure

While the design curve developed in the previous section can be used for the rapid determination of the in-

ternal forces, the original equations will be directly used in the computation for better accuracy.

For the purpose of comparison with existing solutions [61], the member forces are evaluated at sections of $x = 210$, 216 , and 222 ft. The shear lag functions F and F' are determined at these locations, as shown in Table 3.1. Substituting the values of F and F' , both the normal and shear stresses at mid-height of the columns and the shear stresses at the mid-span of the beams are obtained (Tables 3.2, 3.3). The column axial and shear forces and the beam shear forces are then evaluated by integrating the corresponding normal and shear stresses according to Eqs. (3.28) to (3.30), as shown in Tables 3.2 and 3.3. and Fig. 3.7.

3.5.4 Lateral Deflection

The deflected shape and the maximum drift are obtained by using Eqs. (3.31) and (3.32), respectively. The deflected shape is shown in Fig. 3.8, with a maximum value of 113.58×10^{-3} ft.

3.5.5 Comparison of Results

The results obtained using the present method are compared to those obtained by the simplified and finite element methods of Khan and Stafford-Smith [61], as shown in Figs. 3.7 and 3.8, for member internal forces and the lateral deflection, respectively. There is a good agreement between the results of the present method and those of

the detailed finite element analysis which employs 1920 finite elements. This agreement is generally better than that of the simplified method of Khan and Stafford-Smith [61].

3.6 OTHER APPLICATIONS

The present method was also used for analyzing the two extremes of perforated wall structures, (i.e., the solid shear walls and the slender multi-storey multi-bay frames) and the results were in reasonably good agreement with those obtained by detailed computer analyses.

The short solid cantilever wall (Fig. 3.9(a)) was analyzed according to the method described in this Chapter. The normal stresses at Section A-A near the base are plotted in Fig. 3.9(b) which also shows those obtained by finite element analysis employing eighty (10 x 8 in the horizontal and vertical directions, respectively) equal rectangular ordinary plain stress elements.

The present method was also used to analyze the 10-storey slender frame of De Clercq [34] and the column axial forces at the base of the frame are obtained and compared to DeClercq's [34], as shown in Fig. 3.10(b).

3.7 LIMITATIONS

In addition to the apparent limitations of the con-

stant member properties and lateral loads inherent in the present analysis, the solutions are further based on the assumed cubic variation of the normal stress, σ_x (Eq. 3.12) which will be inadequate for representing sharp variation in σ_x distribution caused by high shear lag effect. To quantify the last limitation, consider the assumed expression of σ_x in Eq. (3.12) which can be rewritten in the form:

$$\sigma_x = \eta \{ (1.5M/td^2) + F(\eta^2 - 0.6) \} \quad (3.38)$$

in which

$$\eta = y/d$$

The first term of the expression represents the usual linear distribution of the engineering beam theory and the second term accounts for the shear lag effect. Since the column axial forces which are directly represented by the normal stress σ_x (Eq. (3.28)) should not change signs as the ratio η varies from 0.0 to 1.0 or 0.0 to -1.0, the bracketed term of Eq. (3.38) must be positive (assuming $M > 0$). The minimum value of this term is at $\eta = 0$; and thus the condition is

$$F \leq 2.5(M/td^2) \quad (3.39)$$

Since the shear lag function F is maximum at $x = l$, the condition of Eq. (3.39) can further be expressed by substituting the appropriate values of F and M at $x = l$ as

$$\frac{\omega}{t} \frac{0.25}{SL} \left[\left(\frac{\alpha l}{\cosh \alpha l} - \tan \alpha l \right) \sinh \alpha l + \cosh \alpha l - 1 \right] \leq 1.25 \frac{\omega}{t} (l/d)^2 \quad (3.40)$$

By rearranging the terms, the condition becomes

$$\alpha l \tanh \alpha l \leq K \quad (3.41)$$

in which

$$K = 1 + 20 SL R^2$$

Since αl is generally greater than 3 for most tall structures, $\tanh \alpha l$ can be taken as 1:

$$\alpha l \leq K \quad (3.42)$$

Substituting the appropriate values of αl and K into condition (3.42) yields the following relation:

$$20Z^2 - 9.515 Z + 1 \geq 0 \quad (3.43)$$

in which

$$Z = (SL R^2)^{\frac{1}{2}}$$

which finally yields:

$$SL R^2 \geq 0.10 \quad (3.44)$$

Because the shear lag effect increases with smaller values of SL, the above condition limits the applicability of the simplified approach to cases where the shear lag phenomenon is not too severe. Example structures for which the above limitations are violated will be considered in the subsequent chapters, where a more general method of analysis is presented.

3.8 DISCUSSIONS ON KHAN'S FRAME REDUCTION TECHNIQUE

It can be noticed from Eq. (3.44) that in order that a structure m exhibits the same amount of shear lag as a structure n, the following relation must be satisfied

$$SL_m R_m^2 = SL_n R_n^2 \quad (3.45)$$

or

$$SL_m = SL_n \left(\frac{R_n}{R_m} \right)^2 \quad (3.46)$$

If the two structures have the same overall width and identical storey height, Eq. (3.46) reduces to

$$SL_m = SL_n \left(\frac{N_n}{N_m} \right)^2 \quad (3.47)$$

which indicates that any structure n of N_n stories, can be reduced to an equivalent one of N_m stories ($N_m < N_n$) having the same width by modifying the member stiffnesses

such that Eq. (3.47) is satisfied. The last equation represents a technique which was introduced but not proven by Khan and Amin [67] for reducing an actual framed tube of any number of stories to an equivalent 10-storey one. This technique enables the use of Khan's and Amin's influence curves for the analysis of framed tube structures.

DeClercq [34] later tested the postulate by comparing the lateral deflection and axial forces in columns at the base of a 20-storey, 12-bay frame and its equivalent 10-storey, 12-bay one, and thus showed the validity of the simple reduction technique. Based on the closed-form solutions presented in this chapter, a more solid basis for this hypothesis can be established.

In order to have complete equivalence between the actual and reduced structures, the lateral deflection and member internal forces at any corresponding section, say ξ ($\xi = X/\ell$) from the top of the two structures, must be identical when the section is subjected to the same overturning moment and lateral shear.

Let ℓ and ℓ_r be the total heights of the actual and reduced, equivalent structures, respectively. At the section ξ , the overturning moment due to external forces is

$$M = \omega \frac{(\xi \ell)^2}{2} g(\xi) = \omega_r \frac{(\xi \ell_r)^2}{2} g(\xi) \quad (3.48)$$

in which

ω and ω_r = lateral load intensities at the top of the actual and reduced structures respectively,

and the function $g(\xi)$ represents the load distribution and is equal to 1 for uniform load, and to $\frac{1}{3}(2-\xi)$ for triangular load. From Eq. (3.48) it is obvious that the load to be applied on the reduced structure is

$$\omega_r = \omega \left(\frac{l}{l_r} \right)^2 \quad (3.49)$$

so that the same moment will be applied at the same section. Similarly, the equivalent load giving rise to the same total lateral shear force at the section is

$$\bar{\omega}_r = \omega \left(\frac{l}{l_r} \right) \quad (3.50)$$

It will be shown next that the condition expressed by Eq. (3.47) will produce in the reduced structure the same displacements and axial stresses when used in conjunction with the equivalent load ω_r , and will produce the correct shear when used with the equivalent load $\bar{\omega}_r$. It is interesting to note that both Khan and Amin [67] and DeClercq [34] seemed to ignore the equivalent load for shear. The following discussion will also make clear that in satisfying the condition of Eq. (3.47), only the axial

stiffness of the columns should be adjusted.

For simplicity, only the case of uniform load is considered. The deflection at Section ξ (using Eq. (3.37)) is given, as for the actual structure:

$$\delta_a = c_1 \omega l l [l^2 SL \phi(\xi) + 0.4\psi(\xi)] \quad (3.51)$$

in which

$$c_1 = \frac{2}{3Dt G_{xy}}$$

and ϕ and ψ are functions of ξ , and for the reduced structure

$$\delta_r = c_1 \omega \left(\frac{l}{l_r}\right)^2 l_r l_r [l_r^2 SL_r \phi(\xi) + 0.4\psi(\xi)] \quad (3.52)$$

Note that since the same constant c_1 is used in the above equation, the reduced structure should have the same shear modulus (i.e., the same bay width, storey height, and member bending and shear stiffnesses), thickness, and total width (or number of bays.)

Equating δ_a and δ_r gives

$$l^2 SL = l_r^2 SL_r \quad (3.53)$$

or

$$SL_r = \left(\frac{l}{l_r}\right)^2 SL \quad (3.54)$$

and since G_{xy} of both structures is the same, this condition can be satisfied by adjusting E_x (or column axial stiffnesses.)

To have identical column axial forces in the two structures, it is apparent from Eq. (3.12) that the function F (Eq. 3.33) must be identical in the two structures. To facilitate the subsequent analysis, F can be further expressed as, for the actual structure

$$F_a = c_2 \frac{\omega}{SL} [\phi(\alpha l) \psi(\alpha l \xi) + \theta(\alpha l \xi) - 1.0] \quad (3.55)$$

in which

$$c_2 = \frac{0.25}{t}$$

$$\alpha l = 9.515 l \sqrt{SL}$$

ϕ = function of αl

ψ and θ = functions of $\alpha l \xi$

and for the reduced structure

$$F_r = c_2 \omega \left(\frac{l}{l_r}\right)^2 \frac{1}{SL_r} [\phi(\alpha l)_r \psi(\alpha l \xi)_r + \theta(\alpha l \xi)_r - 1.0] \quad (3.56)$$

Thus to satisfy the equality of F_a and F_r the following two conditions must be satisfied

$$SL_r = \left(\frac{l}{l_r}\right)^2 SL \quad (3.57)$$

and

$$(\alpha l)_r = (\alpha l) \quad (3.58)$$

From the definition of αl , the second condition will be automatically satisfied if the basic condition (Eq. 3.57) is satisfied.

Finally, for equality of shear forces in beams and columns, it is apparent from Eq. (3.14) that the function F' must be identical for the two structures. By using the equivalent load for shear \bar{w}_r it can be shown that the resulting condition is the basic one, i.e., Eq. (3.57).

In summary, the only condition of equivalence is that of Eq. (3.57) which when used in conjunction with the equivalent load for moment \bar{w}_r will result in equal lateral deflection and column axial forces in both the reduced and actual structures, and when used in conjunction with the equivalent load for shear \bar{w}_r will produce identical shear forces in the beams and columns in the two structures.

TABLE 3.1
VALUES OF F AND F'

Height x, ft.	F Eq. (3.23)	F' Eq. (3.24)
210'	2.198	0.218
216'	-----	0.308
222'	5.767	0.427

TABLE 3.2
COLUMN INTERNAL FORCES*

Column No. **	$\frac{Y}{D}$	σ_x Eq. (3.12)	Axial Force ($P=2.198, P'=2.18$) Eq. (3.28)	τ_{xy} Eq. (3.14)	Shearing Force ($F=5.767, F'=4.27$) Eq. (3.29)	σ_x Eq. (3.12)	Axial Force ($P=5.767, P'=4.27$) Eq. (3.28)	τ_{xy} Eq. (3.14)	Shearing Force ($F=5.767, F'=4.27$) Eq. (3.29)
1	0.0	0.0	0.0	4.047	48.57	0.0	0.0	3.984	47.814
2	0.33	9.85	118.20	3.869	46.429	10.468	125.619	4.072	48.869
3	0.67	20.188	242.26	2.652	31.833	22.216	266.6	3.004	36.048
4	0.92	28.557	171.343	.866	5.197	32.641	195.85	1.066	6.397

* The units are ksf and kips for stresses and forces respectively.
(1 ksf = 7.427 KN/m², 1 kip = 4.448 KN)

** Starting from the centre line of the structure and increasing in the outward direction.

TABLE 3.3

BEAM INTERNAL FORCES* (x = 216')

Beam No. **	$\left(\frac{y}{d}\right)$	τ_{xy} Eq. (3.14)	Shearing Force Eq. (3.30)
1	0.167	3.988	57.43
2	0.50	3.375	49.847
3	0.833	1.724	24.828

* The units are ksf and kips for stresses and forces respectively. (1 ksf = 7.427 kN/m², 1 kip = 4.448 kN)

** Starting from the centre lines of the structure and increasing in the outward direction.

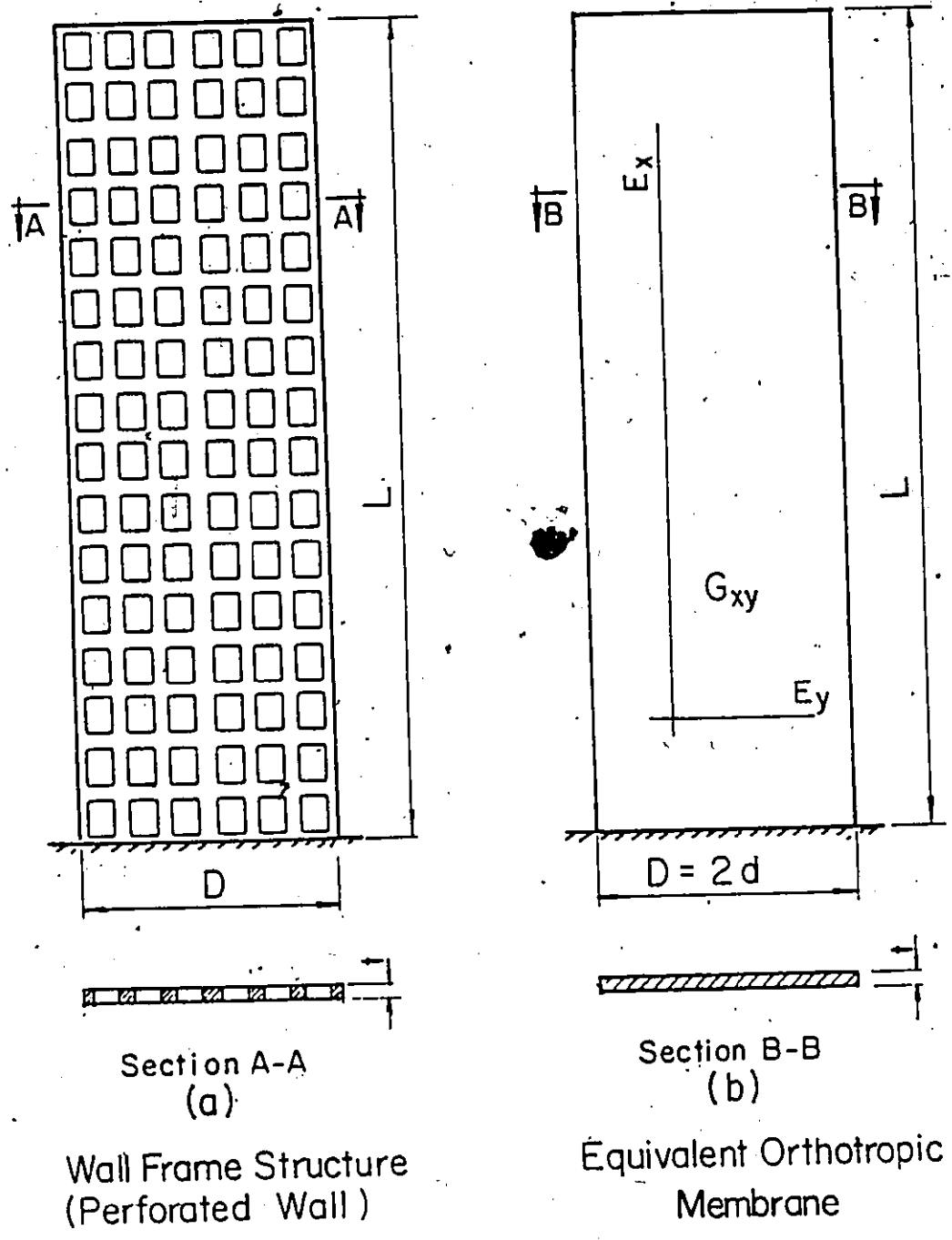


FIG. 3.1 | MODELLING OF WALL-FRAME STRUCTURES

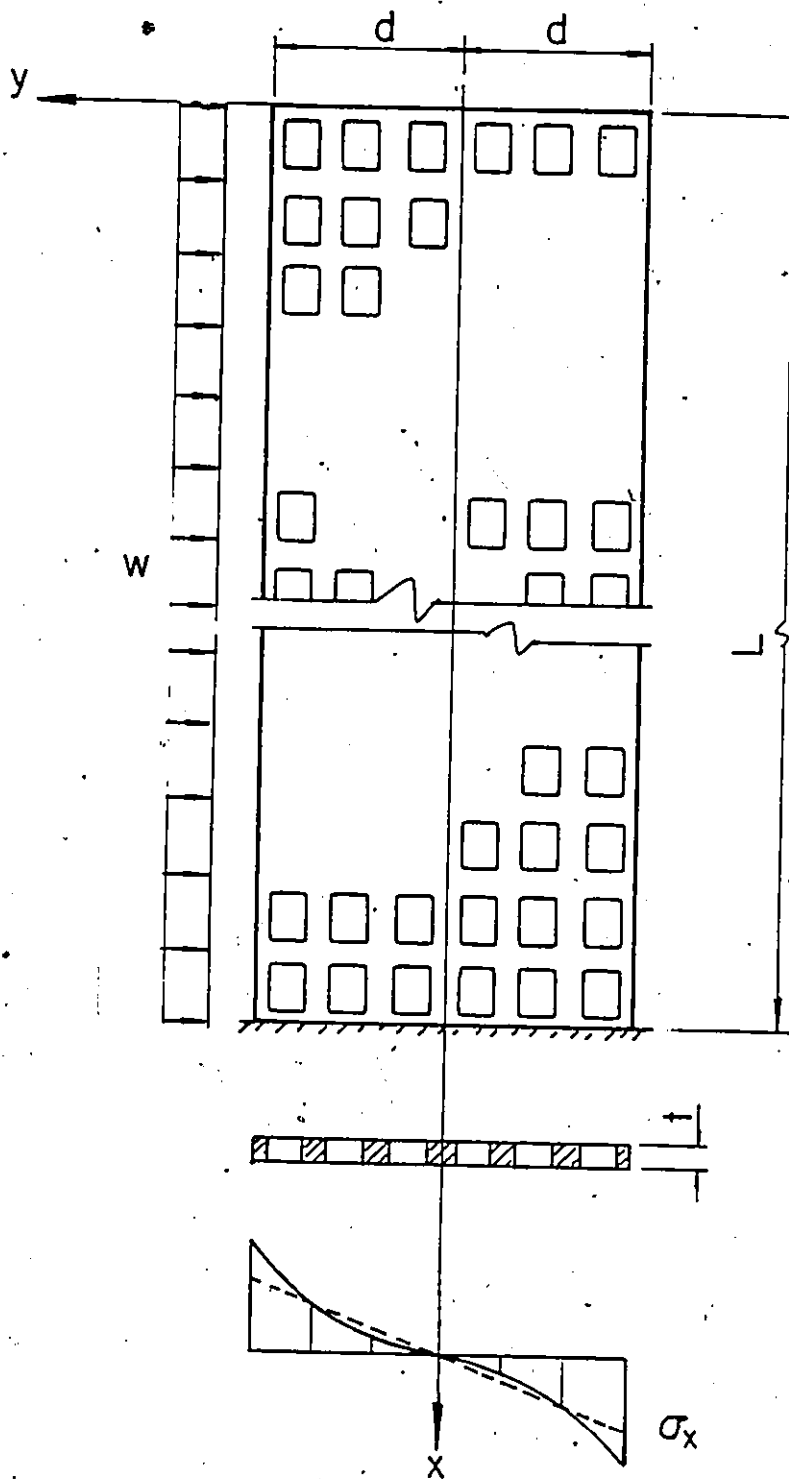


FIG. 3.2 SHEAR LAG EFFECT ON THE DISTRIBUTION OF THE NORMAL STRESS AT THE BASE

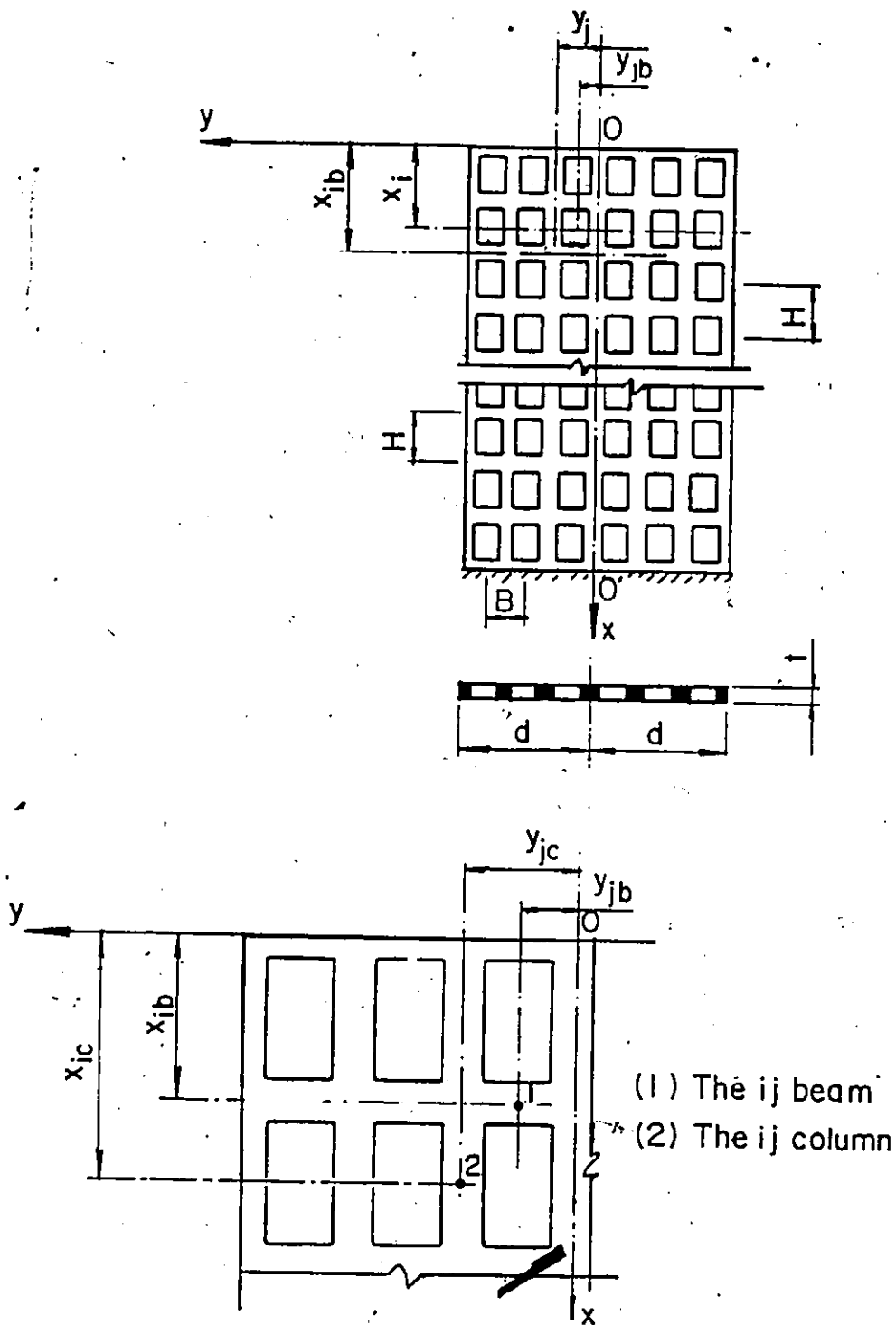
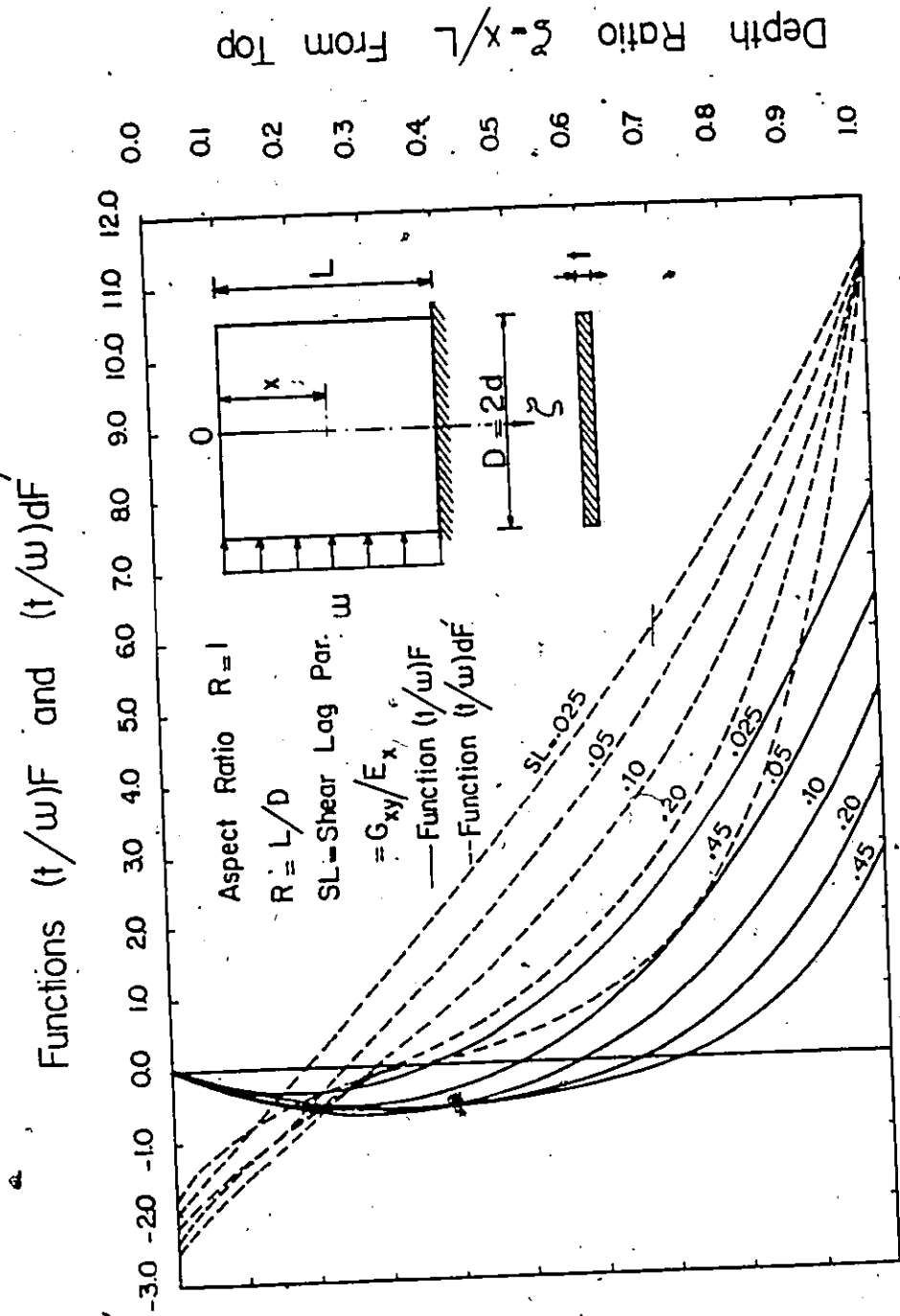


FIG. 3.3 DEFINITION OF SYMBOLS IN EQUATIONS (3.28) TO (3.30)



SHEAR LAG FUNCTIONS (R=1)

FIG. 3.4a

Functions $(t/w)F$ and $(t/w)dF'$

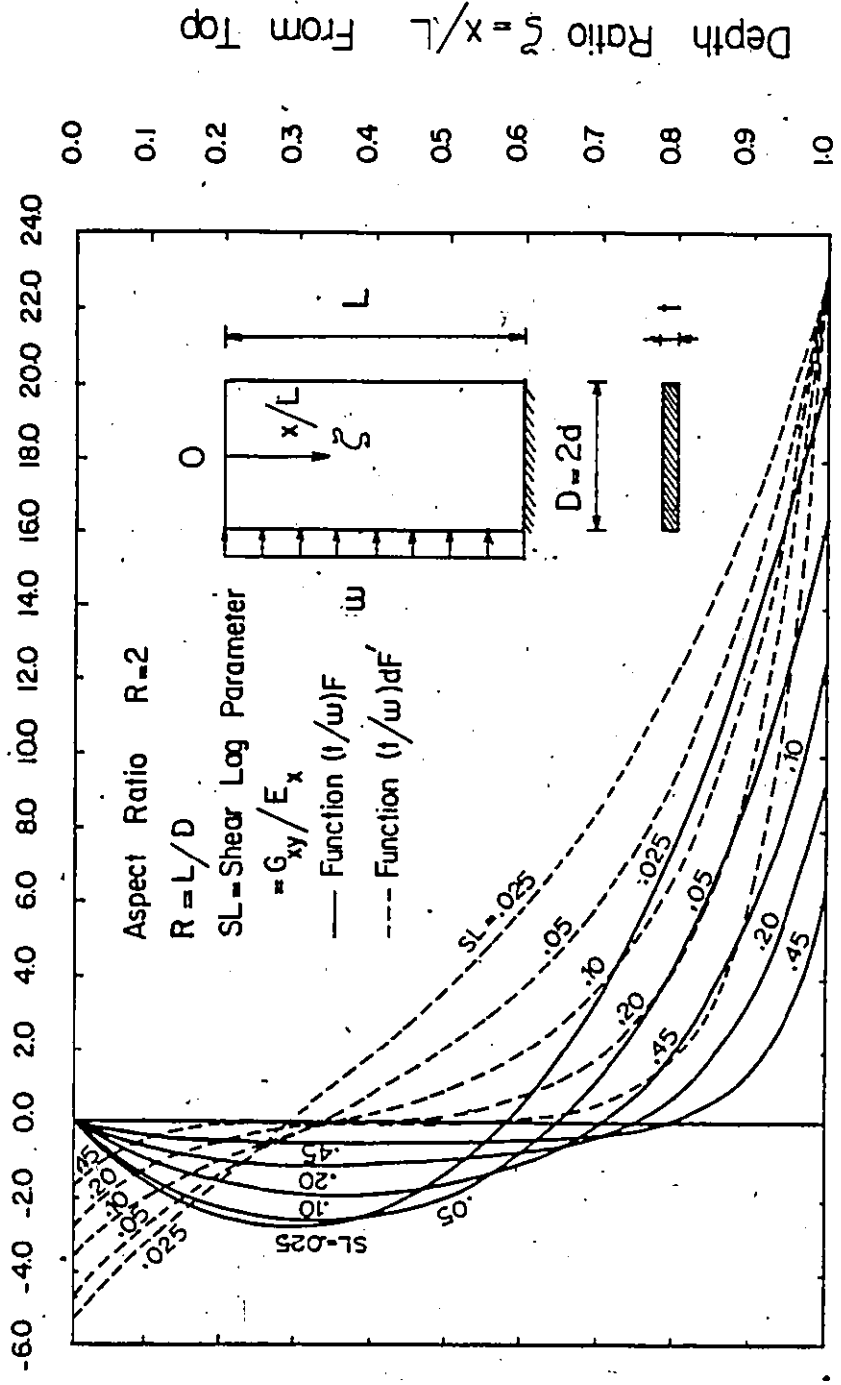


FIG. 3.4b SHEAR LAG FUNCTIONS (R=2)

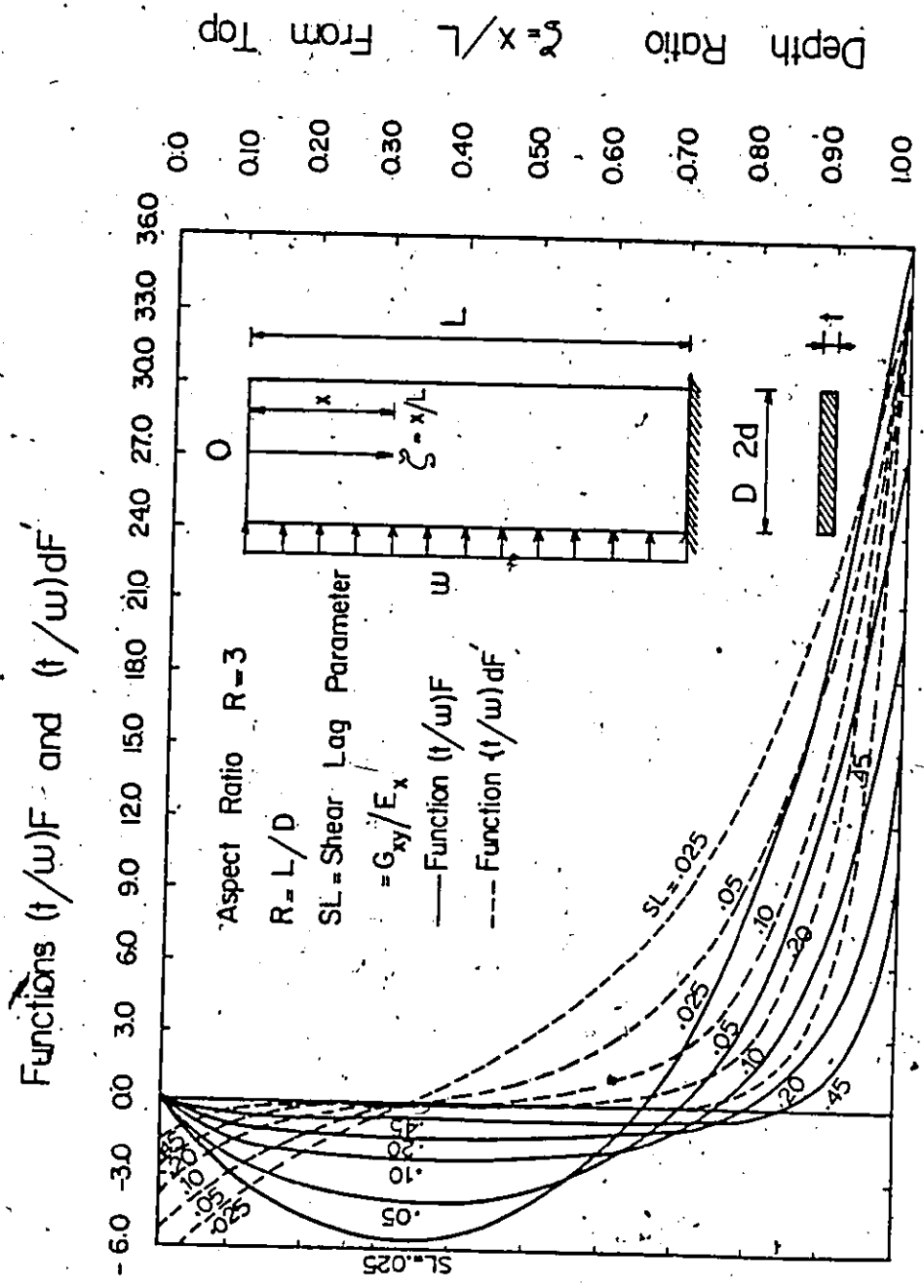


FIG. 3.4c SHEAR LAG FUNCTIONS (R=3)

Functions $(t/w)F$ and $(t/w)dF$

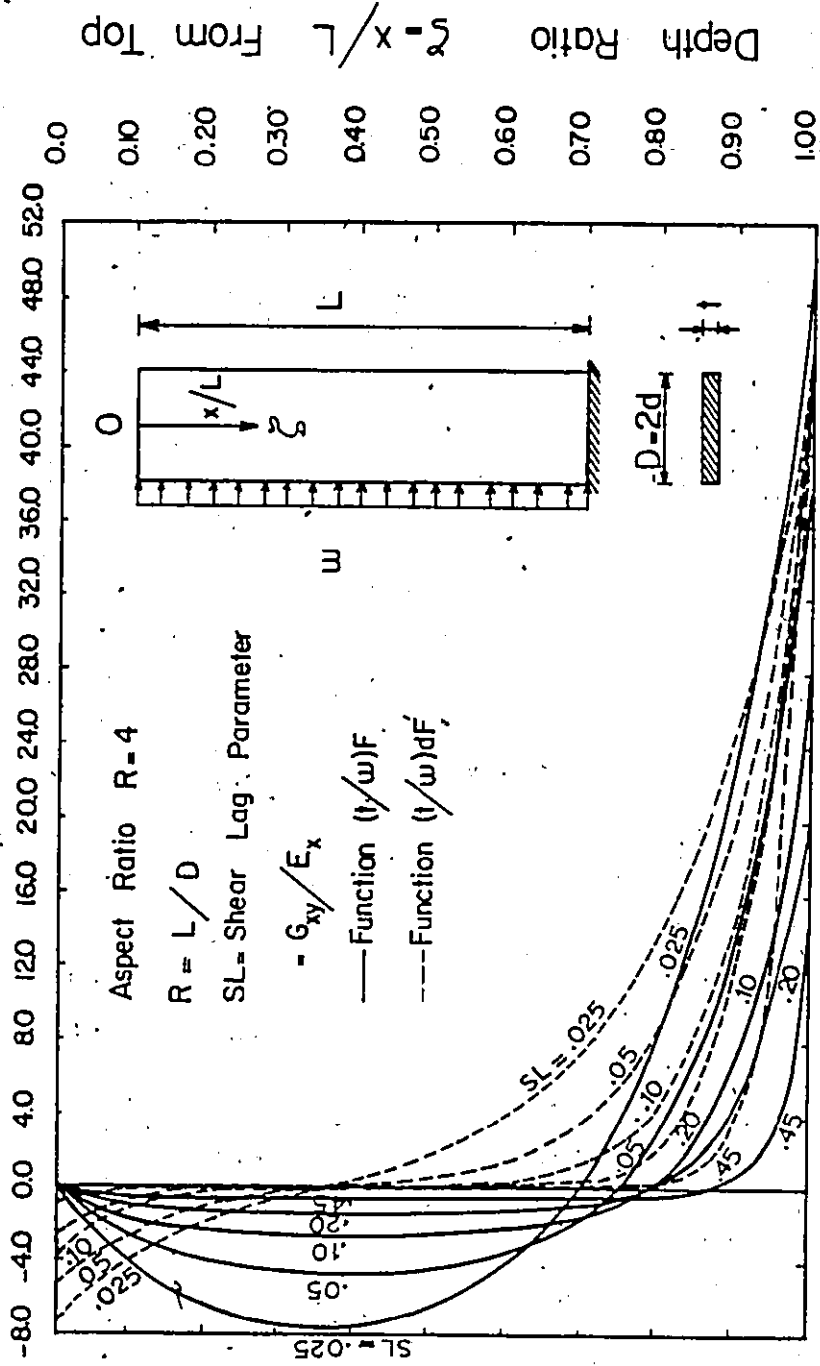


FIG. 3.4d SHEAR LAG FUNCTIONS (R=4)

Functions $(t/w)F$ and $(t/w)dF$

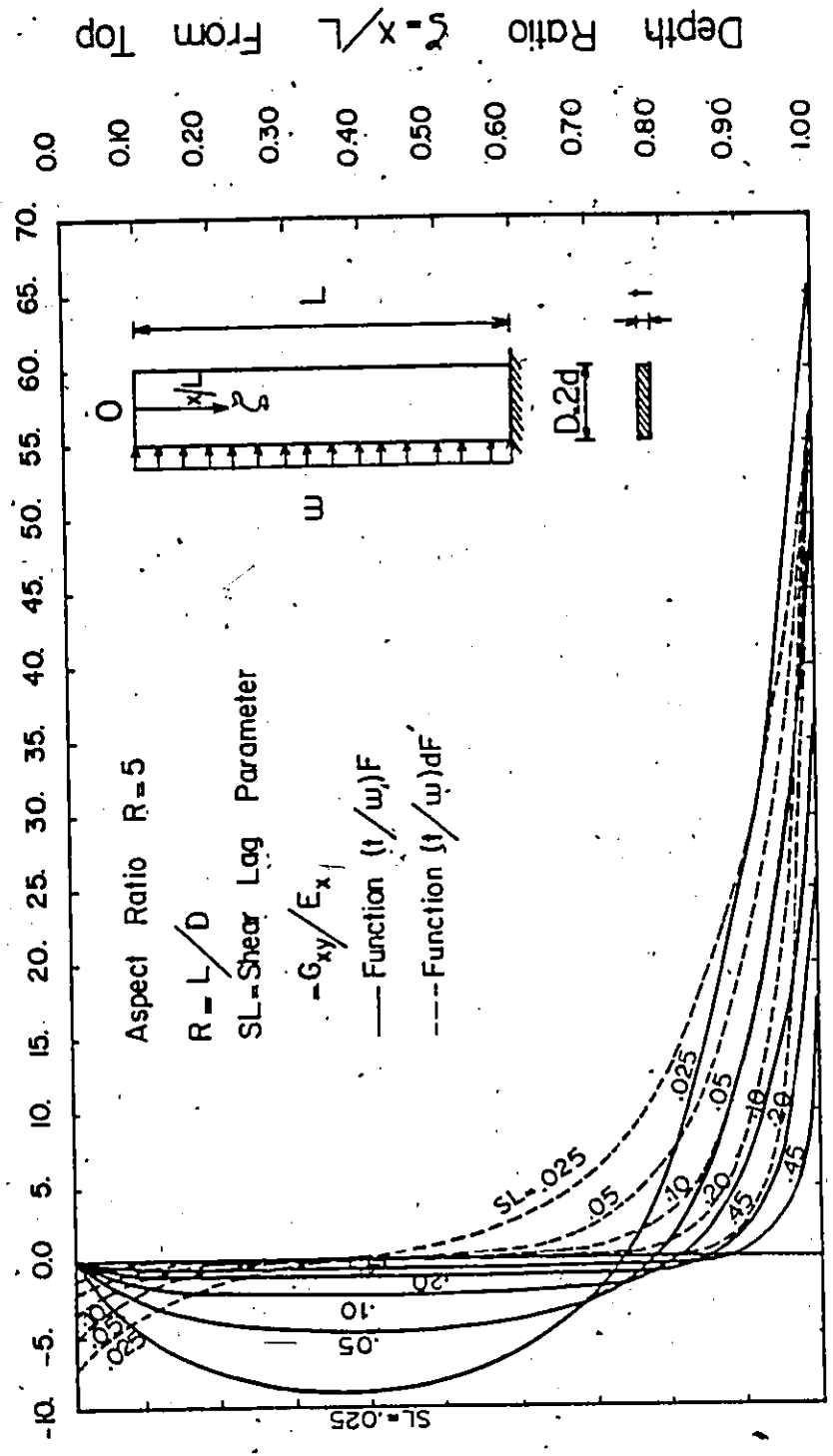


FIG. 3.4e SHEAR LAG FUNCTIONS (R=5)

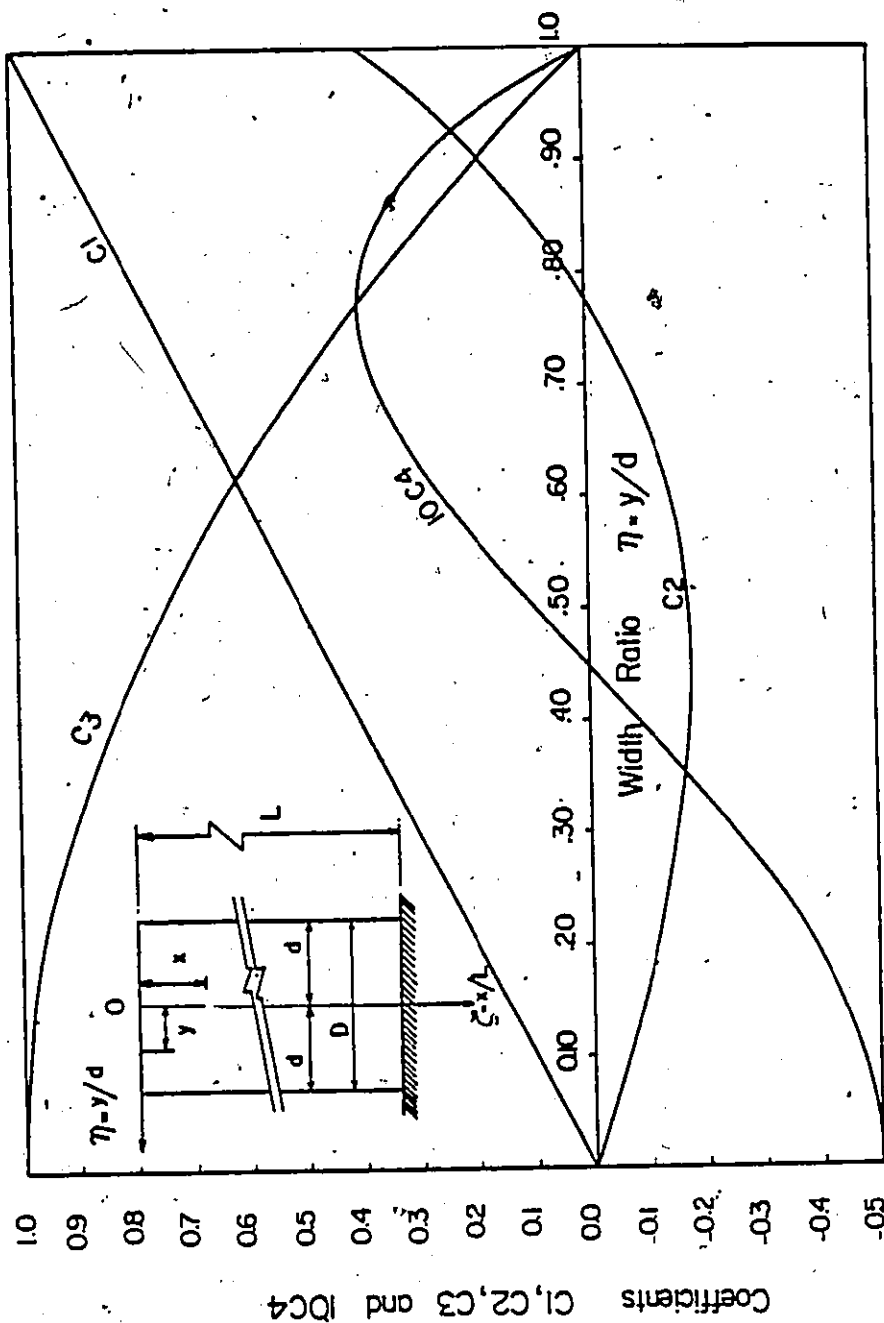


FIG. 3.5 STRESS COEFFICIENTS

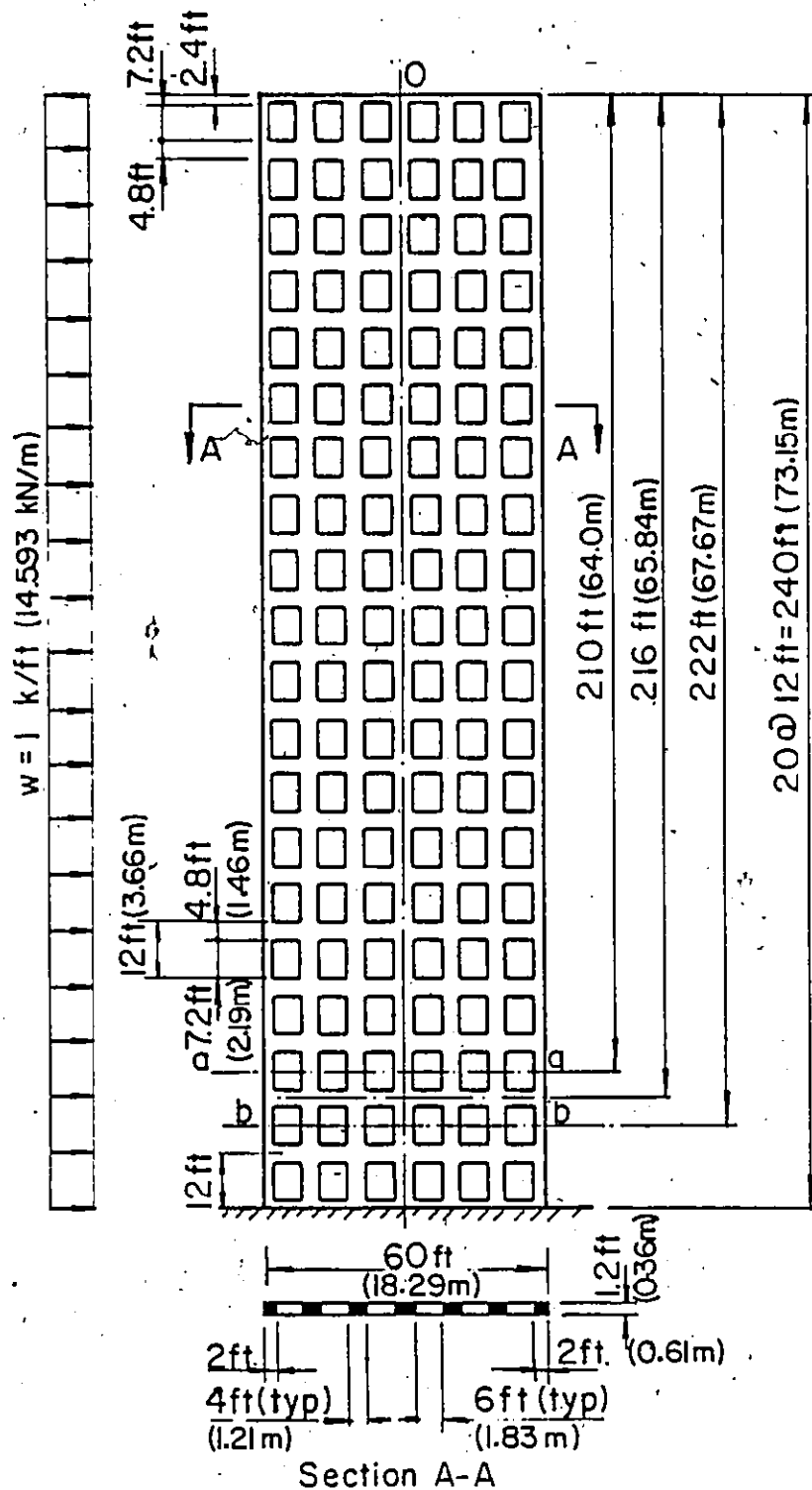


FIG. 3.6 EXAMPLE STRUCTURE (3.1) - KHAN AND STAFFORD-SMITH [61]

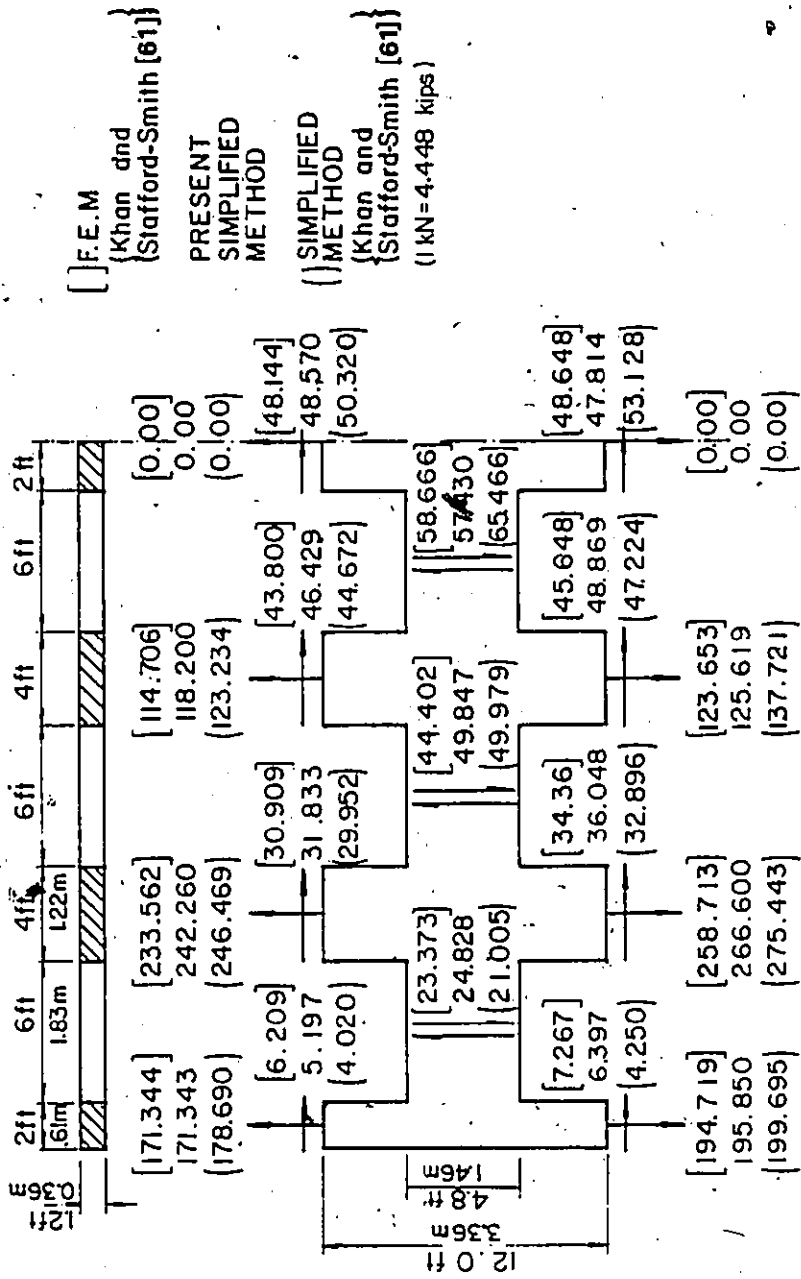


FIG. 3.7 DESIGN FORCES IN COLUMNS AND BEAMS
EXAMPLE 3-1

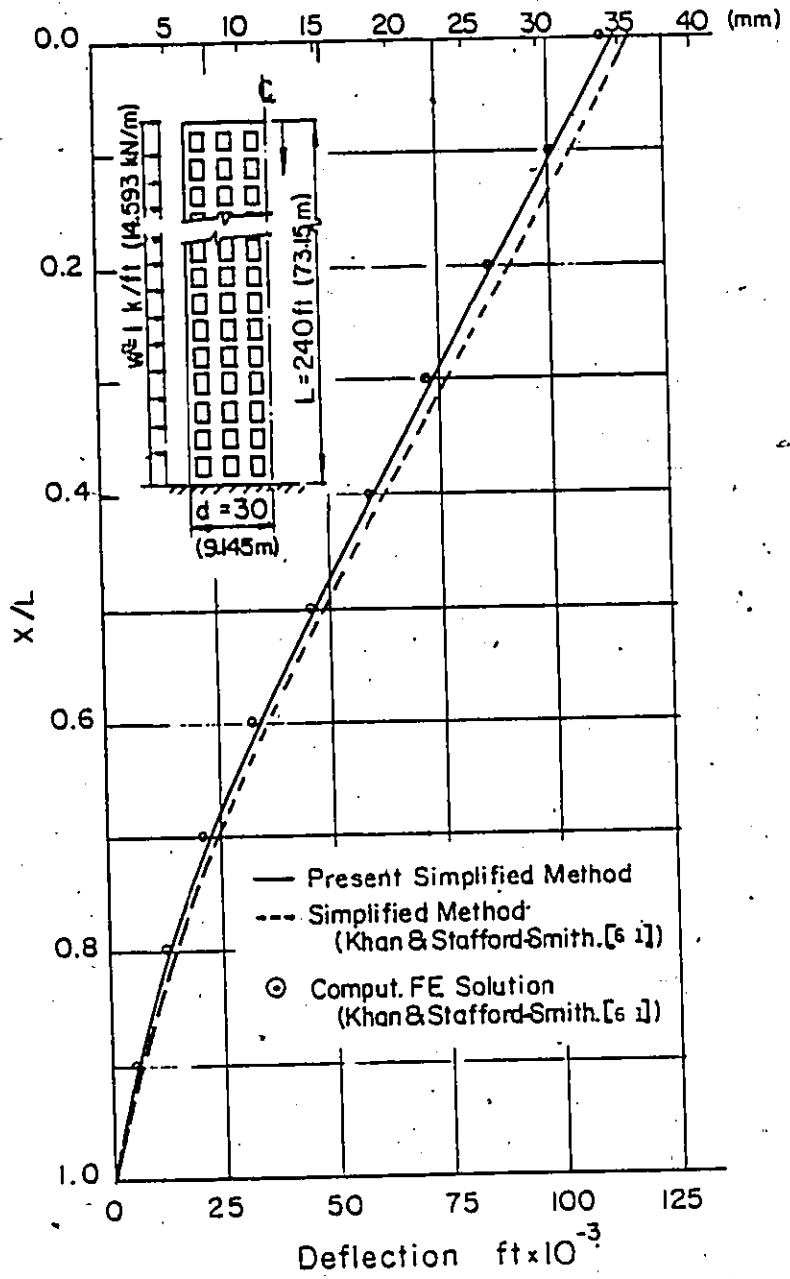


FIG. 3.8 LATERAL DEFLECTION
- EXAMPLE 3-1

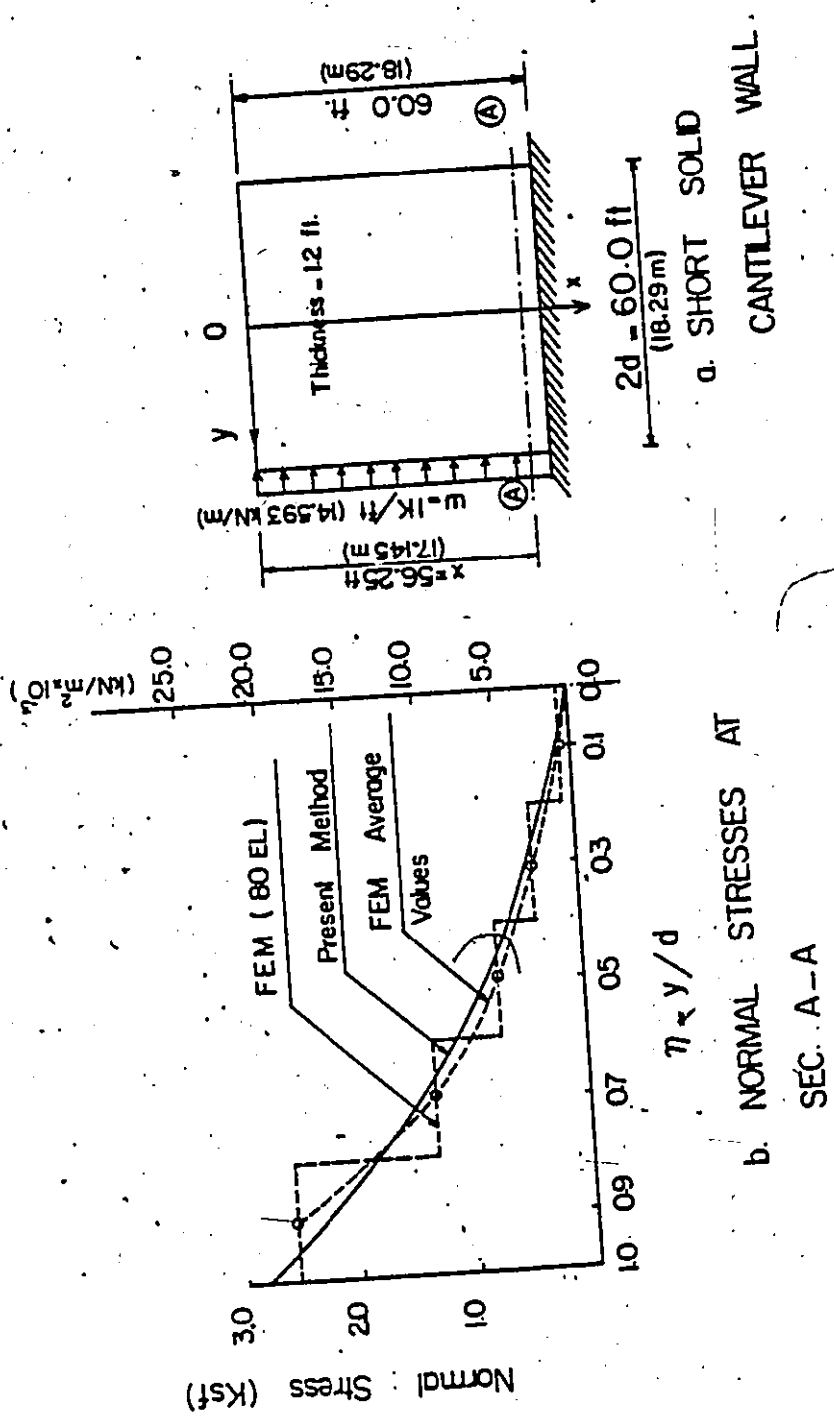
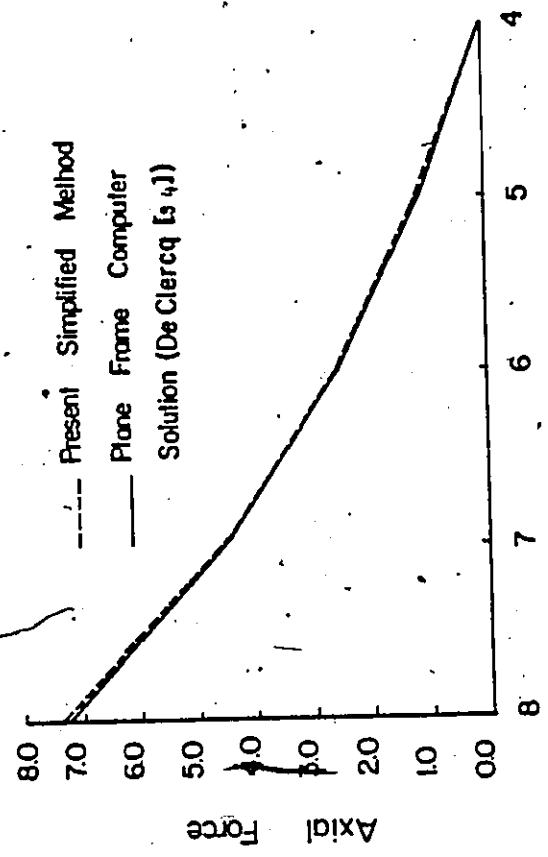
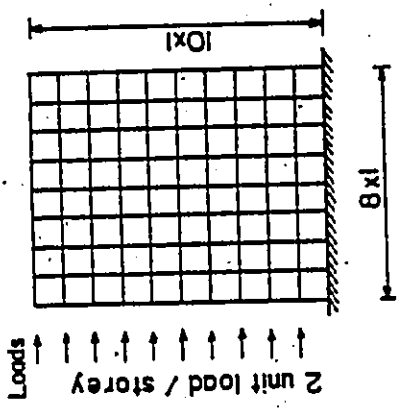


FIG. 3.9 EXAMPLE 3.2

Frame Properties
 $I_{beam} = I_{column} = 1$
 $A_{column} = 12$



a. TEN STOREY PLANE FRAME. (De Clercq [5 4])

b. MAXIMUM AXIAL FORCES IN COLUMNS.

FIG. 3.10 EXAMPLE 3.3

CHAPTER IV

TWO-DIMENSIONAL FINITE ELEMENT ANALYSIS
OF PERFORATED WALLS

CHAPTER IV
TWO-DIMENSIONAL FINITE ELEMENT ANALYSES
OF PERFORATED WALLS

4.1 INTRODUCTION

In the previous chapter, the perforated wall idealized by an equivalent membrane was analyzed employing a continuum approach. The closed-form solutions obtained enable direct determination of the characteristic parameters which control the behavior of the structure. The effects of these parameters on the mode of deformation and distribution of the member internal forces were also discussed.

In this chapter, a more general approach to the problem is presented. The solutions to the idealized equivalent membrane are obtained by the finite element method. The technique can account for moderate variation of the properties of the structure across its width and along its height. Loading, as well as support conditions, can be arbitrary. The technique is applicable to a wide range of tall structures including those where the shear lag effect is severe. As mentioned in the previous chapter, for the latter structures, the assumed cubic variation of the longitudinal stress would be inadequate for representing the sharp stress gradient. In particular, emphasis will be placed on the analysis of large regular multi-storey, multi-bay frames, where significant shear lag effect can be encountered.

A numerical example illustrating the severe shear lag effect on the response of the structure, is considered and the results are compared to those obtained by the "exact" and other simplified methods of analysis. Before developing the present technique, the literature on the analysis of slender multi-storey, multi-bay frames is reviewed.

Since the beam-column framing system was introduced by the Chicago School of Architecture after the turn of the last century [69], engineers have tried to develop approximate hand methods for the lateral load analysis of this structural system. The cantilever and portal methods [108, 123] are the best known among these methods.

With the advent of the electronic computers, the "exact" analysis of framework structures became possible [16, 17, 18, 54, 86, 111]. Nevertheless, because of the large computer time and storage required for such an analysis, engineers are still being challenged to develop simplified methods with the aim of reducing computer time and storage while maintaining sufficient accuracy for design purposes. Foremost among these methods are the substitute or equivalent frame methods [1, 62, 90] where several beams and columns are lumped together to form a reduced equivalent structure. Although these methods are more accurate than the cantilever and portal methods, they are subjected to severe

limitations [6, 34]. For example, the effect of the axial deformation of the columns is either ignored [62] or grossly approximated [1, 90].

To account for the effect of the axial deformation of the columns on the lateral deflection, MacLeod [77] suggested a simple approximate method where only the external columns are assumed to take axial loads. The method, however, does not consider the effect of this deformation on the distribution of member internal forces. Chan and others [12 to 14] have tried to include the effect of the axial deformation of the columns on lateral deflection and member internal forces by assuming the points of contraflexure at mid-span and mid-height of the beams and columns, respectively, and employing an energy approach for the analysis. Only the shear deformations of the beams were considered and the finite size joints were assumed to be infinitely rigid. The micropolar equivalent continuum of Bazant and Christensen [6] discussed in Chapter II, completely ignores the effects of the finite size joints and shear deformation of the members.

Harman and Walker [47] considered the individual columns but lumped the beams at certain "nodal floors". The method yields reasonable results with a considerable saving in computer time. The macroelement method of DeClercq [34] as an extension of the above method, reduces both the number

of nodes on any level and the number of levels. A single element may span several bays and stories. The shape functions are assumed over the region of each element to express the displacements of the beam-column joints in terms of the displacements of the nodes on the boundary of the element. Rigid arms were used in modelling the finite sized joints. Good accuracy and considerable saving in computer time may be achieved if the structure is properly modelled. Although De Clercq pointed out the importance of the P- Δ effect, and the flexibility of the finite sized joints, both aspects were not included in his method.

The objective of this chapter is to develop a general approximate method of analysis for planar perforated walls under the action of lateral loads. The technique should allow for: (i) a variation of the properties of the structure across its width and along its height, (ii) a variation of the lateral loads along the height of the structure, (iii) imposing boundary conditions due to symmetry, (iv) consideration of the P- Δ effect on the lateral deflection and member internal forces, and (v) the effects of axial deformation of the columns and shear deformation of the members, as well as the flexibility of the finite sized joints.

4.2 ANALYSIS PROCEDURE

The frame structure (Fig. 4.1(a)) is idealized by an assemblage of rectangular finite elements (Fig. 4.1(f)). Each element may span several bays and stories of the frame structure. Within each element, the discrete beam-column system forming part of the original frame is replaced by a continuous homogeneous orthotropic membrane which can reproduce the response of the actual beam-column system, as has been shown in Chapter II.

The overall structure stiffness matrix and the load vector is then assembled in the usual way of the displacement method [35]. The equilibrium equations are solved for the nodal displacements and subsequently, the element stresses. From the condition of elastic equivalence, the nodal deflections obtained by the finite element analysis represent directly those of the actual frame. The internal axial and shear forces in the members are obtained by integrating the corresponding stress components, as shown in Chapter III (Sec. 3.2.5). The specific steps of the analysis procedure may be summarized as follows:

- (1) Idealization of the actual frame structure by an elastically equivalent orthotropic membrane having the elastic properties defined in Chapter II.

- (2) Discretization of the equivalent membrane into a number of specially orthotropic finite elements within which the mechanical properties must be constant.
- (3) Computation of element stiffness matrices.
- (4) Assembly of the overall structure stiffness matrix $[K]$ and the load vector $\{P\}$ of the joint equilibrium equations.

$$\{P\} = [K]\{d\} \quad (4.1)$$

in which $\{d\}$ is the nodal displacement vector.

- (5) Introduction of the displacement boundary conditions, and solution of Eq. (4.1) for the unknown nodal displacements $\{d\}$.
- (6) Determination of stresses in each element based on its nodal displacements (obtained in Step 5).
- (7) Evaluation of internal forces in the members of the actual structure by integrating the corresponding stress components (obtained in Step 6).

Details of the above steps are described in the following sections.

4.3 ELEMENT STIFFNESS MATRIX

Research in the field of finite element theory has produced a large number of element types to fit some particular purposes or to be used in the solution of specific problems. As the present work is concerned with modelling a membrane which is subjected to in-plane loads, the search for a suitable element is directed towards two-dimensional plane stress elements. For the present purpose, the rectangular element with linear variations of displacements along the edges seems most suitable [3]. This simple element, which insures compatibility of deformations along the interfaces, has been shown to produce better results than the constant strain triangle or the quadrilateral formed by combining four of such triangles [3]. The element has eight degrees of freedom (8 DOF), two at each of its four corner nodes as shown in Fig. 4.2. As mentioned in Chapter II, the effect of Poisson's ratios of the equivalent orthotropic membrane (μ_{xy} , μ_{yx}) on the analysis is negligible (being zero for slender frames), and hence can be assigned a zero value. Therefore, the 8 x 8 element stiffness matrix $[K_e]$ of Ammar and Nilson [3] can be modified to:

$$[K_e] = \begin{bmatrix}
 K_{11} & & & & & & & & & 1 \\
 K_{21} & K_{22} & & & & & & & & 2 \\
 K_{31} & K_{21} & K_{11} & & & & & & & 3 \\
 -K_{21} & K_{42} & -K_{21} & K_{22} & & & & & & 4 \\
 -\frac{1}{2}K_{11} & -K_{21} & K_{71} & K_{21} & K_{11} & & & & & 5 \\
 -K_{21} & -\frac{1}{2}K_{22} & -K_{21} & K_{82} & K_{21} & K_{22} & & & & 6 \\
 K_{71} & -K_{21} & -\frac{1}{2}K_{11} & K_{21} & K_{31} & -K_{21} & K_{11} & & & 7 \\
 K_{21} & K_{82} & K_{21} & -\frac{1}{2}K_{22} & -K_{21} & K_{42} & -K_{21} & K_{22} & & 8 \\
 1 & 2 & 3 & 4 & 5 & 6 & 7 & 8 & &
 \end{bmatrix}$$

Sym.

in which

$$K_{11} = \frac{t}{3}(E_x/r + rG_{xy})$$

$$K_{21} = \frac{t}{4} G_{xy}$$

$$K_{31} = \frac{t}{6}(-2E_x/r + rG_{xy})$$

$$K_{71} = \frac{t}{6}(E_x/r - 2rG_{xy})$$

$$K_{22} = \frac{t}{3}(rE_y + G_{xy}/r)$$

$$K_{42} = \frac{t}{6}(rE_y - 2G_{xy}/r)$$

$$K_{82} = \frac{t}{6}(-2rE_y + G_{xy}/r)$$

where E_x , E_y , and G_{xy} are the mechanical properties of the equivalent, technically orthotropic membrane and r is the aspect ratio of the element.

4.4 ASSEMBLY OF THE STRUCTURE STIFFNESS MATRIX AND THE LOAD VECTOR

Once the stiffness matrices of all the individual elements are calculated, the structure stiffness matrix is assembled employing the direct stiffness method [35, 107, 118, 128]. The resulting stiffness matrix is symmetric and banded. Thus, it is necessary to store only the coefficients within the band of one triangle of the matrix.

4.5 BOUNDARY CONDITIONS AND SOLUTIONS

The stiffness matrix and the load vector assembled in the previous section are now modified by imposing the kinematic constraints (geometric boundary conditions). Traction boundary conditions are directly incorporated in the load vector $\{P\}$. Natural boundary conditions are implicitly satisfied in the finite element formulation through the implementation of any valid variational principle [35]. Considering the problem at hand, only homogeneous, normal, geometric boundary conditions exist. This enables the partitioning of the global equilibrium equations as follows [35].

$$\begin{bmatrix} [K_{11}] & [0] \\ [0] & [I] \end{bmatrix} \begin{Bmatrix} \{d_1\} \\ \{d_2\} \end{Bmatrix} = \begin{Bmatrix} \{P_1\} - [K_{12}]\{d_2\} \\ \{d_2\} \end{Bmatrix} \quad (4.2)$$

in which $\{d_1\}$ is the vector of unconstrained displacements, and $\{d_2\}$ is that of the specified displacements which is null in the present problem. This simplifies Eq. (4.2) to:

$$\begin{bmatrix} [K_{11}] & [0] \\ [0] & [I] \end{bmatrix} \begin{Bmatrix} \{d_1\} \\ \{0\} \end{Bmatrix} = \begin{Bmatrix} \{P_1\} \\ \{0\} \end{Bmatrix} \quad (4.3)$$

For programming purposes, to preserve the banded nature of the equations, the row and column corresponding to each kinematic constraint are deleted and a unit value is assigned to the diagonal. A computer code for the above procedure is developed by Wilson [124] and used in the present program.

Having set the boundary conditions, a direct (Gaussian elimination) solution of Eq. (4.3) is then performed for the unknown displacement. The code developed by Felippa [37] and based on decomposition of the stiffness matrix and solution by forward reduction and back substitution is adopted in the present program.

4.6 DETERMINATION OF STRESSES

Having determined the nodal displacements $\{d\}$, the element nodal displacements $\{d\}_e$ may now be extracted, and the element strains $\{\epsilon\}$ are then obtained by:

$$\{\epsilon\} = [D]\{d\}_e \quad (4.4)$$

in which $[D]$ is the strain-displacement matrix given (for the element considered herein) by:

$$[D]^T = \begin{array}{ccc} \begin{array}{c} 1 \\ 2 \\ 3 \\ 4 \\ 5 \\ 6 \\ 7 \\ 8 \end{array} & \begin{array}{c} 2 \\ 3 \\ 4 \\ 5 \\ 6 \\ 7 \\ 8 \end{array} & \begin{array}{c} 3 \\ 4 \\ 5 \\ 6 \\ 7 \\ 8 \end{array} \\ \left[\begin{array}{ccc} -\frac{(1-\eta)}{a} & 0 & -\frac{(1-\xi)}{b} \\ 0 & -\frac{(1-\xi)}{b} & -\frac{(1-\eta)}{a} \\ \frac{(1-\eta)}{a} & 0 & -\frac{\xi}{b} \\ 0 & -\frac{\xi}{b} & \frac{(1-\eta)}{a} \\ \frac{\eta}{a} & 0 & \frac{\xi}{b} \\ 0 & \frac{\xi}{b} & \frac{\eta}{a} \\ -\frac{\eta}{a} & 0 & \frac{(1-\xi)}{b} \\ 0 & \frac{(1-\xi)}{b} & -\frac{\eta}{a} \end{array} \right] & \begin{array}{c} 1 \\ 2 \\ 3 \\ 4 \\ 5 \\ 6 \\ 7 \\ 8 \end{array} \end{array}$$

where

a and b = the length and the height of the element, respectively,

$$\xi = \frac{x}{a} \quad \text{and} \quad \eta = \frac{y}{b}$$

Stresses $\{\sigma\}$ are now expressed in terms of strains by:

$$\{\sigma\} = [E]\{\epsilon\} \quad (4.5)$$

in which the $[E]$ matrix defines the constitutive relation between the stresses and strains for an orthotropic medium and is given by:

$$[E] = \frac{1}{\lambda} \begin{bmatrix} E_x & \mu_{yx} E_x & 0 \\ \mu_{xy} E_y & E_y & 0 \\ 0 & 0 & \lambda G_{xy} \end{bmatrix}$$

in which

$$\lambda = (1 - \mu_{xy} \mu_{yx})$$

Since the effect of Poisson's ratios (μ_{xy}, μ_{yx}) on the analysis, as mentioned earlier, is negligible, the $[E]$ matrix can be simplified as

$$[E] = \begin{bmatrix} E_x & 0 & 0 \\ 0 & E_y & 0 \\ 0 & 0 & G_{xy} \end{bmatrix}$$

Stresses are evaluated by substituting the simplified form of the $[E]$ matrix and Eq. (4.4) into Eq. (4.5).

4.7 COMPUTER PROGRAM

A computer program was developed incorporating the ideas presented in the previous sections. The program was written in FORTRAN IV and run on a CDC 6600 computer. The listing of the program is not given here since two-dimensional problems can also be analysed using the more general program, given in Appendix C. The following are some of the program features:

- (1) While properties of the equivalent structure may vary across its width and along its height, they must be kept constant within each element. All elements on the same level must span the same number of stories.
- (2) Nodal points and element data can be automatically generated.
- (3) Boundary conditions simulating symmetry can be imposed.
- (4) The output consists of nodal displacements and element stresses.

4.8 NUMERICAL EXAMPLE

To verify the theory of the present method and to illustrate its application and accuracy, the 52-storey slender frame of Bazant and Christensen [6] is considered.

The frame has uniform properties as shown in Fig. 4.1. The analysis is carried out for the lateral deflection and column axial forces. The results are compared to those obtained by Bazant and Christensen [6] based on:

- (i) "exact" solution;
- (ii) finite difference method applied to an equivalent micropolar continuum; and
- (iii) substitute frames [1,62].

A comparison of the lateral deflection, the variation of column axial forces across the width of the structure, and the variation of the axial force in the external column along the height of the structure, are shown in Figs. 4.3, 4.4, and 4.5, respectively.

It can be seen that the substitute frame methods, as recommended by ACI Committee 442 [1], and as proposed by Khan and Sbarounis [62] are inadequate and cannot reflect completely the behaviour of the original structure. The former underestimates the lateral deflection by 60% and the latter underestimates the maximum column axial force by 52%, as can be seen from Figs. 4.3, 4.5, respectively.

The lateral deflection and column axial forces obtained by the present method are in excellent agreement

with those obtained by the "exact" and the micropolar methods, as shown in Figs. 4.3 to 4.5. However, the number of unknowns required for the solution in the present method is only 7% of the "exact" and 20% of the micropolar. Furthermore, the present method drastically reduces the required computer storage to 1.5% and 6.1% of that required by the other two methods, respectively. Moreover, the micropolar method [6], unlike the present method, is only suitable for the analysis of frames having slender members since it ignores completely the effect of finite size joints and shear deformations of the members.

4.9 DIAPHRAGM ACTION OF FLOORS

Floor slabs normally possess high in-plane rigidity and can be assumed rigid in their own planes [110,129]. According to this assumption all joints on the same floor level would displace laterally the same amount. In the present analysis, the elastic modulus E_x represents such in-plane rigidity. To examine the effect of the above assumption, E_x is assigned different values and the corresponding maximum deflection and column axial force are determined, as shown in Table 4.2. The value of E_x on the first line of the table corresponds to the actual properties of the structure under consideration. By increasing E_x to 10^5 times its actual value, the maximum deflection decreases by only 0.015% and the maximum column

axial force increases insignificantly as shown in Table 4.2.

In summary, a simple method for the analysis of large multi-storey multi-bay framework is presented. The method is based on replacing the actual structure by an elastically equivalent orthotropic membrane which is then analyzed by finite element technique. While the substitute frame methods [1,62] are unacceptably in error, the present method is in excellent agreement with both the micropolar and the "exact" analyses, yet it requires significantly less number of unknowns and computer storage (Table 4.1). The effect of the elastic modulus E_x on the analysis is insignificant and therefore can be assigned an infinite value. In so doing, a further reduction in the required number of unknowns (number of degrees of freedom) and computer storage can be effected, as will be shown in the next Chapter.

TABLE 4.1 COMPARISON OF THE NUMBER OF UNKNOWNNS AND COMPUTER STORAGE

Data	Exact Method Reference [6]	Micropolar Reference [6]	Single Bay Substitute Frame Reference [62]	Present Method
Number of Equations	1,872	648	260	132
Computer Storage*	144,144	34,344	2,600	2,112

* Evaluated as the storage required for the solution of the system of equilibrium equations.

TABLE 4.2 EFFECT OF THE ELASTIC MODULUS E_x ON THE ANALYSIS

Data	Analysis Using Actual E_x (0.3×10^4 ksf)	Analysis Using E_x 0.3×10^9 ksf	Difference From the Actual %
Maximum Lateral Deflection (in)	20.456	20.453	- 0.015
Maximum Column Axial Force (kip)	421.64	421.68	+ 0.0096

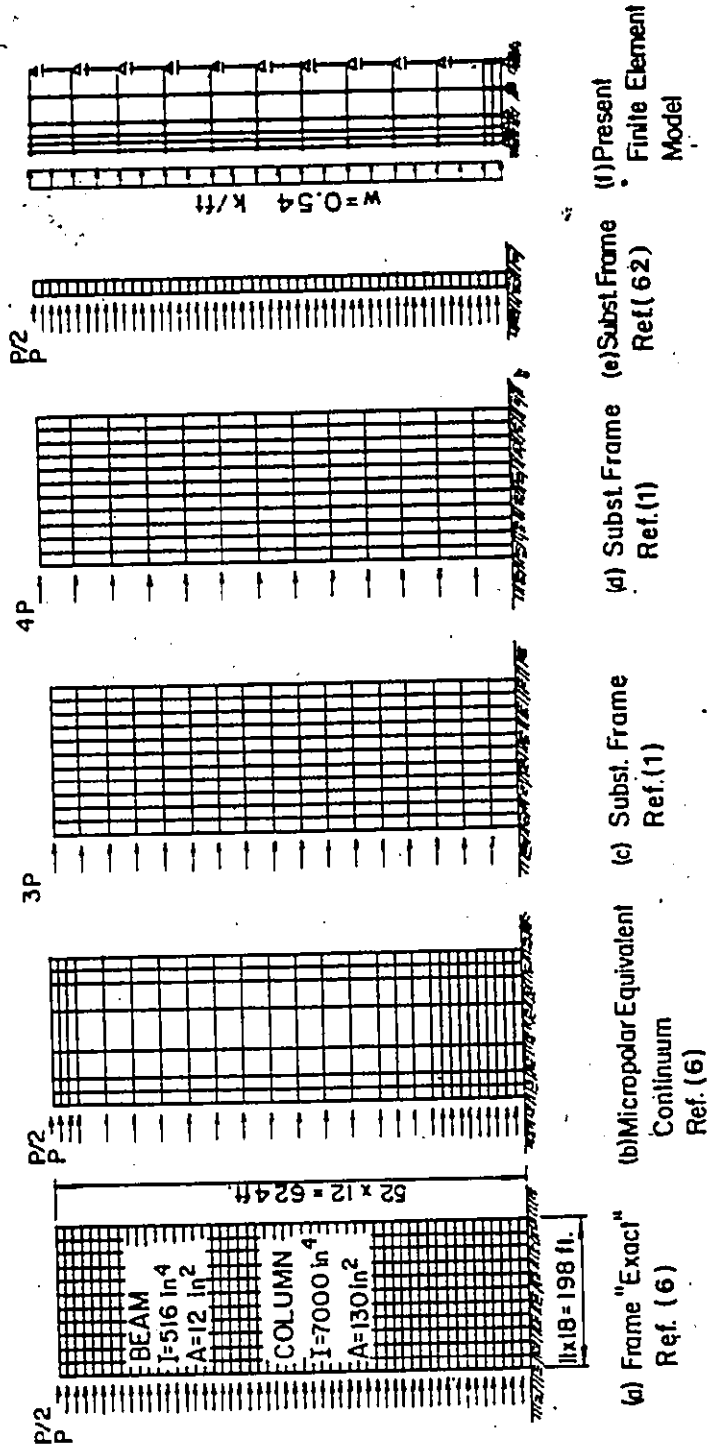


FIG. 4.1 METHODS OF ANALYSIS CONSIDERED IN THE NUMERICAL EXAMPLE (4-1)

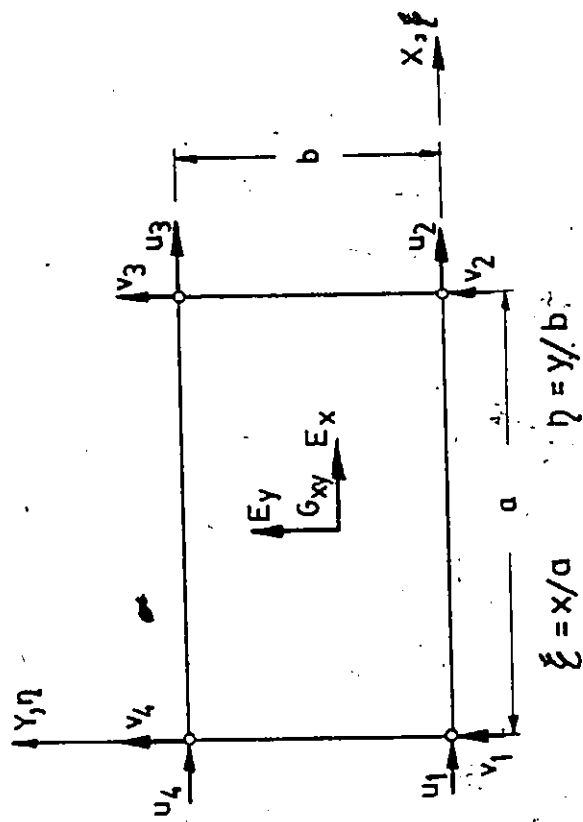


FIG. 4.2 SPECIALLY ORTHOTROPIC ELEMENT OF AMMAR AND NILSON [3]

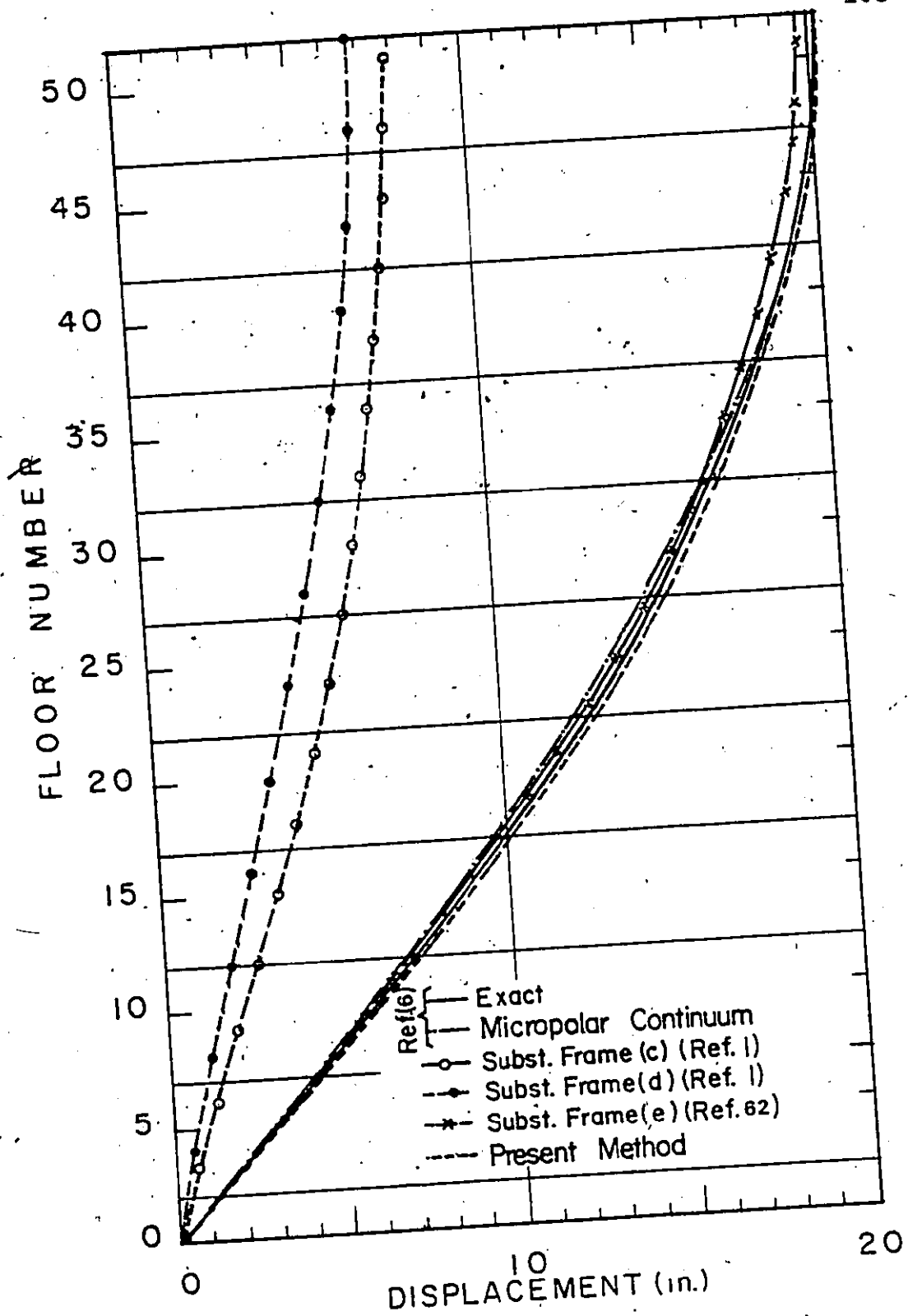


FIG. 4.3

LATERAL DEFLECTION
- EXAMPLE 4-1

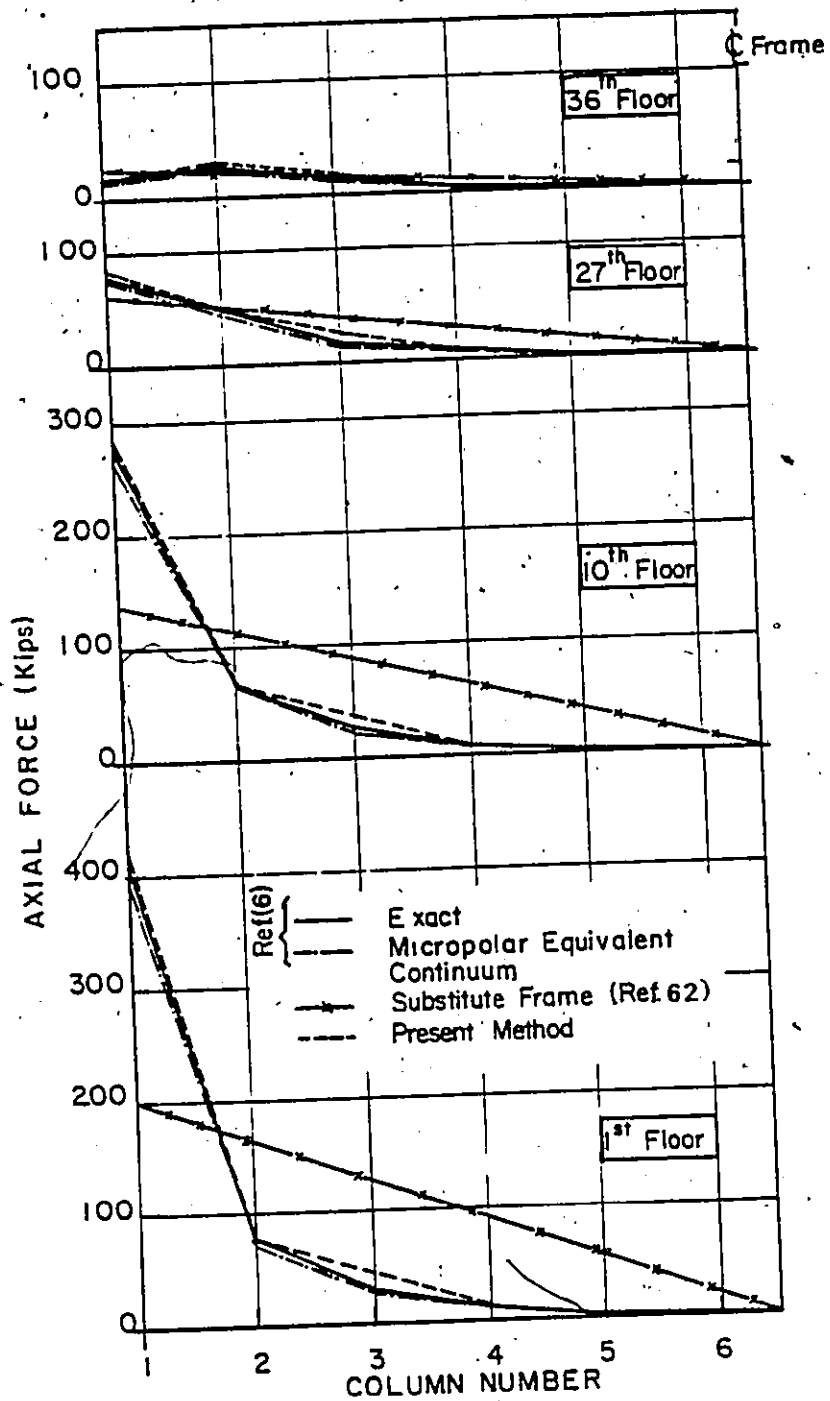


FIG. 4.4 COLUMN AXIAL FORCES
- EXAMPLE 4-1

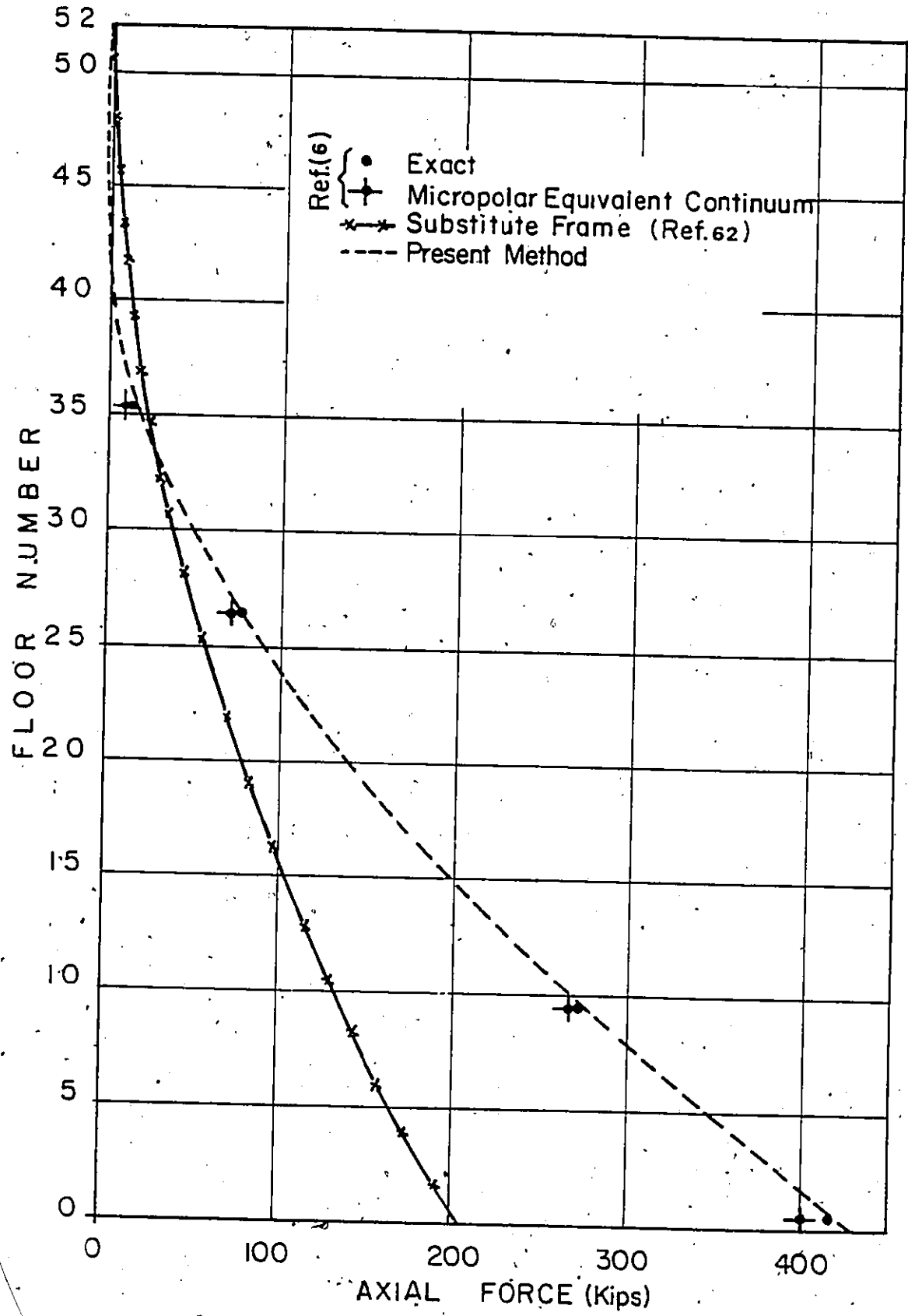


FIG. 4.5 VARIATION OF AXIAL FORCE IN THE EXTERIOR COLUMN - EXAMPLE 4-1

CHAPTER V

SPECIALLY ORTHOTROPIC FINITE ELEMENTS FOR
TALL BUILDING ANALYSIS

CHAPTER V

SPECIALLY ORTHOTROPIC FINITE ELEMENTS FOR
TALL BUILDING ANALYSIS5.1 INTRODUCTION

It has been shown in the previous chapter that the effect of the elastic modulus E_x on the analysis of realistic structures is negligible. Thus, to avoid the unnecessary algebraic equations corresponding to the lateral displacements of nodes on the same level, E_x is assigned an infinite value in the present formulation. This corresponds to the widely accepted assumption of infinite in-plane rigidity of floors in tall building analysis [110].

In this chapter two finite elements are developed incorporating the above assumption. The first is an ordinary element with linear variation of displacements along its edges and the second, a refined element with quadratic displacement functions. Numerical examples are also presented to illustrate the accuracy and applications of the two elements.

5.2 PROCEDURE FOR DERIVING THE ELEMENT STIFFNESS
MATRIX AND THE CONSISTENT LOAD VECTOR

In deriving the stiffness matrix and consistent load vector of the two elements, the principle of minimum total potential energy is used. Expressing the potential energy

functional in terms of some assumed displacement functions and its subsequent minimization will yield the approximate equilibrium equations which automatically define the stiffness matrix and the load vector.

Solutions of an elasto-mechanics problem have to satisfy three types of conditions: compatibility, physical, and equilibrium. Once a displacement model is assumed within an element, and expressed in terms of the nodal displacements $\{d\}$, the strains $\{\epsilon\}$ are obtained by proper differentiation of the displacement functions. In symbolic form

$$\{\epsilon\} = [D]\{d\} \quad (5.1)$$

Equation (5.1) constitutes the relation of compatibility.

The constitutive relation linking stresses to strains expresses the physical nature of the problem as follows:

$$\{\sigma\} = [E]\{\epsilon\} \quad (5.2)$$

in which the $[E]$ matrix represents the mechanical properties of the material.

Now, the third and last condition (i.e., the equilibrium) can be satisfied through the minimization of the total potential energy with respect to the nodal displacements.

The procedure outlined in this section is now employ-

ed in detail in the following two sections.

5.3 FORMULATION OF THE ORDINARY ELEMENT

Consider the rectangular element shown in Fig. 5.1 in accordance with the previously stated assumption of infinite in-plane rigidity of floors, the strain in the x-direction ϵ_x should vanish and consequently the corresponding elastic modulus E_x is considered to be infinite. The displacement function which satisfies this condition, maintains the compatibility along the edges, and satisfies all other requirements for convergence in finite element theory is assumed to be:

$$\left. \begin{aligned} u &= \alpha_1 + \alpha_2 \eta \\ v &= \alpha_3 + \alpha_4 \xi + \alpha_5 \eta + \alpha_6 \xi \eta \end{aligned} \right\} \quad (5.3)$$

in which ξ and η are non-dimensional coordinates equal to x/a and y/b respectively (Fig. 5.1).

Six degrees of freedom are assigned to the element; four vertical displacements at its four nodes and two horizontal displacements at the upper and lower levels as shown in Fig. 5.1. The α coefficients in Eq. (5.3) can further be expressed by means of the nodal displacements as

$$\begin{Bmatrix} u \\ v \end{Bmatrix} = \begin{bmatrix} (1-\eta) \eta & 0 & 0 & 0 & 0 & 0 & 0 \\ 0 & 0 & (1-\xi) & (1-\eta) & \xi(1-\eta) & \xi\eta & \eta(1-\xi) \end{bmatrix} \begin{Bmatrix} u_1 \\ u_2 \\ v_1 \\ v_2 \\ v_3 \\ v_4 \end{Bmatrix} \quad (5.4)$$

or

$$\begin{Bmatrix} u \\ v \end{Bmatrix} = [N]\{d\} \quad (5.5)$$

The strain-displacement relation is:

$$\begin{Bmatrix} \epsilon_x \\ \epsilon_y \\ \gamma_{xy} \end{Bmatrix} = \begin{bmatrix} \partial/\partial x & 0 \\ 0 & \partial/\partial y \\ \partial/\partial y & \partial/\partial x \end{bmatrix} \begin{Bmatrix} u \\ v \end{Bmatrix} \quad (5.6)$$

Substituting Eq. (5.4) into Eq. (5.6) yields:

$$\begin{Bmatrix} \epsilon_x \\ \epsilon_y \\ \gamma_{xy} \end{Bmatrix} = \begin{bmatrix} 0 & 0 & 0 & 0 & 0 & 0 \\ 0 & 0 & -(1-\xi)/b & -\xi/b & \xi/b & (1-\xi)/b \\ -1/b & 1/b & -(1-\eta)/a & (1-\eta)/a & \eta/a & -\eta/a \end{bmatrix} \begin{Bmatrix} u_1 \\ u_2 \\ v_1 \\ v_2 \\ v_3 \\ v_4 \end{Bmatrix} \quad (5.7)$$

or in symbolic form:

$$\{\epsilon\} = [D]\{d\} \quad (5.8)$$

Poisson's ratios μ_{xy} and μ_{yx} of the equivalent orthotropic membrane have zero values in correspondence with the assumption of infinite in-plane rigidity of floors (Section 2.3.1). Therefore the constitutive relation for this specially orthotropic membrane is:

$$\begin{Bmatrix} \sigma_x \\ \sigma_y \\ \gamma_{xy} \end{Bmatrix} = \begin{bmatrix} E_x & 0 & 0 \\ 0 & E_y & 0 \\ 0 & 0 & G_{xy} \end{bmatrix} \begin{Bmatrix} \epsilon_x \\ \epsilon_y \\ \gamma_{xy} \end{Bmatrix} \quad (5.9)$$

or,

$$\{\delta\} = [E] \{\epsilon\} \quad (5.10)$$

Upon minimization of the total potential energy [35], each element in the stiffness matrix can be given by:

$$K = t a b \int_0^1 \int_0^1 [D]^T [E] [D] d\xi d\eta \quad (5.11)$$

Performing the triple matrix product $[D]^T [E] [D]$, the following 6 x 6 matrix is obtained:

$$\begin{array}{l}
 1 \\
 2 \\
 3 \\
 4 \\
 5 \\
 6
 \end{array}
 \left[
 \begin{array}{cccccc}
 b_1 & & & & & \\
 -b_1 & b_1 & & & & \\
 b_2 & -b_2 & (b_4+b_5) & & & \\
 -b_2 & b_2 & (b_6-b_5) & (b_8+b_5) & & \\
 -b_3 & b_3 & (-b_6-b_7) & (-b_8+b_7) & (b_8+b_9) & \\
 b_3 & -b_3 & (-b_4+b_7) & (-b_6-b_7) & (b_6-b_9) & (b_4+b_9)
 \end{array}
 \right]
 \begin{array}{l}
 \\
 \text{Sym.} \\
 \\
 \\
 \\
 \\
 \end{array}
 \left[
 \begin{array}{l}
 \\
 \\
 \\
 \\
 \\
 \\
 \end{array}
 \right]$$

1 2 3 4 5 6

(5.12)

in which

$$b_1 = \frac{G_{xy}}{b^2}$$

$$b_2 = \frac{G_{xy}(1-\eta)}{ab}$$

$$b_3 = \frac{G_{xy}\eta}{ab}$$

$$b_4 = \frac{E_y(1-\xi)^2}{b^2}$$

$$b_5 = \frac{G_{xy}(1-\eta)^2}{a^2}$$

$$b_6 = \frac{E_y \xi(1-\xi)}{b^2}$$

$$b_7 = \frac{G_{xy} \eta(1-\eta)}{a^2}$$

$$b_3 = \frac{E_y \xi^2}{b^2}$$

$$b_3 = \frac{G_{xy} \eta^2}{a^2}$$

Carrying out the double integration of each term in the previous matrix according to Eq. (5.11), the 6 x 6 stiffness matrix for the specially orthotropic rectangular element (Fig. 5.1) is found to be:

$$[K_e] = \begin{bmatrix} K_1 & & & & & \\ -K_1 & K_1 & & & & \\ K_2 & -K_2 & K_3 & & & \\ -K_2 & K_2 & K_4 & K_3 & & \\ -K_2 & K_2 & -\frac{K_3}{2} & K_5 & K_3 & \\ K_2 & -K_2 & K_5 & -\frac{K_3}{2} & K_4 & K_3 \end{bmatrix} \quad (5.13)$$

in which

$$K_1 = \frac{t a G_{xy}}{b}$$

$$K_2 = \frac{t G_{xy}}{2}$$

$$K_3 = \frac{t (E_y \frac{a}{b} + G_{xy} \frac{b}{a})}{3}$$

$$K_4 = \frac{t (E_y \frac{a}{2b} - G_{xy} \frac{b}{a})}{3}$$

and

$$K_s = \frac{t(G_{xy} \frac{b}{2a} - E_y \frac{a}{b})}{3}$$

The integrals which were used to evaluate the K_{ij} terms of the stiffness matrix are given in Appendix A.

Minimization of the total potential energy yields, also, the following expression for the consistent load (kinematically equivalent force) vector:

$$\{P_e\} = \int_s \int [N]^T \{T\} ds \quad (5.14)$$

in which $[N]$ is the shape function expressing the displacement at any point within the element in terms of the nodal displacements as defined in Eq. (5.4), and $\{T\}$ is the in-plane surface tractions vector, acting on the surface s .

In general

$$\{T\}^T = [P_x \ P_y] \quad (5.15)$$

in which P_x and P_y are the prescribed in-plane load intensities along the coordinate directions (Fig. 5.1). These load intensities are distributed load per unit thickness and per unit length measured along the side of the element. In the present application, only P_x will exist. For the case of uniform lateral load p , the consistent load vector can be expressed as

$$\{P_e\} = t b_0 \int_0^1 \begin{bmatrix} (1-\eta) \\ \eta \\ 0 \\ 0 \\ 0 \\ 0 \end{bmatrix} \begin{bmatrix} (1-\xi)(1-\eta) \\ \xi(1-\eta) \\ \xi\eta \\ \eta(1-\xi) \end{bmatrix} \begin{Bmatrix} p \\ 0 \end{Bmatrix} d\eta \quad (5.16)$$

Thus

$$\{P_e\} = \frac{ptb}{2} \begin{Bmatrix} 1 \\ 1 \\ 0 \\ 0 \\ 0 \\ 0 \end{Bmatrix} \quad (5.17)$$

It can be seen from Eq. (5.17), that the consistent loads, for the present element, are identical to the lumped loads. This is also true for the case of linearly varying loads (Fig. 5.1).

5.4 FORMULATION OF THE REFINED ELEMENT

The element has eight nodes and nine associated degrees of freedom (Fig. 5.2). The element is rectangular in shape, of length $2a$, height $2b$ and a uniform thickness t . It is especially orthotropic with respect to the axes x and y which have their origin at the center of the element

as shown in Fig. 5.2.

The procedure for deriving the stiffness matrix and consistent load vector of this element is similar, if not identical, to that given in the previous two sections. Thus, only a brief formulation is given herein. For the complete detailed derivation refer to Appendix B. The assumption of equal lateral displacement for all nodes located on the same level is also incorporated subsequently. The displacement functions satisfying the necessary requirements for convergence in finite element theory [35, 107, 128] may be assumed as

$$\begin{aligned}
 u &= \alpha_1 + \alpha_2 \eta + \alpha_3 \eta^2 \\
 v &= \alpha_4 + \alpha_5 \xi + \alpha_6 \eta + \alpha_7 \xi^2 + \alpha_8 \xi \eta \\
 &\quad + \alpha_9 \xi^2 \eta
 \end{aligned}
 \tag{5.18}$$

The displacement field can further be expressed in terms of the nodal displacement as:

$$\begin{Bmatrix} u \\ v \end{Bmatrix} = [N] \{u_1 \ u_2 \ u_3 \ v_1 \ v_2 \ v_3 \ v_4 \ v_5 \ v_6\}^T
 \tag{5.19}$$

in which $[N]$ is the shape function defined as:

$$[N]^T = \begin{bmatrix} -\frac{1}{2}\eta(1-\eta) \\ 1-\eta^2 \\ \frac{1}{2}\eta(1+\eta) \\ 0 & -\frac{1}{2}\xi(1-\xi-\eta+\xi\eta) \\ 0 & \frac{1}{2}(1-\eta-\xi^2+\xi^2\eta) \\ 0 & \frac{1}{2}\xi(1+\xi-\eta-\xi\eta) \\ 0 & \frac{1}{2}\xi(1+\xi+\eta+\xi\eta) \\ 0 & -\frac{1}{2}(1+\eta-\xi^2-\xi^2\eta) \\ 0 & -\frac{1}{2}\xi(1-\xi+\eta-\eta\xi) \end{bmatrix} \quad (5.20)$$

where ξ and η are non-dimensional coordinates defined as x/a and y/b respectively.

The $[D]$ matrix relating element strains $\{\epsilon\}$ to the nodal displacements $\{d\}$ (Eq. 5.8) can then be expressed by the aid of Eq. (5.6), as shown in Eq. (5.21) on the following page.

The constitutive relation, $[E]$ matrix, relating stresses to strains is the same as that of the ordinary element (Eq. 5.9).

Performing the triple matrix product $[D]^T[E][D]$, a 9×9 matrix is obtained populated by expressions which are functions of ξ and η , as shown in Appendix B.

$$[D]^T = \begin{bmatrix} 0 & 0 & -(1-2\eta)/2b \\ 0 & 0 & -2\eta/b \\ 0 & 0 & (1+2\eta)/2b \\ 0 & \xi(1-\xi)/4b & -(1-2\xi-\eta+2\xi\eta)/4a \\ 0 & -(1-\xi^2)/2b & -\xi(1-\eta)/a \\ 0 & -\xi(1+\xi)/4b & (1+2\xi-\eta-2\xi\eta)/4a \\ 0 & \xi(1+\xi)/4b & (1+2\xi+\eta+2\xi\eta)/4a \\ 0 & (1-\xi^2)/2b & -\xi(1+\eta)/a \\ 0 & -\xi(1-\xi)/4b & -(1-2\xi+\eta-2\xi\eta)/4a \end{bmatrix}$$

(5.21)

Each K_{ij} term of the stiffness matrix is obtained by integrating the corresponding term in the previous matrix. The integration is performed according to Eq. (5.11) except that the lower bounds of the double integration are changed from 0 to -1. The integrals are also included in Appendix B. Finally, the 9 x 9 stiffness matrix of the refined element is obtained as shown on the following page.

Substituting Eq. (5.20) into Eq. (5.14) and carrying out the integrations, the consistent load vector, for the case of uniform lateral loads is:

$$\{P_e\}^T = \frac{ptb}{3} \{1 \ 4 \ 1 \ 0 \ 0 \ 0 \ 0 \ 0 \ 0\} \quad (5.22)$$

$$[K_e] = \begin{bmatrix}
 1 & 7K_1 & & & & & & & & \\
 2 & -8K_1 & 16K_1 & & & & & & & \\
 3 & K_1 & -8K_1 & -7K_1 & & & & & & \\
 4 & 5K_2 & -4K_2 & -K_2 & K_3 & & & & & \\
 5 & 0.0 & 0.0 & 0.0 & K_4 & K_9 & & & & \\
 6 & -5K_2 & 4K_2 & K_2 & K_5 & K_4 & K_3 & & & \\
 7 & -K_2 & -4K_2 & 5K_2 & K_6 & K_7 & K_8 & K_3 & & \\
 8 & 0.0 & 0.0 & 0.0 & K_7 & K_{10} & K_7 & K_4 & K_9 & \\
 9 & K_2 & 4K_2 & -5K_2 & K_8 & K_7 & K_6 & K_5 & K_4 & K_3
 \end{bmatrix}$$

Sym.

1 2 3 4 5 6 7 8 9

(5.23)

in which

$$K_1 = \frac{t G_{xy}}{3r}$$

$$K_2 = \frac{1}{6} t G_{xy}$$

$$K_3 = t \left(\frac{2r}{15} E_Y + \frac{7}{9r} G_{xy} \right)$$

$$K_4 = \frac{1}{3} t \left(\frac{r}{5} E_Y - \frac{8}{3r} G_{xy} \right)$$

$$K_5 = -\frac{1}{6} t \left(\frac{r}{5} E_Y - \frac{2}{3r} G_{xy} \right)$$

$$K_6 = \frac{1}{6} t \left(\frac{r}{5} E_Y + \frac{1}{3r} G_{xy} \right)$$

$$K_7 = -t \left(\frac{r}{15} E_Y + \frac{4}{9r} G_{xy} \right)$$

$$K_8 = -\frac{1}{6} t \left(\frac{4r}{5} E_Y - \frac{7}{3r} G_{xy} \right)$$

$$K_9 = \frac{8}{3}t \left(\frac{r}{5} E_Y + \frac{2}{3r} G_{xy} \right)$$

$$K_{10} = -\frac{8}{3}t \left(\frac{r}{5} E_Y - \frac{1}{3r} G_{xy} \right)$$

where

$r =$ the aspect ratio ($r=a/b$).

For the case of linearly varying lateral loads, as shown in Fig. 5.2, the consistent load vector is:

$$\{P_e\}^T = \frac{p_c t b}{3} \{(1-2\alpha) \quad 4 \quad (1+2\alpha) \quad 0 \quad 0 \quad 0 \quad 0 \quad 0\}$$

(5.24)

in which

$$\alpha = \frac{(p_t - p_c)}{p_c}$$

p_t and $p_c =$ the intensity of the load at the top and the center of the element respectively, as shown in Fig. 5.2

It should be mentioned, however, that only lumped loads are used in the three-dimensional solution as will be shown later in Chapter VI.

5.5 NUMERICAL EXAMPLES

To test the efficiency (in terms of the accuracy versus the required computer time and storage) of the elements developed in Sections 5.3 and 5.4, five examples are considered. The ordinary element is employed in the first three examples and the last two examples are analyzed using the refined element. Also, to illustrate the versatility of the present method incorporating the newly developed elements, the examples are designed to include not only direct static analysis of slender multi-storey, multi-bay frames and those with relatively deep members, but also other aspects such as frames with variable properties, and stability analysis of frames.

The results in all the examples are compared with those obtained by "exact" and other simplified methods of analysis. For the purpose of comparison, member internal forces are divided into two categories, namely those termed "important" and the remainder as defined by De Clercq [34]. Such a division was suggested by the fact that the largest errors, expressed as a percentage, invariably occur near the top of the building, where member sizes tend to be determined by vertical loads rather than lateral loads. Member internal forces are termed "important" if larger than one third of the largest corresponding value recorded in the structure.

5.6.1 Example 5-1

The 20-storey wall frame structure of Khan and Stafford-Smith [61] considered in Chapter III, is reanalyzed (for the convenience of reference, the structure is shown in Fig. 5.3) using the ordinary element developed in Section 5.3. The structure is first replaced by an equivalent orthotropic membrane as in Example 3-1. The equivalent structure is then idealized using 48 ordinary elements; 4 across its width and 12 along its height, as shown in Fig. 5.4b. It should be noted that because of it being antisymmetrical, only one half of the structure need be considered. The results are compared to those of Khan and Stafford-Smith [61] based on a detailed finite element analysis using 1920 plane stress rectangular elements with two degrees of freedom at each node. A typical part of the mesh used is shown in Fig. 5.4a.

An excellent agreement is found between the present method and the detailed finite element of Reference [61], as shown in Figs. 5.5 and 5.6, which include the lateral deflection and a sample of the internal member forces, respectively. A total of 48 elements and 60 unknowns have been used by the present method versus 1920 elements and 4,000 unknowns in Khan and Stafford-Smith's mesh (Fig. 5.4), yet the difference in both the lateral deflection and member internal forces is less than 2%.

5.6.2 Example 5-2

The 52-storey slender frame of Bazant and Christensen [6] considered in the previous Chapter, is also reanalyzed. The finite element mesh of Fig. 4.1(f) will be used. The only change is that the rectangular element of Ammar and Nilson [3] is replaced by the ordinary element, (Section 5.3). The results obtained from the two elements are almost identical as to be expected, since the effect of E_x on the analysis was found to be negligible (Section 4.11). The ordinary element, however, resulted in a considerable reduction of the number of unknowns compared to that of Ammar and Nilson [3] (54.54% for this example structure, as shown in Table 5.1).

5.6.3 Example 5-3

The 20-storey, 12-bay frame with variable properties of De Clercq [34] is considered in this example. The properties of the beams and columns are varied along the height of the frame in six shifts, as shown in Fig. 5.7(a). The frame is subjected to a lateral uniform load of two-unit loads per storey. One-half of the frame is modelled, employing 24 ordinary elements, as shown in Fig. 5.7(b). The analysis is then carried out for the lateral deflection and column axial forces. The results are compared to the "exact" values obtained by De Clercq [34]. Excellent agreement between the results of the "exact" methods and

the present methods, is obtained as clearly illustrated by Figs. 5.7(c) and 5.8 for the maximum column axial forces and the lateral deflection. The error is less than 2% in the latter and 4% in the former. A variation of the shear forces (in the beam adjacent to the centre line of the structure) throughout the height is plotted and compared to that of the macroelement method and the "exact" method [34]. Although the variation of the shear obtained by the three methods is generally in good agreement (Fig. 5.9), the present method employs only 7.6% and 23.3% of the degrees of freedom, DOF, (number of unknowns) used in the "exact" and the macroelement methods, respectively. It can also be seen from Fig. 5.9, that the present method in general, is closer to the "exact" than the macroelement method [34].

In order to demonstrate further the efficiency of the present method versus that of the macroelement [34], the same 20-storey frame is reanalyzed (using the same mesh of Fig. 5.7(b)), but with constant properties such as that of zone-F (Fig. 5.7(d)). This time, in addition to the lateral deflection, the variation of the axial forces in the edge column throughout the height of the structure is considered. Again, the results are in excellent agreement with those obtained by the "exact" and the macroelement methods (as shown in Figs. 5.10 and 5.11), yet only 7.6% and 17.26% of the DOF required by the former and the latter methods, respectively, is used in the present method.

5.6.4 Example 5-4

In this example, the refined element developed in Section 5.4 is employed for the analysis of the same 52-storey frame considered previously in Example 5-2. A total number of 24 elements are used to model the equivalent structure, 3 across its width and 8 along its height, as shown in Fig. 5.12. This particular discretization is used to allow slightly less numbers of degrees of freedom than that used in the previous example, being 64 versus 72, respectively. (i.e., about 11% less), as given in Table 5.1. The analysis is also performed for the lateral deflection and column axial forces. The values of the lateral deflection obtained from the two analyses (using the ordinary and the refined elements, respectively) are almost identical (the maximum difference throughout the height of the structure being less than 0.34%). However, column axial forces obtained in this example (using the refined element) are more accurate than those of the previous example (using the ordinary element), especially at the third column from the outer edge, as shown in Fig. 5.13. This is due to the capacity of the refined element, inherent through its displacement model, to express the shear lag phenomenon more accurately than the ordinary element does.

5.6.5 Example 5-5

A stability (P- Δ) analysis of the 52-storey frame of Bazant and Christensen [6] is considered herein. In addition to the lateral loads of the previous example, the structure is subjected to a uniform compression of 2% of Euler buckling load of a typical column with both ends hinged. The frame is analyzed using the mesh shown in Fig. 5.12. The lateral deflection obtained using the present second-order analysis (Fig. 5.14) is in very good agreement with that obtained from both the "exact" and the micropolar by Bazant and Christensen [6]. However, unlike the first-order analysis (lateral load only) there is a slight deviation from the exact values which increases to a maximum value of less than 6% at the top of the structure. It should be noted that in spite of the close agreement among the three methods, only 64 DOF are used in the present method versus 1,872 in the "exact" and 648 in the micropolar method (i.e., using only 3.4% or 9.87% of the DOF used in the other two methods).

In summary;

- (1) Two plane stress, rectangular, specially orthotropic finite elements are developed. By incorporating the refined evaluation of the mechanical properties of the equivalent membrane given earlier in Chapter II, the two elements have proven to be efficient for

the analysis of slender multi-storey, multi-bay frames and those with relatively deep members, having constant and variable properties, under lateral load and considering the P- Δ effect.

- (2) The two elements are employed in five numerical examples. In the first three examples, the ordinary element is employed for the analysis of a 20-storey reinforced concrete wall-frame structure and a 52-storey steel frame, both being of constant properties. In the third example, a 20-storey frame with variable properties is considered. The refined element is then used, in Examples 4 and 5, for both the first-order lateral load analysis and that including the P- Δ effect of the same 52-storey steel frame, respectively. In all of the examples considered, the lateral deflection is very close to the "exact" values, the error being less than 2% except in the case of second-order (P- Δ) analysis, where it is less than 6%. Member internal forces, however, are in general, slightly less accurate than displacements, yet all important member internal forces had accuracies better than 96% except the shear force in the middle beam, in case of frames with variable properties, where the accuracy has dropped to 92.4%.

- (3) The ordinary element developed in Section 5.3 is more efficient, in the scope of the present work, than that of Ammar and Nilson [3], yielding almost the same accuracy and yet, considerably reducing the number of degrees of freedom in the analysis. Considering the structure in Example 5.2, the degrees of freedom are reduced from 132 to 72 (i.e. reduced to approximately 54.54%.)
- (4) The refined element can be recommended for the cases where the effect of shear lag is significant. This can be judged by the Engineering analyst and with the aid of the study of the behavioral characteristics of perforated walls presented previously in Chapter III. In the general computer program presented later in Appendix C, an option is given to the user to select the type of element to be used in the analysis.

TABLE 5.1 COMPARISON OF THE NUMBER OF UNKNOWN AND COMPUTER STORAGE

Data	"Exact" Reference [6]	Micropolar Reference [6]	Single Bay Frame Reference [62]	Present Method		
				A	B	C
Number of Unknowns	1,872	648	260	132	72	64
Computer Storage*	144,144	34,344	2,600	2,112	864	960
<p>* Evaluated as the storage required for the solution of the system of equilibrium equations.</p> <p>A Using the element of Ammar and Nilson [3] B Using the ordinary element C Using the refined element</p>						

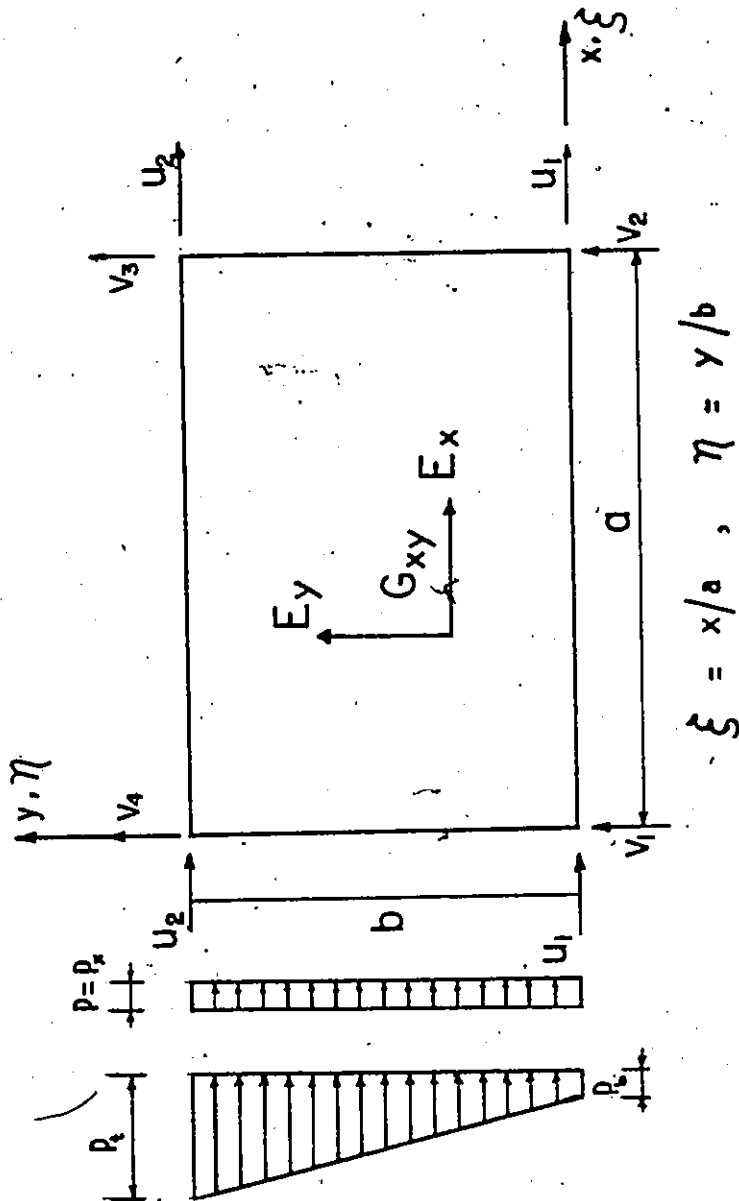


FIG. 5.1 THE ORDINARY ELEMENT

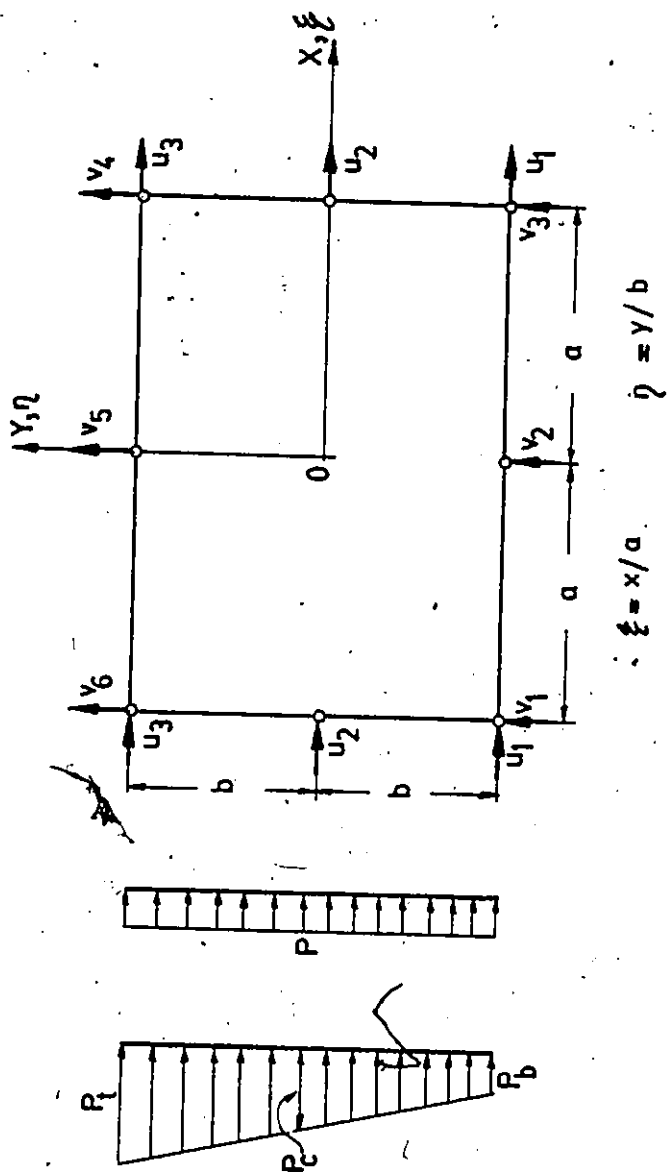


FIG. 5.2 THE REFINED ELEMENT

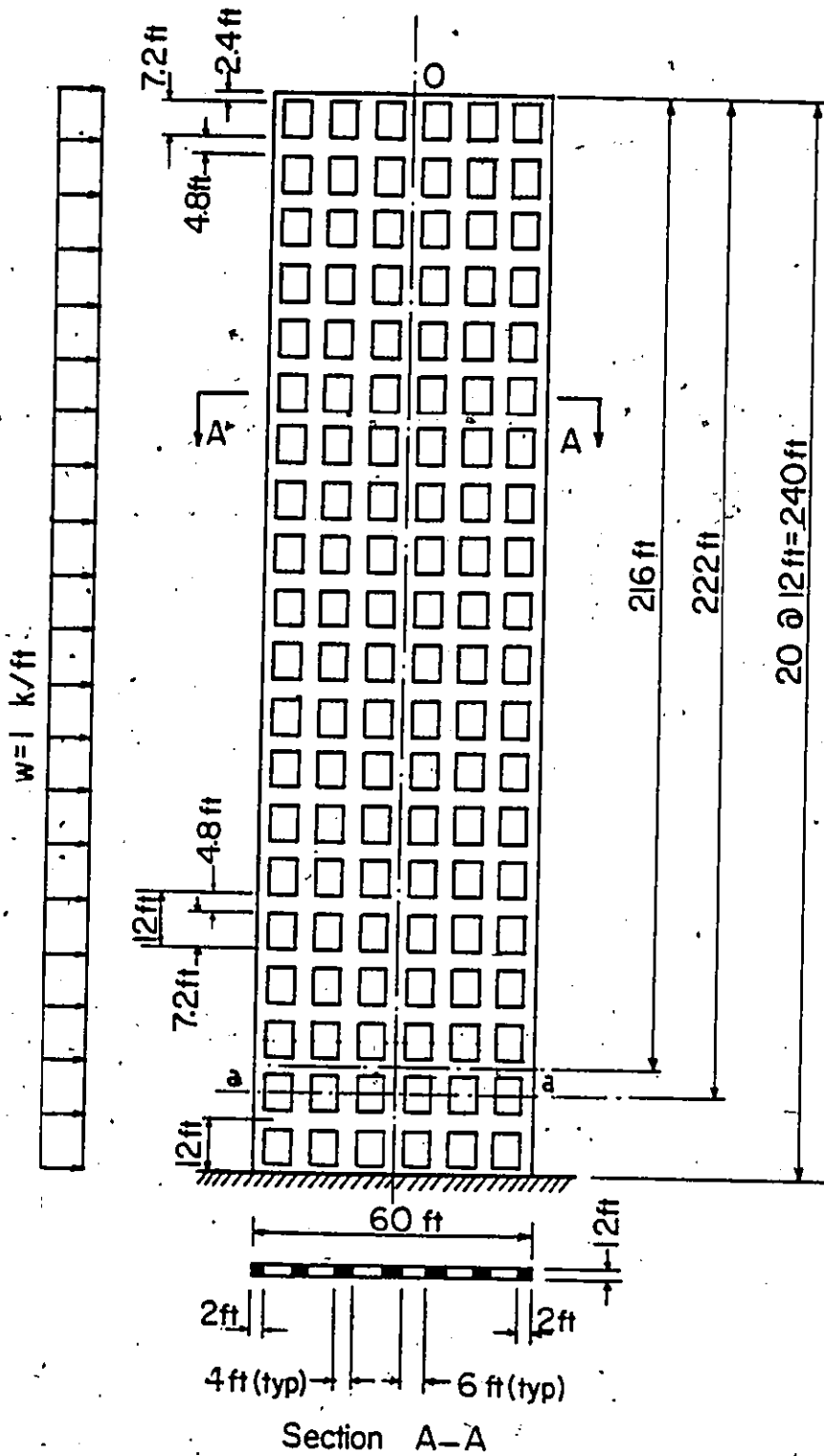


FIG. 5.3 20-STOREY WALL-FRAME STRUCTURE OF KHAN AND STAFFORD-SMITH [61] - EXAMPLE 5-1

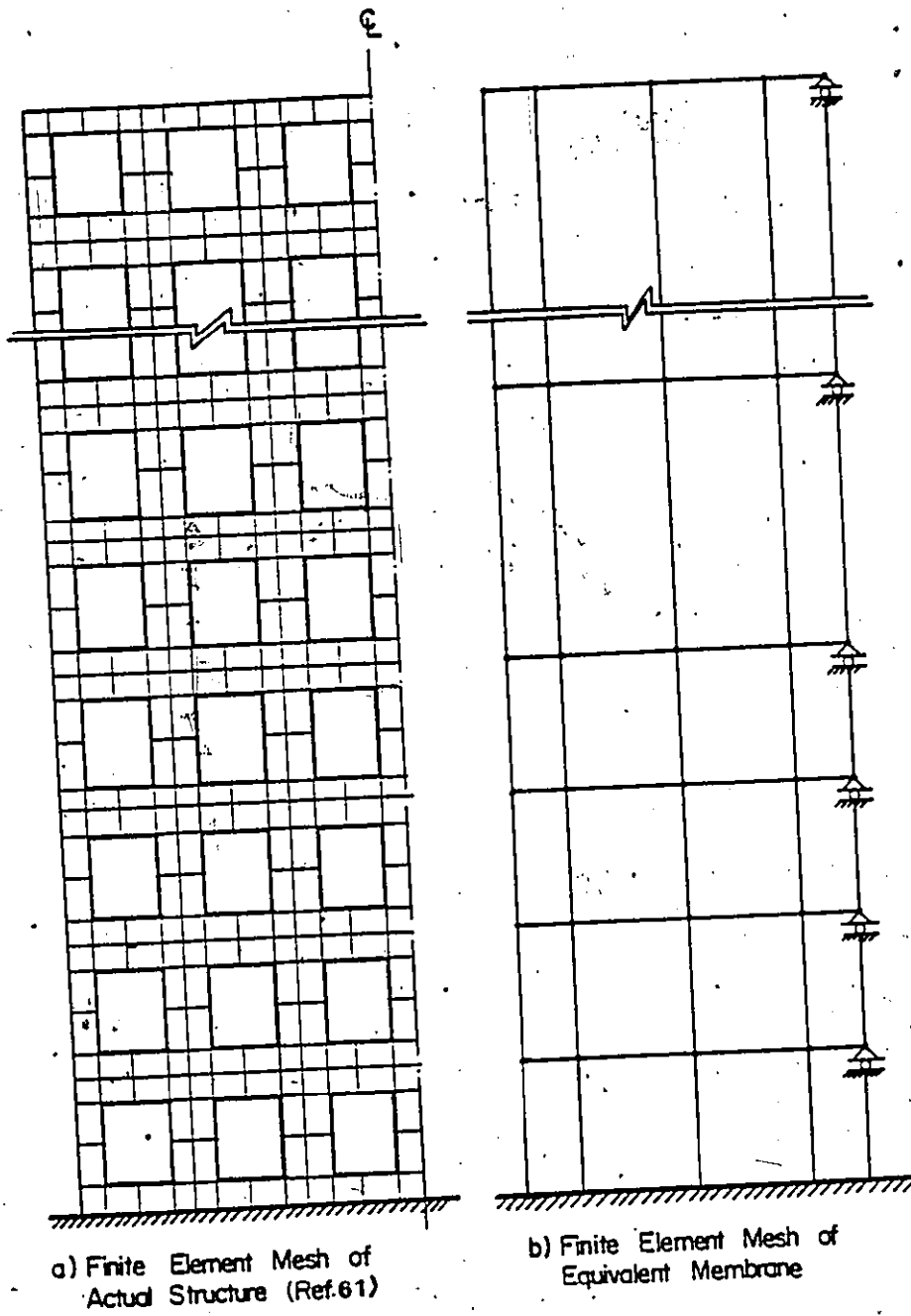


FIG. 5.4 STRUCTURE IDEALIZATION - EXAMPLE 5-1

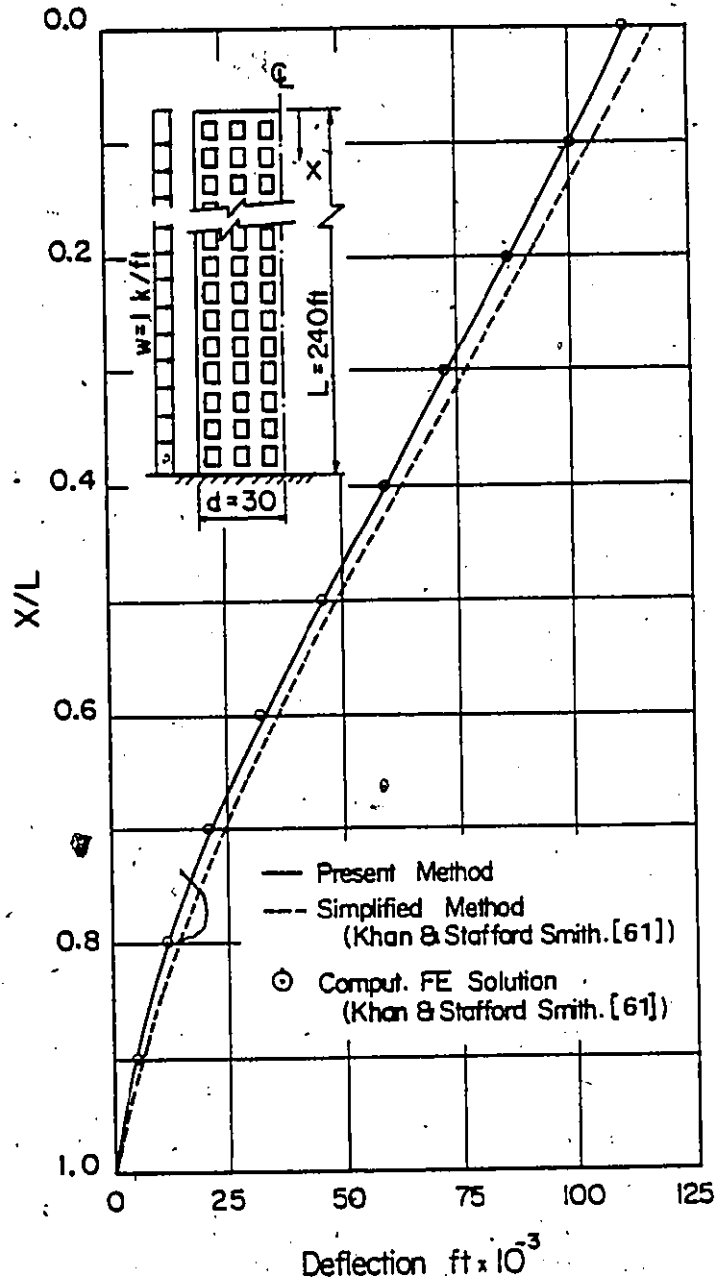


FIG. 5.5 LATERAL DEFLECTION - EXAMPLE 5-1

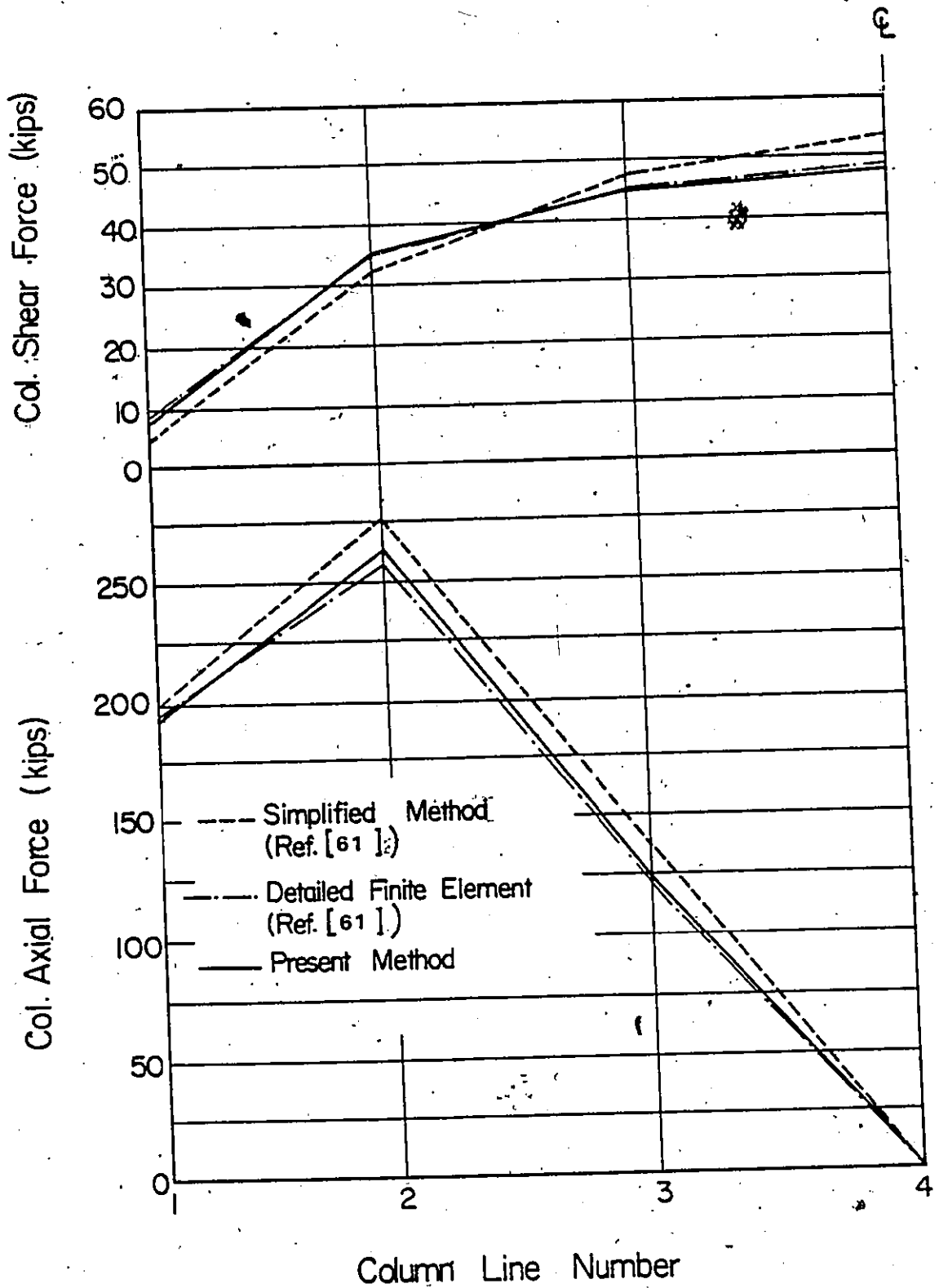
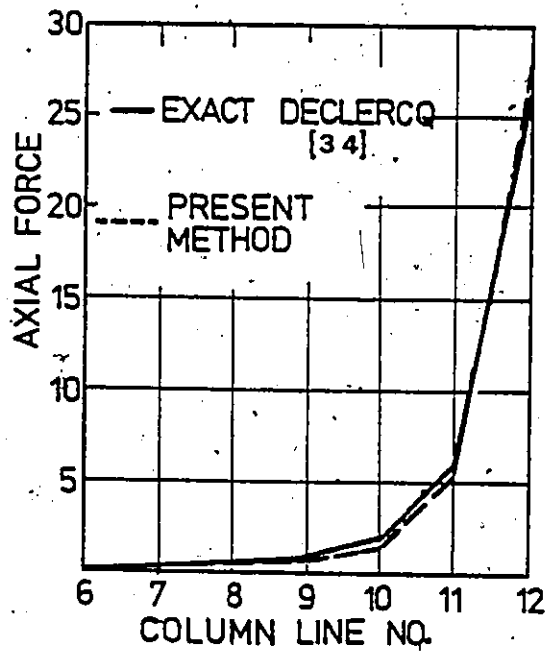
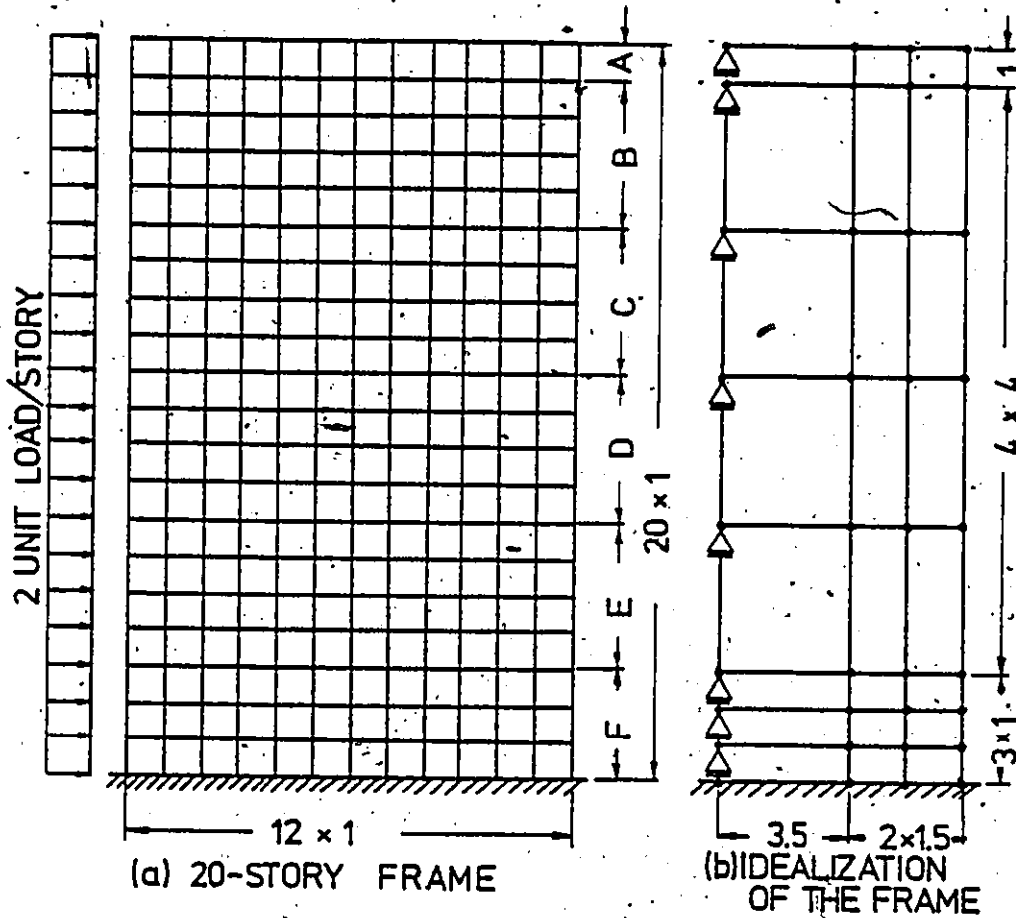


FIG. 5.6 MEMBER INTERNAL FORCES AT SECTION a-a
- EXAMPLE 5-1



ZONE	$\frac{I_b}{I_c}$	A_c
A	0.1	48
B	0.2	96
C	0.4	192
D	0.6	288
E	0.8	384
F	1.0	480

(c) MAXIMUM AXIAL FORCES

(d) MEMBER PROPERTIES

FIG. 5.7 20-STORY FRAME OF DECLERCQ [34]
- EXAMPLE 5-3

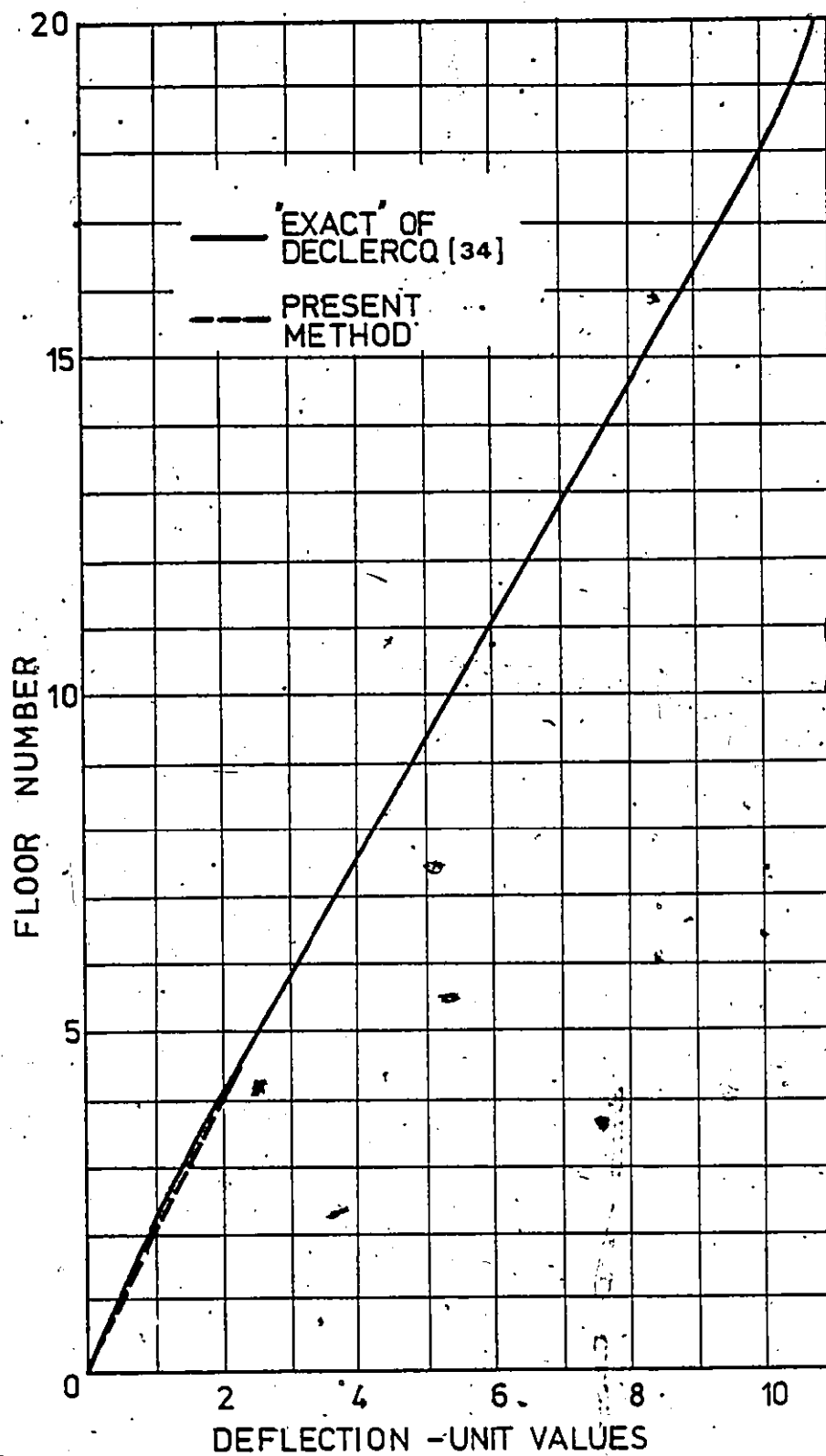


FIG. 5.8 LATERAL DEFLECTION - EXAMPLE 5-3 (VARIABLE PROPERTIES)

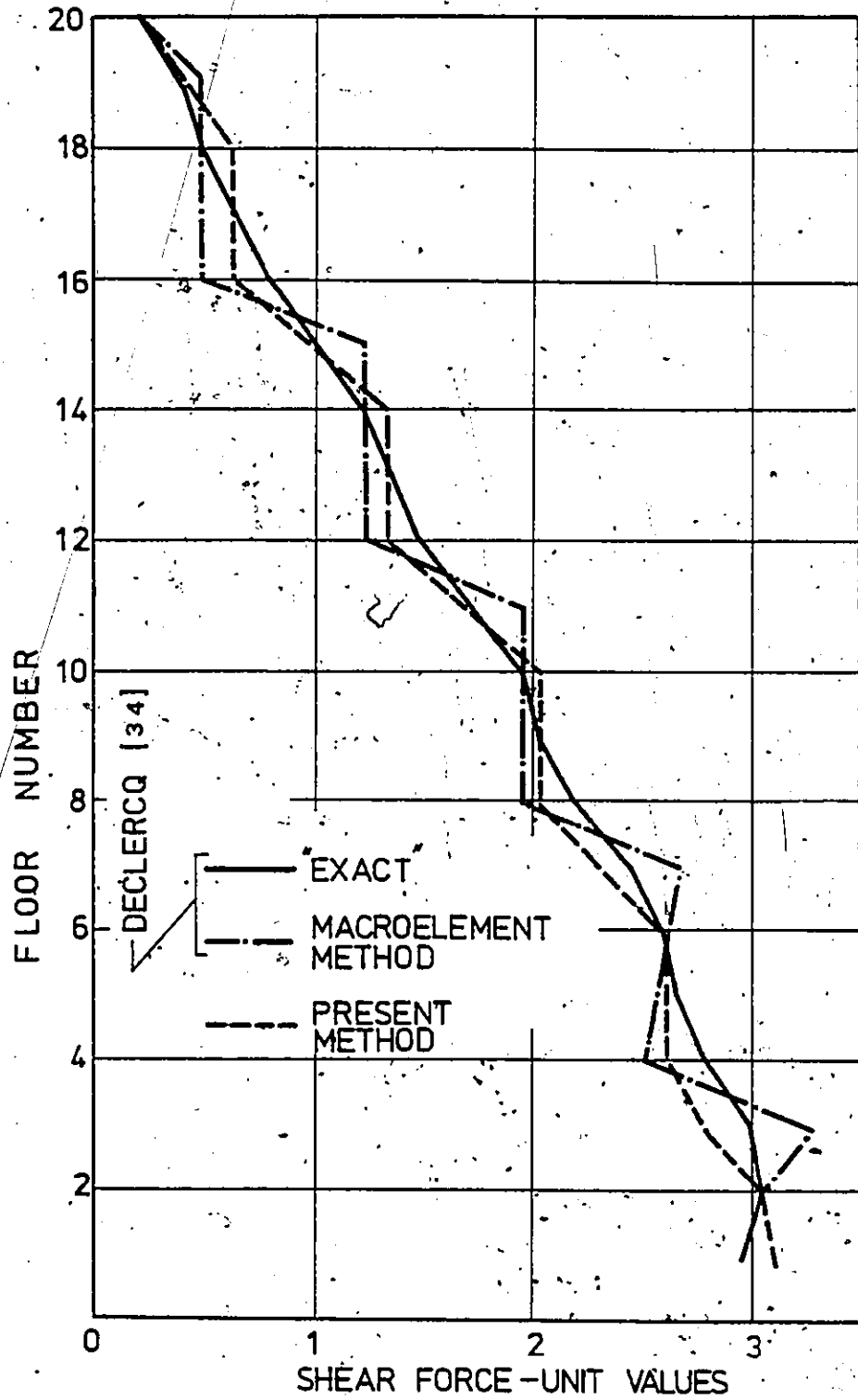


FIG. 5.9 VARIATION OF SHEAR IN MIDDLE BEAM - EXAMPLE 5-3
(VARIABLE PROPERTIES)

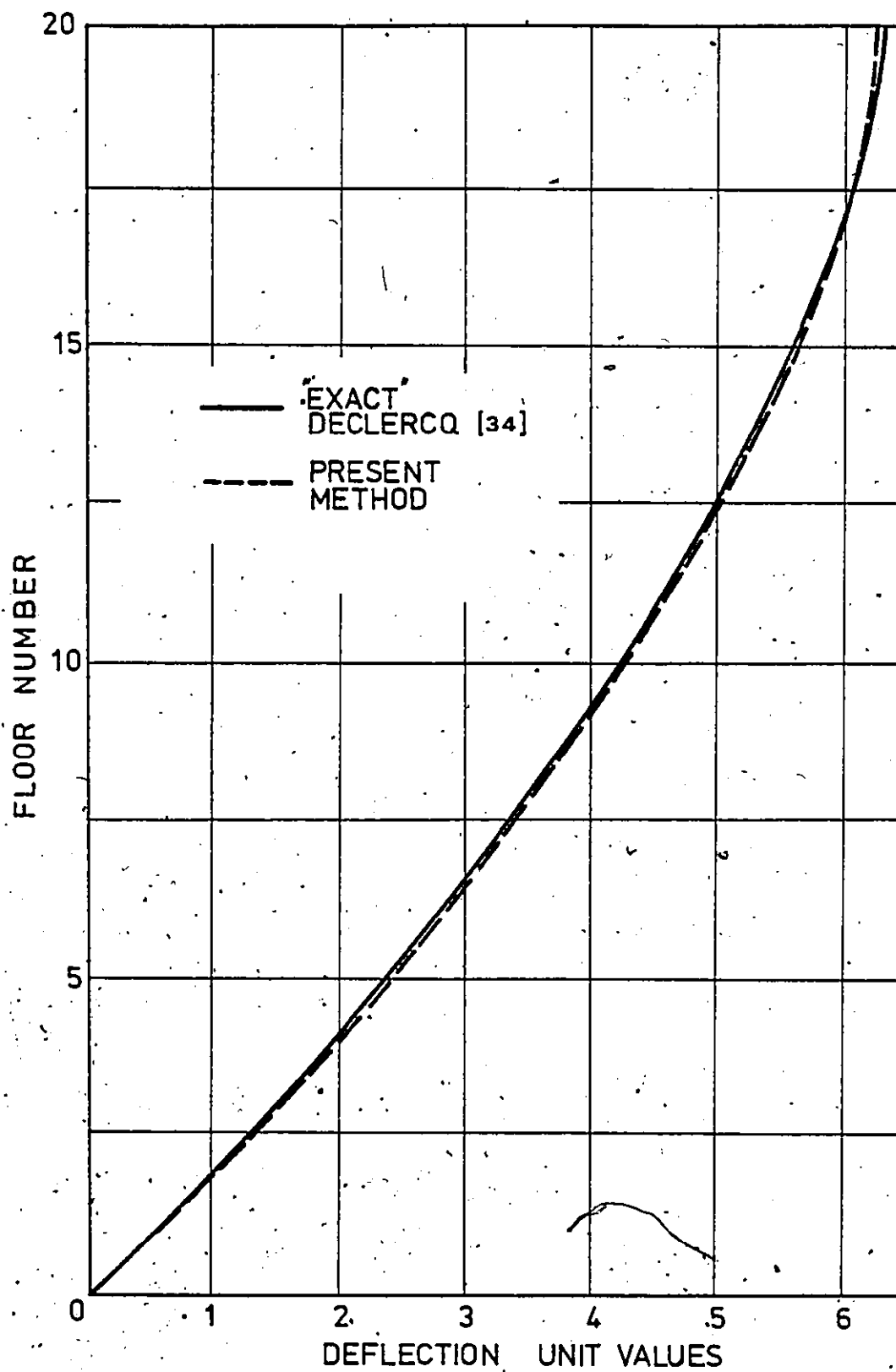


FIG. 5.10 LATERAL DEFLECTION - EXAMPLE 5-3 (CONSTANT PROPERTIES)

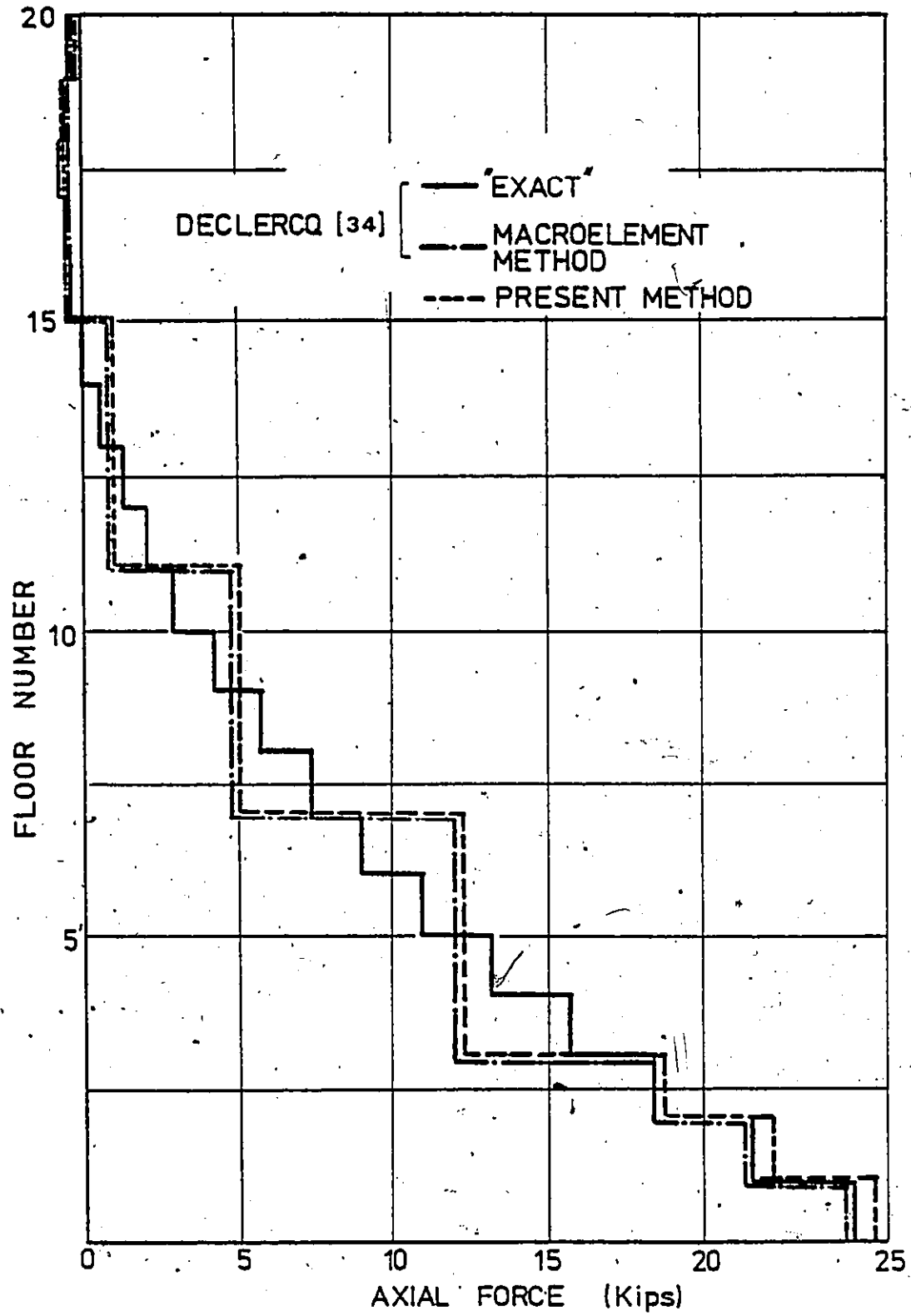


FIG.5.11 VARIATION OF AXIAL FORCE IN THE EDGE COLUMN OF EXAMPLE 5-3 (CONSTANT PROPERTIES)

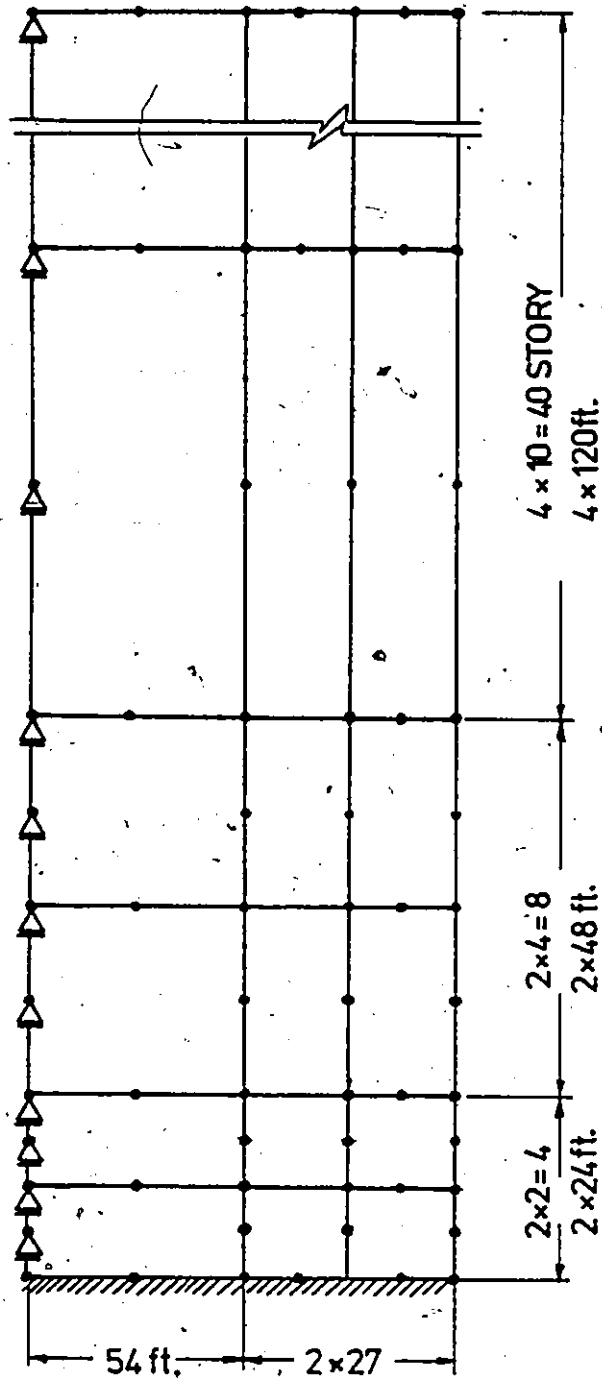


FIG. 5.12 STRUCTURE IDEALIZATION -
 EXAMPLES 5-4 and 5-5

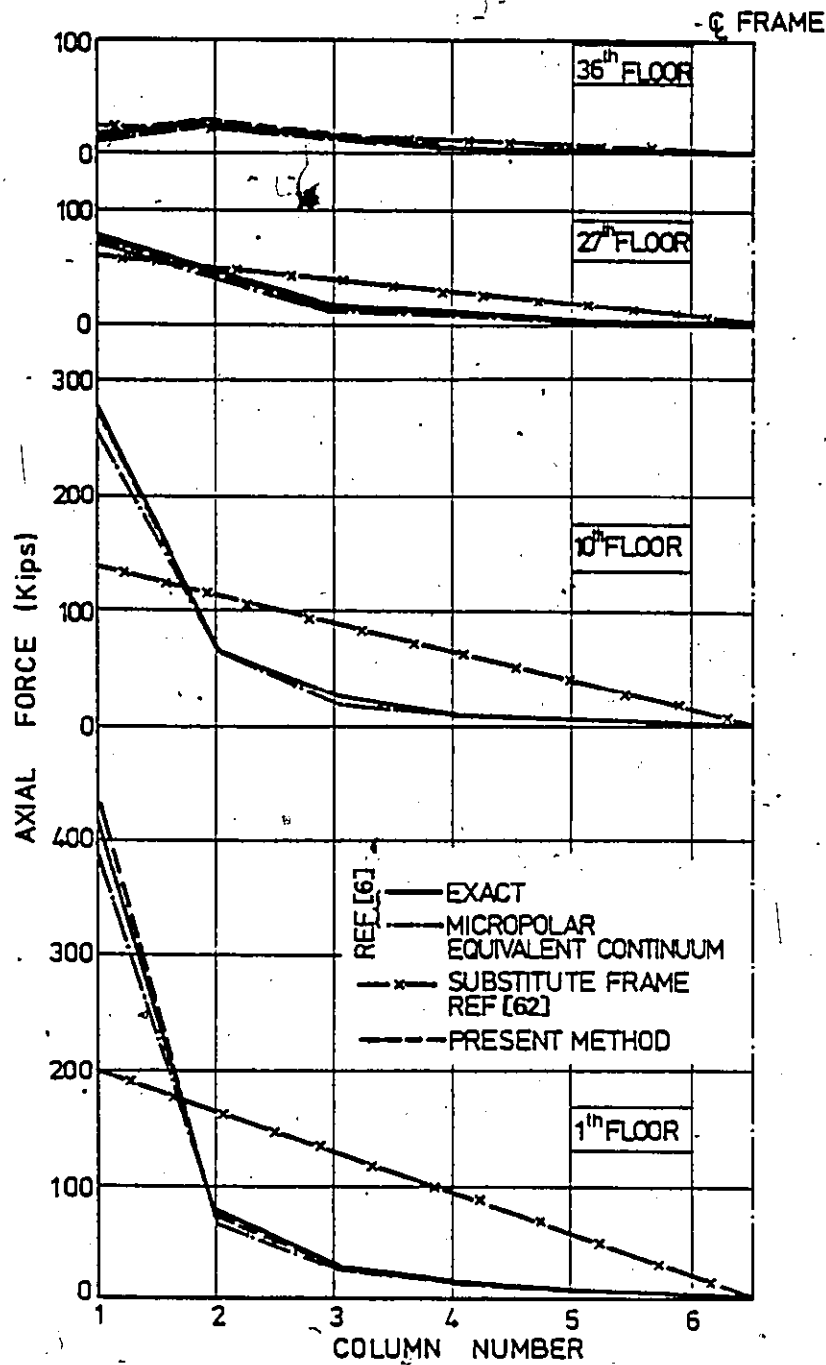


FIG. 5.13 DISTRIBUTION OF AXIAL COLUMN FORCES AT DIFFERENT FLOOR LEVELS - EXAMPLE 5-4

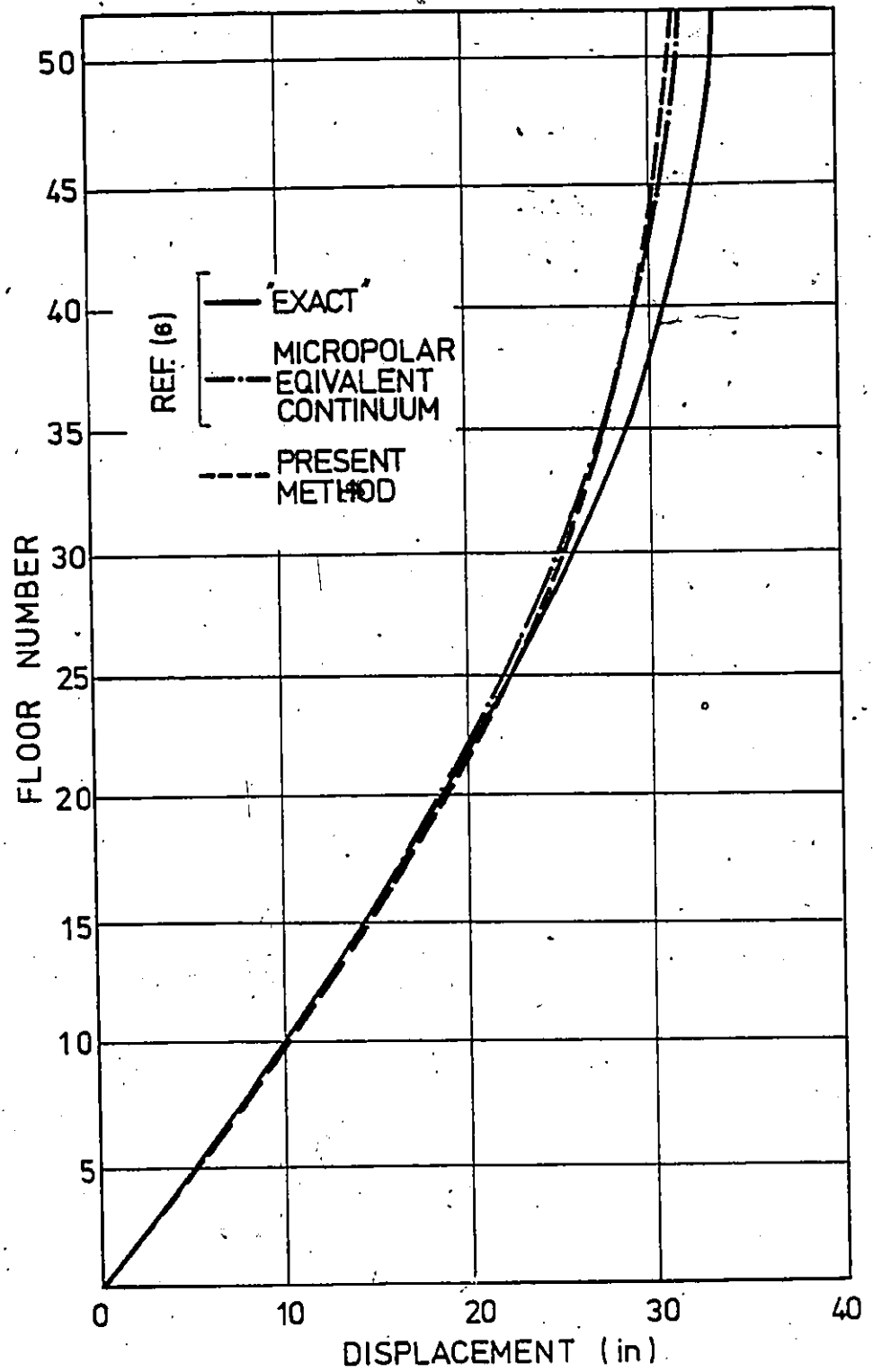


FIG. 5.14 LATERAL DEFLECTION INCLUDING P- Δ EFFECT - EXAMPLE 5-5

CHAPTER VI

ANALYSIS OF TUBE-TYPE TALL BUILDING
STRUCTURES

CHAPTER VI
ANALYSIS OF TUBE-TYPE TALL BUILDING
STRUCTURES

6.1 INTRODUCTION

Tube-like tall building structures may, in general, be assembled from rigid frames (framed tubes), or solid walls connected by bands of lintel beams (core-supported structures). A combination of frames and walls in a tube form is also possible [13]. Before developing the present technique, the literature on the analysis of framed tube and core-supported structures is reviewed.

Framed tube structures are generally composed of a large number of members, in the order of several thousands, interconnecting at the joints. An "exact" analysis of such structure using standard computer programs [54, 111] would be expensive, and the data preparation tedious. This type of analysis would then be impractical especially in the preliminary design stage where member sizes are in the trial stage and the design engineer wants to acquire some feeling of the behavior of the structure and to visualize the order of the design forces and the locations of their peak values. Also, in analyzing these tubular frameworks, the capacity of most currently available computers is overtaxed. The difficulty is further complicated if problems of dynamics, stability, and nonlinear behavior are considered.

Furthermore, it should also be kept in mind that the analysis is "exact" only for structures having slender members where the effect of finite size joints is negligible. However, framed tubes in general are characterized by finite size joints and neither ignoring their effect nor approximating it by introducing infinitely rigid arms would yield an "exact" solution. Ast and Schwaighofer [4] have shown that the latter approximation may result in reducing the lateral deflection of the former approximation by as much as 50% thus illustrating the importance of the effect of such joints. Recently, Khan and Stafford-Smith [61] have demonstrated, experimentally and through a detailed finite element analysis, that by neglecting finite size joints or modelling it by infinitely rigid arms, the lateral stiffness of the structure is underestimated and overestimated respectively.

Considering the approximate methods of analysis, it appears that the method proposed by the ACI Committee on response of buildings to lateral forces [1] is among the earliest ones introduced. In this method, two distinct types of behavior of framed tube structures are recognized, the usual shearing action of the side frames (frames parallel to the acting loads) and the cantilever bending action of the tube. Side frames are then assumed to resist the total horizontal shear force and analyzed by the portal method or other frame methods. In the cantilever bending action, to account

for the shear lag effect of normal frames, the tube structure is reduced to a pair of channels. Thus the shear lag effect of side frames is ignored.

By recognizing the dominant mode of behavior of the structure, Coull and Subedi [28] reduced the conventional three-dimensional analysis to an equivalent two-dimensional one. This was achieved by introducing fictitious connecting members at each storey level to transfer shears from the side to the normal frames which are considered to lie in the same plane as that of the side frames. The stiffnesses of these fictitious members were chosen to allow only for the transmission of shears between the side and normal frames. Although the method considerably reduces the number of unknowns required for the solution, it is restricted to framed tubes having rectangular shape in plan and under the action of bending only. Several investigators have resorted to the equivalent two-dimensional frame concept to establish a more simplified method of analysis.

Khan and Amin [67] have developed "influence curves" in conjunction with a simple reduction model technique for the simplified analysis of framed tubes having rectangular shape in plan and subjected to uniform lateral loads. The method is helpful not only in the preliminary design stage, but also in illustrating the behavior of framed tubes. The method, however, provides incomplete solutions which consider

only the cantilever bending action of the structure. Furthermore, the solutions are available only for the column axial forces and the shearing forces of the side frame beams at the bottom of the structure.

Schwaighofer and Ast [106] have presented tables for the preliminary analysis. The tables were obtained by carrying out a series of analyses, employing also the equivalent plane frame technique, on a range of framed tubes with different geometrical characteristics. The analyses are based on the lateral wind loads specified by the National Building Code of Canada. The tables, however, are only applicable to framed tubes having a square shape in plan and all beams and columns are assumed to have the same dimensions. The solutions are tabulated only for the side frames.

Chan [12], Khan [59], and Coull and Bose [32, 33] employed an energy approach to develop simplified methods of analysis. The discrete beam-column system was considered by Chan [12] and axial deformations of columns were assumed in terms of that of the corner columns. The latter were determined from the minimization of the total potential energy of the structure and subsequently member internal forces were evaluated. Khan [59] also assumed the chord-wise displacement, but for an equivalent isotropic tube. Internal forces in the actual structure were evaluated by some specially defined stress concentration factors. Both bending and torsional analyses were considered. The method is subject to

the same limitations stated earlier in Chapter III.

Coull and Bose [32] replaced the perforated tube by an equivalent orthotropic one. Chord-wise normal stresses were assumed instead of displacements, and the energy solution resulted in the planar stress components of the equivalent tube. Member internal forces, in the actual structure, were then obtained by integrating the corresponding stress component. The mechanical properties of the equivalent orthotropic membrane (or plate) were grossly approximated, as shown in Chapter II.

In all the previously mentioned methods, which are based on energy solution, only the structures having rectangular shape in plan and subjected to specific loadings can be analyzed. Structures are also assumed to have uniform properties everywhere (i.e., no variation of material and dimensions of members across the width of the structure and along its height). Also, in cases where high gradient of stress occurs across the frame facades, the assumed displacement or stress functions are inadequate and poor accuracy would be expected.

Of significant importance is the "Macroelement Method" advanced by De Clercq [34], in which, a macroelement may span several bays and stories of the original structure, and its deformation pattern is explicitly specified by some assumed displacement functions. Interior joint displacements with-

in the elements are then obtained in terms of those at the element nodes. The method considerably reduces the required computer time and storage. Structures with arbitrary shape in plan, variable properties, and subjected to arbitrary lateral loads can be efficiently analyzed. Although the method can account for the consideration of symmetry, this cannot be implemented when a facade includes an odd number of bays since an element must span a complete number of bays and storey heights. The effects of the $P-\Delta$ (stability), flexibility of finite size joints, and deformation of the supporting soil on the analysis were not considered. Finally, the method still requires considerable computer time and effort for data preparation, due to its lack of efficient transformation, assembly, and consideration of symmetry.

With regard to core-supported structures, these central cores which usually house elevators and service ducts provide the main lateral resistance of many high-rise buildings. The cores are basically nonplanar shear walls having either an open section [102, 113, 117] or partially closed section, coupled through a band or more of lintel beams or connecting slabs, at the floor levels [51, 60, 109, 112]. In general, the cores are subjected to torsion as well as to shear and bending. The torsion usually results from asymmetry of the cross-section of the core itself or of the applied lateral loads. The dimensions and behavior of the

cores are such that they may be classified as thin-walled beams [60,109]. Such structures when subjected to torsion suffer warping stresses which can be of the same order as the bending stresses [109,112,113]. Most of the presently available methods of analysis [9,10,50,51,60,94,102,109,112,113,117], except that presented recently by MacLeod and Hosny [82] are based on Vlasov's theory for thin-walled elastic beams [119] in conjunction with the continuous connection method [7]. In all methods based on Vlasov's theory, the total behavior of the structure is considered by superimposing the bending and the torsional analyses. Torsional moments are considered with respect to the shear centre of the core cross-section. Its location is commonly determined, based on an open section assumption, thus completely ignoring the effect of coupling beams. Recognizing that such an assumption may result in a significant reduction of the torsional stiffness of the structure, especially for cases of deep lintel beams, Khan and Stafford-Smith [60] have presented a method based on an equivalent closed section analysis to account for the shift of the shear centre due to the stiffness of the coupling beams.

MacLeod and Hosny [82] have presented a discrete frame method for the analysis of cores of rectangular shape in plan. It is a direct extension of the equivalent frame concept as applied to the analysis of planar coupled shear walls [49,78 to 81,104]. The method is simple and can be

readily incorporated into conventional frame computer programs. The method, however, requires the incorporation of a stiff member to brace the core cross-section against any distortion. The method cannot be applied to cores of arbitrary shape in cross-section due to its lack of proper coordinate transformation.

Each of the above-mentioned methods has its relative merits, and constitutes a forward step in meeting the persistent challenge of reducing the cost and effort of the analysis while improving the accuracy of the results. However these methods are subjected to a number of limitations, some of which have been already mentioned in the previous chapters. For example, (1) the effect of finite size joints is either neglected [28,67,90] or grossly approximated by introducing infinitely rigid arms to model these joints [4,12,32,34,83]; (2) "exact" analyses require large computer storage and time in addition to tedious data preparation; (3) simplified methods based on energy approach generally do not allow for the variation of geometry, loads, and structure properties; (4) while substitute frames [1,62,90] can provide reasonably accurate modelling under certain circumstances, their limitations are substantial, resulting in a very poor accuracy [6,34] as already shown in Chapter IV; (5) the macro-element method cannot be directly applied for the analysis of spatial shear wall assemblies. Flexibility of finite-size joints is also neglected. The method requires considerable effort for data preparation; and finally, (6) none of

these methods considers the second-order (stability) effects.

6.2 SCOPE

The method to be presented in this Chapter is for the analysis of ~~of~~ tube-type tall building structures with the following characteristics:

- 1) The behavior is elastic.
- 2) The structure may consist of an assembly of planar frames, or solid shear walls in conjunction with uniform bands of lintel beams, or any combination of these.
- 3) Planar frames consist only of rigidly connected vertical columns and horizontal beams.
- 4) Both static and stability analyses are considered under the same general assumptions stated earlier in Chapter I.

The present method is seen to combine both features of the ordinary finite element and macroelement [34] methods. In the former, an element represents only a small finite region within a structural member unlike the macroelement [34] and the element of the present method.

6.3 ANALYSIS PROCEDURE

The perforated tube of arbitrary cross-section is first replaced by an equivalent unperforated tube, as shown in Fig. 6.1. The equivalent structure is then idealized by an assemblage of rectangular plane stress elements developed in Chapter V. These elements are connected together only at the nodal points dividing the structure to a number of levels, as shown in Fig. 6.1(b). Adopting the assumption of rigid floor diaphragm, each story of the structure would have three degrees of freedom: two translations and a rotation in the plane of the floor. However, in order to maintain compatibility of the vertical displacements at the junction of any two facades, an additional degree of freedom corresponding to the vertical translation is introduced at each corner of the structure for each level. These degrees of freedom will be referred to as "global degrees of freedom" which may be associated with an arbitrary reference point in each level (Fig. 6.2). Other displacements associated with interior nodes within an individual facade are termed "internal facade degrees of freedom" which will be eliminated by static condensation before the global structure stiffness matrix is formed.

Solutions are first obtained for the global degrees of freedom, which then allow the recovery of the eliminated internal facade degrees of freedom. Stresses and hence,

member internal forces can be subsequently determined. The major steps in the analysis procedure are summarized below.

- 1) Assembly of the individual facade local stiffness matrix taking directly into account the boundary and symmetry conditions. The facades are assumed to have negligible resistance against out-of-plane deformations.
- 2) Condensation of all internal degrees of freedom in each facade stiffness matrix leaving only those at the edges of the facade.
- 3) Transformation of the condensed facade stiffness matrices into the global coordinate system taking into account the global symmetry conditions.
- 4) Assembly of the overall structure stiffness matrix from the transformed facade stiffness matrices obtained in the previous step.
- 5) Assembly of the overall load vector in the global axis system.
- 6) Solution for the global displacements or degrees of freedom.
- 7) Extraction and transformation of the external global nodal displacements of each facade into its local system.

- 8) Recovery of the internal local displacements of each facade and calculation of the stresses within each element.
- 9) Determination of member internal forces in the actual structure by integrating the corresponding stress component.

The above-mentioned steps are described in detail below, with particular attention given to the programming aspects.

6.4 STRUCTURE IDEALIZATION

To illustrate the rules and definitions which govern the process of idealization, the hypothetical framed tube structure shown in Fig. 6.1(a) is considered. It consists of an assembly of three vertical frames or "facades" intersecting each other at three "corners" (Fig. 6.1(c)). The facades are numbered in a counter-clockwise direction starting with the lower left corner with respect to the global coordinate system as shown in Figs. (6.1(a)) and (6.1(c)).

The actual framed tube is replaced by an equivalent orthotropic tube which is then discretized into a number of finite elements* (Fig. 6.1(b)) according to the following rules and definitions:

- 1) An element normally extends over one or more complete stories and one or more complete bays depending on the accuracy required. The boundary of the elements need not coincide with the lines of beams or columns as shown in Fig. 6.1(b). However, all elements at a given height in the building must include the same number of stories. Thus, the elements divide the structure into a number of levels called "structure levels" consecutively numbered from the bottom to the top as shown in Fig. 6.1.
- 2) Properties of the structure may vary across its width and along its height but not within an element. In other words, within each element the following properties must be constant: bay width and storey height; moment of inertia, area and shear area of columns; moment of inertia and shear area of beams; and finally, dimensions of the finite sized joints (i.e., column depth and beam depth.)
- 3) For each facade, the element corner nodes are numbered from the bottom to the top starting from the left to the right, as shown in Fig. 6.3(a). If the refined element is used, numbering of mid-height and mid-width element nodes are considered one after the other, starting after that of the

corner nodes and in the same fashion as the latter as shown in Fig. 6.3(b).

- 4) Element numbering system is independent of the type of element used in the analysis. Elements are numbered from the left to the right, starting from the bottom to the top, as shown in Figs. 6.3(a) and 6.3(b).
- 5) Element incidences or connectivity are specified by starting from the lower left corner node in a counter clock-wise manner.

The discretization process (node numbering, and element numbering, connectivity and type) is generated automatically from the given number of elements in the horizontal and vertical directions of each facade, thus reducing the effort in data preparation and at the same time eliminating possible data errors.

6.5 ASSEMBLY OF FACADE STIFFNESS MATRIX IN LOCAL AXES

Since the facade coordinate system coincides with that of its individual elements, the element stiffness matrices are assembled directly without transformation to form the facade stiffness matrix. At this stage, zero-dis-

placement at the boundaries to simulate the supports or possible symmetry conditions are imposed by not setting up the equilibrium equations corresponding to the restrained displacements. This allows some savings in computer storage and computation time especially in cases of symmetry. The bottom nodes (i.e., level 0) are assumed to be fixed; however, the effect of foundation settlement can be taken into account by introducing a bottom strip of elements simulating the supporting soil.

In the present method, symmetry is considered at two levels: global structure level, and local facade level. The latter may not exist with the presence of the former, but not the reverse. Facade stiffness matrix is assembled element-by-element according to the degrees of freedom associated with each element. These degrees of freedom are generated differently according to the type of facade symmetry as follows:

6.5.1 No Symmetry

In this case degrees of freedom are assigned as shown in Figs. 6.4(a) and 6.4(b) for the ordinary and refined element assemblies, respectively. In the case of the ordinary element, lateral degrees of freedom are assigned first starting from the bottom to the top, i.e., identical to the level numbering. Vertical degrees of freedom are then assigned sequentially to the nodes of the leftmost

edge, rightmost edge, and those in between in that order, starting from the bottom to the top, as shown in Fig. 6.4(a). In the case of the refined element, degrees of freedom are assigned to nodes on the exterior, lateral mid-height, vertical interior at corners, and finally vertical interior at mid-width in that order, exactly the same as the previous case (Fig. 6.4(b)).

6.5.2 Symmetry Type One

If the normal stress (σ_y), which represents the distribution of column axial forces, is symmetrical about the center line of a facade, only one half of this facade need be considered with all nodes at the line of symmetry restrained from lateral movement (Figs. 6.4(c) and 6.4(d)). Degrees of freedom are assigned exactly in the same order and fashion as that given in the previous section.

6.5.3 Symmetry Type Two

This type of symmetry describes an anti-symmetric distribution of column axial forces in the facade and only the half of the facade on the left is to be considered. In this case, the vertical movements of all nodes on the symmetry axis are restrained. Degrees of freedom are then assigned following the same format given in Section 6.5.1, as shown in Figs. 6.4(e) and 6.4(f), according to the type

of elements.

6.5.4 Symmetry Type Three

This type of symmetry within a facade is similar to type two, except that the right half of the facade is being analyzed, and thus vertical displacements of all nodes on the symmetry axis are restrained (Fig. 6.4(g) and 6.4(h)).

In the computer program described in the last Appendix, the facade degrees of freedom are generated automatically, incorporating the details given in the previous sections.

Since the facade stiffness matrix, $[K_F]$, is symmetric, only its upper triangle is assembled and stored.

$$[K_F] = \begin{bmatrix} K_{11} & K_{12} & \dots & K_{1j} & \dots & K_{1n} \\ & K_{22} & \dots & K_{2j} & \dots & K_{2n} \\ & & & K_{ij} & \dots & K_{in} \\ & & & & & K_{nn} \end{bmatrix} \quad (6.1)$$

in which

n = total number of degrees of freedom of a facade

For the efficient use of computer storage, $[K_F]$ is stored in a singly subscripted array column-by-column

$$[K_F] = \{a_1 \ a_2 \ \dots \ a_\ell \ \dots \ a_m\} \quad (6.2)$$

in which

ℓ = storage location of the element K_{ij} (Eq.6.1)

in the row matrix (Eq.6.2) and

m = the order of the row matrix given by

$$m = n(n+1)/2 \quad (6.3)$$

The mapping function is

$$\ell = i + \{(j-1)j\}/2 \quad (6.4)$$

6.6 CONDENSATION OF FACADE INTERNAL DEGREES OF FREEDOM

In an effort to minimize the computer storage requirement as well as the computation time, the facade internal degrees of freedom (i.e. those not required for maintaining compatibility with the adjacent facades) are eliminated by the process of static condensation which is briefly described below. [46].

The facade stiffness equation may be written in partitioned form as

$$\begin{bmatrix} [K_{11}] & [K_{12}] \\ [K_{21}] & [K_{22}] \end{bmatrix} \begin{Bmatrix} \{d_r\} \\ \{d_e\} \end{Bmatrix} = \begin{Bmatrix} \{P_r\} \\ \{P_e\} \end{Bmatrix} \quad (6.5)$$

in which

$\{d_r\}$ and $\{d_e\}$ = the remaining and eliminated degrees of freedom, respectively.

Expanding Eq. (6.5) and solving for $\{d_e\}$ gives

$$\{d_e\} = [K_{22}]^{-1} [K_{21}] \{d_r\} + [K_{22}]^{-1} \{P_e\} \quad (6.6)$$

Substituting this result into the first part of Eq. (6.5) yields

$$[\bar{K}_r] \{d_r\} = \{\bar{P}_r\} \quad (6.7)$$

in which $[\bar{K}_r]$ and $\{\bar{P}_r\}$ are the "reduced" or condensed facade stiffness matrix and load vectors, respectively, and are defined by

$$[\bar{K}_r] = [K_{11}] - [K_{12}] [K_{22}]^{-1} [K_{21}] \quad (6.8)$$

$$\{\bar{P}_r\} = \{P_r\} - [K_{12}] [K_{22}]^{-1} \{P_e\} \quad (6.9)$$

The static condensation procedure described by Eqs. (6.8) and (6.9) is not suitable for digital computation and can be more efficiently carried out by a symmetric backward Gaussian elimination which is quite well known [11]. Wilson [25] has given a FORTRAN routine to perform this

operation; however, it is applicable only when the full storage for the stiffness matrix is provided. The main structure of Wilson's routine is adapted to the present triangular storage scheme and also extended for other operations.

After a partial backward elimination of the unknowns $\{d_r\}$ has been completed, Eq. (6.5) has the form

$$\begin{bmatrix} [\bar{K}_{11}] & [0] \\ [\bar{K}_{21}] & [\bar{K}_{22}] \end{bmatrix} \begin{Bmatrix} \{d_r\} \\ \{d_e\} \end{Bmatrix} = \begin{Bmatrix} \{\bar{P}_r\} \\ \{\bar{P}_e\} \end{Bmatrix} \quad (6.10)$$

In this equation the elements of the submatrix $[\bar{K}_{22}]$ above the main diagonal are all zero's, and the submatrix $[\bar{K}_{11}]$ directly represents the required condensed facade stiffness matrix $[\bar{K}_F]$.

It should also be noted that the above condensation procedure, as described by Eq. (6.10) can directly be used for the solution of any system of linear algebraic equations having the form of Eq. (6.7). The solution can be achieved by setting the number of the remaining degrees of freedom to one, in Eq. (6.10). This would result in a complete backward elimination of all but the first unknown, and thus only a forward substitution is required to obtain the rest of the unknowns.

Finally, the eliminated or condensed displacements $\{d_e\}$ can simply be "recovered" after the determination of the remaining displacements $\{d_r\}$ by a forward substitution starting from the row $NR + 1$ of Eq. (6.10), where NR is the number of the remaining degrees of freedom.

6.7 ASSEMBLY OF THE GLOBAL STRUCTURE STIFFNESS MATRIX

Since the in-plane stiffness of a facade can resist both translation and twisting of the three-dimensional structure and the facade could be arbitrarily located in the plan, it is necessary to transform the condensed facade stiffness matrix of the previous section into the global coordinate system. This may be done by means of the transformation matrix T defined as

$$\{d_r\} = [T] \{d_r^*\} \quad (6.11)$$

in which

$\{d_r^*\}$ = a set of global degrees of freedom affecting the facade deformations

To facilitate the presentation and the derivation of the transformation matrix $[T]$, a specific ordering system of the global as well as the local facade degrees of freedom is chosen:

$$\{d_I\}_{3L \times 1} = \left\{ \begin{array}{l} \{\Delta\}_{L \times 1} \\ \{\omega_I\}_{L \times 1} \\ \{\omega_J\}_{L \times 1} \end{array} \right\} \quad (6.12)$$

and

$$\{d_I^*\}_{5L \times 1} = \left\{ \begin{array}{l} \{d_C\}_{3L \times 1} \\ \{\omega_I\}_{L \times 1} \\ \{\omega_J\}_{L \times 1} \end{array} \right\} \quad (6.13)$$

in which .

$\{\Delta\}$ = the lateral degrees of freedom at each level in the facade with respect to the local axis system

$\{\omega_I\}$ and $\{\omega_J\}$ = the vertical degrees of freedom at each level along the two edges of the facade in both the local and global coordinate systems

$\{d_C\}$ = the degrees of freedom associated with the arbitrarily located centre or reference point at each level, and is defined by

$$\{d_C\}^T = \{u_1 \ v_1 \ \theta_1 \ u_2 \ v_2 \ \theta_2 \ \dots \ u_L \ v_L \ \theta_L\} \quad (6.14)$$

L = number of levels

To derive the transformation matrix T , the effects of translations and twisting of the building on the lateral in-plane local displacement of the facade are first considered.

Refer to Fig. 6.2, the lateral displacement of the facade at level i can be written as

$$\Delta_i = \{\cos\alpha \ \sin\alpha \ D\} \begin{Bmatrix} u_i \\ v_i \\ \theta_i \end{Bmatrix} \quad (6.15)$$

in which

α = the angle measured from the x-axis to the positive direction of the facade (Fig. 6.2).

It should be noted that the positive direction of the facade is from the first specified edge to the other edge (i.e., facade 1-2 \neq facade 2-1).

D = the perpendicular distance between the facade and the z-axis.

Let $\{\cos\alpha \ \sin\alpha \ D\}$ be denoted as $\{\lambda\}$, Eq. (6.15) can be generalized for L levels:

$$\{\Delta\}_{L \times 1} = [T_1] \{d_c\}_{3L \times 1} \quad (6.16)$$

in which

$$[T_1] = \begin{bmatrix} \{\lambda\} & & & \\ & \{\lambda\} & & \\ & & \ddots & \\ & & & \{\lambda\} \end{bmatrix}_{L \times 3L} \quad (6.17)$$

The complete transformation matrix $[T]$ can now be written

$$[T] = \begin{bmatrix} [T_1] & & & \\ & [I]_{L \times L} & & \\ & & [I]_{L \times L} & \\ & & & [I]_{L \times L} \end{bmatrix} \quad (6.18)$$

where the identity matrix $[I]$ reflects the fact that the vertical displacements of the corner nodes are the same in both the global and local coordinate systems.

From Eq. (6.11), the contragradient law of transformation yields

$$\{\bar{P}_R^*\} = [T]^T \{\bar{P}_R\} \quad (6.19)$$

which, by substituting Eq. (6.7) into it, becomes

$$\{\bar{P}_R^*\} = [T]^T [\bar{K}_F] \{d_R\} \quad (6.20)$$

From Eq. (6.11), the above equation can further be written in the form

$$\{\bar{P}_R^*\} = [T]^T [\bar{K}_F] [T] \{d_R^*\} \quad (6.21)$$

Thus the transformed stiffness matrix can be recognized as

$$[\bar{K}_F^*] = [T]^T [\bar{K}_F] [T] \quad (6.22)$$

The transformation described above requires storage and manipulation of large matrices and is not convenient for programming purposes. A more efficient scheme can be achieved by rearranging the order of numbering for the degrees of freedom.

Let $\{d_i\}$ represent the three local displacements of level i in the sequence: lateral displacement, vertical displacements of the left and right edges, respectively. The local facade stiffness matrix can be written in the form

$$\begin{Bmatrix} P_1 \\ P_2 \\ \vdots \\ P_i \\ \vdots \\ P_n \end{Bmatrix}_{3L \times 1} = \begin{bmatrix} K_{11} & K_{12} & \dots & K_{1i} & \dots & K_{1L} \\ & K_{22} & \dots & K_{2i} & \dots & K_{2L} \\ & & & & & \\ & & & K_{ii} & \dots & K_{iL} \\ & & & & & \\ & & & & & K_{LL} \end{bmatrix}_{3L \times 3L} \begin{Bmatrix} d_1 \\ d_2 \\ \vdots \\ d_i \\ \vdots \\ d_n \end{Bmatrix}_{3L \times 1} \quad (6.23)$$

in which K_{ij} is a 3×3 sub-matrix representing the stiff-

ness coupling of the i^{th} level with the j^{th} level. In actual programming, all the terms of the sub-matrix $[K_{ij}]$ can be extracted from the upper triangle of the condensed facade stiffness matrix of Eq. (6.23).

The global degrees of freedom at the i^{th} level (Fig. 6.2) are also grouped together in the vector $\{d_i^*\}$ defined as

$$\{d_i^*\}^T = \{u_i \ v_i \ \theta_i \ \omega_{1i} \ \omega_{2i}\} \quad (6.24)$$

The local displacements at the i^{th} level $\{d_i\}$ are related to those in the global system $\{d_i^*\}$ as follows:

$$\{d_i\} = [T_i] \{d_i^*\} \quad (6.25)$$

The transformation matrix for the complete facade is

now

$$[T] = \begin{bmatrix} [T_1]_{3 \times 5} & & & & \\ & [T_2]_{3 \times 5} & & & \\ & & \ddots & & \\ & & & \ddots & \\ & & & & [T_L]_{3 \times 5} \end{bmatrix} \quad (6.26)$$

and the transformed stiffness matrix of Eq. (6.22) making use of Eqs. (6.26) and (6.23) yields the following express-

ion

$$[K_{ij}^*] = [T_i]^T [K_{ij}] [T_j] \quad (6.27)$$

Thus, the transformation is now performed for the sub-matrices $[K_{ij}]$ one by one, instead of the complete facade stiffness matrix. It should be noted that for all the types of structures considered throughout this thesis $[T_i]$ equals $[T_j]$.

For the case of no symmetry, there are five global displacements at each level. The transformation matrix $[T_i]$ is

$$[T_i] = \begin{matrix} & \begin{matrix} u & v & \theta & \omega_1 & \omega_2 \end{matrix} \\ \begin{matrix} \text{cosa} & \text{sina} & D & 0 & 0 \\ 0 & 0 & 0 & 1 & 0 \\ 0 & 0 & 0 & 0 & 1 \end{matrix} \end{matrix} \quad (6.28)$$

Having transformed the condensed facade stiffness matrices, the overall global structure stiffness matrix $[K_s]$ is assembled by direct summation of all individual global stiffness sub-matrices $[K_{ij}^*]$ in each facade and only its upper triangle is stored in a row fashion as that of a facade (Eq. 6.2).

6.8 TRANSFORMATION MATRICES FOR DIFFERENT STRUCTURAL SYMMETRY CONDITIONS

Symmetry conditions of loading and geometry would allow significant reduction of data input, as well as comput-

er storage and time. To take advantage of this, the arbitrary reference point where global degrees of freedom are attached must be located on the symmetry axis.

For the case of structural symmetry Type 1, the structure is restrained from twisting and translating in the y-direction. The remaining global degrees of freedom are the x-displacement and the vertical displacements at the corners. The transformation matrix is modified, in this case, to

$$[T_i]_1 = \begin{matrix} & u & \omega_1 & \omega_2 \\ \begin{bmatrix} \cos\alpha & 0 & 0 \\ 0 & 1 & 0 \\ 0 & 0 & 1 \end{bmatrix} & & & \end{matrix} \quad (6.29)$$

The structural symmetry Type 2 is similar to the above type except that the x-displacement is restrained instead of the y-displacement. The appropriate transformation matrix is

$$[T_i]_2 = \begin{matrix} & v & \omega_1 & \omega_2 \\ \begin{bmatrix} \sin\alpha & 0 & 0 \\ 0 & 1 & 0 \\ 0 & 0 & 1 \end{bmatrix} & & & \end{matrix} \quad (6.30)$$

If the loading and the geometry are such that only twisting occurs, the appropriate transformation matrix for this third type of structural symmetry is

$$[T_i]_3 = \begin{matrix} & \theta & \omega_1 & \omega_2 \\ \begin{bmatrix} D & 0 & 0 \\ 0 & 1 & 0 \\ 0 & 0 & 1 \end{bmatrix} & & & \end{matrix} \quad (6.31)$$

It should be noted that the sub-matrix $[K_{ij}]$ of Eq. (6.27) is normally of order 3×3 and its terms can be extracted from the condensed facade stiffness matrix. However, when symmetry of a facade is considered, the order of the sub-matrix $[K_{ij}]$ is reduced to 2×2 which is then extended to size 3×3 before performing the transformation to allow the use of the above transformation matrices (Eqs. (6.29) to (6.31)).

6.9 SOLUTION FOR DISPLACEMENTS

Nodal displacements are determined in two stages: the first stage deals with the global structure displacements, and the second considers the local displacements of nodes within each facade.

Having established the global structure stiffness matrix and the associated overall load vector, the global structure displacements can now be obtained by solving the set of equations

$$\{P^*\} = [K_s^*] \{d^*\} \quad (6.32)$$

The solution technique is based on Gauss elimination as was described in Section 6.6.

Determination of the local internal nodal displacements within each facade is now considered in the second stage. Considering each facade at a time, the global displacements associated with it are first extracted from those obtained in the first stage for the whole structure. These extracted displacements are then transformed (Eqs. (6.28) to (6.31)) to the local facade system level by level. The latter displacements constitute the remaining facade degrees of freedom which can be used to recover the internal nodal displacements, as explained in Section 6.6.

6.10 DETERMINATION OF STRESSES

The facade nodal displacements are then extracted to yield the displacements associated with each element within the facade and subsequently the strains and stresses are calculated as given in Chapter V. It should be remembered that these stresses are for the facade membrane. Member internal forces of the actual discrete beam-column system of the actual structures are evaluated, based on these stresses, as described in Chapter III.

6.11 COMPUTER PROGRAM

A large capacity computer program (program TUBE) was developed for the analysis of most currently available planar and tubular structural systems for tall buildings. The program incorporates not only the theoretical developments of this chapter, but also those of Chapters II, III, and V. A description, user's guide, and FORTRAN listing of the program are presented in Appendix C.

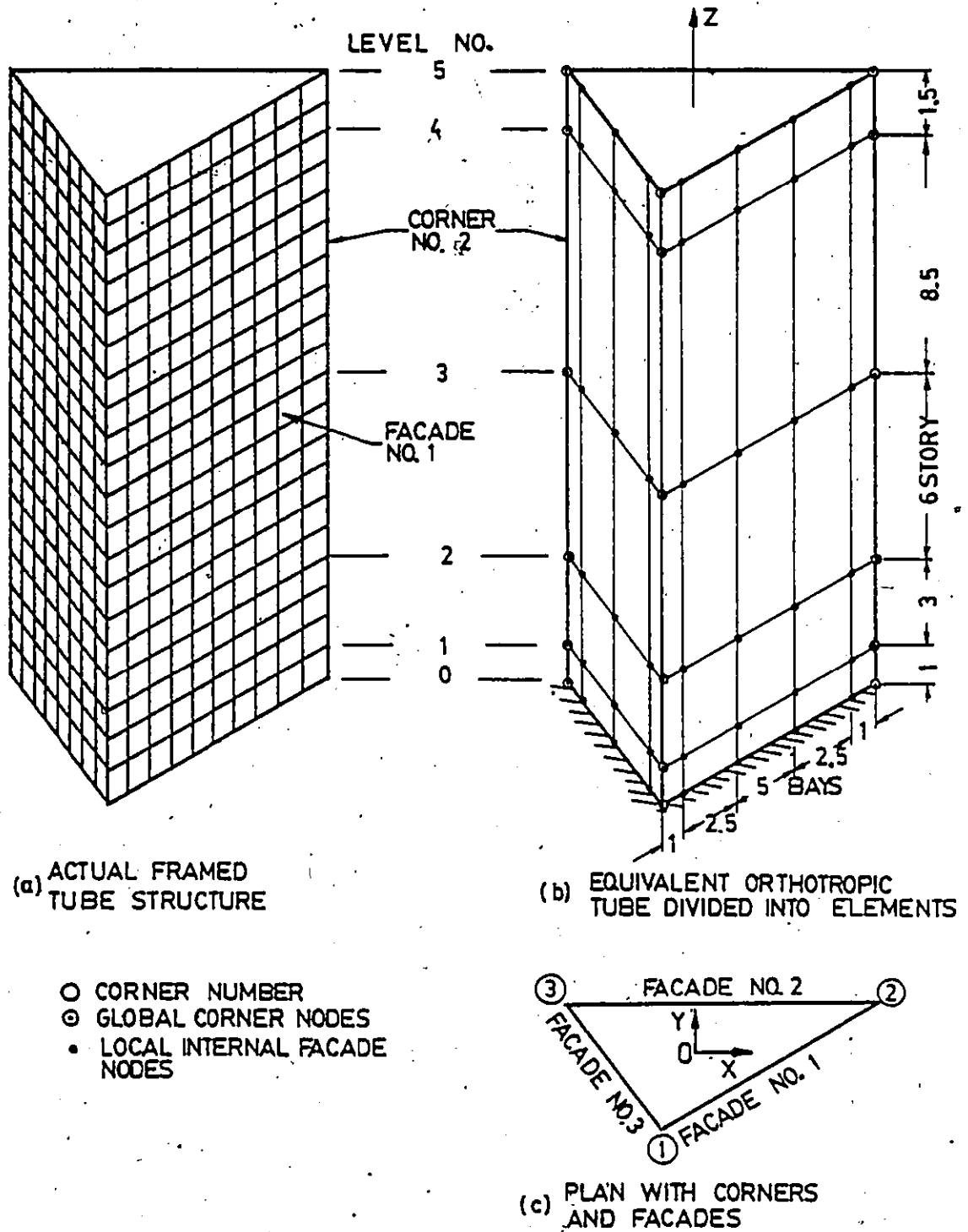


FIG. 6.1 STRUCTURE IDEALIZATION

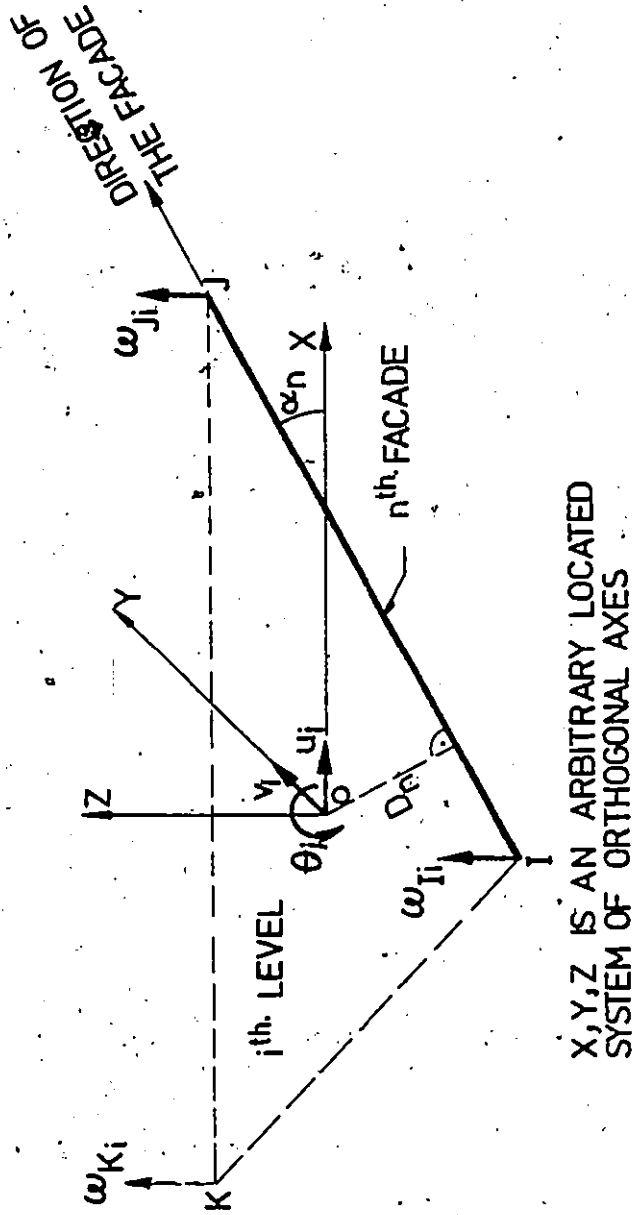
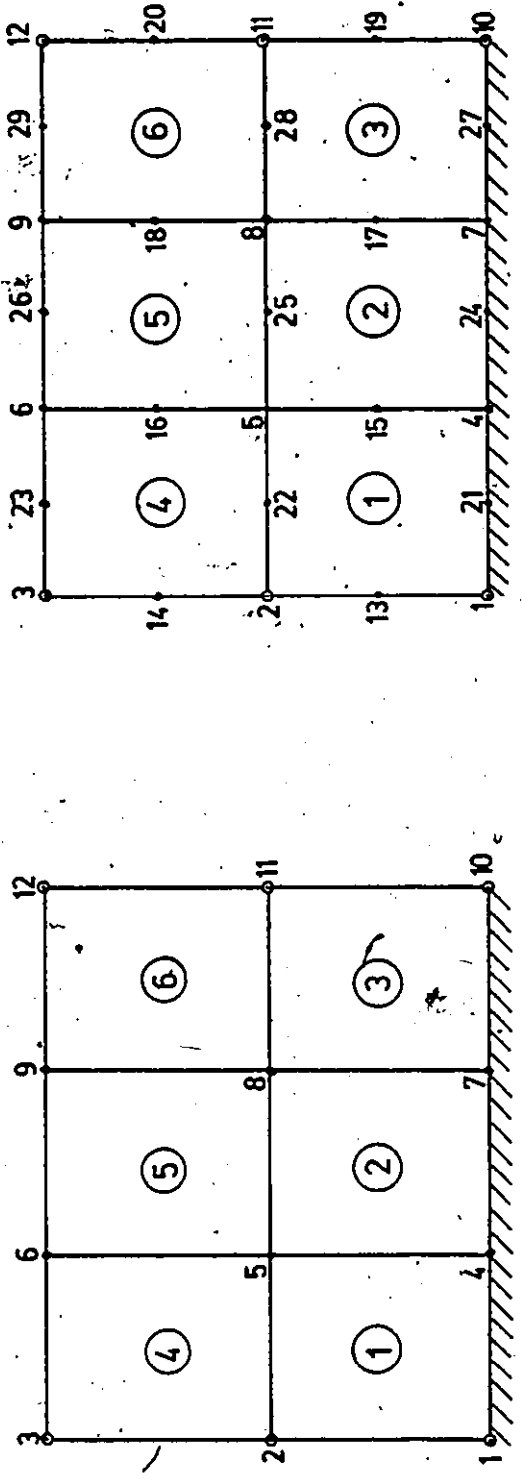


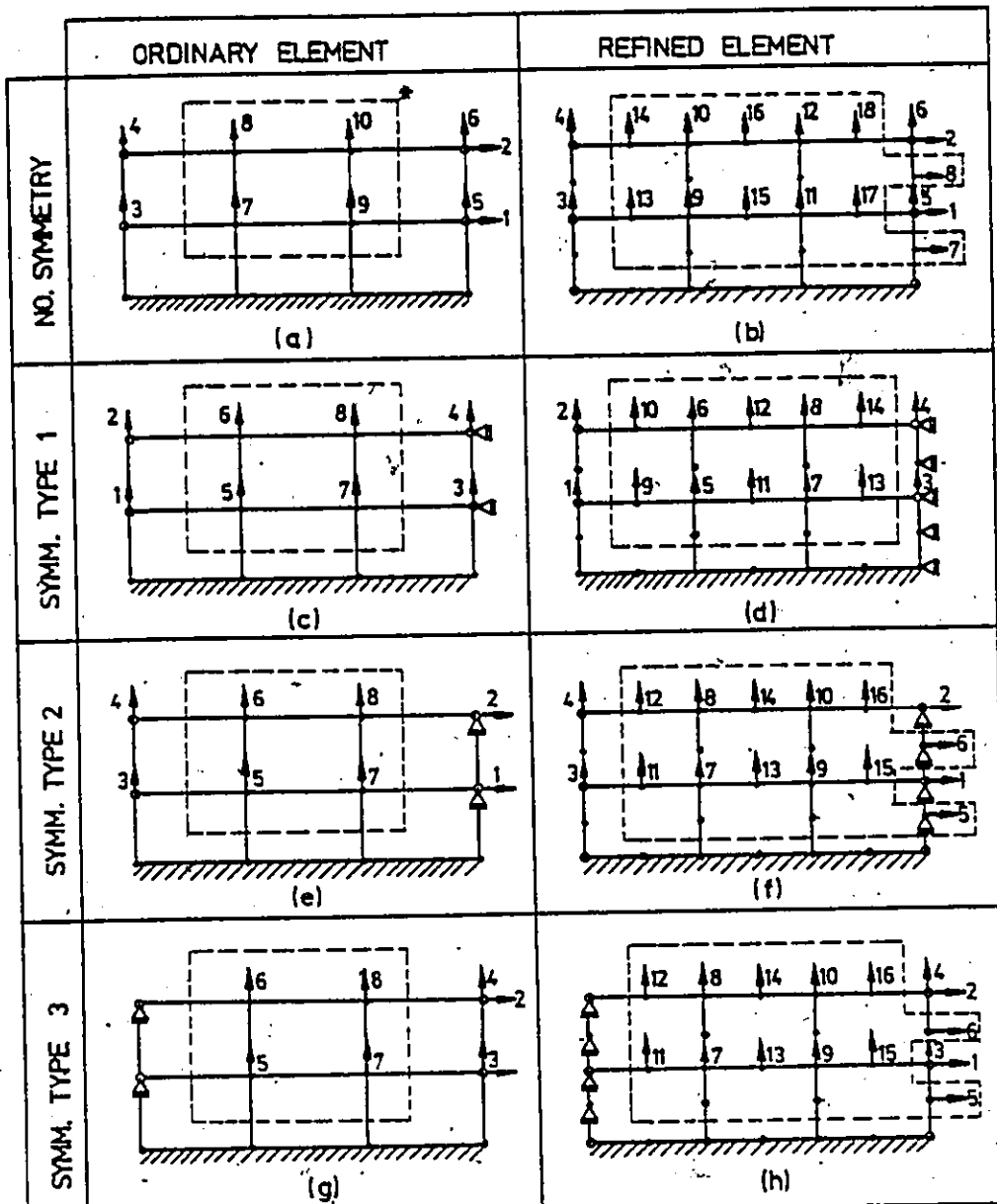
FIG. 6.2 GLOBAL DEGREES OF FREEDOM AT THE i TH LEVEL



(a) ORDINARY ELEMENT

(b) REFINED ELEMENT

FIG. 6.3 AUTOMATED NUMBERING SYSTEM OF NODES AND ELEMENTS



INTERNAL DEGREES OF FREEDOM ARE THOSE SURROUNDED BY THE DOTTED LINE.

FIG. 6.4 AUTOMATED FACADE DEGREES OF FREEDOM SYSTEM

CHAPTER VII

APPLICATIONS TO THE ANALYSIS OF TUBE-TYPE
TALL BUILDING STRUCTURES

CHAPTER VII
APPLICATIONS TO THE ANALYSIS OF TUBE-TYPE
TALL BUILDING STRUCTURES

7.1 INTRODUCTION

The Equivalent Orthotropic Macroelement Method was developed in an attempt to minimize the computer time and storage required in analyzing planar and tubular tall buildings. Application of the method to a number of planar structures has been presented in Chapter V. In this chapter, the method is applied to the analysis of three-dimensional framed tube and core-supported structures.

The objectives of this chapter are:

- (1) To verify the validity of the theoretical developments of Chapter VI with particular emphasis on those aspects such as: the bending analysis of framed tube structures taking symmetry into account, combined bending and torsional analysis of core-supported structures,
- (2) To investigate the effect of the mesh size on the accuracy of the results, and
- (3) To illustrate the efficiency of the present method as applied to the analysis of tube-type tall building structures.

7.2 APPLICATION TO FRAMED TUBE STRUCTURES

In this section three different examples are considered: the 16-storey framed tube of Chan [12], the ten-storey framed tube of DeClercq [34], and the 36-storey plexiglass framed tube model [12]. The results are compared to those obtained from the "exact" analysis, experimental data and from other simplified methods whenever these are available. The basic assumptions affecting the response of framed tube structures to lateral loads, (i.e., line members, shear deformations of members, infinitely rigid joints, and flexibility of these joints) are investigated in the first example. Effect of the mesh size, in modelling structures employing the present method, is also examined in the first two examples. The refined modelling of finite size joints, developed previously in Chapter II, is applied to the analysis of the plexiglass model in the third example.

7.2.1 Example 7.1

In this example the 16-storey framed tube of Chan [12] is considered. The structure is square in plan with each facade consisting of a 12-bay, 16-storey frame. Typical dimensions and properties of the structure are given in Fig. 7.1. The discrete beam-column system is first replaced, for the analysis, by an elastically equiva-

lent orthotropic membrane. In order to investigate the effects of some commonly used simplifications on the structural response, five different analyses are carried out considering respectively:

- (1) bending deformations in members with rigid finite size joints [32];
- (2) shear deformations of beams in addition to (1) [12];
- (3) shear deformations in columns in addition to those in (2) [34, 106];
- (4) flexibility of finite size joints in addition to (3); and
- (5) line members (i.e., joint size is ignored) with their bending stiffness only [67, 90].

Due to symmetry conditions, only one quarter of the structure needs to be modelled utilizing a total of 24 ordinary elements per facade (three across its width and eight along its height), as shown in Fig. 7.1(c).

The results (Fig. 7.2) show that ignoring the effects of finite size joints (analysis No. 5) may result in underestimating the rigidity of the structure to almost one half of that based on infinitely rigid finite joints (analysis No. 1). This was also pointed out by Ast and Schwaighofer [4]. It should be noted that the rigidity of

the structure as modelled by No. 1 and No.5 represents the upper and lower bounds respectively since the actual rigidity, considering shear deformations in members and joints, obviously should lie within these two bounds, as shown in Fig. 7.2. It should also be emphasized that while the lateral deflection predicted by the method of Chan [12] coincides with that obtained by the present method under the same assumptions, the consideration of shear deformations of columns and joints increases its value by about 13%.

In order to examine the effect of mesh size on the accuracy of the results, four different meshes (Figs. 7.1(c) and 7.3) are considered. Surprisingly, it is observed that the maximum lateral deflection is little affected by the mesh size and is within 3% of the "exact" value. However, member internal forces, especially the column axial forces, are significantly affected by the mesh size to the extent of making mesh-4 unacceptable as shown in Table 7.1 and Fig. 7.4, yet rapid convergence is obtained (Figs. 7.4 and 7.5) resulting in an error of less than 3% with the finest mesh used. The number of unknowns (degrees of freedom) in the finest mesh is only 19% of that used in the "exact" analysis. It should be noted that "exact" method referred to here, is based on a two-dimensional frame idealization [28] and hence is limited to framed tube structures having rectangular shape in plan and subjected to symmetric bending

action.

Since the accuracy obtained with mesh-2 (Fig. 7.1(c)) is quite acceptable, it was decided to carry out a more detailed analysis of the same structure using this mesh. The results are compared to those obtained from the "exact" and simplified methods by Chan [12] as well as to those obtained by employing the simplified method of Coull and Bose [32] for the analysis of the same structure. As shown in Figs. 7.2 and 7.6 to 7.9, both the lateral deflection and "important" member internal forces are calculated with errors less than 3% and 5% respectively, yet employing a fraction (8%) of the number of degrees of freedom in the "exact" analysis. The simplified methods, especially that of Coull and Bose, on the other hand, show serious errors. It should be mentioned that for the purpose of comparison, the member internal forces were obtained based on the same basic assumptions of Chan [12] (i.e., infinitely rigid finite size joints and only shear deformations of beams in addition to the bending deformations of the members.)

As mentioned in the introduction, the accuracy resulted from the application of the elastic equivalent concept depends primarily on the elastic properties of the equivalent continuum and the modelling. This is clearly illustrated in Figs. 7.6 to 7.9, in which the results obtained by the present method are in close agreement with

the "exact" values whereas those by Coull and Bose [32] method are unacceptably in error even though both methods are based on the same equivalent concept. It should be noted that the poor results, especially those in column axial forces, by Coull and Bose's theory, were expected since it is obvious that the assumed second-degree parabolic distribution of normal stresses in the normal frames cannot represent the severe variation of the axial forces. As a consequence, the maximum corner column axial force is underestimated by 41.5% and that of the adjacent column is overestimated by 24.6% (Figs. 7.6 and 7.7, respectively.) It can also be seen that the assumed stress functions resulted in extremely unacceptable shear distribution in the beams intersecting at the corner (Figs. 7.8 and 7.9), especially that in the normal frames (Fig. 7.9).

7.2.2 Example 7.2

This is the 10-storey framed tube structure of DeClercq [34]. The structure is subjected to a uniform lateral load and has the dimensions and properties shown in Fig. 7.10. As usual, the discrete beam-column system is replaced, for the analysis, by an equivalent orthotropic membrane. In this example, the refined element is employed for modelling the equivalent structure and five different meshes (Figs. 7.10(c) and 7.11) are used to test further the effect of mesh size on the accuracy. Again, it is

found that the mesh size has a negligible effect on the lateral deflection. The errors in all cases do not exceed 3% of that obtained by the "exact" three-dimensional frame analysis. Column axial forces are shown to be the most greatly affected by the mesh size. However, unlike the previous example, none of the five meshes used has resulted in unacceptable errors. This is due to both the use of the refined element and the moderate shear lag effects. The maximum error in both column base axial forces and the maximum shear forces in spandrel beams, is less than 13% (Figs. 7.12 and 7.14) for the coarsest mesh (number of degrees of freedom is less than 4% of that in the "exact" analysis).

In general, as the mesh gets finer, the error reduces, but nevertheless, the "exact" solutions may not be reached even when each element spans a one-bay, one-storey area, as shown in Fig. 7.12 (Case E). This is because a basic approximation was introduced in assuming the inflection points at the mid-lengths of the members when the elastically equivalent membrane was derived. In addition, it should be pointed out that while equilibrium exists at the nodal points of the equivalent macroelements, individual joints of the actual structure will not generally be in equilibrium. This situation also occurs in the macroelement method of DeClercq [34] and that of Ha [45] and may be explained by the fact that the structure is constrained to

deform as prescribed by the assumed displacement functions, and thus true equilibrium configuration is not obtained.

7.2.3 Example 7.3

In this example the 36-storey plexiglass framed tube model of Chan [12] is analyzed. The elastic properties of the equivalent membrane are evaluated taking into consideration both the bending and shear deformations of members, axial deformation of columns, and the flexibility of the finite size joints. Due to symmetry conditions, only one quarter of the structure is analyzed (Fig. 7.15) with each of its two facades modelled by 12 refined elements as shown in Fig. 7.15(c). The analysis is carried out for two load cases; a top concentrated lateral load of 10 lbs and a uniform lateral load of 1 lb/in. The lateral deflection and column axial stresses at mid-height of the fifth storey were obtained experimentally and theoretically by Chan [12] and are compared with those predicted by the present method.

In the two load cases considered the experimental values of the lateral deflection (Figs. 7.16 and 7.18) were found to be less than those obtained by the simplified method of Chan [12]. This is contrary to what is to be expected since the Chan method treats finite size joints as infinitely rigid and ignores shear deformations of columns.

Chan [12] attributed this apparent contradiction to the use of non-frictionless pulleys (in the loading system) which reduced the load transferred to the structure. The actual applied loads were evaluated by using the experimental values of the axial stresses in columns and reduction factors of 0.873 and 0.84 were obtained for the two cases respectively. Upon applying these reduction factors, both the lateral deflection and column axial stresses (obtained by the present method) are found to be in very close agreement and theoretically consistent with the experimental values as shown in Figs. 7.16 to 7.19.

7.3 APPLICATION TO CORE-SUPPORTED STRUCTURES

The core-supported structure of Stafford-Smith and Taranath [109] is considered herein. The structure has 15 stories at 12.5 ft each, 50 x 50 sq. ft. in plan, and is subjected to uniform wind load of 25 psf as shown in Fig. 7.20. The supporting core consists of 4 one-ft. thick 20-ft wide concrete ($E = 576,000$ ksf) walls forming a tube of square cross-section, as shown in Fig. 7.20. One of these walls is regularly perforated by door openings (10 x 11 sq. ft.) resulting in a band of lintel beams each having a depth of 1.5 ft.

7.3.1 Structure Idealization

The band of lintel beams is replaced, for the analysis, by an elastically equivalent orthotropic membrane having a uniform thickness of one ft. The shear modulus (G_{xy}) of the equivalent membrane is evaluated from Eq. (2.4) to be 1,464 ksf, and the elastic modulus (E_y) is assigned a very small value (10^{-6} that of the solid walls, i.e., $E_y = 0.576$ ksf).

Due to the lack of symmetry in the loading with respect to the structure orientation, twisting (in addition to the lateral displacement) of the structure will occur. Therefore, none of the types of the global structural symmetry, discussed in the previous chapter, can be used and consequently, a three-dimensional idealization of the complete structure is necessary. The mesh used is shown in Fig. 7.21 and consists of 176 ordinary elements (8 elements in the vertical direction and 22 elements around the periphery of the structure) with a total of 182 degrees of freedom, of which only 56 are the boundary or global degrees of freedom.

7.3.2 Comparison and Discussion of Results

Both the floor rotation and stresses at the base of the core structure are obtained and compared to those of (1) Stafford-Smith and Taranath [109]; (2) Heidebrecht and Stafford-Smith [51]; and (3) Khan and Stafford-Smith [60]; and (4) MacLeod and Hosny [82].

The last authors used a discrete modified frame method and the other authors employed Vlasov's theory for thin-walled elastic beams [119].

Fig. 7.22 displays a very close agreement among the different methods on the floor rotation. Comparison of maximum rotation at the top of the structure is shown in Table 7.2. The distribution of the axial stresses at the base of the structure are shown in Fig. 7.23 and their peak values in Table 7.2. It can be seen that the stresses of the different methods are generally in reasonable agreement, but not as close as in the case of rotations.

It should be emphasized that all the methods employed here except the present method assume a linear variation of axial stresses. This assumption is reasonable only when the shear lag effect is small [88, 89, 122, 127]. Severe shear lag tends to increase stresses at the edges of the facades (especially those acting as flanges), and reduce them near the centre, and this effect increases with the increase of the aspect ratio of the structure in plan and elevation.

TABLE 7.1
EFFECT OF MESH SIZE ON THE ACCURACY
(EXAMPLE 7.1)

Data	Exact (2-D)	Mesh-1	Mesh-2	Mesh-3	Mesh-4	
		Value & Error Value & Error Value & Error Value & Error	Value & Error Value & Error Value & Error Value & Error	Value & Error Value & Error Value & Error Value & Error	Value & Error Value & Error Value & Error Value & Error	
Number of Degrees of Freedom	672*	130	56	30	15	
Number of Elements	432	120	48	25	12	
Maximum Lateral Deflection, ft x 10 ⁻²	23	23.7	+3 23.6	2.6 23.5	2.17 23.4	1.74
Maximum Column Axial Load, kips	180	174.56	-3 171.4	4.77 147.7	17.94 136	24.4
Maximum Column Shear, kips	30.05	32	+6.48 31.9	6.15 31.8	5.82 31.8	5.82
Maximum Beam Shear, kips	47.5	45	-5.26 45	5.26 44.9	5.47 45	5.26
Execution Time, sec.		5.617	4.132 ^{**}	3.159	2.415	

* This value is only for the equivalent two-dimensional (2-D) frame method. In case of 3-D analysis considering 1/4 tube (due to symmetry), this number becomes 1,248.

** Further savings can be effected if member internal forces are evaluated at mid-height of elements and interpolating linearly between these values. In this case the execution time is reduced from 4.132 to 2.69 sec. (i.e. reduced by 35%.)

TABLE 7.2
 COMPARISON OF RESULTS OBTAINED BY DIFFERENT METHODS (CORE-SUPPORTED
 STRUCTURE)

Method of Analysis	Maximum Rotation Radians x 10 ⁻³	Stress (ksf) at significant locations		
		a	b	c
Stafford-Smith and Taranath [109], and Heidebrecht and Stafford-Smith [51]	2.95	92.88	8.35	75.31
Khan and Stafford- Smith [60]	3.32	91.65	7.63	73.58
MacLeod and Hosny [82],	2.8*	83.10	12.96	90.43
Present Method	2.85	81.02	14.09	72.41

* Obtained from the rotation curve of Reference [82].

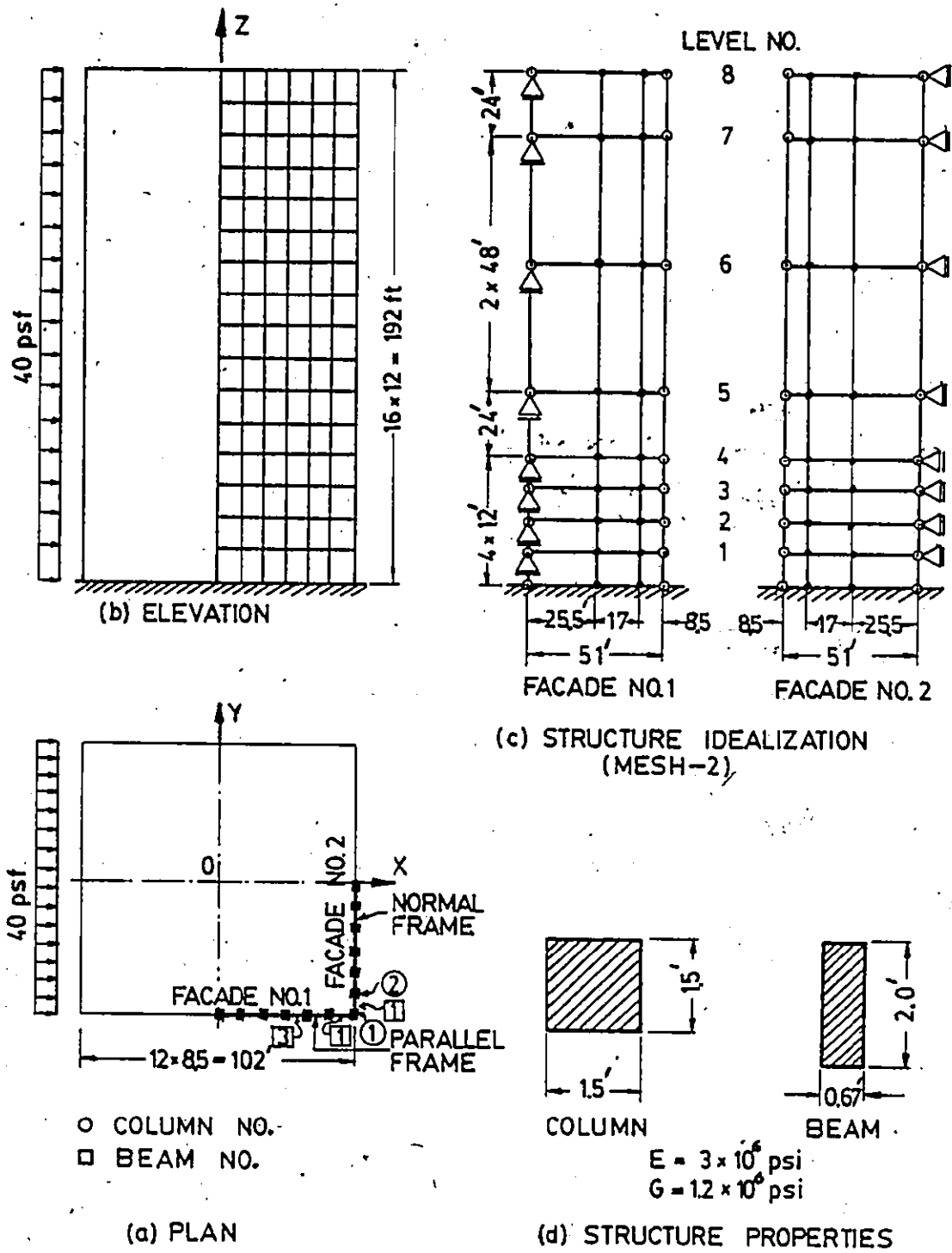


FIG. 7.1 16-STORY FRAMED TUBE OF CHAN [12]
 - EXAMPLE 7-1

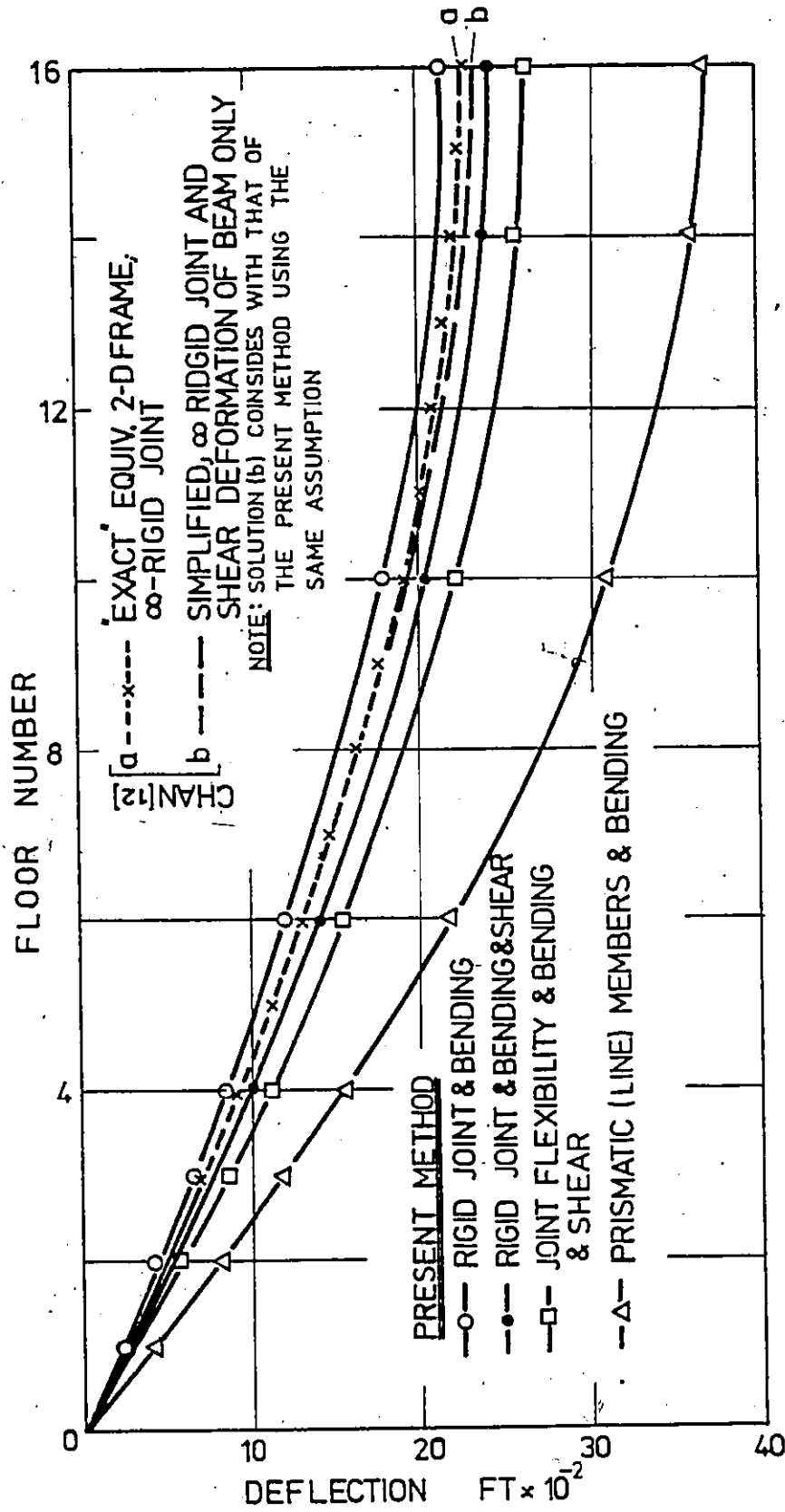


FIG. 7.2 LATERAL DEFLECTION - EXAMPLE 7-1

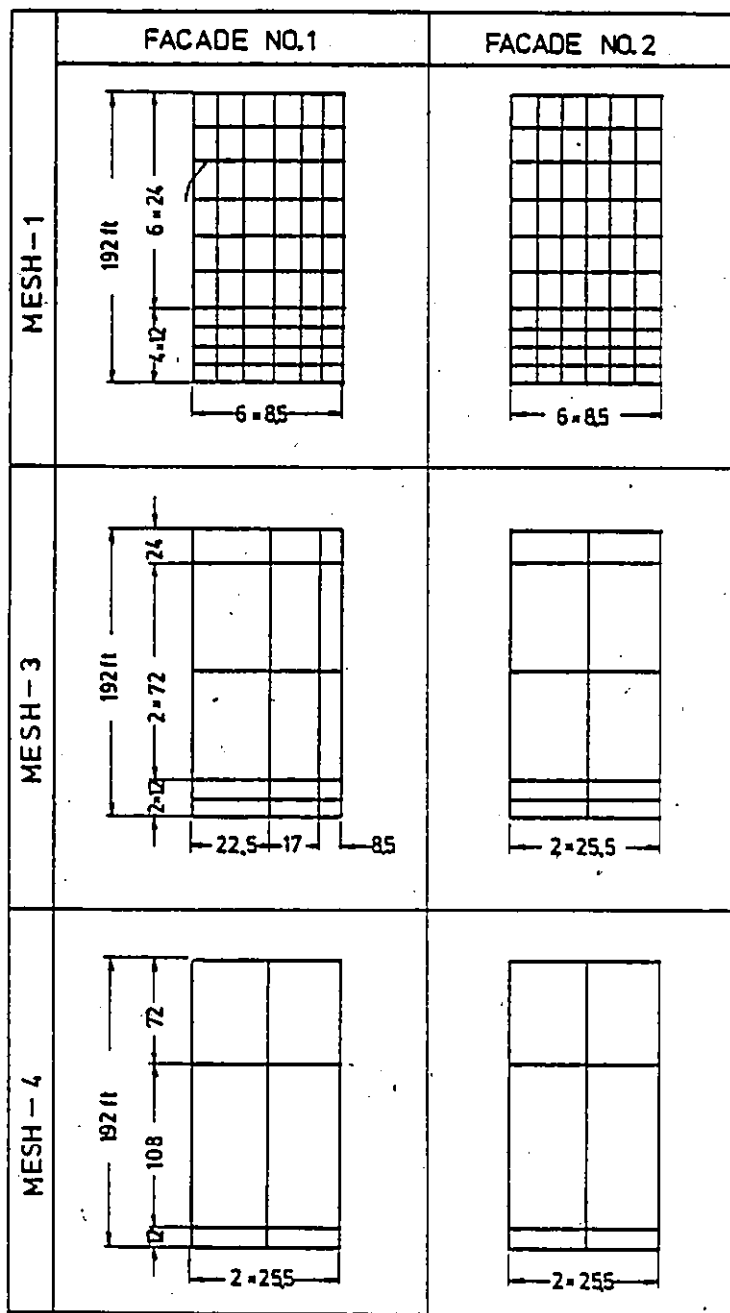


FIG. 7.3 DIFFERENT MESHES USED IN STRUCTURE IDEALIZATION - EXAMPLE 7-1

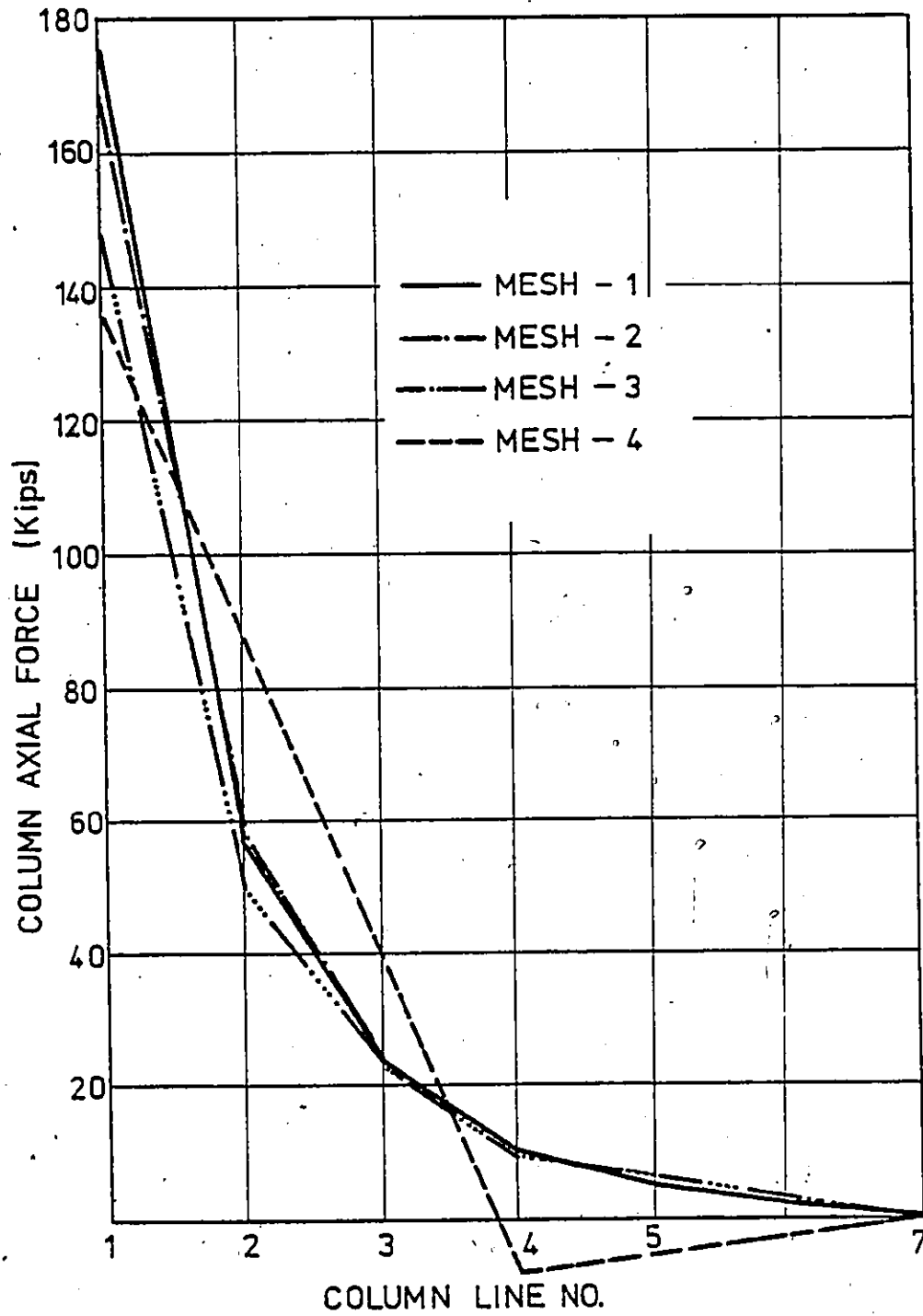


FIG. 7.4 EFFECT OF MESH SIZE ON DISTRIBUTION OF COLUMN AXIAL FORCES - EXAMPLE 7-1

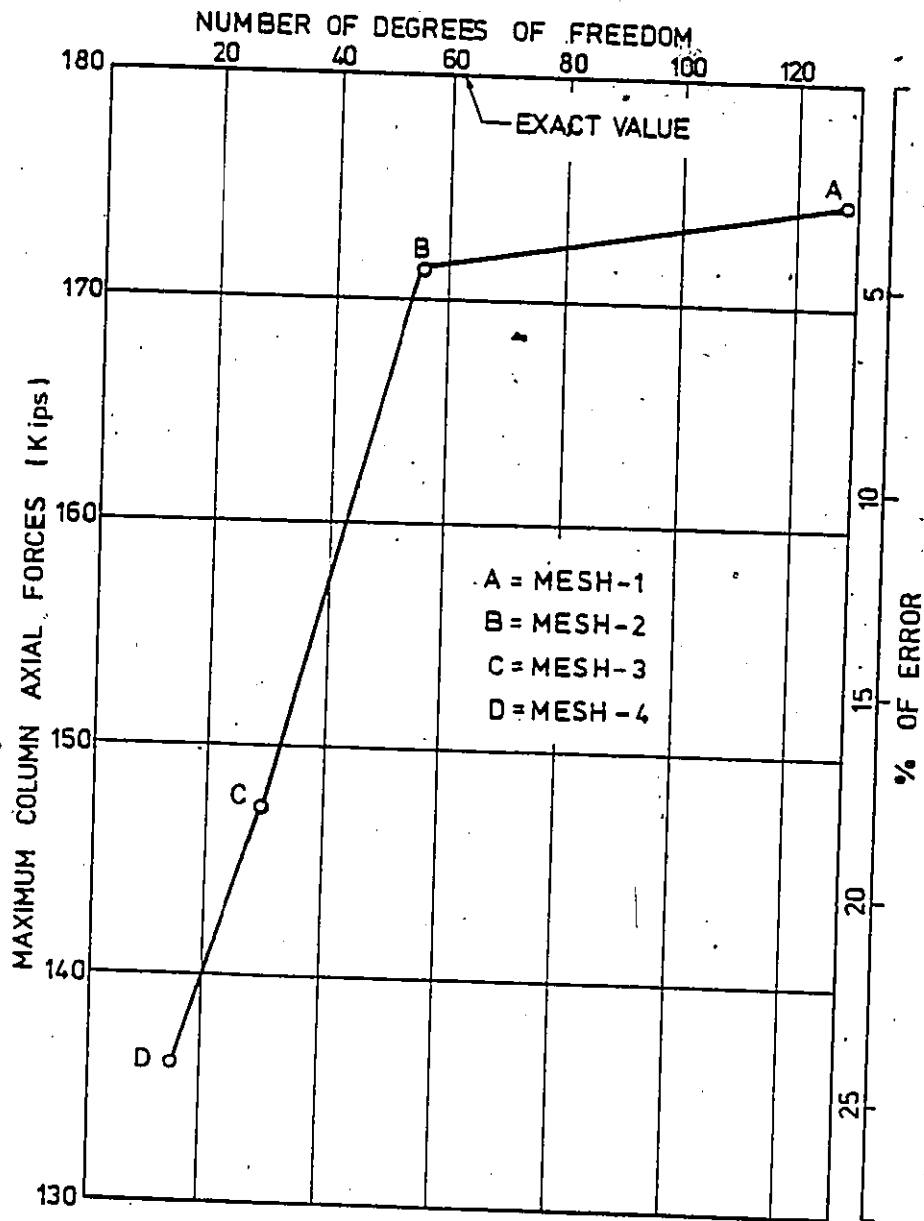


FIG. 7.5 CONVERGENCE OF MAXIMUM COLUMN AXIAL FORCE - EXAMPLE 7-1

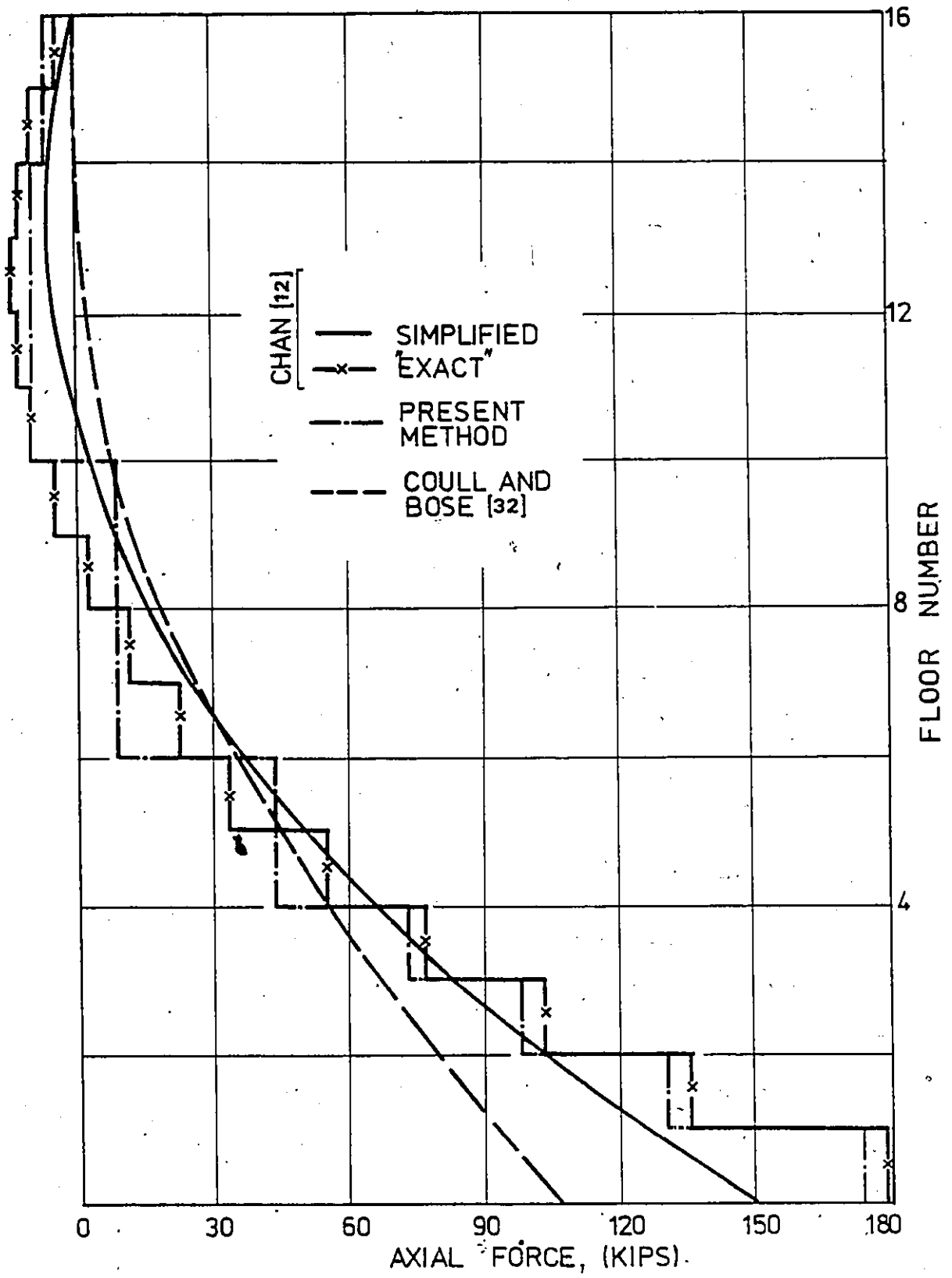


FIG. 7.6 VARIATION OF AXIAL FORCES IN TYPICAL CORNER COLUMNS - EXAMPLE 7-1

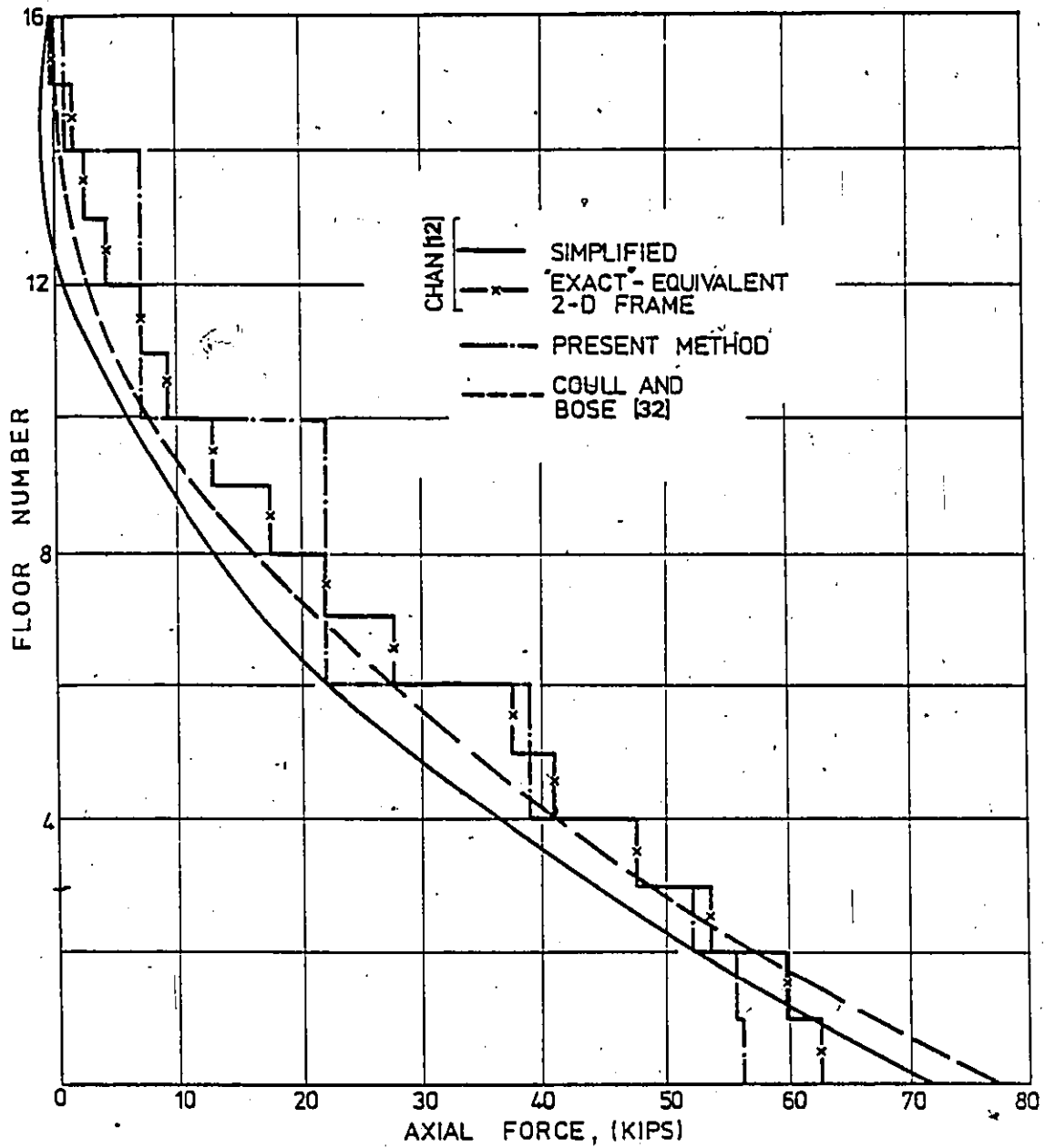


FIG. 7.7 VARIATION OF AXIAL FORCE IN COLUMN - 2 OF NORMAL FRAMES - EXAMPLE 7-1

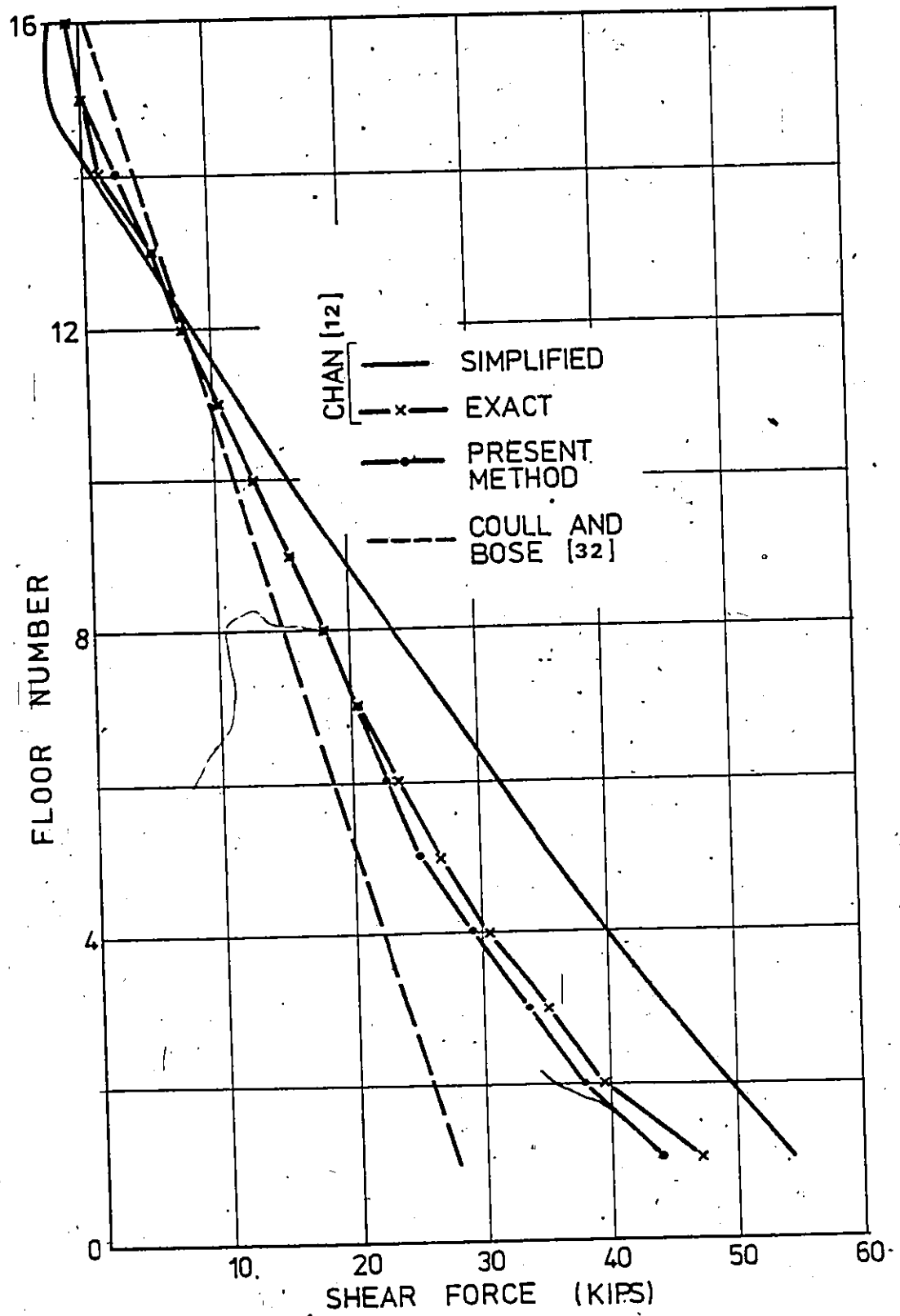


FIG. 7.8 ENVELOPE OF SHEAR FORCES IN BEAM 1 OF PARALLEL FRAMES - EXAMPLE 7-1

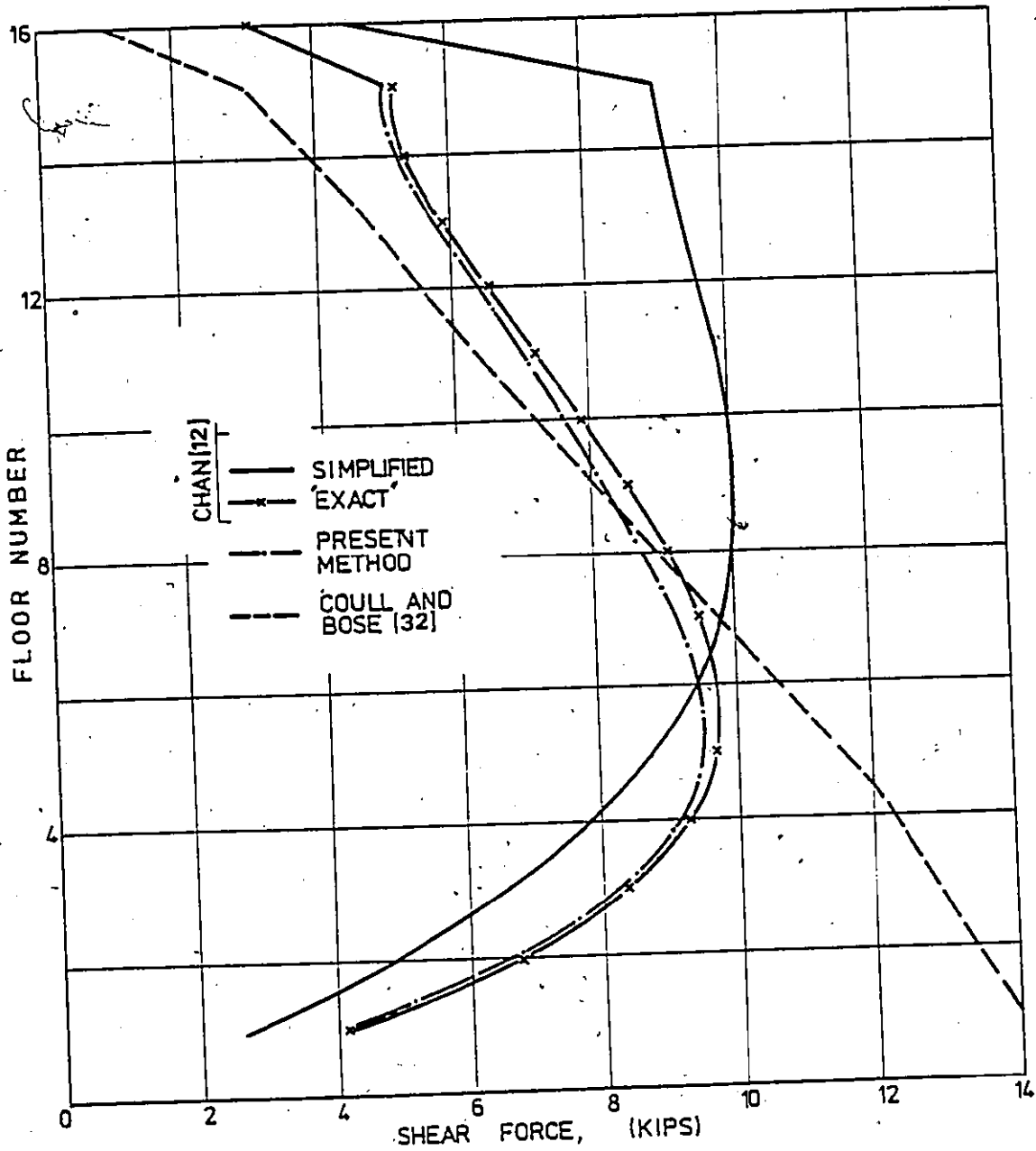
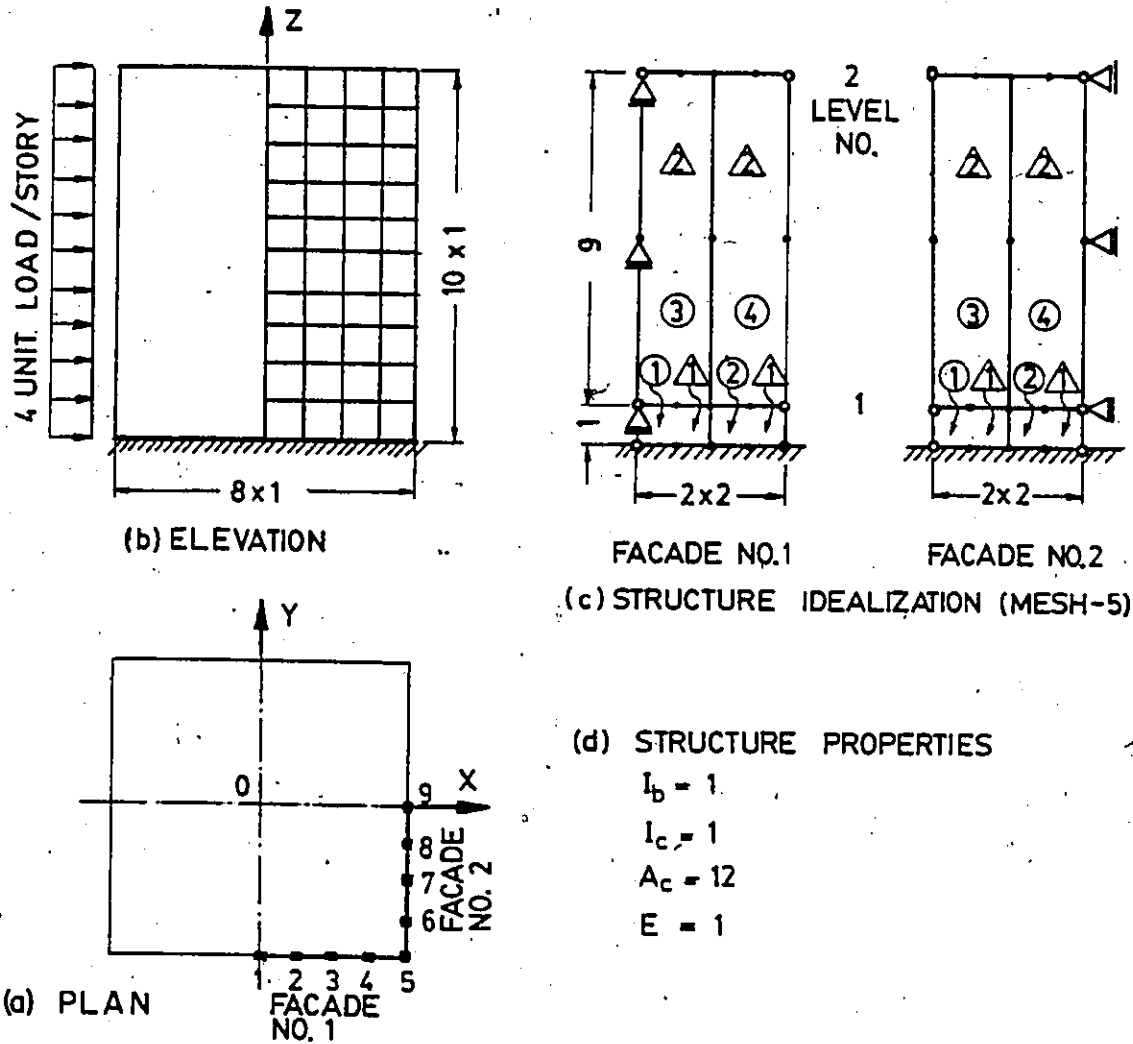


FIG. 7.9 ENVELOPE OF SHEAR FORCES IN BEAM-1 OF NORMAL FRAMES - EXAMPLE 7-1



FACADE DATA	FACADE NO.1	FACADE NO.2
NUMBER OF HORIZONTAL ELEMENTS	2	2
NUMBER OF VERTICAL ELEMENTS	2	2
NUMBER OF DIFFERENT MATERIAL TYPES	1	1
NUMBER OF DIFFERENT ELEMENT TYPES	2	2
NUMBER OF SYMMETRY TYPES	3	1

FIG. 7.10 10-STOUREY FRAMED TUBE OF DECLERCQ [34] - EXAMPLE 7-2

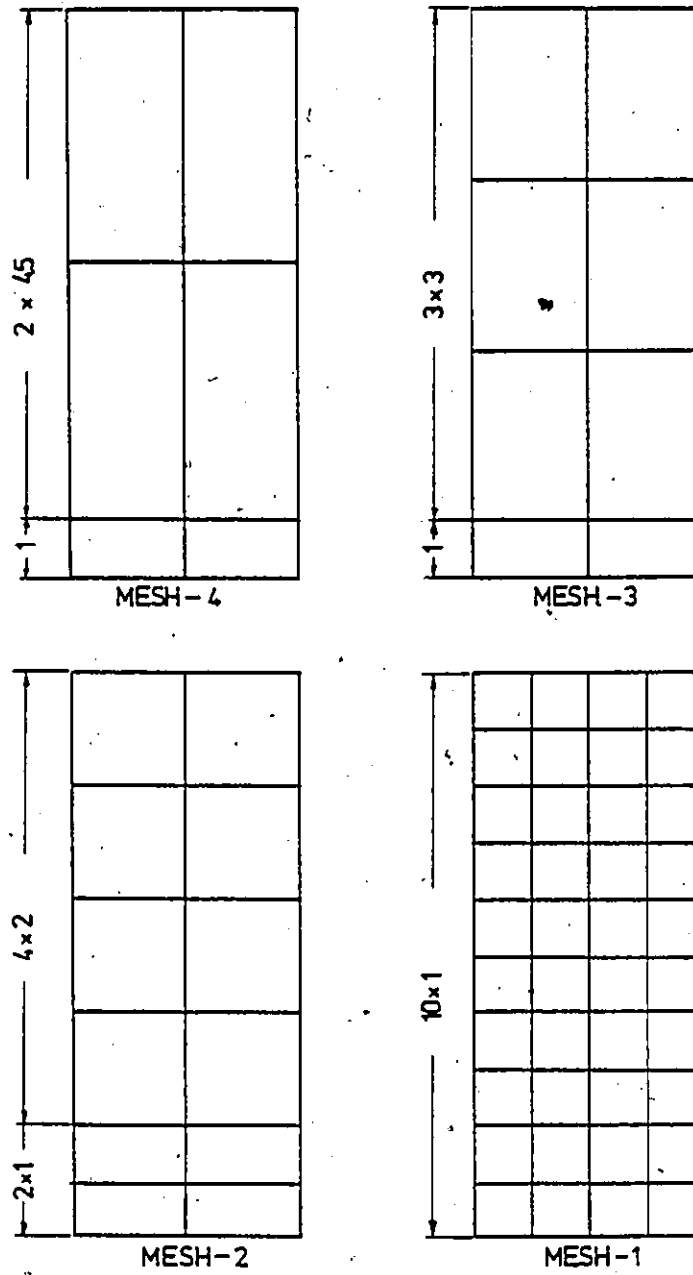


FIG. 7.11 DIFFERENT MESHES USED IN STRUCTURE IDEALIZATION - EXAMPLE 7-2

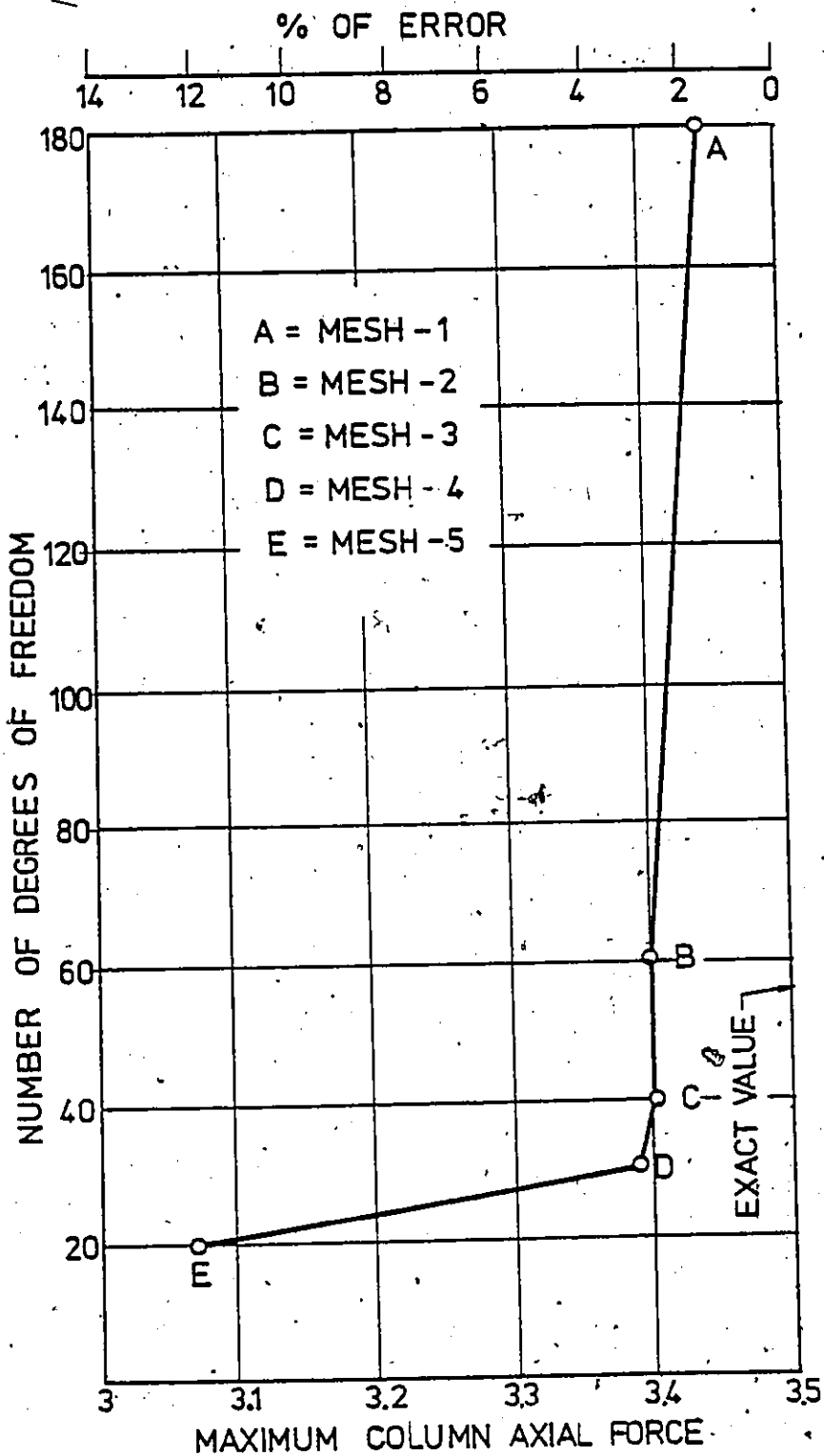


FIG. 7.12 CONVERGENCE OF MAXIMUM COLUMN AXIAL FORCE - EXAMPLE 7-2

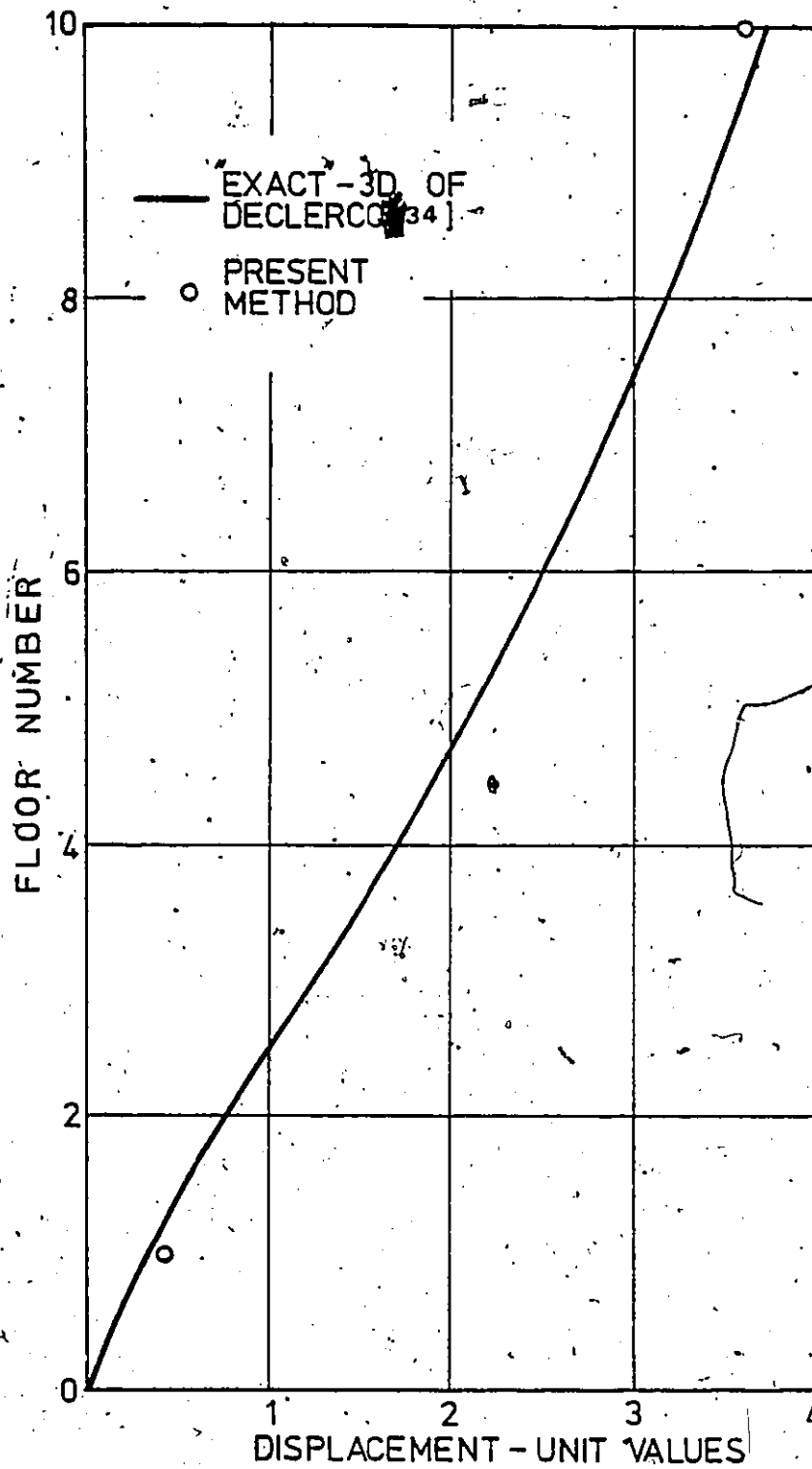
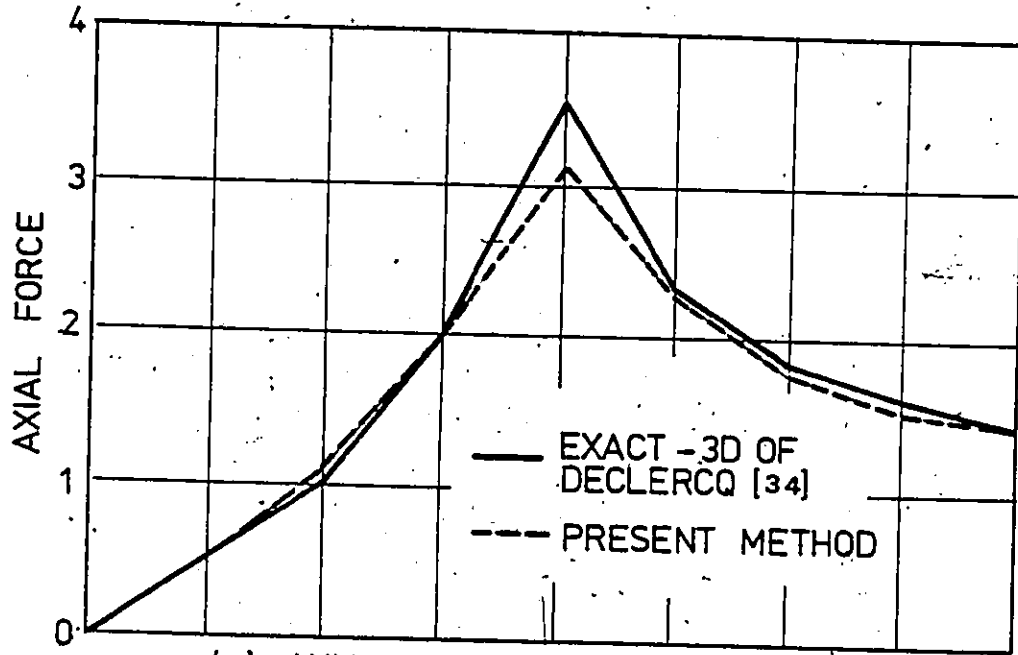
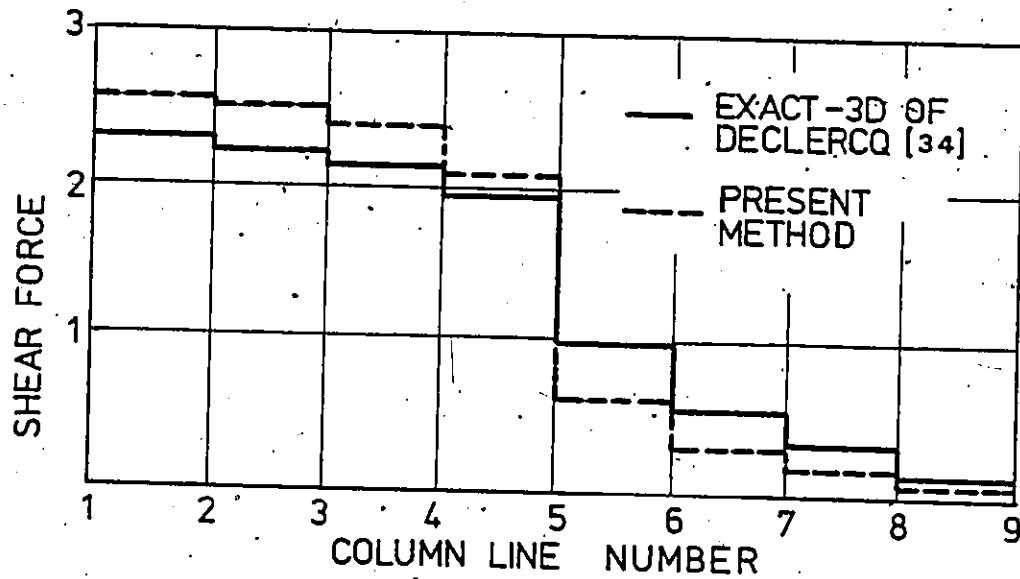


FIG. 7:13 LATERAL DEFLECTION - EXAMPLE 7-2



(a) AXIAL FORCES IN COLUMNS



(b) MAXIMUM SHEARS IN BEAMS

FIG. 7.14 MEMBER INTERNAL FORCES AT FIRST FLOOR - EXAMPLE 7-2

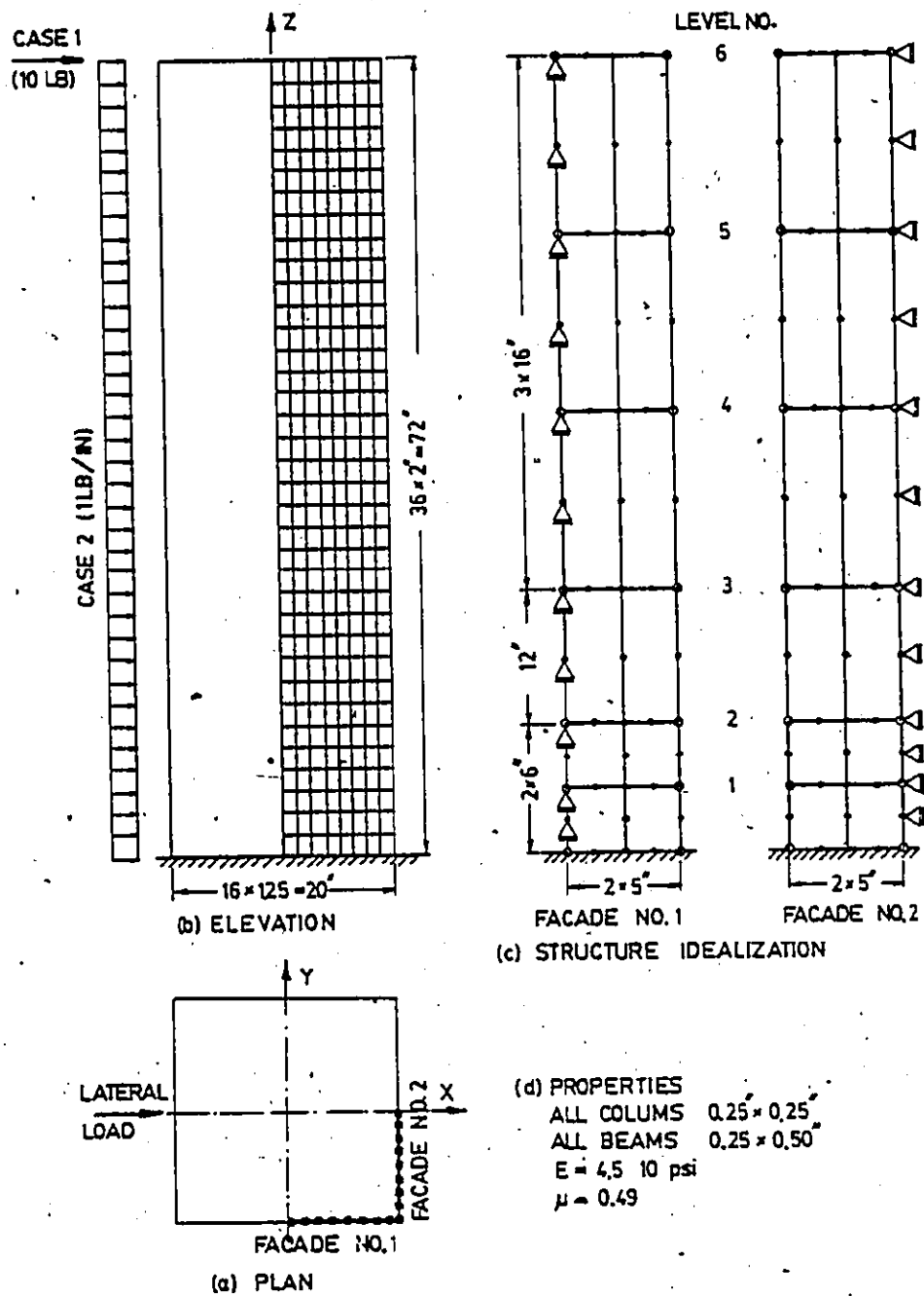


FIG. 7.15 36-STOUREY FRAMED TUBE MODEL OF CHAN [12]
- EXAMPLE 7-3

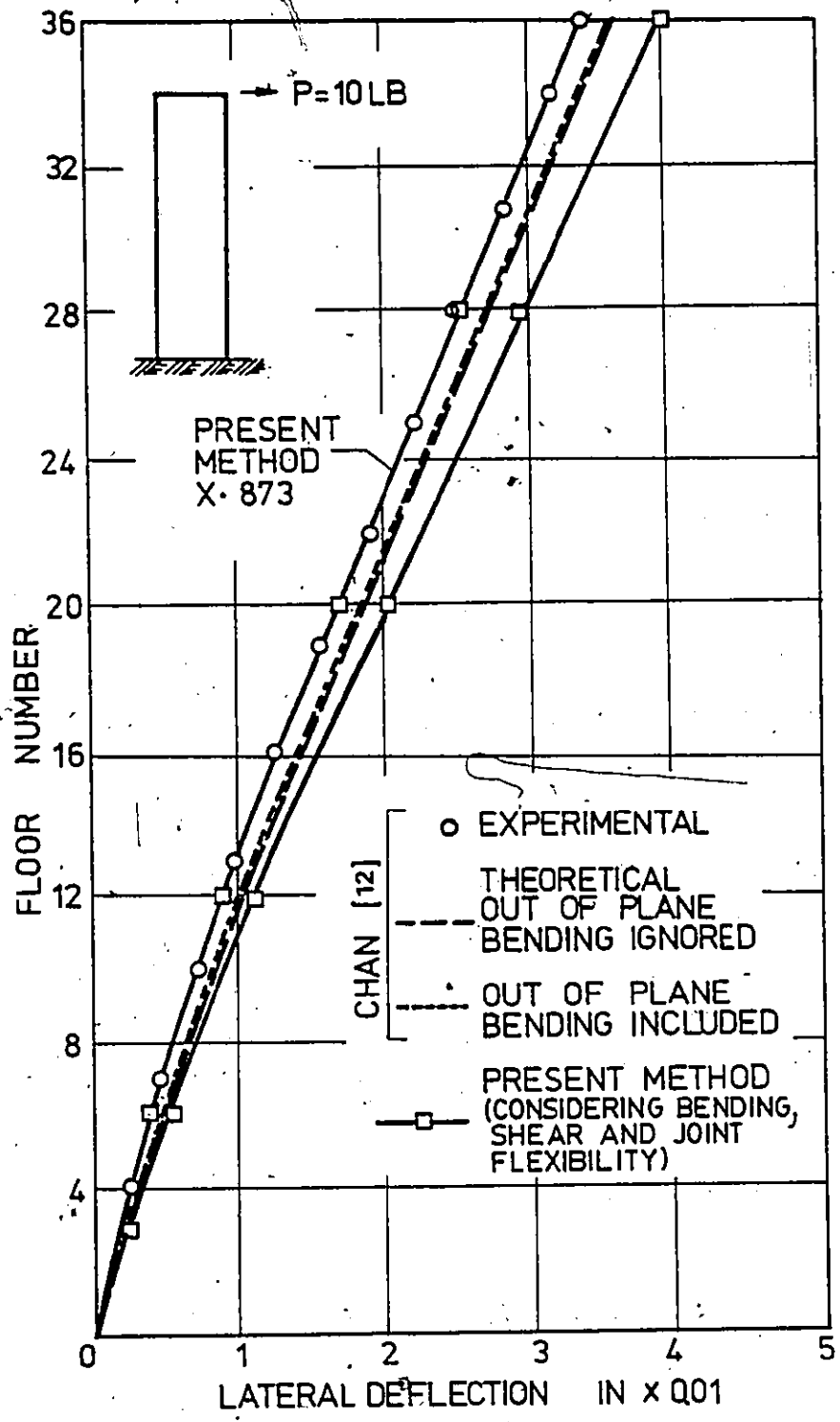


FIG. 7.16 LATERAL DEFLECTION OF THE MODEL UNDER P = 10 LB - EXAMPLE 7-3

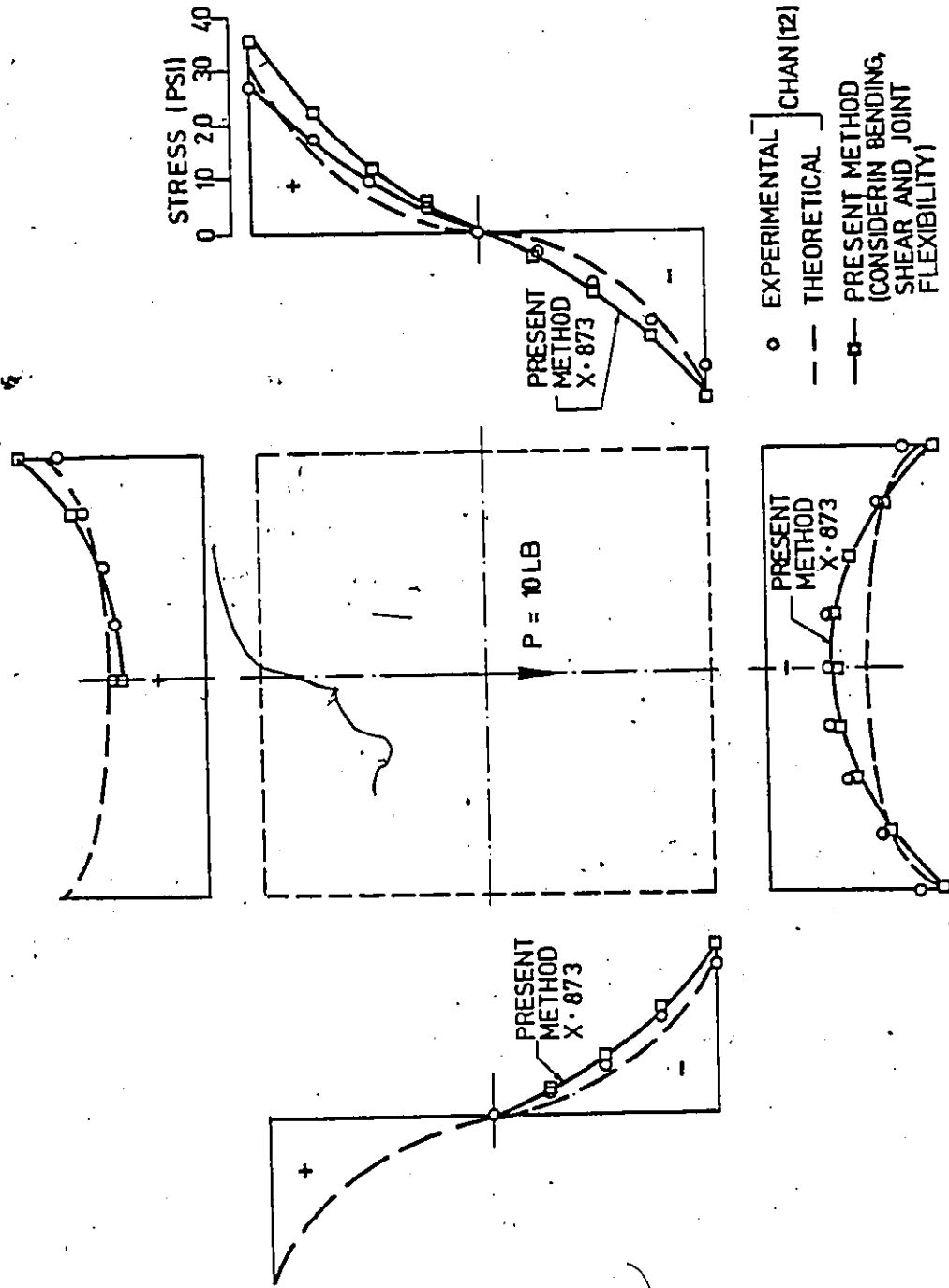


FIG.7.17 VARIATION OF COLUMN AXIAL STRESSES AT MID-HEIGHT OF THE FIFTH-STORY OF THE MODEL UNDER $P = 10 \text{ LB}$ - EXAMPLE 7-3

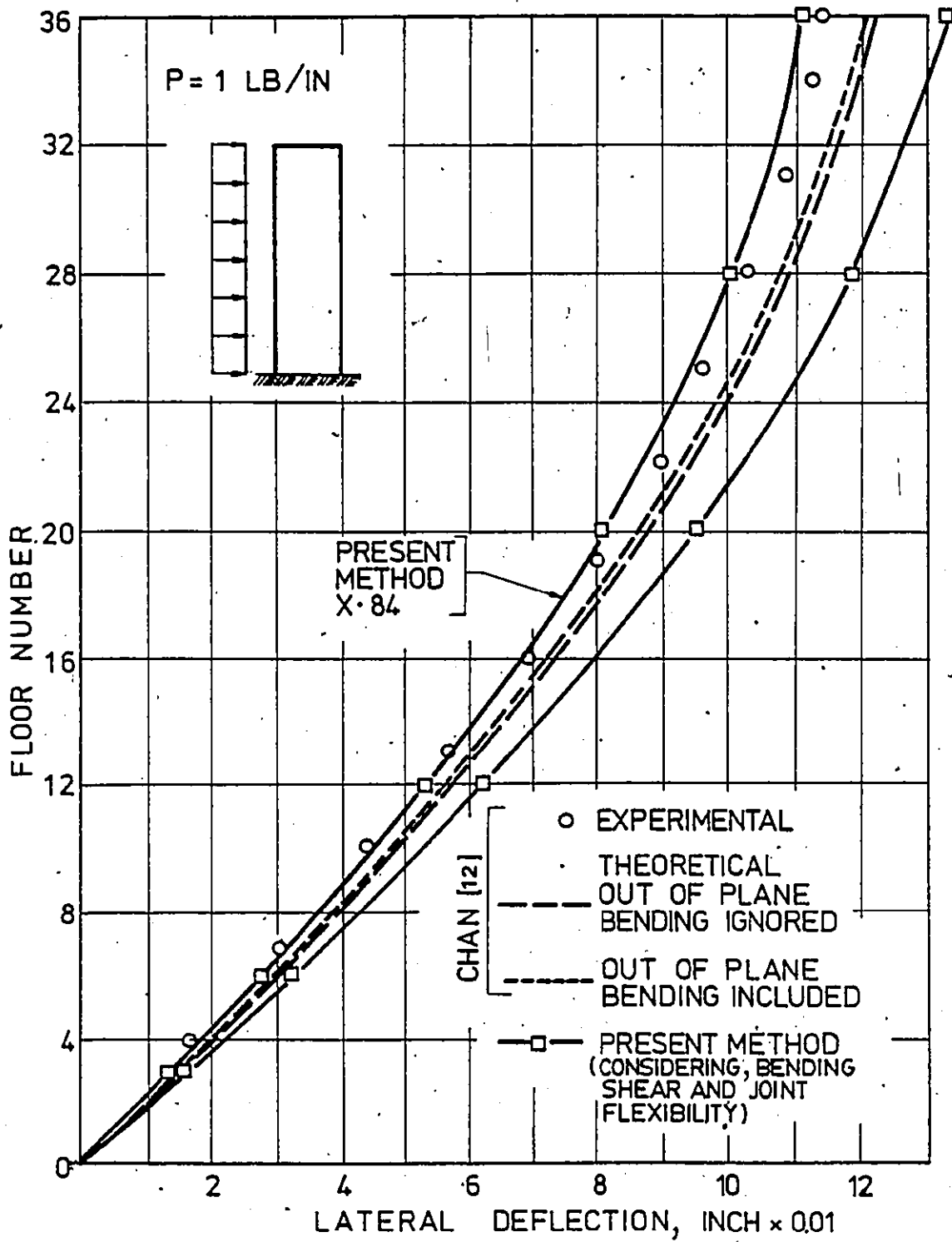


FIG. 7.18 LATERAL DEFLECTION OF THE MODEL UNDER UNIFORM LOAD DISTRIBUTION OF INTENSITY 1 LB PER INCH - EXAMPLE 7-3

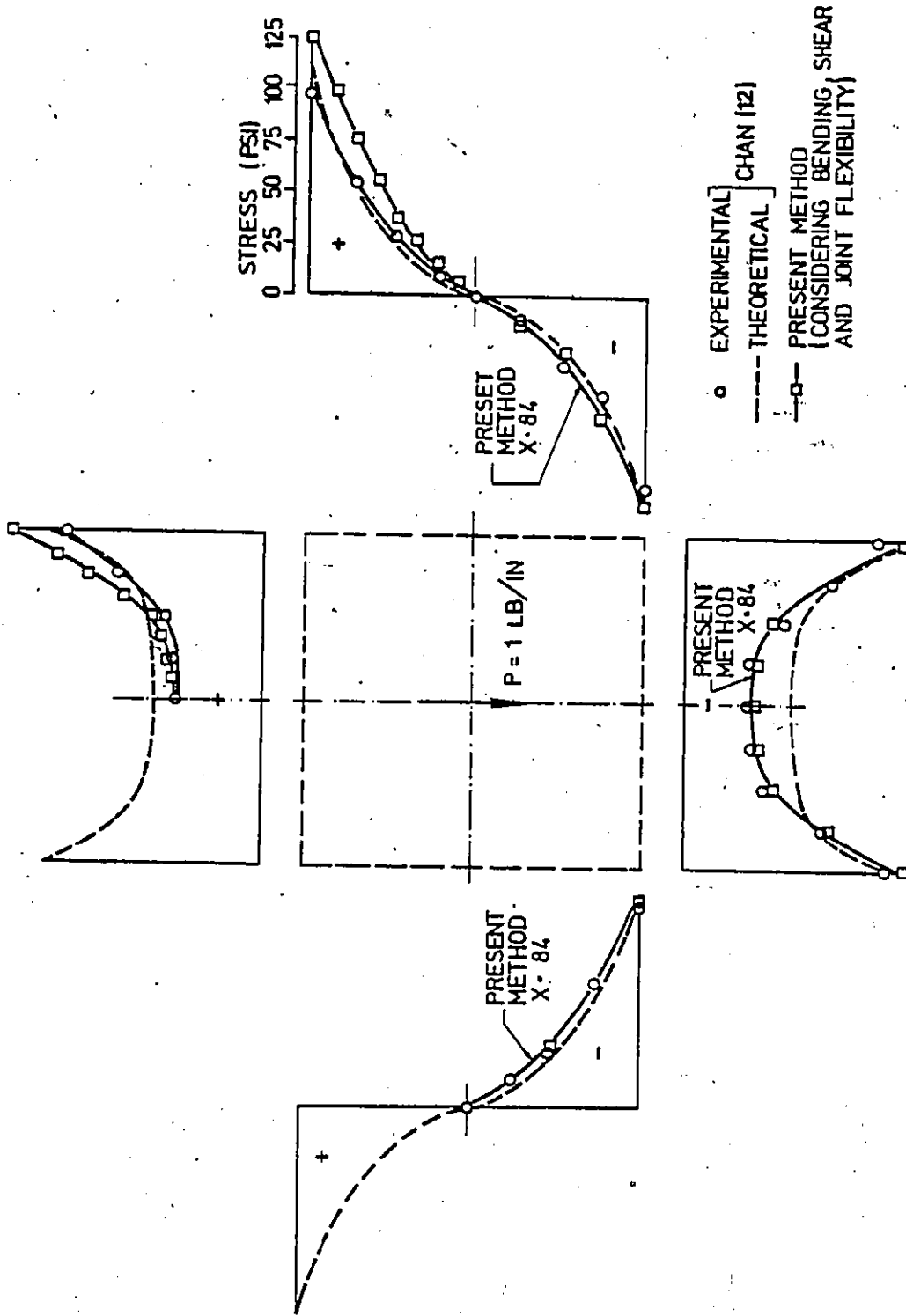
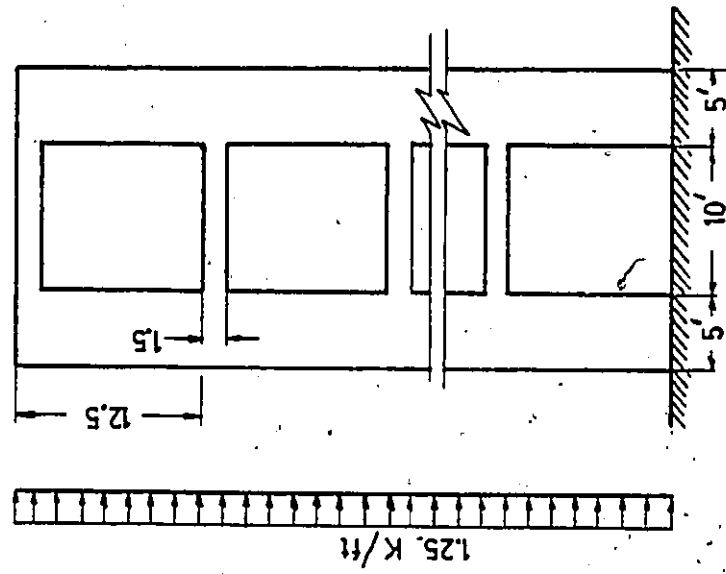
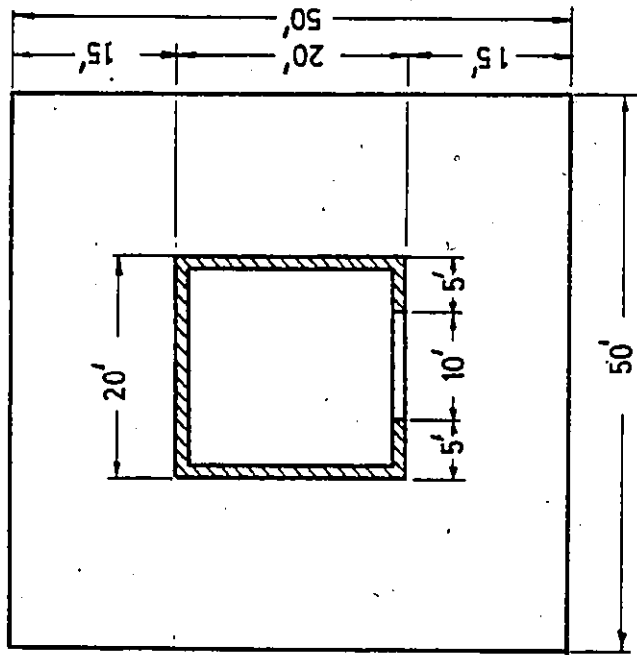


FIG. 7.19 VARIATION OF COLUMN AXIAL STRESSES AT MID-HEIGHT OF THE FIFTH STOREY OF THE MODEL UNDER UNIFORM LOAD DISTRIBUTION OF 1 LB PER INCH - EXAMPLE 7-3



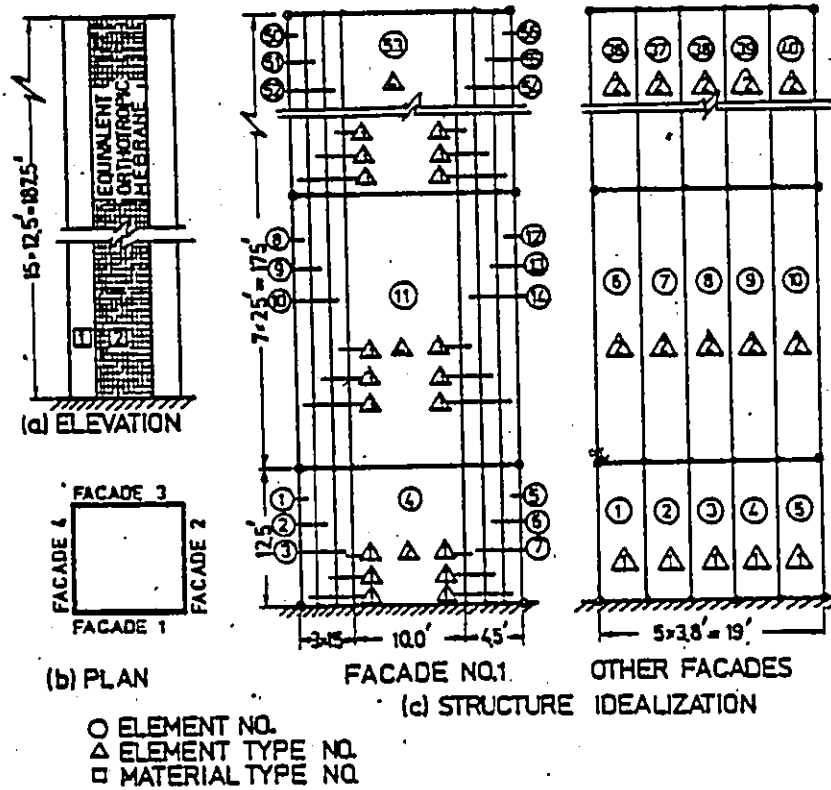
(b) ELEVATION OF SUPPORTING CORE.



(a) PLAN



FIG. 7.20 DIMENSIONS AND LOADING OF THE CORE-SUPPORTED STRUCTURE - REF. [109]



CONTROLLING PARAMETERS	FACADE NO.1	OTHER FACADES
SYMMETRY	NO	NO
NO. OF HORIZONTAL ELEMENTS	7	5
NO. OF VERTICAL ELEMENTS	8	8
NO. OF DIFFERENT MATERIAL TYPES	2	1
NO. OF DIFFERENT ELEMENT TYPES	4	2

FIG. 7.21 STRUCTURE IDEALIZATION

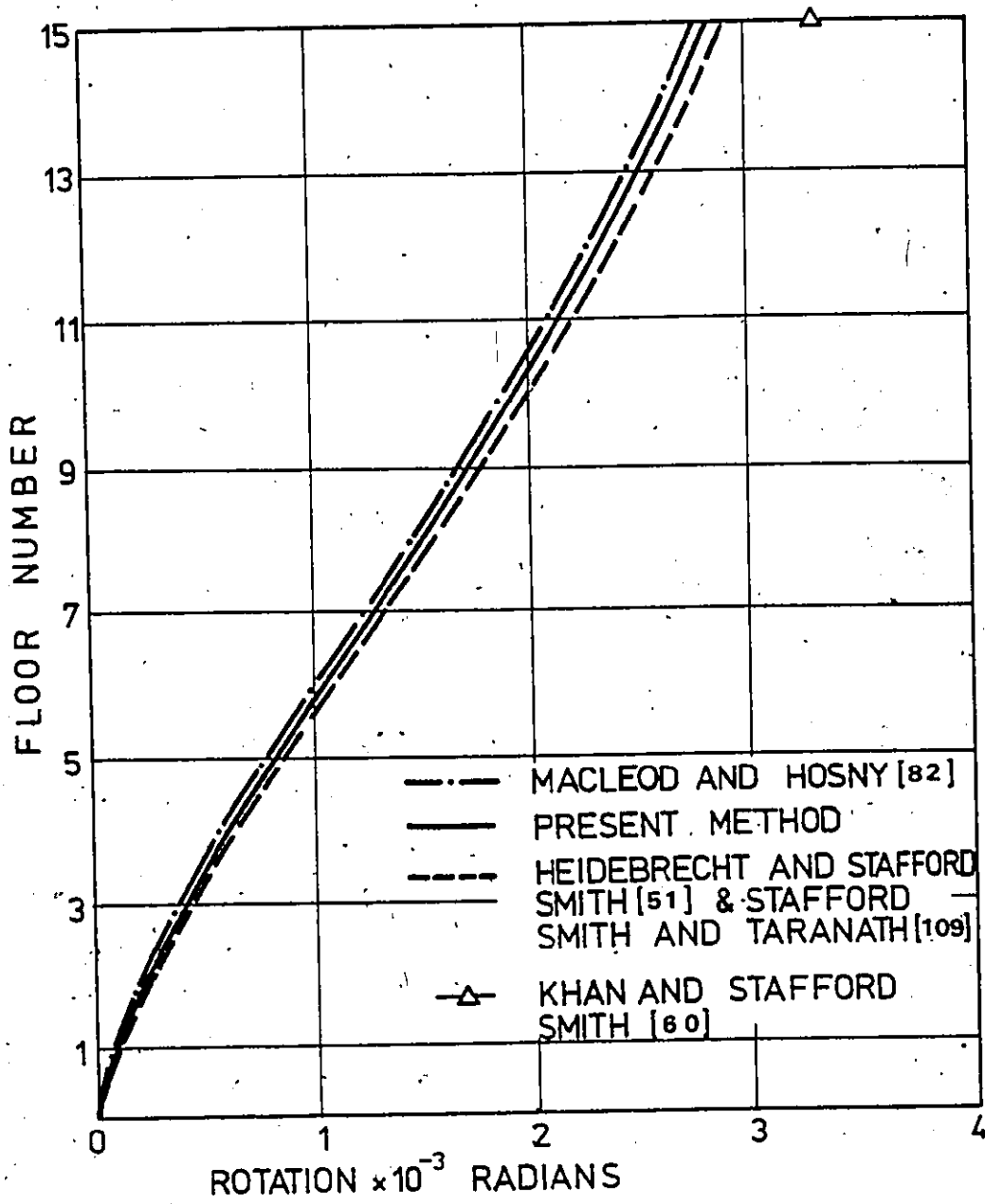


FIG. 7.22 ROTATION

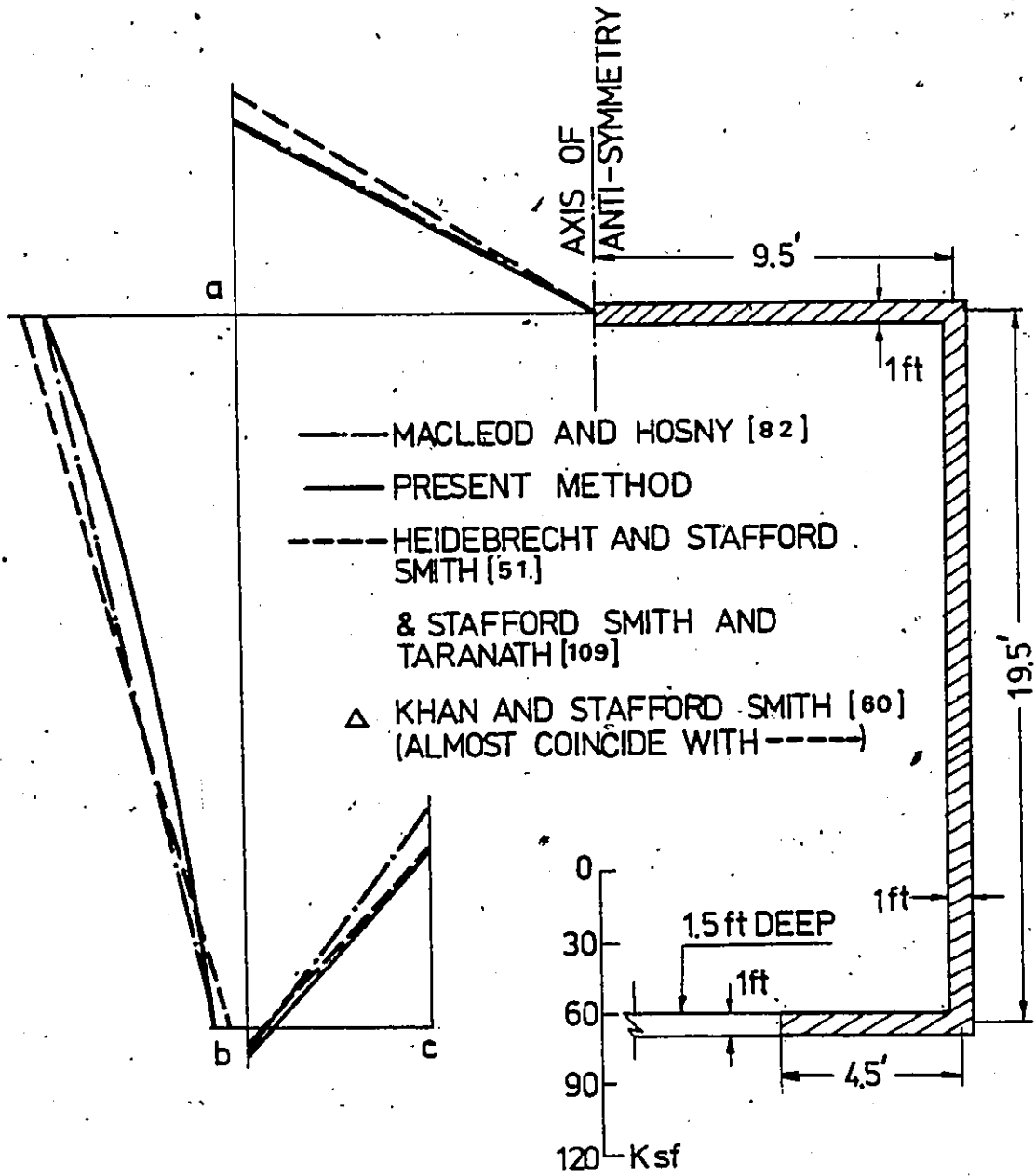


FIG. 7.23 NORMAL STRESSES AT THE BASE OF THE STRUCTURE

CHAPTER VIII

CONCLUSIONS AND RECOMMENDATIONS

CHAPTER VIII

CONCLUSIONS AND RECOMMENDATIONS

8.1 CONCLUSIONS

The Equivalent Orthotropic Macroelement Method has been developed and implemented for the efficient analysis of planar and tube-type tall buildings consisting of frames, shear walls, coupled shear walls, or their combinations. Frame-type structures are assumed to consist of rigidly connected horizontal beams and vertical columns. Repetition of dimensions and member sizes over parts of a structure is necessary for efficient implementation of the method.

The analysis technique is based on replacing the discrete beam-column system and any band of coupling beams by an elastically equivalent orthotropic membrane. Refined expressions for the mechanical properties of the equivalent membrane were developed taking into account the axial deformations of columns, bending and shear deformations of members, the reduction in stiffness due to the presence of axial forces in members, and the deformations of finite size joints.

For the case of planar regularly perforated walls, closed-form solutions were also presented which enable not only the development of design curves and a complete reduc-

tion technique, but also the determination of the characteristic parameters controlling the behavior of these structures. The two specially orthotropic finite elements developed in this work and incorporated in the present method provide a more general solution to the problem and have proven to be very efficient for the analysis of a variety of two and three-dimensional tall building structures.

A general large capacity computer program (program TUBE) was developed with the capability for analyzing most existing large planar and tubular structural systems for tall buildings. The program requires minimal computer memory storage, as well as effort for data preparation, as compared to those programs used in the "exact" and other simplified methods.

In general, excellent results have been obtained for both planar and tubular structures, and in common with most finite element solutions, the displacements tend to be more accurate than stresses and member internal forces. The errors are within 3% and 10% for the displacements and stresses, respectively.

The closed-form solutions when applied to a typical wall-frame structure yielded results comparable to those obtained from a detailed finite element analysis. The errors are less than 3% and 6% for the maximum lateral deflection and member internal forces, respectively. The error in the

shear force in the edge column is more significant, being 16%; however, this is still less than the 35% error produced by the simplified method of Khan and Stafford-Smith [61].

With regard to the accuracy of the Equivalent Orthotropic Macroelement Method when applied to planar frames of various characteristics, the error in the maximum lateral deflection is less than 2% except in the case of second-order (P- Δ) analysis where the error is still less than 6%. "Important" member internal forces were obtained with accuracy better than 96% except for beam shear in the case of frames with variable properties where the accuracy drops to 92.4%. All of these results have been obtained with the TUBE program with the total number of degrees of freedom less than 7% and 24% of those required by the "exact" and other simplified methods, respectively. The efficiency of the present method becomes more pronounced when applied to the analysis of framed tube structures, especially when a full three-dimensional analysis is needed. In all the examples considered on framed tube structures, the maximum lateral deflection was obtained with accuracies better than 97%, even when using as few as two or three elements in the vertical direction in modelling the structure. Convergence study has shown that the deflections are little affected by the mesh size, however internal forces seem to converge toward the "exact" solutions upon refining the mesh. Finally, it is worthwhile noting that although the equivalent proper-

ties of the membrane have been derived analytically, taking into account many factors, it is possible to determine them experimentally or by detailed finite element analysis.

In view of the versatility, the accuracy and the great efficiency offered by the present method, it is believed that the technique should be of value to designers of tall building structures.

8.2 RECOMMENDATIONS FOR FURTHER STUDIES

The present work has been confined to the static and stability analyses. Extension of the technique for dynamic analysis and optimization study of three-dimensional tall building structures would be possible. In addition to these natural extensions of the method, the following points could also be explored.

- (1) Improvement of the equivalent membrane properties by experimental or detailed finite element analysis of the basic frame unit.
- (2) Improvement of the finite element stiffness matrices by using hybrid stress elements or incompatible displacement models.
- (3) Extension of the program code for the analysis of tube-in-tube structural system.

- (4) Since the frame reduction technique has shown to be useful in static analysis of tall frames, it would be interesting to investigate its validity for vibration analysis.

REFERENCES

REFERENCES

- [1] ACI Committee 442, "Response of Buildings to Lateral Forces", J. Am. Concrete Inst., Feb. 1971, pp. 81-106.
- [2] Adams, P.F., "Stability of Three-Dimensional Building Frames", Proc. Int. Conf. on Planning and Design of Tall Buildings, Lehigh, Technical Committee No. 16, Report No. 4, Vol. II, 1972, pp. 483-497.
- [3] Ammar, A.R., and Nilson, A.H., "Analysis of Light Gage Steel Shear Diaphragms", Report No. 351, Part II, Dept. of Str. Engg., Cornell University, July 1973, pp. 34-143; 230-238.
- [4] Ast, P.F., and Schwaighofer, J., "Economical Analysis of Large Framed-Tube Structures", Building Sci., Vol. 9, 1974, pp. 73-77.
- [5] Barnard, P.R., and Schwaighofer, J., The Interaction of Shear Walls Connected Solely Through Slabs, Tall Building, Pergamon Press, 1967, pp. 157-173.
- [6] Bazant, Z.P., and Christensen, M., "Continuous Approximation of Large Regular Frameworks and the Problem of a Substitute Frame", Paper 13, ACI Publication SP-36: Response of Multistorey Concrete Buildings to Lateral Forces, 1973, pp. 257-280.
- [7] Beck, H., "Contribution to the Analysis of Coupled Shear Walls", J. Am. Concrete Inst., Aug. 1962, pp. 1055-1070.
- [8] Bergmann, R., "The First Bank Tower in Toronto", Proc. of the Symposium on Tall Buildings, Vanderbilt University, Nashville, Tennessee, November, 1974, pp. 19-60.
- [9] Biswas, J.K., "Three-Dimensional Analysis of Shear Wall Multi-storey Buildings", Ph.D. Thesis, McMaster

University, Hamilton, Ontario, Canada, 1974.

- [10] Biswas, J.K., and Tso, W.K., "Three-Dimensional Analysis of Shear Wall Buildings to Lateral Loads", J. Struc.Div., ASCE, Vol.100, No. ST5, May 1974, pp.1019-1036.
- [11] Cantin, G., "An Equation Solver of Very Large Capacity", International Journal of Numerical Methods in Engineering, Vol. 3, 1971, pp.379-388.
- [12] Chan, P.C.K., "Static and Dynamic Analysis of Framed-Tube Structures", Ph.D.Thesis, McMaster University, Hamilton, Ontario, Canada, 1973.
- [13] Chan, P.C.K., Tso, W.K., and Heidebrecht, A.C., "Effect of Normal Frames on Shear Walls", Building Science, Vol. 9, 1974, pp.197-209.
- [14] Chan, P.C.K., Heidebrecht, A.C., and Tso, W.K., "Approximate Analysis of Multistorey Multibay Frames", J. Struc.Div., ASCE, Vol.101, No.ST 5, May 1975, pp.1020-1035.
- [15] Cheong-Siat-Moy, F., "Consideration of Secondary Effects in Frame Design", J. Struc.Div., ASCE, Oct. 1977, pp.2005-2019.
- [16] Clough, R.W., Wilson, E.L., and King, L.P., "Large Capacity Multistory Frame Analysis Programs", J.Struc: Div., ASCE, Vol. 89, No. ST 4., Aug. 1963, pp.179-204.
- [17] Clough, R.W., King, I.P., and Wilson, E.L., "Structural Analysis of Multi-Storey Buildings", J. Struc. Div., ASCE, Vol. 90, ST3, June 1964, pp. 19-34.
- [18] Clough, R.W., and King, I.P., "Analysis of Three-Dimensional Building Frames", International Assoc. of Bridge and Struc.Engg., Vol.24, 1964, pp.15-30.

- [19] Coull, A., and Choudhurry, J.R., "Stresses and Deflections in Coupled Shear Walls", J. Amer. Concrete Inst., Feb. 1967, pp.65-72.
- [20] Coull, A., and Choudhurry, J.R., "Analysis of Coupled Shear Walls", J. Am. Concrete Inst., Sept. 1967, pp.587-593.
- [21] Coull, A. and Puri, R.D., "Analysis of Coupled Shear Walls of Variable Thickness", Building Science, Vol.2, 1967, pp.181-188.
- [22] Coull, A. and Puri, R.D., "Analysis of Pierced Shear Walls", J. Struct. Div., ASCE, Vol. 94, ST1, Jan. 1968, pp.71-82.
- [23] Coull, A. and Puri, R.D., "Analysis of Coupled Shear Walls of Variable Cross-Section", Building Science, Vol. 2, 1968, pp.313-320.
- [24] Coull, A. and Irwin, A.W., "Design of Connecting Beams in Coupled Shear Wall Structures", J. Amer. Concrete Inst., March, 1969, pp.205-209.
- [25] Coull, A. and Irwin, A.W., "Analysis of Load Distribution in Multi-Storey Shear Wall Structures", Struc. Engr., Aug. 1970, pp.301-306.
- [26] Coull, A., "Interaction of Coupled Shear Walls With Elastic Foundations", J. Amer. Concrete Inst., June 1971, pp.456-461.
- [27] Coull, A., "Coupled Shear Walls Subjected to Differential Settlement", Building Science, Vol.6, 1971, pp.209-212.
- [28] Coull, A., and Subedi, N.K., "Framed-Tube Structures for High-Rise Buildings", J. Struc. Div., ASCE, Vol.97, ST8, Aug. 1971, pp.2097-2105.
- [29] Coull, A., and Subedi, N.K., "Coupled Shear Walls With Two and Three Bands of Openings", Building

Science, Vol.7, 1972, pp.81-86.

- [30] Coull, A., and Puri, R.D., and Tottenham, H., "Numerical Elastic Analysis of Coupled Shear Walls", Proc. Inst. of Civil Engrs., 1973, pp.109-128.
- [31] Coull, A., "Stiffening of Coupled Shear Walls Against Foundation Movement", Struc.Engr., No.1, Vol.52, Jan. 1974, pp.23-26.
- [32] Coull, A., and Bose, B., "Simplified Analysis of Framed-Tube Structures", J. Struc. Div., ASCE, Vol. 101, No. ST-11, Nov.1975, pp.2223-2240.
- [33] Coull, A., and Bose, B., "Torsion of Framed-Tube Structures", J. Struc. Div., ASCE, Vol.102, No.ST-12, December, 1976, pp.2366-2370.
- [34] De Clercq, H., "Analysis and Design of Tube-Type Tall Building Structures", Ph.D.Thesis, University of California, Berkeley, 1975.
- [35] Desai, C.S., and Abel, J.F., Introduction to the Finite Element Method, Van Nostrand Reinhold Co., N.Y., 1970.
- [36] Fazio, P., and Ha, H.K., "Analysis of Three-Dimensional Orthotropic Sandwich Plate Structures by Finite Element Method", Report No. SBC XX, CE-72-4, Dept. of Civil Engr., Sir George Williams University, Montreal, Canada, 1972.
- [37] Felippa, C.A., "Refined Finite Element Analysis of Linear and Nonlinear Two-Dimensional Structures", Ph.D.Thesis, Dept. of Civil Engr., University of California, Berkeley, 1966.
- [38] Fintel, M., Editor, Handbook of Concrete Engineering, Van Nostrand Reinhold Co., 1973, Chapter 10, pp.287-344.

- [39] Flower, W.R., and Schmidt, L.C., "Analysis of Space Truss as Equivalent Plate", J. Struc. Div., ASCE, Vol.97, No. ST-12, Dec. 1971, pp.2777-2789.
- [40] Flügge, W., Stresses in Shells, Springer-Verlag, N.Y., 2nd Edition, 1973, pp.295-310.
- [41] Goldberg, J.E., "Buckling Formulas for Design", Proc. Int. Conference on Planning and Design of Tall Buildings, Lehigh, 1972, Technical Committee No.16, Report No.7, Vol.II, 1972, pp.581-589.
- [42] Goldberg, J.E., "Approximate Methods In Stress and Stability Analysis of Tall Building Frames", Regional Conference on Tall Buildings, Bangkok, Jan. 1974, pp.177-193.
- [43] Graham, J., and Godden, W.G., Structural Engineering Handbook. McGraw-Hill Book Company, New York, N.Y., 1968, Section 1.
- [44] Ha, H.K., "Analysis of Three-Dimensional Orthotropic Sandwich Plate Structures by Finite Element Method", D.Eng. Thesis, Sir George Williams University, Montreal, Quebec, Canada, 1972.
- [45] Ha, H.K., "Tall Frame Analysis by Reduced Generalized Coordinates", J. Struc.Div., ASCE, Vol.104, ST-3, March, 1978, pp.527-536.
- [46] Ha, H.K., "Private Communication".
- [47] Harman, D.J., and Walker, W.H., "Analysis of Tall Buildings Using Member Groups", J. Struc.Div., ASCE, Vol.101, No. ST 3, March. 1975, pp.567-583.
- [48] Harrison, H.B., Computer Methods in Structural Analysis, Prentice-Hall, Inc., Englewood Cliffs, N.J., 1973.

- [49] Harrison, T., et al., "A Modified Beam Stiffness Matrix for Interconnected Shear Walls", Building Science, 1975, Vol.10, pp.89-94.
- [50] Heidebrecht, A.C. and Swift, R.D., "Analysis of Asymmetrical Coupled Shear Walls", J. Struc.Div., ASCE, Vol.97, ST5, May 1971, pp.1407-1422.
- [51] Heidebrecht, C., and Stafford-Smith, B., "Approximate Analysis of Open-Section Shear Walls Subject to Torsional Loading", J. Struc. Div. Proc. ASCE, Vol.99, No.St-12, Dec. 1973, pp.2355-2373.
- [52] Heidebrecht, A.C. and Stafford-Smith, B., "Approximate Analysis of Tall Wall-Frame Structures", J. Struc. Div. ASCE, Vol.99, ST2, Feb. 1973, pp.199-221.
- [53] Hisatoku, T., and Nishikawa, F., "Mixed and Composite Concrete and Steel Systems", Proc. Int. Conference on Planning and Design of Tall Buildings, Lehigh, 1972, Technical Committee No. 3, Report No. 6, Vol.1a, 1972, pp.501-513.
- [54] ICES STRUDL-II, Engineering User's Manual, M.I.T., Cambridge, 1968.
- [55] Iffland, J.S.B., "Design for Stability in High-Rise Buildings", Proc. Int. Conference on Planning and Design of Tall Buildings, Lehigh, Technical Committee No. 16, Report No. 2, Vol.II, 1972, pp.445-462.
- [56] Iyengar, H.S., "Preliminary Design and Optimization of Steel Building Systems," Proc. Int. Conference on Planning and Design of Tall Buildings, Lehigh, 1972. Technical Committee No. 14, SOA Report No.2, Vol.II, 1972, pp.185-200.
- [57] Iyengar, H.S., "Stability of Overall Structural Systems", Proc. Int. Conference on Planning and Design of Tall Buildings, Lehigh, Technical Committee No. 16, Report No. 4, Vol.II, 1972, pp.564-567.

- [58] Iyengar, H.S., "Composite or Mixed Steel-Concrete Construction for Buildings", State-of-the-Art Report, ASCE, 1977.
- [59] Khan, A.H., "Analysis of Tall Shear Wall-Frame and Tube Structures", Ph.D. Thesis, University of Southampton, U.K., March, 1974.
- [60] Khan, A.H., and Stafford-Smith, B., "Restraining Action of Bracing in Thin-Walled Open Section Beams", Proc. Inst. Civ. Engrs., Part 2, 1975, 59, Mar, 67-78.
- [61] Khan, A.H., and Stafford-Smith, B., "A Simple Method of Analysis for Deflection and Stresses in Wall-Frame Structures", Building and Environment, Vol.11, 1976, pp.69-78.
- [62] Khan, F.R., and Sbarounis, J.A., "Interaction of Shear Walls and Frames", J. Struc. Div., ASCE, Vol.90, ST3, June, 1964, pp.285-335.
- [63] Khan, F.R., Current Trends in Concrete High-Rise Buildings, Tall Building, Pergamon Press, 1967, pp.571-590.
- [64] Khan, F.R., "Recent Structural Systems in Steel for High-Rise Buildings", Proc. Conference on Steel in Architecture, London, 1969, pp.55-65.
- [65] Khan, F.R., "Influence of Design Criteria on Selection of Structural Systems for Tall Buildings", Canadian Structural Engineering Conference, 1972.
- [66] Khan, F.R., and Iyengar, H.S., "Optimization Approach for Concrete High-Rise Buildings", Paper 4, ACI Publication SP-36: Response of Multi-Storey Concrete Structures to Lateral Forces, 1973, pp.61-74.
- [67] Khan, F.R., and Amin, N.R., "Analysis and Design of Framed Tube Structures for Tall Concrete Buildings", Paper 3, ACI Publication SP-36: Response of Multi-storey Concrete Structures to Lateral Forces, 1973, pp.39-60.

- [68] Khan, F.R., Tubular Structures for Tall Buildings, Handbook of Concrete Engineering (ed. Mark Fintel), Van Norstrand Comp., 1974., Chapter 11, pp.345-355.
- [69] Khan, F.R., "New Structural Systems for Tall Buildings and Their Scale Effects on Cities", Proc. Symposium on Tall Buildings, Vanderbilt Univ., Nashville, Tennessee, Nov. 1974, pp.19-60.
- [70] König, G., "Cast-in-Place Reinforced Concrete Systems", Proc. Int. Conference on Planning and Design of Tall Buildings, Lehigh, Technical Committee No.3, Report No.2, Vol.II, 1972, pp.445-462.
- [71] Korn, G.A., and Korn, T.M., Mathematical Hand-book, McGraw-Hill Book Company, New York, N.Y., 1968, pp.344-357.
- [72] Kozak, J., "Structural Systems of Tall Buildings With Core Structures", Proc. Int. Conference on Planning and Design of Tall Buildings, Lehigh, Technical Committee No.3, Report No.8, Vol. Ia, 1972, pp.537-565.
- [73] Lim, L.C., and McNamara, R.J., "Stability of Novel Building System," Proc. Int. Conference on Planning and Design of Tall Buildings, Lehigh, 1972, Technical Committee No. 16, SOA Report No.5, Vol.II, 1972, pp.499-524.
- [74] Lu, L.W., et al, "Strength and Drift Characteristics of Steel Frames", J. Struc. Div., ASCE, Vol.103, No. ST-11, Nov.1977, pp.2225-2241.
- [75] MacGregor, J.G., "Stability of Reinforced Concrete Building Frames", Proc. Int. Conference on Planning and Design of Tall Buildings, Lehigh, 1972, Technical Committee No. 23, Report No. 1, Vol. III, 1972, pp. 517-536.
- [76] MacGregor, J.G., and Hage, S.E., "Stability Analysis and Design of Concrete Frames", J. Struc.Div.ASCE, Vol.103, No.ST-10, Oct.1977, pp.1953-1970.

- [77] MacLeod, I.A., "Simplified Equations for Deflection of Multi-Storey Frames", Building Science, Vol.6, 1971, pp.25-31.
- [78] MacLeod, I.A., "Analysis of Shear Wall Buildings by the Frame Method", Proc.Inst. Civ.Engrs, 1973, 55, Sept., pp.593-603.
- [79] MacLeod, I.A., and Green, D.R., "Frame Idealization for Shear Wall Support Systems", Struc.Engr., 1973, 51, No.2, Feb., pp.71-74.
- [80] MacLeod, A., "General Frame Element For Shear Wall Analysis", Proc. Inst. Civ.Engrs., Part 2, 1976, 61, Dec., pp.785-790.
- [81] MacLeod, I.A., and Hosny, H.M., "The Distribution of Vertical Load in Shear Wall Buildings", Struct.Engr., 1976, 54, No.2, pp.62-71.
- [82] MacLeod, I.A., and Hosny, H.M., "Frame Analysis of Shear Wall Cores", J. Struc. Div., ASCE, Vol.103, No.ST-10, Oct. 1977, pp. 2037-2047.
- [83] Mazzeo, L.A., and De Fries, A., "Perimetral Tube for 37-Storey Steel Building", J. Struc.Div., ASCE, Vol.98, No.ST 6, June 1972, pp.1255-1272.
- [84] Moselhi, O., Fazio, P., and Zielinski, Z., Discussion of "Torsion of Framed-Tube Structures", J. Struc. Div., ASCE, Vol.103, No. ST-12, pp.2426-2428.
- [85] Moselhi, O., Fazio, P., and Zielinski, Z., "Simplified Analysis of Wall-Frame Structures", J.Can.Soc. of Civ.Engg., Vol.5, No.2, June 1978.
- [86] Nair, R.S., "Linear Structural Analysis of Multi-storey Buildings", J. Struc.Div., ASCE, Vol.101, No.ST 3, March 1975, pp.551-565.
- [87] Nixon, D., Beaulieu, D., and Adams, P.F., "Simplified Second-Order Frame Analysis", Can.J. Civ.Engg., Vol.2, No.4, Dec.1975, pp.602-605.

- [88] Reissner, E., "Analysis of Shear Lag in Box Beams by the Principle of Minimum Potential Energy", Quart. Applied Maths., Vol. 4, Oct. 1946, pp. 268-278.
- [89] Richmond, B., "Twisting of Thin-Walled Box Girders", Proc. I.C.E., April, 1966.
- [90] Richter, P.J., Reddy, D.P., and Agbabian, M.S., "Three-Dimensional Dynamic Analysis of Multistorey Concrete Office Buildings", Paper 8, ACI Publication SP-36: Response of Multistorey Concrete Structures to Lateral Forces, 1973, pp. 151-186.
- [91] Rosman, R., "An Approximate Method of Analysis of Walls of Multi-Storey Buildings", Civ. Engg. and Public Works Rev., London, Vol. 59, Jan. 1964, pp. 67-69.
- [92] Rosman, R., "Approximate Analysis of Shear Walls Subject to Lateral Loads", J. Am. Conc. Inst., June 1964, pp. 717-732.
- [93] Rosman, R., Laterally Loaded Systems Consisting of Walls and Frames, Tall Building, Pergamon Press, 1967, pp. 273-289.
- [94] Rosman, R., "Torsion of Perforated Concrete Shafts", J. Struc. Div., ASCE, Vol. 95, ST5, May, 1969, pp. 991-1010.
- [95] Rosman, R., "Analysis of Spatial Concrete Shear Wall Systems", Proc. Inst. of Civ. Engrs., Supplement (vi), 1970, pp. 131-151.
- [96] Rosman, I.R., "Statics of Non-Symmetric Shear Wall Structures", Proc. Inst. Civ. Engrs., Supplement xii, 1971, pp. 211-244.
- [97] Rosman, R., "The Continuum Analysis of Shear-Wall Structures", Proc. Intl. Conf. on Planning and Design of Tall Buildings, Lehigh, 1972, Technical Committee No. 21, Discussion No. 4, Vol. III, 1972, pp. 271-276.

- [98] Rosman, R., "Dynamics and Stability of Shear Wall Building Structures", Proc. Inst. of Civ. Engrs., 1973, Part 2, pp.411-423.
- [99] Roy, H.E.H., "Design for Lateral Loads", Structural Concrete Symposium, University of Toronto, May, 1971, pp.146-175.
- [100] Rutenberg, A., Discussion on "Framed-Tube Structures for High-Rise Buildings", by A. Coull and N.K. Subedi, J. Struc.Div., ASCE, Vol.97, ST4, April 1972, pp.942-943.
- [101] Rutenberg, A., Discussion on "Perimetral Tube for 37-Storey Steel Building", by Mazzeo, A., and De Fries, A., J. Struc.Div., ASCE, Vol. , No.ST3, March 1973, pp.586-588.
- [102] Rutenberg, A.V., and Tso, W.K., "Torsional Analysis of Perforated Core Structure", J. Struc.Div., ASCE, Vol.101, No.ST3, March, 1975, pp.539-549.
- [103] Schwaighofer, J., "Door Openings in Shear Walls", J. Am. Concrete Inst. Nov.1967, pp.730-734.
- [104] Schwaighofer, J., and Microys, H.F., "Analysis of Shear Walls Using Standard Computer Programs", J. Am. Concrete Inst., Dec. 1969, pp.1005-1007.
- [105] Schwaighofer, J., "Shear Wall Structures", Structural Concrete Symposium, University of Toronto, 1971, pp.119-145.
- [106] Schwaighofer, J., and Ast.P.A., "Tables for the Analysis of Framed-Tube Buildings", Publication 72-01, Dept. Civ.Engrg., University of Toronto, Canada, Mar. 1972.
- [107] Segerlind, L.J., Applied Finite Element Analysis, John Wiley & Sons, Inc., N.Y. 1976.

- [108] Smith, A., and Wilson, C.A., "Wind Stresses in the Steel Frames of Office Buildings", J. Western Soc. of Engrs., April, 1915, pp.365-390.
- [109] Stafford-Smith, B., and Taranath, B.S., "The Analysis of Tall Core-Supported Structures Subjected to Torsion", Proc. Inst. of Civ.Engrs. Vol.53, Sept. 1972, pp.173-187.
- [110] Stafford-Smith, Editor, Planning and Design of Tall Buildings, Vol.CB, Chapter 21C, Revised Draft 1, March 1976.
- [111] Stress, A., User's Manual, M.I.T. Press, Cambridge, Mass., U.S.A., 1964.
- [112] Taranath, B.S., and Stafford-Smith, B., "Torsion Analysis of Shear Core Structures", ACI Publication: SP-35, 1974, pp.239-263.
- [113] Taranath, B.S., "Analysis of Interconnected Open Section Shear Wall Structures", J. Struc.Div., ASCE, Vol.101, No.ST11, Nov. 1975, pp:2367-2384.
- [114] Timoshenko, S.P., and Goodier, J.N., Theory of Elasticity, Third edition, McGraw-Hill Book Company, 1970, pp.53-60.
- [115] Troitsky, M.S., Orthotropic Bridges - Theory and Design, The James F. Lincoln Arc Welding Foundation, Cleveland, Ohio, 1967.
- [116] Troitsky, M.S., Stiffened Plates - Bending, Stability and Vibrations, Elsevier Scientific Publ.Co., N.Y., 1976.
- [117] Tso, W.K. and Biswas, J.K., "General Analysis of Non-Planar Coupled Shear Walls", J. Struc.Div., ASCE, Vol.99, ST3, Mar.1973, pp.365-380.

- [118] Turner, M.J., "The Direct Stiffness Method of Structural Analysis", Structures and Materials, Panel Paper, AGARD Meeting, Aachen, Germany, Sept. 17, 1959.
- [119] Vlasov, V.S., "Thin-Walled Elastic Beams", English Translation, National Science Foundation, Washington, D.C., 1961.
- [120] Wang, C.K., Computer Methods in Advanced Structural Analysis, Intext Press, Inc., N.Y., 1973.
- [121] Weaver, W. and Nelson, M.F., "Three-Dimensional Analysis of Tier Buildings", J. Struc. Div., ASCE, Vol.92, ST6, Dec.1966, pp.385-404.
- [122] Williams, D., An Introduction to the Theory of Aircraft Structures, Edward Arnold Ltd., 1960.
- [123] Wilson, C.A., "Wind Bracing With Knee-Braces or Gusset Plates", Engineering Record, Sept. 1908, pp. 272-274.
- [124] Wilson, E.L., "Programme Listing", Short course on Finite Element Method, University of California, Berkeley, 1967.
- [125] Wilson, E.L., "The Static Condensation Algorithm", International Journal of Numerical Methods in Engineering, Vol.8, No.1, 1974, pp.198-203.
- [126] Yarimci, E., "The Equivalent Beam Approach in Tall Building Stability Analysis", Proc. Intl. Conference on Planning and Design of Tall Buildings, Lehigh, 1972, Technical Committee No. 16, Report No.3, Vol.II, 1972, pp.553-563.
- [127] Younger, J.E., Mechanics of Aircraft Structures, 2nd Ed., McGraw-Hill, Inc., N.Y., 1942.

[128] Zienkiewicz, O.C., The Finite Element Method in Engineering Sciences, 2nd Edition, McGraw-Hill Book Co., N.Y., 1971.

[129] Zienkiewicz, O.C., Parekh, C.J., and Teply, B., "Three-Dimensional Analysis of Buildings Composed of Floor and Wall Panels", Proc. Inst. of Civ. Engrs. Vol. 49, July, 1971, pp. 319-332.

APPENDIX A

THE INTEGRALS USED IN EVALUATING THE TERMS
OF THE ORDINARY ELEMENT STIFFNESS MATRIX

APPENDIX A

THE INTEGRALS USED IN EVALUATING THE TERMS
OF THE ORDINARY ELEMENT STIFFNESS MATRIX

Each K_{ij} term in the element stiffness matrix (Eq. 5.13) is obtained by integrating the corresponding term of Eq. (5.12) according to Eq. (5.11) as follows:

$$K_{11} = t ab \int_0^1 \int_0^1 (G_{xy}/b^2) d\xi d\eta = tr G_{xy}$$

$$K_{21} = -K_{11}$$

$$K_{31} = t ab \int_0^1 \int_0^1 G_{xy} [(1-\eta)/ab] d\xi d\eta = \frac{1}{2} t G_{xy}$$

$$K_{41} = -K_{31}$$

$$K_{51} = -\frac{t}{2} ab \int_0^1 \int_0^1 G_{xy} (\eta/ab) d\xi d\eta = -\frac{1}{2} t G_{xy} = -K_{31}$$

$$K_{61} = K_{31}$$

$$K_{22} = K_{11}$$

$$K_{32} = -K_{31}$$

$$K_{42} = K_{31}$$

$$K_{52} = K_{31}$$

$$K_{62} = -K_{31}$$

$$K_{33} = t ab \left[\int_0^1 \int_0^1 E_Y \{(1-2\xi+\xi^2)/b^2\} d\xi d\eta + \int_0^1 \int_0^1 G_{XY} \{(1-2\eta+\eta^2)/a^2\} d\xi d\eta \right] = \frac{t}{3} [r E_Y + G_{XY}/r]$$

$$K_{43} = t ab \int_0^1 \int_0^1 E_Y \{(\xi-\xi^2)/b^2\} d\xi d\eta - \frac{t}{3} G_{XY}/r = \frac{t}{3} \left[\frac{1}{2} r E_Y - G_{XY}/r \right]$$

$$K_{53} = -\frac{t}{6} [r E_Y + G_{XY}/r] = -\frac{1}{2} K_{33}$$

$$K_{63} = \frac{t}{3} \left[-r E_Y + \frac{1}{2} G_{XY}/r \right]$$

$$K_{44} = K_{33}$$

$$K_{54} = t ab \left[\int_0^1 \int_0^1 -E_Y (\xi^2/b^2) d\xi d\eta + \int_0^1 \int_0^1 G_{XY} \{\eta(1-\eta)/a^2\} d\xi d\eta \right] = \frac{t}{3} \left[-r E_Y + \frac{1}{2} G_{XY}/r \right] = K_{63}$$

$$K_{64} = -\frac{t}{6} [r E_Y + G_{XY}/r] = -\frac{1}{2} K_{33}$$

$$K_{55} = K_{33}$$

$$K_{65} = \frac{t}{3} \left[\frac{1}{2} r E_y - G_{xy}/r \right] = K_{43}$$

$$K_{66} = K_{33}$$

where

$$r = a/b$$

t = the thickness of the element

APPENDIX B

DERIVATIONS OF THE REFINED ELEMENT STIFFNESS
MATRIX

APPENDIX B

DERIVATIONS OF THE REFINED ELEMENT STIFFNESS MATRIX

Each K_{ij} term in the element stiffness matrix, as explained previously in Chapter V, is obtained by integrating the corresponding B_{ij} term of the matrix resulting from the triple matrix product $[D]^T[E][D]$. The B_{ij} terms are first evaluated as follows:

$$B_{11} = \frac{G_{xy}}{4b^2} (1-2\eta)^2$$

$$B_{21} = \frac{G_{xy}}{b^2} \eta(1-2\eta)$$

$$B_{31} = -\frac{G_{xy}}{4b^2} (1+2\eta)(1-2\eta)$$

$$B_{41} = \frac{G_{xy}}{8ab} (1-2\xi-\eta+2\xi\eta)(1-2\eta)$$

$$B_{51} = \frac{G_{xy}}{2ab} \xi(1-\eta)(1-2\eta)$$

$$B_{61} = -\frac{G_{xy}}{8ab} (1+2\xi-\eta-2\xi\eta)(1-2\eta)$$

$$B_{71} = -\frac{G_{xy}}{8ab} (1+2\xi+\eta+2\xi\eta)(1-2\eta)$$

$$B_{81} = \frac{G_{xy}}{2ab} \xi(1+\eta)(1-2\eta)$$

$$B_{91} = \frac{G_{xy}}{8ab} (1-2\xi+\eta-2\xi\eta) (1-2\eta)$$

$$B_{22} = \frac{4G_{xy}}{b^2} \eta^2$$

$$B_{32} = \frac{G_{xy}}{b^2} \eta (1+2\eta)$$

$$B_{42} = \frac{G_{xy}}{2ab} \eta (1-2\xi-\eta+2\xi\eta)$$

$$B_{52} = \frac{2G_{xy}}{ab} \eta \xi (1-\eta)$$

$$B_{62} = \frac{G_{xy}}{2ab} \eta (1+2\xi-\eta-2\xi\eta)$$

$$B_{72} = -\frac{G_{xy}}{2ab} \eta (1+2\xi+\eta+2\xi\eta)$$

$$B_{82} = \frac{2G_{xy}}{2ab} \eta \xi (1+\eta)$$

$$B_{92} = \frac{G_{xy}}{2ab} \eta (1-2\xi+\eta-2\xi\eta)$$

$$B_{33} = \frac{G_{xy}}{4b^2} (1+2\eta)^2$$

$$B_{43} = -\frac{G_{xy}}{8ab} (1+2\eta) (1-2\xi-\eta+2\xi\eta)$$

$$B_{53} = \frac{G_{xy}}{2ab} \xi(1-\eta)(1+2\eta)$$

$$B_{63} = \frac{G_{xy}}{8ab} (1+2\eta)(1+2\xi-\eta-2\xi\eta)$$

$$B_{73} = \frac{G_{xy}}{8ab} (1+2\eta)(1+2\xi+\eta+2\xi\eta)$$

$$B_{83} = \frac{G_{xy}}{2ab} \xi(1+\eta)(1+2\eta)$$

$$B_{93} = -\frac{G_{xy}}{8ab} (1+2\eta)(1-2\xi+\eta-2\xi\eta)$$

$$B_{44} = \frac{E_y}{16b^2} \xi^2(1-\xi)^2 + \frac{G_{xy}}{16a^2} (1-2\xi-\eta+2\xi\eta)^2$$

$$B_{54} = -\frac{E_y}{8b^2} \xi(1-\xi)(1-\xi^2) + \frac{G_{xy}}{4a^2} \xi(1-\eta)(1-2\xi-\eta+2\xi\eta)$$

$$B_{64} = \frac{E_y}{16b^2} \xi^2(1-\xi^2) - \frac{G_{xy}}{16a^2} (1-2\xi-\eta+2\xi\eta)(1+2\xi-\eta-2\xi\eta)$$

$$B_{74} = \frac{E_y}{16b^2} \xi^2(1-\xi^2) - \frac{G_{xy}}{16a^2} (1-2\xi-\eta+2\xi\eta)(1+2\xi+\eta+2\xi\eta)$$

$$B_{84} = \frac{E_y}{8b^2} \xi(1-\xi)(1-\xi^2) + \frac{G_{xy}}{4a^2} \xi(1+\eta)(1-2\xi-\eta+2\xi\eta)$$

$$B_{94} = -\frac{E_y}{16b^2} \xi^2(1-\xi)^2 + \frac{G_{xy}}{16a^2} (1-2\xi+\eta-2\xi\eta)(1-2\xi-\eta+2\xi\eta)$$

$$B_{55} = \frac{EY}{4b^2} (1-\xi^2)^2 + \frac{G_{xy}}{a^2} \xi^2 (1-\eta)^2$$

$$B_{65} = \frac{EY}{8b^2} \xi(1+\xi)(1-\xi^2) - \frac{G_{xy}}{4a^2} \xi(1-\eta)(1+2\xi-\eta-2\xi\eta)$$

$$B_{75} = -\frac{EY}{8b^2} (1+\xi)(1-\xi^2) - \frac{G_{xy}}{4a^2} \xi(1-\eta)(1+2\xi+\eta+2\xi\eta)$$

$$B_{85} = \frac{EY}{4b^2} (1-\xi^2)^2 + \frac{G_{xy}}{a^2} \xi^2 (1-\eta^2)$$

$$B_{95} = \frac{EY}{8b^2} \xi(1-\xi)(1-\xi^2) + \frac{G_{xy}}{4a^2} \xi(1-\eta)(1-2\xi+\eta-2\xi\eta)$$

$$B_{66} = \frac{EY}{16b^2} \xi^2(1+\xi)^2 + \frac{G_{xy}}{a^2} \xi^2(1-\eta)^2$$

$$B_{76} = -\frac{EY}{16b^2} \xi^2(1+\xi)^2 + \frac{G_{xy}}{16a^2} (1+2\xi-\eta-2\xi\eta)(1+2\xi+\eta+2\xi\eta)$$

$$B_{86} = -\frac{EY}{8b^2} \xi(1+\xi)(1-\xi^2) - \frac{G_{xy}}{4a^2} \xi(1+\eta)(1+2\xi-\eta-2\xi\eta)$$

$$B_{96} = \frac{EY}{16b^2} \xi^2(1-\xi^2) - \frac{G_{xy}}{16a^2} (1+2\xi-\eta-2\xi\eta)(1-2\xi+\eta-2\xi\eta)$$

$$B_{77} = \frac{EY}{16b^2} \xi^2(1+\xi)^2 + \frac{G_{xy}}{16a^2} (1+2\xi+\eta+2\xi\eta)^2$$

$$B_{87} = \frac{EY}{8b^2} \xi(1+\xi)(1-\xi^2) - \frac{G_{xy}}{4a^2} \xi(1+\eta)(1+2\xi+\eta+2\xi\eta)$$

$$B_{97} = -\frac{E_Y}{16b^2} \xi^2 (1-\xi^2) - \frac{G_{xy}}{16a^2} (1+2\xi+\eta+2\xi\eta) (1-2\xi+\eta-2\xi\eta)$$

$$B_{88} = \frac{E_Y}{4b^2} (1-\xi^2)^2 + \frac{G_{yx}}{a^2} \xi^2 (1+\eta)^2$$

$$B_{98} = -\frac{E_Y}{8b^2} \xi (1-\xi) (1-\xi^2) + \frac{G_{xy}}{4a^2} \xi (1+\eta) (1-2\xi+\eta-2\xi\eta)$$

$$B_{99} = \frac{E_Y}{16b^2} \xi^2 (1-\xi)^2 + \frac{G_{xy}}{16a^2} (1-2\xi+\eta-2\xi\eta)^2$$

Each of the above terms is then doubly integrated with respect to ξ and η to yield the corresponding term in the element stiffness matrix, viz.:

$$K_{11} = \frac{t}{4} r G_{xy} \int_{-1}^1 \int_{-1}^1 (1-4\eta+4\eta^2) d\xi d\eta = \frac{7}{3} tr G_{xy}$$

$$K_{21} = tr G_{xy} \int_{-1}^1 \int_{-1}^1 (\eta-2\eta^2) d\xi d\eta = -\frac{8}{3} rt G_{xy}$$

$$K_{31} = tr G_{xy} \int_{-1}^1 \int_{-1}^1 (1-4\eta^2) d\xi d\eta = \frac{1}{3} rt G_{xy}$$

$$K_{41} = \frac{1}{8} t G_{xy} \int_{-1}^1 \int_{-1}^1 (1-2\xi-3\eta+6\xi\eta+2\eta^2-4\xi\eta^2) d\xi d\eta =$$

$$= \frac{5}{6} t G_{xy}$$

$$K_{51} = 2t G_{xy} \int_{-1}^1 \int_{-1}^1 \xi (1-3\eta+2\eta^2) d\xi d\eta = 0.0$$

$$K_{61} = -\frac{1}{2} t G_{xy} \int_{-1}^1 \int_{-1}^1 (1+2\xi-3\eta-6\xi\eta+2\eta^2+4\xi\eta^2) d\xi d\eta =$$

$$= -\frac{5}{6} t G_{xy}$$

$$K_{71} = -\frac{1}{8} t G_{xy} \int_{-1}^1 \int_{-1}^1 (1+2\xi-\eta-2\xi\eta-2\eta^2+4\xi\eta^2) d\xi d\eta =$$

$$= -\frac{1}{6} t G_{xy}$$

$$K_{81} = \frac{1}{2} t G_{xy} \int_{-1}^1 \int_{-1}^1 \xi(1-\eta-2\eta^2) d\xi d\eta = 0.0$$

$$K_{91} = \frac{1}{8} t G_{xy} \int_{-1}^1 \int_{-1}^1 (1-2\xi-\eta+2\xi\eta-2\eta^2+4\xi\eta^2) d\xi d\eta =$$

$$= \frac{1}{6} t G_{xy}$$

$$K_{22} = 4 \operatorname{tr} G_{xy} \int_{-1}^1 \int_{-1}^1 \eta^2 d\xi d\eta = \frac{16}{3} \operatorname{tr} G_{xy}$$

$$K_{32} = -\operatorname{tr} G_{xy} \int_{-1}^1 \int_{-1}^1 \eta(1+2\eta) d\xi d\eta$$

$$K_{32} = -\frac{8}{3} \operatorname{tr} G_{xy}$$

$$K_{42} = \frac{1}{2} t G_{xy} \int_{-1}^1 \int_{-1}^1 (1-2\xi-\eta+2\xi\eta) d\xi d\eta = -\frac{2}{3} t G_{xy}$$

$$K_{52} = 2t G_{xy} \int_{-1}^1 \int_{-1}^1 \xi\eta(1-\eta) d\xi d\eta = 0.0$$

$$K_{62} = -\frac{1}{2} t G_{xy} \int_{-1}^1 \int_{-1}^1 \eta(1-2\xi-\eta-2\xi\eta) d\xi d\eta = \frac{2}{3} t G_{xy}$$

$$K_{72} = -\frac{1}{2} t G_{xy} \int_{-1}^1 \int_{-1}^1 \eta(1+2\xi+\eta+2\xi\eta) d\xi d\eta = \frac{2}{3} t G_{xy}$$

$$K_{82} = 2t G_{xy} \int_{-1}^1 \int_{-1}^1 \xi\eta(1+\eta) d\xi d\eta = 0.0$$

$$K_{92} = \frac{1}{2} t G_{xy} \int_{-1}^1 \int_{-1}^1 \eta(1-2\xi+\eta-2\xi\eta) d\xi d\eta = \frac{2}{3} t G_{xy}$$

$$K_{33} = \frac{1}{4} \text{tr} G_{xy} \int_{-1}^1 \int_{-1}^1 (1+4\eta+4\eta^2) d\xi d\eta = \frac{7}{3} \text{tr} G_{xy}$$

$$K_{43} = -\frac{1}{8} t G_{xy} \int_{-1}^1 \int_{-1}^1 (1-2\xi+\eta-2\xi\eta-2\eta^2+4\xi\eta^2) d\xi d\eta =$$

$$= -\frac{1}{6} t G_{xy}$$

$$K_{53} = -\frac{1}{2} t G_{xy} \int_{-1}^1 \int_{-1}^1 \xi(1+\eta-2\eta^2) d\xi d\eta = 0.0$$

$$K_{63} = \frac{1}{8} t G_{xy} \int_{-1}^1 \int_{-1}^1 (1+2\xi+\eta+2\xi\eta-2\eta^2-4\xi\eta^2) d\xi d\eta =$$

$$= \frac{1}{6} t G_{xy}$$

$$K_{73} = \frac{1}{8} t G_{xy} \int_{-1}^1 \int_{-1}^1 (1+2\xi+3\eta+6\eta\xi+2\eta^2+4\xi\eta^2) d\xi d\eta =$$

$$= \frac{5}{6} t G_{xy}$$

$$K_{83} = -\frac{1}{2} t G_{xy} \int_{-1}^1 \int_{-1}^1 \xi(1+3\eta+2\eta^2) d\xi d\eta = 0.0$$

$$K_{93} = -\frac{1}{8} t G_{xy} \int_{-1}^1 \int_{-1}^1 (1-2\xi+3\eta-6\eta\xi+2\eta^2-4\xi\eta^2) d\xi d\eta =$$

$$= -\frac{5}{6} t G_{xy}$$

$$\begin{aligned}
K_{44} &= \frac{1}{16} \operatorname{tr} E_Y \int_{-1}^1 \int_{-1}^1 \xi^2 (1-2\xi+\xi^2) d\xi d\eta + \\
&+ \frac{1}{16} \frac{t}{r} G_{xy} \int_{-1}^1 \int_{-1}^1 (1-2\xi-\eta+2\xi\eta)^2 d\xi d\eta = \\
&= \frac{2}{15} \operatorname{tr} E_Y + \frac{7}{9} \frac{t}{r} G_{xy}
\end{aligned}$$

$$\begin{aligned}
K_{54} &= -\frac{1}{8} \operatorname{tr} E_Y \int_{-1}^1 \int_{-1}^1 (\xi-\xi^2-\xi^3+\xi^4) d\xi d\eta + \\
&+ \frac{1}{4} \operatorname{tr} G_{xy} \int_{-1}^1 \int_{-1}^1 \xi (1-2\xi-2\eta+4\xi\eta+\eta^2-2\xi\eta^2) d\xi d\eta = \\
&= \frac{1}{15} \operatorname{tr} E_Y + \frac{8}{9} \frac{t}{r} G_{xy}
\end{aligned}$$

$$\begin{aligned}
K_{64} &= -\frac{t}{16} r E_Y \int_{-1}^1 \int_{-1}^1 (\xi^2-\xi^4) d\xi d\eta - \\
&- \frac{t}{16} \frac{1}{r} G_{xy} \int_{-1}^1 \int_{-1}^1 (1-2\eta-4\xi^2+8\xi^2\eta+\eta^2-4\xi^2\eta^2) d\xi d\eta = \\
&= -\frac{1}{30} \operatorname{tr} E_Y + \frac{1}{9} \frac{t}{r} G_{xy}
\end{aligned}$$

$$\begin{aligned}
K_{74} &= \frac{t}{16} r E_Y \int_{-1}^1 \int_{-1}^1 (\xi^2-\xi^3) d\xi d\eta - \\
&- \frac{1}{16} \frac{t}{r} G_{xy} \int_{-1}^1 \int_{-1}^1 (1-4\xi^2-\eta^2+4\xi^2\eta^2) d\xi d\eta = \\
&= \frac{1}{30} \operatorname{tr} E_Y + \frac{1}{18} \frac{t}{r} G_{xy}
\end{aligned}$$

$$\begin{aligned}
K_{84} &= \frac{t}{8} r E_Y \int_{-1}^1 \int_{-1}^1 (\xi - \xi^2 - \xi^3 + \xi^4) d\xi d\eta + \\
&+ \frac{1}{4} \frac{t}{r} G_{xy} \int_{-1}^1 \int_{-1}^1 \xi (1 - 2\xi - \eta^2 + 2\xi\eta^2) d\xi d\eta = \\
&= -\frac{1}{15} \text{tr } E_Y - \frac{4}{9} \frac{t}{r} G_{xy}
\end{aligned}$$

$$\begin{aligned}
K_{94} &= -\frac{t}{16} r E_Y \int_{-1}^1 \int_{-1}^1 \xi^2 (1 - 2\xi + \xi^2) d\xi d\eta + \\
&+ \frac{1}{16} \frac{t}{r} G_{xy} \int_{-1}^1 \int_{-1}^1 (1 - 4\xi + 4\xi^2 - \eta^2 + 4\xi\eta^2 - 4\xi^2\eta^2) d\xi d\eta = \\
&= -\frac{2}{15} \text{tr } E_Y + \frac{7}{18} \frac{t}{r} G_{xy}
\end{aligned}$$

$$\begin{aligned}
K_{55} &= \frac{t}{4} r E_Y \int_{-1}^1 \int_{-1}^1 (1 - 2\xi^2 + \xi^4) d\xi d\eta + \\
&+ \frac{t}{r} G_{xy} \int_{-1}^1 \int_{-1}^1 \xi^2 (1 - 2\eta + \eta^2) d\xi d\eta = \\
&= \frac{8}{15} \text{tr } E_Y + \frac{16}{9} \frac{t}{r} G_{xy}
\end{aligned}$$

$$\begin{aligned}
K_{65} &= \frac{t}{8} r E_Y \int_{-1}^1 \int_{-1}^1 (\xi + \xi^2 - \xi^3 - \xi^4) d\xi d\eta - \\
&- \frac{1}{4} \frac{t}{r} G_{xy} \int_{-1}^1 \int_{-1}^1 \xi (1 + 2\xi - 2\eta - 4\xi\eta + \eta^2 + 2\xi\eta^2) d\xi d\eta = \\
&= \frac{1}{15} \text{tr } E_Y - \frac{8}{9} \frac{t}{r} G_{xy}
\end{aligned}$$

$$\begin{aligned}
 K_{75} &= -\frac{t}{8} r E_Y \int_{-1}^1 \int_{-1}^1 (\xi + \xi^2 - \xi^3 - \xi^4) d\xi d\eta - \\
 &\quad - \frac{1}{4} \frac{t}{r} G_{xy} \int_{-1}^1 \int_{-1}^1 \xi (1 + 2\xi - \eta^2 - 2\eta^2 \xi) d\xi d\eta = \\
 &= -\frac{1}{15} \text{tr } E_Y - \frac{4}{9} \frac{t}{r} G_{xy}
 \end{aligned}$$

$$\begin{aligned}
 K_{85} &= -\frac{t}{4} r E_Y \int_{-1}^1 \int_{-1}^1 (1 - 2\xi^2 + \xi^4) d\xi d\eta + \\
 &\quad + \frac{t}{r} G_{xy} \int_{-1}^1 \int_{-1}^1 \xi^2 (1 - \eta^2) d\xi d\eta = \\
 &= -\frac{8}{15} \text{tr } E_Y + \frac{8}{9} \frac{t}{r} G_{xy}
 \end{aligned}$$

$$\begin{aligned}
 K_{95} &= \frac{t}{8} r E_Y \int_{-1}^1 \int_{-1}^1 (\xi - \xi^2 - \xi^3 + \xi^4) d\xi d\eta + \\
 &\quad + \frac{1}{4} \frac{t}{r} G_{xy} \int_{-1}^1 \int_{-1}^1 \xi (1 - 2\xi - \eta^2 + 2\xi \eta^2) d\xi d\eta = \\
 &= \frac{1}{15} \text{tr } E_Y - \frac{4}{9} \frac{t}{r} G_{xy}
 \end{aligned}$$

$$\begin{aligned}
 K_{66} &= \frac{t}{16} r E_Y \int_{-1}^1 \int_{-1}^1 \xi^2 (1 + 2\xi + \xi^2) d\xi d\eta + \\
 &\quad + \frac{1}{16} \frac{t}{r} G_{xy} \int_{-1}^1 \int_{-1}^1 (1 + 4\xi - 2\eta - 8\xi\eta + 4\xi^2 - 8\xi^2\eta + \eta^2 + \\
 &\quad + 4\xi\eta^2 + 4\xi^2\eta^2) d\xi d\eta = \frac{2}{15} \text{tr } E_Y + \frac{7}{9} \frac{t}{r} G_{xy}
 \end{aligned}$$

$$\begin{aligned}
K_{76} &= -\frac{t}{16} r E_Y \int_{-1}^1 \int_{-1}^1 \xi^2 (1+2\xi+\xi^2) d\xi d\eta + \\
&+ \frac{1}{16} \frac{t}{r} G_{xy} \int_{-1}^1 \int_{-1}^1 (1+4\xi+4\xi^2-\eta^2-4\xi\eta^2-4\xi^2\eta^2) d\xi d\eta = \\
&= -\frac{2}{15} \text{tr } E_Y + \frac{7}{18} \frac{t}{r} G_{xy}
\end{aligned}$$

$$\begin{aligned}
K_{86} &= -\frac{t}{8} r E_Y \int_{-1}^1 \int_{-1}^1 (\xi+\xi^2-\xi^3-\xi^4) d\xi d\eta - \\
&- \frac{1}{4} \frac{t}{r} G_{xy} \int_{-1}^1 \int_{-1}^1 \xi(1+2\xi-\eta^2-2\xi\eta^2) d\xi d\eta = \\
&= -\frac{1}{15} \text{tr } E_Y - \frac{4}{9} \frac{t}{r} G_{xy}
\end{aligned}$$

$$\begin{aligned}
K_{96} &= \frac{t}{16} r E_Y \int_{-1}^1 \int_{-1}^1 \xi^2 (1-\xi^2) d\xi d\eta - \\
&- \frac{1}{16} \frac{t}{r} G_{xy} \int_{-1}^1 \int_{-1}^1 (1-4\xi^2-\eta^2+4\xi^2\eta^2) d\xi d\eta = \\
&= \frac{1}{30} \text{tr } E_Y + \frac{1}{18} \frac{t}{r} G_{xy}
\end{aligned}$$

$$\begin{aligned}
K_{77} &= \frac{t}{16} r E_Y \int_{-1}^1 \int_{-1}^1 \xi^2 (1+2\xi+\xi^2) d\xi d\eta + \\
&+ \frac{1}{16} \frac{t}{r} G_{xy} \int_{-1}^1 \int_{-1}^1 (1+2\xi+\eta+2\xi\eta)^2 d\xi d\eta = \\
&= \frac{2}{15} \text{tr } E_Y + \frac{7}{9} \frac{t}{r} G_{xy}
\end{aligned}$$

$$\begin{aligned}
K_{87} &= \frac{t}{8} r E_Y \int_{-1}^1 \int_{-1}^1 (\xi + \xi^2 - \xi^3 - \xi^4) d\xi d\eta - \\
&- \frac{1}{4} \frac{t}{r} G_{xy} \int_{-1}^1 \int_{-1}^1 (\xi + 2\xi^2 + 2\xi\eta + 4\xi^2\eta + \xi\eta^2 + 2\xi^2\eta^2) d\xi d\eta = \\
&= \frac{1}{15} \text{tr } E_Y - \frac{8}{9} \frac{t}{r} G_{xy}
\end{aligned}$$

$$\begin{aligned}
K_{97} &= -\frac{t}{16} r E_Y \int_{-1}^1 \int_{-1}^1 (\xi^2 - \xi^4) d\xi d\eta - \\
&- \frac{1}{16} \frac{t}{r} G_{xy} \int_{-1}^1 \int_{-1}^1 (1 + 2\eta - 4\xi^2 - 8\xi^2\eta + \eta^2 - 4\xi^2\eta^2) d\xi d\eta = \\
&= -\frac{1}{30} \text{tr } E_Y + \frac{1}{9} \frac{t}{r} G_{xy}
\end{aligned}$$

$$\begin{aligned}
K_{88} &= \frac{t}{4} r E_Y \int_{-1}^1 \int_{-1}^1 (1 - 2\xi^2 + \xi^4) d\xi d\eta + \\
&+ \frac{t}{r} G_{xy} \int_{-1}^1 \int_{-1}^1 (\xi^2 + 2\eta\xi^2 + \xi^2\eta^2) d\xi d\eta = \\
&= \frac{8}{15} \text{tr } E_Y + \frac{16}{9} \frac{t}{r} G_{xy}
\end{aligned}$$

$$\begin{aligned}
K_{98} &= -\frac{t}{8} r E_Y \int_{-1}^1 \int_{-1}^1 (\xi - \xi^2 - \xi^3 + \xi^4) d\xi d\eta + \\
&+ \frac{1}{4} \frac{t}{r} G_{xy} \int_{-1}^1 \int_{-1}^1 (\xi - 2\xi^2 + 2\xi\eta - 4\xi^2\eta + \xi\eta^2 - 2\xi^2\eta^2) d\xi d\eta = \\
&= \frac{1}{15} \text{tr } E_Y - \frac{8}{9} \frac{t}{r} G_{xy}
\end{aligned}$$

$$\begin{aligned}
K_{99} &= \frac{t}{16} r E_y \int_{-1}^1 \int_{-1}^1 (\xi^2 - 2\xi^3 + \xi^4) d\xi d\eta + \\
&+ \frac{1}{16} \frac{t}{r} G_{xy} \int_{-1}^1 \int_{-1}^1 (1 - 4\xi - 2\eta - 8\xi\eta + 4\xi^2 + 6\xi^2\eta + \eta^2 - \\
&- 4\xi\eta^2 + 4\xi^2\eta^2) d\xi d\eta = \frac{2}{15} tr E_y + \frac{7}{9} \frac{t}{r} G_{xy}
\end{aligned}$$

in which

$$r = a/b$$

t = the thickness of the element.

APPENDIX C
COMPUTER PROGRAM

APPENDIX C
COMPUTER PROGRAM

C.1 INTRODUCTION

A large capacity computer program (program TUBE) has been developed for the analysis of most currently available planar and tube-type tall building structures, incorporating the developments presented in Chapters II, III, V and VI. The program is written in FORTRAN IV and was run on a CDC 6600 computer. Efficient use of the memory storage has been achieved by employing the transformation and the global assembly techniques of Chapter VI and by the aid of auxiliary storage via six magnetic tapes.

As with the finite element method, a feeling for the physical behavior of the structure is desirable for the efficient use of the program which is based on the equivalent orthotropic macroelement method. The developments of Chapter III are intended to serve this purpose. Other studies on the behavioral characteristics of other structures that may be analyzed by the TUBE program [1,6,34,60,67,73] are also recommended.

Generally, the reduction in computer time and storage is obtained at the expense of some loss in accuracy. Such loss in accuracy can be minimized if the structure under

consideration is properly idealized. In this case the program can yield results very close to those obtained from the "exact" analysis. This has been demonstrated for planar and tubular structures as shown in Chapters V and VII, respectively.

The amount of input data required for the program is kept to a minimum by implementing automatic data generation wherever it is possible. Subsequently, both the effort of data preparation and the possible data errors are minimized.

The objective of this Appendix is to describe clearly the logic of the program through its different stages and to express its essential features. This will serve two purposes:

- (1) Assisting the user to implement the TUBE program correctly and efficiently,
- (2) facilitating any further developments to update and/or modify the current version of the program.

C.2 SCOPE

The program TUBE performs approximate elastic static and stability analyses for a number of planar and tube-type tall building structures. Frames consisting of slender or relatively deep members, coupled shear walls, frames interacting with shear walls, and clad-frames are direct examples

of the planar structural systems which can be analyzed using the TUBE program. The tubular systems which the program can be implemented for their analysis include primarily framed tubed structures, core supported structures with open or closed section, and structures consisting of interacting shear walls with normal frames. These tubular systems can be seen as the three-dimensional assembly of the first three planar systems respectively.

The structures to be analyzed by the program should preferably possess a high degree of regularity. For framed structures, bay widths, storey heights, and member sizes should not change over large parts of the structure. This is also true for structures containing coupling lintel beams. This does not constitute a severe restriction; high degree of regularity is inherent in most, if not all, tall building structures due to aesthetic reasons and to ensure ease of construction and consequent savings in time and money [34].

Planar frames and their spacial assembly must consist of horizontal beams rigidly connected to vertical columns. Structures must also satisfy the assumptions stated earlier in Chapter I.

C.3 DESCRIPTION OF THE PROGRAM

The major part of the program logic follows the section on analysis procedure presented in Chapter VI. The program can be divided into three main stages. In the first stage, the data is entered on two levels: global structure level through subroutine DATA1 and local facade and element level through subroutine DATA2. Basically in the global level the geometry of the tube view plan is specified and the overall load vector is directly assembled. Facade properties (number of elements and properties of each element type) are specified at the local level. Construction of the global structure stiffness matrix which corresponds to the overall load vector constitutes the second main stage of the program. In this stage the mechanical properties of the equivalent orthotropic membrane, if not given directly, are evaluated in subroutine EMAT. Discretization including element connectivity and type is generated automatically in ELCON. Individual element stiffness matrices are generated in RECT and then assembled to form the local facade stiffness matrix in ASMBL 1. This assembly is based on the degrees of freedom associated with each element. The degrees of freedom are automatically generated in LABEL and adjusted in SYMM if any type of symmetry exists within the facade. The facade stiffness matrix is then condensed by eliminating all internal degrees of freedom using GAUSS and transformed to the global system

using the technique explained in Sections 6.6 and 6.7.

Different transformation matrices are used for the different symmetry types of the global structure. Facade properties including the condensed stiffness matrix, global interacting level stiffness matrices, and the corresponding transformation matrix are stored on tapes 1, 2 and 5, respectively. Global interacting level stiffness matrices are finally assembled using LABS in ASMBL2 to form the global structure stiffness matrix. In the third and final stage, displacements, stresses and member internal forces are evaluated respectively via (GAUSS), (STRESS) and (STRESS and FORCE).

C.4 USER'S GUIDE

To minimize any possible data errors and to ensure efficient implementation of the program, a detailed discussion on data preparation including suggestions to improve the accuracy of the analysis is given in this section.

These suggestions are based on the findings of Chapter III, the experience gained through implementing the program for the analysis of a variety of structures, and previous work [6, 34, 51, 52, 60, 67, 73].

6.4.1 Structure Modelling

Besides the rules and definitions given previously in Section 6.4, the following simple, systematic steps may be followed.

Step 1:

Draw a plan view and elevation for the structure to be analyzed indicating the reference axes, lateral loads, and the number of each level, corner and facade as shown in Fig. 7.1.

Step 2:

Decide on whether the ordinary element (4-corner nodes and 6-degrees-of-freedom) or the refined element (8-nodes, and 9-degrees-of-freedom), is to be used in the analysis. The latter is recommended for cases where the effect of shear lag is significant, as shown earlier in Chapter V.

Step 3:

In case of symmetry decide on the degrees of freedom to be restrained in the part of the structure. Thus, indicate the symmetry type number for the whole structure and within each facade.

Step 4:

Since each facade is almost considered separately in the program, draw a separate elevation for each facade discretized to a number of elements, indicating the number of each element and its type. Note that while dividing a

facade into a number of elements, the vertical and horizontal lines used for this purpose need not coincide with the center-lines of columns and beams, respectively. A table may be arranged in conjunction with the drawings as shown in Fig. 7.10.

Step 5:

Decide on the type of output (i.e., stresses or member internal forces), and the levels at which these values should be printed.

In addition to these five steps, the following suggestions may prove helpful while dividing the structure, to a number of levels and consequently, each facade to a number of elements:

- (1) In general, as many as five to ten stories can be incorporated in an element. In the cases treated, this represents approximately from one-third to one-fourth the total number of stories in the structure.
- (2) The use of three more single storey levels near the base of the structure [6,34], appears to be a sound rule.

- (3) At the top of the structure, a single-storey level or more in some cases is desirable. This is not crucial for the overall behavior of the structure [34]. However, such consideration is more important in structures deforming in a predominant bending mode.
- (4) In dividing each facade to a number of elements, always provide a finer mesh at the area of stress concentration (i.e., near the edges of the facade.) In general, the elements adjacent to the corners of the building are desirable to incorporate only one bay; especially when using the ordinary element.

C.4.2 Input Data

Units must be consistent and data cards for each problem must be in the sequence shown below. Integers and reals are specified in 5-and-10-column fields respectively throughout all data cards.

A. PROBLEM NUMBER AND TITLE (I5,3X,9A8) - One Card

Columns 1-5: Problem number

Columns 9-80: Title of the problem to be printed
as output heading

B. STRUCTURE CONTROLLING PARAMETERS (715) -- One Card

- Columns 1-5: Number of façades
- Columns 6-10: Number of levels
- Columns 11-15: Number of joint loads
- Columns 16-20: Basic element type code:
- 0: Use the ordinary element in the analysis (see Chapter V)
 - 1: Use the refined element in the analysis (see Chapter V)
- Columns 21-25: Plan view shape code:
- 0: Closed cross-section
 - 1: Open cross-section
- Columns 26-30: Symmetry type code:
- 0: No symmetry
 - 1: Besides the vertical displacements of corners, the structure is only allowed to displace laterally in the x-direction (i.e. $v=\theta=0.0$)
 - 2: As in 1 but with respect to the y-direction (i.e. $u=\theta=0.0$)
 - 3: As in 1 but with respect to the rotation about the z-axis (i.e. $u=v=0.0$)

Columns 31-35: Type of output code:

- 0: Member internal forces
- 1: Stresses at the mid-height of the element and at specified column centerlines
- 2: Stresses at element centroid of the ordinary element and each half (dividing width-wise) of the refined element

C. COORDINATES OF CORNERS (I5,2F10.0) - One card for each corner

Columns: 1-5: Corner number
 6-10: Its X-coordinate
 11-15: Its Y-coordinate

D. GEOMETRY OF FACADES (5I5, F10.0) - One card for each facade

Columns: 1-5: Facade number
 6-10: Number of its first side
 11-15: Number of its second side
 16-20: Number of horizontal elements
 21-25: Number of vertical elements
 26-35: Perpendicular distance between the facade and the reference center of

the structure

- E. APPLIED LATERAL LOADS (I5,3F10.0) - One card for each loaded level

Columns: 1-5: Level number
 6-15: Value of load component in the direction of global X-axis
 16-25: Value of the load component in the direction of global Y-axis
 26-35: Value of the torsional moment about the global Z-axis

- F. STRESSES AND INTERNAL FORCES PRINTING CODE (16I5)

As many cards as needed (one card in most - if not all - cases.) Each 5-column field corresponds to a level in sequence starting from first level.

- 0: Do not calculate stresses and member internal forces in all elements bounded by this level and the one below it.
- 1: Calculate and print stresses or member internal forces (according to the type of output indicated in B) in all elements bounded by this level and the one below it.

G. The following group of cards, from G.1 to G.5, is to be repeated for each facade.

G.1 FACADE TITLE (8A10) - One card

Columns 1-80: Title of the facade

G.2 FACADE CONTROLLING PARAMETERS (6I5) - One card

Columns 1-5: Number of horizontal elements

6-10: Number of vertical elements

11-25: Number of different material types

16-20: Number of different element types

21-25: Symmetry type code:

0: No symmetry

1: Facade is not allowed to translate laterally in its plane

2: All nodes located on the second side of the facade are restrained from the vertical displacement

3: As in 2 but with respect to the first side.

Columns 26-30: Material input code:

- 0: Beam, column, and the original material properties should be entered (see G3.1, G3.2, and G3.3.)
- 1: Mechanical properties of the equivalent membrane are entered directly. (See G.3 below.)

Cards from G.3.1 to G.3.3 are to be prepared only if the material input code, given in G.2, equals zero. This set of cards should be repeated whenever any of the properties included in it is different.

G.3.1 MATERIAL PROPERTIES (2E10.3) - One card

Columns 1-10: Young's modulus (E)
 11-20: Poisson's ratio (μ)

G.3.2 BEAM PROPERTIES (3F10.0) - One card

Columns 1-10: Span
 11-20: Depth
 21-30: Thickness

G.3.3 COLUMN PROPERTIES (3F10.0) - One card

Columns	1-10:	Height
	11-20:	Depth
	21-30:	Thickness

G.3 EQUIVALENT MATERIAL PROPERTIES (4E10.3) - One card

To be prepared only if the material input type code, given in G.2, equals one.

Columns	1-10:	Corresponds to E_x and may be left blank
	11-20:	Value of E_y
	21-30:	Value of G_{xy}
	31-40:	Thickness

G.4 ELEMENT TYPE PROPERTIES (I5,2F10.0,3I5) - One card

for each element type

Columns	1-5:	Type number
	6-15:	Width
	16-25:	Height
	26-30:	Material type number
	31-35:	Number of bays
	36-40:	Number of stories

G.5 ASSIGNMENT OF A TYPE NUMBER FOR EACH ELEMENT (4I5) -

One card for each element type

Columns	1-5:	N1
	6-10:	N2
	11-15:	I
	16-20:	NT

All elements from number N1 through number N2 with increment I. are assigned an element type number of NT.

Repeat the whole group of data cards from A to G.5 for each new problem. After those of the last problem place a BLANK CARD at the end of the complete set of data cards.

G.6 PROGRAM OUTPUT

To ensure direct checking of input data, most of the input information and those automatically generated are printed out. In case of errors resulting from core allocation, or any operation on the algebraic equilibrium equations, a corresponding message will be printed out.

Global structure displacements which include:

lateral displacement in the X-direction (u), lateral displacement in the Y-direction (v), rotation (θ) about the Z-axis, and vertical displacement at each corner are printed at each level.

According to the codes which indicate the type of the printed output and its location, stresses or member internal forces are printed at the specified locations.

C.6 PROGRAM LISTING

The FORTRAN listing of the TUBE program is documented below.

COMPUTER PROGRAM LISTING

73/172 OPT=1

FTN 4.6+446

73/01/31. 19.34

PROGRAM TUBE (INPUT,OUTPUT,TAPE1,TAPE2,TAPE3,TAPE4,TAPE5,TAPE6)

```

*****
*****THE PURPOSE OF THE PROGRAM IS TO ANALYZE TUBULAR *****
*****TALL BUILDING STRUCTURES. THE ANALYSIS IS LINEARLY *****
*****ELASTIC AND STATIC. *****
*****

```

PROGRAM VARIABLES

```

*   NF =NO. OF FACADES
*   NL =NC. OF LEVELS
*   NJL =NC. OF JOINT LOADS
*   NHEL=NO. OF HORIZONTAL ELEMENTS IN ONE FACADE
*   NVEL=NO. OF VERTICAL ELEMENTS IN ONE FACADE
*   NMAT=NO. OF DIFFERENT MATERIALS IN ONE FACADE
*   NTYPE=NO. OF ELEMENT TYPES IN ONE FACADE
*   NEQ =NO. EQUATIONS FOR THE TUBE STRUCTURE

```

*****PROGRAM ARRAYS

```

*   FP(N,5) =5 PROPERTIES FOR EACH FACADE, N= NO OF FACADE
*   FP(N,1) =NO. OF FIRST CORNER LINE
*   FP(N,2) =NO. OF SECOND CORNER LINE
*   FP(N,3) =NHEL
*   FP(N,4) =NVEL
*   FP(N,5) =DISTANC OF FACADE FROM CENTRE LINE OF TUBE STRUCTURE
*   X(N)   = X-COORDINATE OF A CORNER LINE, N=NO. OF FACADE
*   Y(N)   = Y-COORDINATE OF A CORNER LINE, N=NO. OF FACADE
*   EX(M)..
*   EY(M)..
*   GXY(M)..
*   GXY(M) =ELASTIC PROPERTIES OF EQUIVALENT ORTHOTROPIC
*           MEMBRANE, M= MATERIAL TYPE NO.
*   EC(NP) = ELEMENT CONNECTIVITY, NP=NODE NO.
*   EL(N0) = ELEMENT LABEL, N0=NO. OF ELEMENT DOF
*   QK     = ELEMENT STIFFNESS MATRIX
*   T      = TRANSFORMATION MATRIX
*   K----- LOCAL SUB STIFFNESS MATRIX
*   S----- GLOBAL SUB STIFFNESS MATRIX
*   ETN(N) = ELEMENT TYPR NO IN SEQUENCE FROM 1 TO N
*   BB     = STRAIN DISPLACEMENT MATRIX
*   C      = STRESS STRAIN MATRIX
*   R      = GENERALIZED LOAD OR DISPLACEMENT VECTOR
*           OR LOCAL FACADE DISPLACEMENT VECTOR
*   AK     = FACADE STIFFNESS MATRIX BEFORE AND AFTER CONDENSATION
*           OR GLOBAL TUBE STRUCTURE STIFFNESS MATRIX
*   Q, SIG = ELEMENT NOOAL DISPLACEMENTS AND C.G. STRESSES ON
*   B, BBCLK, LN, FD, FLD, ... ARRAYS FOR MATRIX MANIPULATION

```

73/172 OPT=1

FTN 4.6+446

7

```

C .....
C
60 C
C DIMENSION TITLE(9)
C COMMON ON STRUCTURAL LEVEL.....INPUT
COMMON NF,NL,NJL,NOOF,NSHAPE,NSSYM,NOUT
C COMMON ON FAÇADE LEVEL .....INPUT
65 COMMON/P1/ FP(4,4),RFP(4),X(4),Y(4),NPRINT(10)
COMMON/P2/NHEL,NVEL,NMAT,NTYPE,NEOF,LMAX,NSYM,NPR,NBAY,NSTOR
1EX(6),EY(6),GXY(6),TH(6),EC(8),EL(6),LEL(9),
2ET(12,2),ETM(12),ETN(90),OK(9,9),IEH(12),IEH(12)
COMMON/P3/ T(3,5),K(3,3),S(5,5),B(3,5)
70 C COMMON ON STRUCTURAL LEVEL .....SOLUTION
COMMON/P4/NEQ,R(70),AK(6105)
INTEGER FP,EC,EL,ETM,ETN
INTEGER AMAX
DATA MAXNF,MAXNL,MAXMAT,MAXTYP,MAXFEL
75 1 / 4, 10, 6, 12, 90/
C
C REWIND 3
C
C PROBLEM IDENTIFICATION AND DESCRIPTION
80 C
9999 READ 100,NPROB,(TITLE(I),I=1,9)
IF(NPROB.LE.0) GO TO 999
PRINT 200,NPROB,(TITLE(I),I=1,9)
C
85 C READ OVERALL STRUCTURAL DATA
C
CALL DATA1(MAXNF,MAXNL,ISTOP1)
IF(ISTOP1.GT.0) GO TO 999
C
90 C COMPUTE REQ. STORAGE FOR GLOBAL TUBE STIFF MATRIX.
C
AMAX = (NEQ*NEQ-NEQ)/2+NEQ
C
C READ EACH FAÇADE DATA
95 REWIND 1
REWIND 2
REWIND 5
REWIND 6
00 500 N=1,NF
100 CALL DATA2(MAXMAT,MAXTYP,MAXFEL,ISTOP2,NCOF)
IF(ISTOP2.GT.0) STOP
C
C
C 1....ASSEMBLE EACH FAÇADE STIFF. MATRIX
105 C 2....CONDENSE INTERNAL DOF.
C 3....SAVE CONDENSED STIFF. MATRIX ON TAPE1
C 4....EXTRACT SUB MATRICES K 3X3 FROM MATRIX IN STEP 3
C 5....TRANSFORM EACH K TO GLOBAL SYSTEM FORMING S 5X5
C 6....SAVE ALL S MATRICES ON TAPE2
110 C
CALL ASMBL1(N,NL,NOOF,NSSYM)
500 CONTINUE
C
C ASSEMBLE OVERALL STRUCTURAL STIFF. MATRIX AK

```

PROGRAM TUBE 73/172 OPT=1

FTN 4.6+446

7

```

115      C
          CALL ASMBL2(NL,NEQ,AMAX,AK,NF,NSHAPE,NSSYM)
      C
      C SOLVE FOR GENERALIZED SRTUCRE DISPLACEMENTS AND PRINT IT
      C
120      C      CALL GAUSS(AK,R,NEQ,NLO,1,DET,1)
      C
          IF(NSSYM.NE.0) GO TO 10
          PRINT 300
          NC=(NEQ/NL)-3
125          DO 1000 II=1,NL
              I=(NEQ/NL)*(II-1)
              PRINT 400,II,R(I+1),R(I+2),R(I+3),(R(I+3+J),J=1,NC)
1000         CONTINUE
              GO TO 444
130          10 CONTINUE
              NC=(NEQ/NL)-1
              IF(NSSYM.EQ.1) GO TO 30
              IF(NSSYM.EQ.2) GO TO 40
              PRINT 800
135              GO TO 222
              30 CONTINUE
              PRINT 600
              GO TO 222
              40 CONTINUE
              PRINT 700
140              222 CONTINUE
                  DO 1100 II=1,NL
                      I=(NEQ/NL)*(II-1)
                      PRINT 900,II,R(I+1),(R(I+1+J),J=1,NC)
145              1100 CONTINUE
                  444 CONTINUE
                      WRITE(3) (R(I),I=1,NEQ)
      C
      C CALCULATE STRESSES
150      C
          CALL STRESS(NL,NF,NDOF,NSHAPE,NSSYM,NOUT)
      C
          GO TO 9999
      C
155      100 FORMAT(I5,3X,9A8)
          200 FORMAT(/8H1PROBLEM,I5,3H.,9A8/)
          300 FORMAT(38H1OUTPUT TABLE 1.. GLOBAL DISPLACEMENTS //
              1 2X,5HLEVEL,8X,7HX-DISP.,8X,7HY-DISP.,8X,7H ROT-O .16X,
              2 25HVERTICAL DISP. OF CORNERS/ )
160      400 FORMAT(I7,3E15.3,5X,4(E10.3,3X))
          600 FORMAT(38H1OUTPUT TABLE 1.. GLOBAL DISPLACEMENTS //
              1 * LEVEL NO. X-DISPL. DISPLACEMENT OF
              1 CORNERS *///)
165      700 FORMAT(38H1OUTPUT TABLE 1.. GLOBAL DISPLACEMENTS //
              1 * LEVEL NO. Y-DISPL. DISPLACEMENT OF
              1 CORNERS *///)
          800 FORMAT(38H1OUTPUT TABLE 1.. GLOBAL DISPLACEMENTS //
              1 * LEVEL NO. ROTATION DISPLACEMENT OF
              1 CORNERS *///)
170      900 FORMAT(I10,4X,E10.3,4(4X,E10.3))
      C
          999 CONTINUE
          STOP
          END

```


SUBROUTINE DATA1

73/172 OPT=1

FTN 4.6+446

7

```

1      SUBROUTINE DATA1(MAXNF,MAXNL,ISTOP1)
      C .....
      C *
      C *   THIS SUBROUTINE READS PROPERTIES OF THE TUBE STRUCTURE *
      C * .....
5      COMMON NF,NL,NJL,NDOF,NSHAPE,NSSYM,NOUT
      COMMON/P1/ FP(4,4),RFP(4),X(4),Y(4),NPRINT(10)
10     COMMON/P4/NEQ,R(70),AK(6105)
      INTEGER FP,EC,EL,ETM,ETN
      REAL MT

      C
15     READ 1,NF,NL,NJL,NDOF,NSHAPE,NSSYM,NOUT
      PRINT 101,NF,NL,NJL
      IF(NDOF.EQ.0) GO TO 90
      PRINT 95
      GO TO 91
20     90 CONTINUE
      PRINT 100
      91 CONTINUE

      C
25     C CHECK TO BE SURE INPUT DATA DOES NOT EXCEED STORAGE CAPACITY
      C
      ISTOP1=0
      IF(NF.LE.MAXNF) GO TO 10
      ISTOP1=ISTOP1+1
      PRINT 20,MAXNF
30     10 IF(NL.LE.MAXNL) GO TO 11
      ISTOP1=ISTOP1+1
      PRINT 21,MAXNL
      11 IF(ISTOP1.EQ.0) GO TO 12
      PRINT 22,ISTOP1
35     STOP
      12 CONTINUE

      C
40     C COMPUT TUBE DOF (NO. OF EQUATIONS)
      C
      IF(NSSYM.NE.0) GO TO 60
      IF(NSHAPE.NE.0) GO TO 50
      NEQ=(3+NF)*NL
      GO TO 51
45     50 CONTINUE
      NEQ=(4+NF)*NL
      51 CONTINUE
      GO TO 61
      60 CONTINUE
      NEQ=NL*(1+NF)
50     61 CONTINUE

      C
      C READ AND PRINT PROPERTIES OF FACADES
      C
55     PRINT 102
      IF(NSHAPE.NE.0) GO TO 14
      I=NF
      GO TO 15

```

SUBROUTINE DATA1 73/172 OPT=1

FTN 4.6+446

7

```

14 CONTINUE
   I=NF+1
60 15 CONTINUE
      DO 29 N=1,I
      READ 2, NN,X(N),Y(N)
      PRINT 52,N,X(N),Y(N)
29 CONTINUE
E5 C
      PRINT 103
      DO 30 N=1,NF
      READ 3,NN,(FP(N,I),I=1,4),RFP(N)
      PRINT 53,N,(FP(N,I),I=1,4),RFP(N)
70 30 CONTINUE
C
C READ, PRINT DIRECT LOAD
C READ, PRINT DIRECT JOINT LOADS AND SET UP OVERALL LOAD VECTOR R
C FOR SIMPLICITY, JLN=NO. OF CORRESPONDING LEVEL
75 C
      PRINT 104
C INITIALIZE LOAD VECTOR
C
      DO 40 I=1,NEQ
      R(I)=0.0
80 40 CONTINUE
      J2=NEQ/NL
      IF(NSSYM.NE.0) GO TO 42
      DO 41 J=1,NJL
      READ 4,J1,FX,FY,MT
85 PRINT 54,J1,FX,FY,MT
      J3=J1+J2-J2
      R(J3+1)=FX
      R(J3+2)=FY
      R(J3+3)=MT
90 41 CONTINUE
      GO TO 444
C
95 42 CONTINUE
      DO 70 I=1,NJL
      READ 4,J1,FX,FY,MT
      PRINT 54,J1,FX,FY,MT
      J3=J1+J2-J2
      IF(NSSYM.EQ.1) GO TO 44
      IF(NSSYM.EQ.2) GO TO 45
100 R(J3+1)=MT
      GO TO 70
      44 CONTINUE
      R(J3+1)=FX
      GO TO 70
105 45 CONTINUE
      R(J3+1)=FY
      70 CONTINUE
110 444 CONTINUE
      READ 80, (NPRINT(I),I=1,NL)
C
1 FOPMAT(7IS)
101 FORMAT(35H INPUT TABLE 1.. BASIC PARAMETERS //
1 5X, 40H NUMBER OF FACADES .....I5/

```

SUBROUTINE DATA1

73/172 OPT=1

FTN 4.6+446

```

115      2      5X, 40H NUMBER OF LEVELS. . . . .,I5/
        3      5X, 40H NUMBER OF LOADED JOINTS . . . . .,I5)
100     FORMAT(/** ANALYSIS IS PERFORMED USING THE ORDINARY ELEMENT WITH
        1 6DOF**/)
120     95     FOPMAT(/** ANALYSIS IS PERFORMED USING THE REFINED ELEMENT WITH
        1 9DOF**/)
        20     FORMAT(//// 28+ TOO MANY FACADES. MAXIMUM = .I5)
        21     FORMAT(//// 28+ TOO MANY LEVELS.. MAXIMUM = .I5)
        22     FOPMAT(//// 28H EXECUTION HALTED BECAUSE OF,I5,13H FATAL ERRORS //)
        2      FORMAT(I5,2F10.0)
125     102    FORMAT(//35H0INPUT TABLE 2.. FACADE PROPERTIES //
        1      12H CORNER NO.,8X,12HX-COORDINATE,8X,12HY-COORDINATE)
        52     FORMAT(I12,2F20.4)
        3      FORMAT(I5,5F10.0)
130     103    FORMAT(// 12H FACADE NO.,4X,1HI,4X,1HJ,4X,4HNHEL,4X,4HNVEL,4X,
        1      17HDIST. FROM CENTRE//)
        53     FORMAT(I12,2I5,2I8,F20.4)
        4      FORMAT(I5,3F10.0)
        104    FORMAT(//26H INPUT TABLE 3.. LOAD DATA //
        1      10H LEVEL NO. ,5X,7HFORCE-X,5X,7HFORCE-Y,5X,7HTORSION)
135     54     FOPMAT(I10,3F12.4)
        60     FORMAT(10I5)
C
999     RETURN
      END

```

SUBROUTINE DATA2

73/172 OPT=1

FTN 4.6+446

7

```

1      SUBROUTINE DATA2(MAXMAT,MAXTYP,MAXFEL,ISTOP2,NOOF)
      C
      C
      C *****
      C * THIS SUBROUTINE READS AND PRINTS FACADE'S PROPERTIES *
      C * *****
      C
10     COMMON/P2/NHEL,NVEL,NMAT,NTYPE,NEOF,LMAX,NSYM,NPR,NBAY,NSTOR,
      1EX(6),EY(6),GXY(6),TH(6),EC(6),EL(6),LEL(9),
      2ET(12,2),ETH(12),ETN(90),QK(9,9),IEH(12),IEH(12)
      DIMENSION TITLE(8)
      INTEGER FP,EC,EL,ETH,ETN
15     C
      C
      C READ 99,TITLE
      C PRINT 100,TITLE
      C READ 1, NHEL,NVEL,NMAT,NTYPE,NSYM,INCCDE
20     NEL=NHEL*NVEL
      C PRINT 101,NHEL,NVEL,NMAT,NTYPE
      C
      C CHECK TO BE SURE THAT INPUT DATA DOES NOT EXCEED STORAGE CAPACITY
      C
25     ISTOP2=0
      C IF(NEL.LE.MAXFEL) GO TO 10
      C ISTOP2=ISTOP2+1
      C PRINT 20,MAXFEL
30     10 IF(NMAT.LE.MAXMAT) GO TO 11
      C ISTOP2=ISTOP2+1
      C PRINT 21,MAXMAT
      C 11 IF(NTYPE.LE.MAXTYP) GO TO 12
      C ISTOP2=ISTOP2+1
      C PRINT 22,MAXTYP
35     12 IF(ISTOP2.EQ.0) GO TO 13
      C ISTOP2=ISTOP2+1
      C PRINT 23,ISTOP2
      C STOP
40     13 CONTINUE
      C READ AND PRINT MATERIAL PROPERTIES
      C
      C IF(INCODE.NE.0) GO TO 14
      C CALL EMAT
      C GO TO 15
45     14 CONTINUE
      C READ 2, (EX(I),EY(I),GXY(I),TH(I),I=1,NMAT)
      C 15 CONTINUE
      C PRINT 102
50     PRINT 52, (I,EX(I),EY(I),GXY(I),TH(I),I=1,NMAT)
      C
      C
      C READ AND PRINT ELEMENT TYPE PROPERTIES
      C
      C READ TYPR OF EACH ELEMENT
55     C
      C PRINT 103

```

SUBROUTINE DATA2

73/172 OPT=1

FTN 4.6+446

```

60      DO 30 J =1, NTYPE
          READ 3, NN, (ET(J,I), I=1,2), ETM(J), IEW(J), IEH(J)
          PRINT 53, J, (ET(J,I), I=1,2), ETM(J), IEW(J), IEH(J)
30      CONTINUE
C
C GENERATE AND PRINT ELEMENT CONNECTIVITY AND TYPE
C
65      PRINT 104
          DO 35 I=1, NTYPE
            READ 4, NS, NE, INC, NELT
            DO 35 II=NS, NE, INC
              ETN(II)=NELT
35      CONTINUE
          DO 40 I=1, NEL
            CALL ELCON(I, NDOF)
            IF(NDOF.NE.0) GO TO 41
            NNP=4
            GO TO 42
75      41 CONTINUE
            NNP=8
          42 CONTINUE
          PRINT 54, I, (EC(J), J=1, NNP), ETN(I)
80      40 CONTINUE
C
99      FORMAT(8A10)
100     FORMAT(1H1///2X, 8A10)
1      FORMAT(6I5)
85     101  FORMAT(35H INPUT TABLE A.. FACADE PROPERTIES //
          1      5X, 40H NUMBER OF HORIZONTAL ELEMENTS . . . . .I5/
          2      5X, 40H NUMBER OF VERTICAL ELEMENTS . . . . .I5/
          3      5X, 40H NUMBER OF DIFFERENT MATERIALS . . . . .I5/
          4      5X, 40H NUMBER OF DIFFERENT ELEMENT TYPES . . . . .I5)
90     2      FORMAT(4E10.3)
102     FORMAT(//36H INPUT TABLE B.. MATERIAL PROPERTIES //
          1      10H MATERIAL, 5X, 10H MODULUS, 5X, 10H MODULUS,
          2      6X, 7H SHEAR, 7X, 8H MATERIAL/
          3      4X, 6H NUMBER, 10X, 2HEX, 13X, 2HEY, 11X, 7H MODULUS, 6X, 9H THICKNES)
95     52     FORMAT(I10, 4E15.4)
          3      FORMAT(I5, 2F10.0, 3I5)
103     FORMAT(//30H INPUT TABLE C.. ELEMENT TYPES //
          1      10H ELEMENT, 8X, 7HELEMENT, 8X, 7HELEMENT, 2X, 8H MATERIAL,
          1      4X, 6H NO. OF, 4X, 6H NO. OF/
          2      6X, 4H TYPE, 8X, 7H WIDTH-A, 7X, 8H HEIGHT-B, 6X, 4H TYPE,
100     3      6X, 4H BAYS, 4X, 7H STORIES/)
          53     FORMAT(I10, 2F15.4, 3I10)
          4      FORMAT(4I5)
104     FORMAT(/** ELEMENT CONNECTIVITY AND TYPE*/)
105     54     FORMAT(10I5)
          20     FORMAT(/**TOO MANY ELEMENTS IN FACADE, MAXIMUM=*, I5)
          21     FORMAT(/**TOO MANY DIFFERENT MATERIALS, MAXIMUM= *, I5)
          22     FORMAT(/**TOO MANY ELEMENT TYPES ,MAXIMUM= *, I5)
          23     FORMAT(/**EXECUTION HALTED BECAUSE OF *, I5, *FATAL ERRORS*/)
110     C
          RETURN
          END

```

SUBROUTINE EMAT

73/172 OPT=1

FTN 4.6+446

7

```

1      SUBROUTINE EMAT
      C
      C *****
      C * THIS SUBROUTINE EVALUATES THE ELASTIC PROPERTIES *
      C * OF THE EQUIVALENT ORTHOTROPIC MEMBRANE *
      C *****
10     COMMON/P2/NHEL,NVEL,NMAT,NTYPE,NEOF,LMAX,NSYM,NPR,NBAY,NSTOR,
      1EX(6),EY(6),GXY(6),TH(6),EC(8),EL(6),LEL(9),
      2ZET(12,2),ETM(12),ETN(90),OK(9,9),IEH(12),IEH(12)
      INTEGER FP,EC,EL,ETM,ETN
      REAL MU
      C
      C
20     DO 9999 I=1,NMAT
      READ 1, E,MU
      READ 2, B,BD,BT
      READ 2, H,CD,CT
      TT=BT
      G=E/2.*(1.+MU)
      Q=1./(CD*BT)
      X=CD/2.
      Y=BD/2.
      C
      C
30     C FIRST DELTA OF PARTS 1 AND 3
      DCOL=(H-BD)/(CD*CT*E)
      PRINT 91,DCOL
      91 FORMAT(// * DEFORMATION OF PARTS 1 AND 3 = * ,E15.4)
      C DELTA OF PART 2 DUE TO UNIFORM STRESS ONLY
      VUNIF=Q*CD*BD/(B*E)
      PRINT 92, VUNIF
35     92 FORMAT( * EDFORMATION DUE TO UNIFORM STRESS ..PART 2.. * ,
      1E15.4)
      C DELTA OF PART 2 DUE TO INIFNIT FOURIER SERIES ONLY
      TERM=0.
40     DO 10 M=1,50
      AL=M*22./(7.*B/2.)
      ALA=AL*CD/2.
      ALC=AL*BD/2.
      ALX=AL*X
      ALY=AL*Y
      T1=SIN(ALA)/(AL*M)
      T2=(1.+MU)*ALC*COSH(ALC)*SINH(ALY)
      T3=(1.-MU)*SINH(ALC)*SINH(ALY)
      T4=(1.+MU)*(ALY*COSH(ALY)-SINH(ALY))*SINH(ALC)
      T5=COS(ALX)/(SINH(2.*ALC)+2.*ALC)
      TERM=TERM+T1*(T2+T3-T4)*T5
50     10 CONTINUE
      VFUNC=TERM*4.*Q/(E*22./7.)
      PRINT 93, VFUNC
55     93 FORMAT( * EDFORMATION DUE TO FOURIER TERMS .. PART 2 .. * ,
      1E15.4)
      E2=H/(B*TT*(DCOL+VUNIF+2.*VFUNC))

```

SUBROUTINE EMAT

73/172 OPT=1

FTN 4.6+446

7

```

        EY(I)=0.
        EY(I)=EY(I)+E2
60      PRINT 999, E2
        999 FORMAT(////* EQUIVALENT ELASTIC MODULUS EY = *.F15.4)
C
C EQUIVALENT SHEAR MODULUS GXY
C
65      T1=(H-B0)/H
        CI=CT*CD**3.
        BI=BT*B0**3.
        DELTAB=(T1*(H-B0)*(H-B0)/CI)+ (H/B)*((B-CD)/B)*((B-CD)*(B-CD)/BI)
        DELTAB=DELTAB/E
70      DELTAV=H*(B-CD)/(B*B*BT*B0/1.2)+1.2*T1/(CT*CD)+
        1 ((B-CD)/B+T1-1)**2.)/(BT*CD*(1-T1))
        DELTAV=DELTAV/G
        DB=DELTAB
        DV=DELTAV
75      G12=1./(TT*B*(DB+DV))
        GXY(I)=0.
        GXY(I)=GXY(I)+G12
        TH(I)=0.
        TH(I)=TH(I)+TT
80      PRINT 111, G12
        111 FORMAT(//* EQUIVALENT SHEAR MODULUS = *.F15.4)
        9999 CONTINUE
        1 FORMAT(2E10.3)
        2 FORMAT(3F10.0)
85      RETURN
        END

```

SUBROUTINE ELCON

73/172 OPT=1

FTN 4.6+446

7.

```

1      SUBROUTINE ELCON(I,NDOF)
      COMMON/P2/NHEL,NVEL,NMAT,NTYPE,NEOF,LPAX,NSYM,NPR,NBAY,NSTOR,
      1EX(6),EY(6),GXY(6),TH(6),EC(8),EL(6),LEL(9),
      2ET(12,2),ETM(12),ETN(90),OK(9,9),IEW(12),IEH(12)
5      INTEGER FP,EC,EL,ETM,ETN
      C
      C *****
      C *
      C *   THIS SUBROUTINE GENERATE ELEMENT CONNECTIVITY
      C *
      C *****
10     THIS CAN BE ACHIEVED BY RELATING THE ELEMENT NO. TO ITS
      C FIRST NODE(L/WER, LEFT)
      C
      C JJ=(I-1)/NHEL
      C II=I-JJ*NHEL
20     N1=(II-1)/NHEL+1+(II-1)*(NVEL+1)+JJ
      C N2=N1+NVEL+1
      C IF(NDOF.NE.0) GO TO 10
      C EC(1)=N1
      C EC(2)=N2
25     EC(3)=EC(2)+1
      C EC(4)=EC(1)+1
      C GO TO 999
      C 10 CONTINUE
      C N=(NHEL+1)*(NVEL+1)
      C EC(1)=N1
30     EC(2)=EC(1)+N+NVEL*(NHEL+1)
      C EC(3)=N2
      C EC(4)=N+II*NVEL+JJ+1
      C EC(5)=N2+ 1
35     EC(6)=EC(2)+1
      C EC(7)=N1 +1
      C EC(8)=EC(4)-NVEL
      C 999 CONTINUE
      C RETURN
40     END

```


SUBROUTINE ASMBL1

73/172 OPT=1

FTN 4.6+446

7

```

1      SUBROUTINE ASMBL1(N,NL,NCOF,NSSYM)
      C
      C *****
      C
5      C * THIS SUBROUTINE ASSEMBLES EACH FACADE STIFF. MATRIX .
      C * CONDENSE IT, AND FORMS LOCAL(K) LEVEL SUBMATRICES AND
      C * AND GLOBAL SUBMATRICES (S).
      C *****
10     COMMON/P1/ FP(4,4),RFP(4),X(4),Y(4),NPRINT(10)
      COMMON/P2/NHEL,NVEL,NMAT,NTYPE,NEQF,LMAX,NSYM,NPR,NBAY,NSTOP,
      1EX(6),EY(6),GXY(6),TH(6),EC(8),EL(6),LEL(9),
      2ET(12,2),ETN(12),ETN(90),QK(9,9),IEW(12),IEW(12)
15     COMMON/P3/ T(3,5),K(3,3),S(5,5),B(3,5)
      COMMON/P4/NEQ,R(70),AK(6105)
      DIMENSION LK(3),LN(3)
      C
      REAL K
20     INTEGER FP,EC,EL,ETH,ETN
      C
      C
      WRITE(2) NSYM
      NEL=NHEL*NVEL
25     C
      C EVALUATE NO. OF EQUATIONS FOR FACADE "NEQF" AND
      C THE REQ. STORAGE FOR ITS STIFF. MATRIX
      C
30     IF(NDOF.NE.0) GO TO 11
      IF(NSYM.NE.0) GO TO 12
      NEQF=NVEL+(NHEL+1)*NVEL
      GO TO 111
      12 CONTINUE
      NEQF=NVEL*(1+NHEL)
      GO TO 111
35     11 CONTINUE
      IF(NSYM.NE.0) GO TO 15
      NEQF=NVEL*(2*NHEL+3)
      GO TO 111
      15 CONTINUE
40     IF(NSYM.EQ.1) GO TO 14
      NEQF=NVEL*(2*NHEL+2)
      GO TO 111
      14 CONTINUE
      NEQF=NVEL*(2*NHEL+1)
45     111 CONTINUE
      LMAX=(NEQF*NEQF-NEQF)/2+NEQF
      C
      C INITIALIZE FACADE STIFF. MATRIX AK
50     DO 1 I=1,LMAX
      AK(I)=0.0
      1 CONTINUE
      PRINT 100
      IF(NDOF.NE.0) GO TO 5
      LIM=6
55     DO 99 M=1,NEL
      C
      C PROCEDURE IN THIS SUBROUTINE WILL BE AS FOLLOWS..

```

SUBROUTINE ASMBL1

73/172 OPT=1

FTN 4.6+446

73/01/31. 1°

```

C          U.. FORM LOCAL ELEMENT ETIFF. MATRIX QK
C          2.. ASSEMBEL EACH QK TO FORM FACADE STIFF. MATRIX AK
60 C          3.. CONDENSE AK
C          4.. TRANSFORM EACH SUB MATRIX K JXJIN AK-CONDENSED
C          TO GLOBAL SYSTEM FORMING S 5X5
C          5.. ASSEMBEL EACH S FOR EACH FACADE TO FORM OVERALL
65 C          STRUCTURE STIFF. MATRIX IN SAME LOCATION AK
C
C FORM ELEMENT LABEL VCTOR "EL"
C
C          CALL LABEL(M,NDOF)
C          PRINT 200,M,(EL(I),I=1,6)
70 C
C FORM ELEMENT STIFF. MATRIX QK
C
C          CALL RECT(M,NDOF)
75 C
C S
C ASSEMBEL EACH QK ACCORDING TO THE CORRSPOING LABEL VECTOR "EL"
C NOTE . LIM= NO. OF ELEMENT DOF
C
C          DO 10 LL=1,LIM
C          I=EL(LL)
C          DO 10 MM=1,LIM
C          J=EL(MM)
80 C
C ASSEMBEL ONLY THE LOWER TRIANGLE . ROW BY ROW
C OR
C THE UPPER TRIANGLE COL. BY COL. ... NOTICE THAT BOTH ARE IDENTICAL
C
C          IF(I.GT.J) GO TO 10
C          IF(I.EQ.0) GO TO 10
C          LOC=((J-1)*J)/2+I
C          AK(LOC)=AK(LOC)+QK(LL,MM)
90 C          10 CONTINUE
C          99 CONTINUE
C          GO TO 6
95 C
C
C          5 CONTINUE
C          LIM=9
100 C          DO 88 M=1,NEL
C          CALL LABEL(M,NDOF)
C          PRINT 200, M, (LEL(I),I=1,9)
C          CALL RECT(M,NDOF)
C          DO 8 LL=1,LIM
C          I=LEL(LL)
105 C          DO 8 MM=1,LIM
C          J=LEL(MM)
C          IF(I.GT.J) GO TO 8
C          IF(I.EQ.0) GO TO 8
C          LOC=((J-1)*J)/2+I
C          AK(LOC)=AK(LOC)+QK(LL,MM)
110 C          8 CONTINUE
C          88 CONTINUE
C          6 CONTINUE

```

SUBROUTINE ASMRL1 73/172 CPT=1

FTN 4.6+446

75/01/31. 19.

```

115 C
C CONDOENSE INTERNAL DOF IN ABOVE AK
C
      IF(NSYM.NE.0) GO TO 17
      NR=3*NL
120 GO TO 16
      17 CONTINUE
      NP=2*NL
      16 CONTINUE
      CALL GAUSS(AK,R,NEQF,0,NR,DET,1)
125 WRITE(1) NSYM,NEQF,LMAX,NEL,NMAT,NTYPE
      WRITE(1) (AK(I),I=1,LMAX),(ETN(J),J=1,NEL)
      WRITE(1) (EX(I),EY(I),GX(I),TH(I),I=1,NMAT)
      WRITE(1) (ETH(I),IEW(I),IEH(I),(ET(I,J),J=1,2),I=1,NTYPE)
C
130 C *****NOTICE***** FP(N,1)....UP TO FP(N,5) ARE FRST NODE LIN, SECOND NODE LINE,
C FORM TRANSFORMATION MATRIX T 3X5.
C *****NOTICE***** FP(N,1)....UP TO FP(N,5) ARE F
C 1ST, NODE LINE, 2ND, NODE LINE, NHEL, NVEL, DIST, OF FACADE
135 C FROM-STRUCTURE CENTRE LINE FOR THE N TH. FACADE
C
      II=FP(N,1)
      JJ=FP(N,2)
      D=RFP(N)
140 XX=X(JJ)-X(II)
      YY=Y(JJ)-Y(II)
      FW=SQRT(XX*XX+YY*YY)
      SA=YY/FW
      CA=XX/FW
      NROT=0
145 C
      IF(NSSYM.NE.0) GO TO 60
      JT=5
      NROT=3
150 DO 20 I=1,3
      DO 20 J=1,5
      20 T(I,J)=0.0
      T(1,1)=CA
      T(1,2)=SA
155 T(1,3)=0
      T(2,4)=1.
      T(3,5)=1.
      WRITE(5) T
      GO TO 6666
160 C
      60 CONTINUE
      JT=3
      DO 62 I=1,3
      DO 62 J=1,3
165 T(I,J)=0.0
      62 CONTINUE
      T(2,2)=1.
      T(3,3)=1.
170 IF(NSSYM.EQ.1) GO TO 63
      IF(NSSYM.EQ.2) GO TO 64
      NROT=1

```

SUBROUTINE ASMBL1 73/172 CPT=1

FTN 4.6+446 78/01/31, 19.

```

      T(1,1)=0
      GO TO 666
175     53 CONTINUE
      T(1,1)=CA
      GO TO 666
      64 CONTINUE
      T(1,1)=SA
180     666 CONTINUE
      WRITE(5) T
      6666 CONTINUE
      C
      C
      C
185     C
      C EXTRACT EACH SMALL SUBMATRIX K 3X3 (REPRESENTING LEVEL STIFF.)
      C FROM CONDENSED FACADE STIFF. MATRIX
      C
      DO 30 I=1,NL
190     DO 30 J=1,NL
      IF(I.GT.J) GO TO 30
      LK(1)=I
      LK(2)=I+NL
      LK(3)=I+2*NL
195     LN(1)=J
      LN(2)=J+NL
      LN(3)=J+2*NL
      IF(NSYM.EQ.0) GO TO 25
      LK(3)=0
      LN(3)=0
200     25 CONTINUE
      C
      C INITIALIZE SUBMATRIX K
      C
205     DO 31 I1=1,3
      DO 31 J1=1,3
      K(I1,J1)=0.0
      31 CONTINUE
      C
210     IF(I.NE.J) GO TO 33
      DO 32 II=1,3
      DO 32 JJ=1,3
      IF(II.GT.JJ) GO TO 32
      LLK=LK(II)
      LLN=LN(JJ)
215     IF((LLK.EQ.0).OR.(LLN.EQ.0)) GO TO 32
      LOC=((LLN-1)*LLN)/2+LLK
      K(II,JJ)=AK(LOC)
      32 CONTINUE
220     C
      C FORM FULL K
      C
      K(2,1)=K(1,2)
      K(3,1)=K(1,3)
      K(3,2)=K(2,3)
225     GO TO 333
      C
      C

```

SUBROUTINE ASMBL1

73/172 CPT=1

FTN 4.6+446

75/01/31. 19

```

230      C
          33 CONTINUE
          DO 34 II=1,3
          DO 34 JJ=1,3
             LLK=LK(II)
             LLN=LN(JJ)
235             IF((LLK.EQ.0).OR.(LLN.EQ.0)) GO TO 34
             IF(II.GT.JJ) GO TO 35
             LOC=((LLN-1)*LLK)/2+LLK
             K(II,JJ)=AK(LOC)
             GO TO 34
240             35 LOC=((LLK-1)*LLK)/2+LLN
             K(II,JJ)=AK(LOC)
          34 CONTINUE
          333 CONTINUE
      C
245      C IF NSYM=1 MODIFY K TO HAVE ZERO FIRST COL. AND ROW
      C INSTEAD OF THIRDO
      C
          IF(NSYM.NE.1) GO TO 50
          K(3,3)=K(2,2)
250          K(3,2)=K(2,1)
          K(2,3)=K(1,2)
          K(2,2)=K(1,1)
          K(1,1)=0.
          K(1,2)=0.
255          K(1,3)=0.
          K(2,1)=0.
          K(3,1)=0.
          GO TO 55
260          50 CONTINUE
          IF(NSYM.NE.3) GO TO 55
          K(1,3)=K(1,2)
          K(3,1)=K(2,1)
          K(3,3)=K(2,2)
          K(2,1)=0.
265          K(2,2)=0.
          K(2,3)=0.
          K(1,2)=0.
          K(3,2)=0.
          55 CONTINUE
270      C EVALUATE TRANSFORMED SUB MATRIX S 5X5
      C S=T TRANSPOSE TIMES K TIMES T
      C
          DO 40 II=1,3
          DO 40 JJ=1,3T
275      C MULTIPLY K TIMES T AND STORE IN B
          B(II,JJ)=0.0
          DO 40 L=1,3
             B(II,JJ)=B(II,JJ)+K(II,L)*T(L,JJ)
          40 CONTINUE
280      C COMPUTE T TRANSPOSE TIMES B AND STORE IN S
          DO 41 II=1,3T
          DO 41 JJ=1,3T
             S(II,JJ)=0.0
             DO 41 L=1,3
                S(II,JJ)=S(II,JJ)+T(L,II)*B(L,JJ)
285

```

SUBROUTINE ASHPL1

73/172 OPT=1

FTN 4.6+646

78/01/31. 19.

41 CONTINUE

C

WRITE (2) ((S(II,JJ),JJ=1,JT),II=1,JT)

30 CONTINUE

290

100 FORMAT(//* ELEMENT NO.

DEGREES OF FREEDOM

*//)

200 FORMAT(I14,5X,9I5)

RETURN

END

SUBROUTINE LABEL

73/172 OPT=1

FTN 4.6+446

78/01/31. 19.

```

1      SUBROUTINE LABEL(M,NDOF)
      COMMON/P2/NHEL,NVEL,NMAT,NTYPE,NEOF,LHAX,NSYM,NPR,NBAY,NSTOR,
      1EX(6),EY(6),GXY(6),TH(6),EC(8),EL(6),LEL(9),
5      2ET(12,2),ETM(12),ETN(90),OK(9,9),IEW(12),IEH(12)
      INTEGER FP,EC,EL,ETM,ETN
      C
      C *****
      C
      C          THIS SUBROUTINE FORMS THE LABEL(NUMBERING OF DOF) FOR EACH ELEMENT
10      C *****
      C
      C FIRST HORIZONTAL DOF
      C
15      L=(M-1)/NHEL
      NPR=L+1
      C LIM=NO. OF DOF PER ELEMENT
      C NP= NO. OF NODES PER ELEMENT
      LIM=6
      NP=LIM*2
      DO 1 I=1,NP
      IF(I.GT.2) GO TO 2
      EL(1)=L
      GO TO 1
25      2 EL(2)=L+1.
      1 CONTINUE
      C
      C SECOND VERTICAL DOF
      C
30      LL=M-L*NHEL
      LLL=NVEL*(LL+1)
      C
      C 1... ELEMENTS FIXED TO FOUNDATION
35      C
      IF(L.NE.0) GO TO 10
      EL(3)=0
      EL(4)=0
      IF(M.EQ.1) GO TO 11
      IF(M.EQ.NHEL) GO TO 12
      EL(6)=LLL+1
      EL(5)=EL(6)+NVEL
      GO TO 111
40      11 EL(5)=3*NVEL+1
      EL(6)=NVEL+1
      GO TO 111
45      12 EL(5)=NVEL*2+1
      EL(6)=NVEL*(NHEL+1)+1
      GO TO 111
50      C
      C 2... REST OF ELEMENTS
      C
      C          A.. ELEMENTS ON THE LEFT MOST SIDE
55      C
      10 IF(LL.NE.1) GO TO 20
      EL(3)=NVEL+L
      EL(4)=NVEL*3+L

```

SUBROUTINE LABEL

73/172 OPT=1

FTN 4.6+446

75/01/31. 19.

```

        EL(5)=EL(4)+1
        EL(6)=EL(3)+1
60      GO TO 111
      C
      C      B.. ELEMENTS ON THE RIGHT MOST SIDE
      C
      20 IF(LL.NE.NHEL) GO TO 30
65      EL(3)=NVEL*(NHEL+1)+L
        EL(4)=NVEL*2+L
        EL(5)=EL(4)+1
        EL(6)=EL(3)+1
        GO TO 111
      C
      C      C.. INTERIOR ELEMENTS
      C
      30 EL(3)=LLL+L
        EL(4)=EL(3)+NVEL
75      EL(5)=EL(4)+1
        EL(6)=EL(3)+1
      111 CONTINUE
        IF(NDOF.NE.0) GO TO 70
        IF(NSYM.NE.0) CALL SYMM(NDOF,LL)
80      WRITE(6) EL,NPR
        GO TO 999
      70 CONTINUE
      C
      C      C GENERATE DOF FOR THE REFINED ELEMENT *** BASED **
      C      C ON THOSE OF THE ORDINARY ELEMENT
      C
        LEL(1)=EL(1)
        LEL(2)=NVEL*3+1+L
90      LEL(3)=EL(2)
      C 1.... ELEMENTS FIXED TO FOUNDATION
      C
        IF(L.NE.0) GO TO 80
        LEL(4)=0
95      LEL(5)=0
        LEL(6)=0
        IF(LL.EQ.NHEL) GO TO 81
        LEL(7)=EL(5)+NVEL
        GO TO 82
100     81 CONTINUE
        LEL(7)=EL(5)
        82 CONTINUE
        LEL(8)=NVEL*(3+NHEL)+(LL-1)*NVEL+1
        IF(LL.EQ.1) GO TO 83
105     LEL(9)=EL(6)+NVEL
        GO TO 84
        83 CONTINUE
        LEL(9)=EL(6)
        84 CONTINUE
110     GO TO 91
      C
      C 2.... REST OF ELEMENTS
      C
      80 CONTINUE

```


SUBROUTINE LABEL

73/172 OPT=1

FTN 4.6+446

75/01/31. 19-

```
115      LEL(4)=EL(3)+NVEL
        LEL(5)=NVEL*(3+NHEL)+(LL-1)*NVEL+L
        LEL(6)=EL(4)+NVEL
        LEL(7)=LEL(6)+1
        LEL(8)=LEL(5)+1
120      LEL(9)=LEL(4)+1
        IF(LL.NE.1) GO TO 90
        LEL(4)=EL(3)
        LEL(9)=LEL(4)+1
90      CONTINUE
125      IF(LL.NE.NHEL) GO TO 91
        LEL(6)=EL(4)
        LEL(7)=LEL(6)+1
91      CONTINUE
        IF(NSYM.NE.0) CALL SYMM(NDOF,LL)
130      WRITE(6) LEL,NPR
999     CONTINUE
        RETURN
        END
```

SUBROUTINE SYMM

73/172 OPT=1

FTN 4.6+446

78/01/31. 19.

```

1      SUBROUTINE SYMM(NDOF,LL)
      C *****
      C *
      C *   THIS SUBROUTINE MODIFIES ELEMENT LABEL TO ACCOUNT FOR *
5      C *   SYMMETRY CONDITIONS *
      C *
      C *****
      C
10     COMMON/P2/NMEL,NVEL,NMAT,NTYPE,NEOF,LMAX,NSYM,NPR,NBAY,NSTOR,
      1EX(6),EY(6),GXY(6),TH(6),EC(8),EL(6),LEL(9),
      2ET(12,2),ETM(12),ETN(90),OK(9,9),IEH(12),IEH(12)
      INTEGER FP,EC,EL,ETM,ETN
      C
15     C *** MODIFICATION
      C *** MODIFY ELEMENT LABEL ACCORDING TO SYMM. CONDITIONS
      C *** NOTE THAT FOR NO SYMM. NSYM=0, SYMM. NSYM=1, ANTI-SYMM. NSYM=2
      C
20     IF(NDOF.NE.0) GO TO 80
      IF(NSYM.NE.1) GO TO 40
      C
      C FOR CASE OF SYMM. NSYM=1
      C
25     EL(1)=0
      EL(2)=0
      EL(3)=EL(3)-NVEL
      EL(4)=EL(4)-NVEL
      EL(5)=EL(5)-NVEL
30     EL(6)=EL(6)-NVEL
      GO TO 444
      40 CONTINUE
      C
      C FOR CASE OF ANTI-SYMM. NSYM=2
35     C
      IF(LL.EQ.1) GO TO 41
      IF(LL.EQ.NMEL) GO TO 42
      C A..... INTERNAL ELEMENTS
40     EL(3)=EL(3)-NVEL
      EL(4)=EL(4)-NVEL
      EL(5)=EL(5)-NVEL
      EL(6)=EL(6)-NVEL
      GO TO 444
45     41 CONTINUE
      C
      C B..... ELEMENTS ON THE LEFT MOST SIDE
      EL(4)=EL(4)-NVEL
      EL(5)=EL(5)-NVEL
50     IF(NSYM.NE.3) GO TO 444
      EL(3)=0
      EL(6)=0
      GO TO 444
      42 CONTINUE
      C
55     C..... ELEMENTS ON THE RIGHT MOST SIDE
      C
      EL(3)=EL(3)-NVEL

```

SUBROUTINE SYMM

73/172 OPT=1

FTN 4.6+446

78/01/

```

        EL(4)=EL(4)-NVEL
        EL(5)=EL(5)-NVEL
60      EL(6)=EL(6)-NVEL
        IF(NSYM.NE.2) GO TO 444
        EL(4)=0
        EL(5)=0
        444 CONTINUE
65      DO 4444 I=1,6
        IF(EL(I).GE.0) GO TO 4444
        EL(I)=0
        4444 CONTINUE
        GO TO 9999

70      C
        C
        80 CONTINUE
        C
        C ***** MODIFICATION FOR REFINED ELEMENT
75      C
        C IF(NSYM.NE.1) GO TO 81
        C
        C FOR CASE OF SYMM.
        C
80      LEL(1)=0
        LEL(2)=0
        LEL(3)=0
        NN=2*NVEL
85      IF(LL.EQ.1) GO TO 82
        IF(LL.EQ.NVEL) GO TO 83
        LEL(4)=LEL(4)-NN
        LEL(5)=LEL(5)-NN
        LEL(6)=LEL(6)-NN
        LEL(7)=LEL(7)-NN
90      LEL(8)=LEL(8)-NN
        LEL(9)=LEL(9)-NN
        GO TO 888
        82 CONTINUE
        C
95      C LEFT MOST SIDE ELEMENTS
        C
        LEL(4)=LEL(4)-NVEL
        LEL(5)=LEL(5)-NN
        LEL(6)=LEL(6)-NN
100     LEL(7)=LEL(7)-NN
        LEL(8)=LEL(8)-NN
        LEL(9)=LEL(9)-NVEL
        GO TO 888
        83 CONTINUE
105     C RIGHT MOST SIDE ELEMENTS
        LEL(4)=LEL(4)-NN
        LEL(5)=LEL(5)-NN
        LEL(6)=LEL(6)-NVEL
        LEL(7)=LEL(7)-NVEL
110     LEL(8)=LEL(8)-NN
        LEL(9)=LEL(9)-NN
        GO TO 888
        81 CONTINUE
        C

```

SUBROUTINE SYMM

73/172 OPT=1

FTN 4.6+446

78/01,

```
115      C FOP CASE OF ANTI-SYMM.
        LEL(2)=LEL(2)-NVEL
        IF(LL.EQ.1) GO TO 84
        IF(LL.EQ.N+EL) GO TO 85
        LEL(4)=LEL(4)-NVEL
120      LEL(5)=LEL(5)-NVEL
        LEL(6)=LEL(6)-NVEL
        LEL(7)=LEL(7)-NVEL
        LEL(8)=LEL(8)-NVEL
        LEL(9)=LEL(9)-NVEL
125      GO TO 888
        84 CONTINUE
        LEL(5)=LEL(5)-NVEL
        LEL(6)=LEL(6)-NVEL
        LEL(7)=LEL(7)-NVEL
        LEL(8)=LEL(8)-NVEL
130      IF(NSYM.NE.3) GO TO 888
        LEL(4)=0
        LEL(9)=0
        C
135      GO TO 888
        85 CONTINUE
        LEL(4)=LEL(4)-NVEL
        LEL(5)=LEL(5)-NVEL
        LEL(6)=LEL(6)-NVEL
140      LEL(7)=LEL(7)-NVEL
        LEL(8)=LEL(8)-NVEL
        LEL(9)=LEL(9)-NVEL
        IF(NSYM.NE.2) GO TO 888
        LEL(6)=0
        LEL(7)=0
145      888 CONTINUE
        DO 8888 I=1,9
        IF(LEL(I).GE.0) GO TO 8888
        LEL(I)=0
150      8888 CONTINUE
        9999 CONTINUE
        RETURN
        END
```

```

SUBROUTINE RECT          73/172  CPT=1          FTN 4.6+446          79/01/

1      SUBROUTINE RECT(M,NDOF)
      COMMON/P2/NHEL,NVEL,NMAT,NTYPE,NEGF,LMAX,NSYM,NPR,NBAY,NSTOR,
      1EX(6),EY(6),GXY(6),TH(6),EC(8),EL(6),LEL(9),
      2ET(12,2),ETH(12),ETN(90),QK(9,9),IEW(12),IEH(12)
      5      INTEGER FP,EC,EL,ETM,ETN

      C
      C *****
      C
      C          THIS SUBROUTINE FORMS EZCH ELEMENT STIFF. MATIX
      C *****
10     C
      C
      C ELEMNNT PROPERTIES
15     C
      C          IT=ETN(M)
      C          A=ET(IT,1)
      C          B=ET(IT,2)
      C          IM=ETH(IT)
      C          E1=EX(IM)
      C          E2=EY(IM)
      C          G12=GXY(IM)
      C          TT=TH(IM)
      C          R=A/B
20     C
      C          IF(NDOF.NE.0) GO TO 50
25     C
      C
      C INITIALIZE ELEMENT STIFF. MATRIX QK
30     C
      C          DO 10 I=1,6
      C          DO 10 J=1,6
      C          QK(I,J)=0.0
      C          10 CONTINUE
35     C
      C FORM STIFF. MATRIX OF ORDINARY ELEMENT
      C
      C          QK(1,1)=TT*R*G12
      C          QK(2,1)=-QK(1,1)
      C          QK(3,1)= .5*TT*G12
      C          QK(4,1)=-QK(3,1)
      C          QK(5,1)=-QK(3,1)
      C          QK(6,1)= QK(3,1)
40     C
      C          QK(2,2)=QK(1,1)
      C          QK(3,2)=-QK(3,1)
      C          QK(4,2)= QK(3,1)
      C          QK(5,2)=QK(3,1)
      C          QK(6,2)=-QK(3,1)
45     C
      C          QK(3,3)=(E2*R+G12/R)*TT/3.
      C          QK(4,3)=(.5*E2*R-G12/R)*TT/3.
      C          QK(5,3)=-.5*QK(3,3)
      C          QK(6,3)=(.5*G12/R-E2*R)*TT/3.
50     C
      C          QK(4,4)=QK(3,3)
      C          QK(5,4)=QK(6,3)
55     C

```

SUBROUTINE RECT

73/172 CPT=1

FTN 4.6+446

73/01/

```

        QK(6,4)=-.5*QK(3,3)
60      C
        QK(5,5)=QK(3,3)
        QK(6,5)=QK(4,3)
        C
        QK(6,6)=QK(3,3)
65      C
        DO 20 I=1,6
        DO 20 J=1,6
        IF(J.LE.I) GO TO 20
        QK(I,J)=QK(J,I)
        20 CONTINUE
70      GO TO 999
        C
        C
        50 CONTINUE
75      C
        C FORM STIFF. MATRIX OF THE REFINED ELEMENT
        C
        C INITIALIZE QK 9X9
        DO 55 I=1,9
        DO 55 J=1,9
        QK(I,J) =0.0
80      55 CONTINUE
        C
        C
        S1=TT*G12*P/12.
        S2=TT*G12/12.
        S3=TT*E2*P/60.
        S4=TT*G12/(P*36.)
85      C
        C
        QK(1,1)=28.*S1
        QK(2,1)=-32.*S1
        QK(3,1)=4.*S1
        QK(4,1)=10.*S2
        QK(6,1)=-10.*S2
        QK(7,1)=-2.*S2
        QK(9,1)=2.*S2
90      C
        C
        QK(2,2)=64.*S1
        QK(3,2)=QK(2,1)
        QK(4,2)=-8.*S2
        QK(6,2)=-QK(4,2)
        QK(7,2)=QK(4,2)
        QK(9,2)=-QK(4,2)
95      C
        C
        QK(3,3)=QK(1,1)
        QK(4,3)=QK(7,1)
        QK(6,3)=-QK(7,1)
        QK(7,3)=QK(4,1)
        QK(9,3)=-QK(4,1)
100     C
        C
        QK(4,4)=8.*S3+28.*S4
        QK(5,4)=4.*S3-32.*S4
        QK(6,4)=-2.*S3+4.*S4
        QK(7,4)=2.*S3+2.*S4
110     C

```

FTN 4.6+446

75/01,

SUBROUTINE RECT

73/172 OPT=1

```

115      QK(8,4)=-4.*S3-16.*S4
      QK(9,4)=-8.*S3+14.*S4
      C
      QK(5,5)=32.*S3+64.*S4
      QK(6,5)=QK(5,4)
120      QK(7,5)=QK(8,4)
      QK(8,5)=-32.*S3+32.*S4
      QK(9,5)=QK(8,4)
      C
      QK(6,6)=QK(4,4)
      QK(7,6)=QK(9,4)
125      QK(8,6)=QK(8,4)
      QK(9,6)=QK(7,4)
      C
      QK(7,7)=QK(4,4)
      QK(8,7)=QK(5,4)
130      QK(9,7)=QK(6,4)
      C
      QK(8,8)=QK(5,5)
      QK(9,8)=QK(5,4)
135      C
      QK(9,9)=QK(4,4)
      C
      C
140      DO 60 I=1,9
      DO 60 J=1,9
      IF(J.LE.I) GO TO 60
      QK(I,J)=QK(J,I)
      60 CONTINUE
      999 CONTINUE
145      RETURN
      END

```

SUBROUTINE GAUSS

73/172 CPT=1

FTN 4,6+446

78/01.

```

1      SUBROUTINE GAUSS(AK,R,NEQ,NLO,NR,DET,NCODE)
        DIMENSION R(70,1),AK(6105)
C
C      *****
C
5      AK CONTAINS COEFF. IN ONE TRIANGLE OF ASYM. MATRIX
        CO.L. BY COL. IF UPPER TRIANGLE, ROW BY ROW
        IF LOWER TRIANGLE.
C
C      R= RIGHT HAND SIDE MATRIX IN (AK)(X)=(R)
C
10     NEQ= NO. OF EQUATIONS
        NLC=NO. OF LOAD CASES, I.E. COLS. OF R
        NR= NO. OF EQUATIONS REMAINED IN CONDENSATION
        ***** NOTICE***** ELEMENATED DOF STORED LAST
C
C      DET= DETERMINANT
C
15     NCODE= 1 FORWARD ELIMINATION AND BACK SUBSTITUTION
        2 ELIMINATION OF RIGHT HAND SIDE AND BACK SUBSTITU.
C
C      NR.LT.0=MODIFY MATRIX AK AND BACK SUBSTITUTE TO
        RECOVER ELIMINATED UNKNOWNNS. KNOWN VALUES OF
        R MUST BE IN POSITION BEFORE.
C
C      *****CALLING ARGUMENTS *****
C
C      FOR SOLUTIONS GAUSS(AK,R,NEQ,NLO,1,DET,1)
C
25     FOR NEW RIGHT HAND SIDE GAUSS(AK,R,NEQ,NLO,1,DET,2)
        FOR DETERMINANT GAUSS(AK,0,NLO,0,1,DET,1)
        FOR CONDENSATION GAUSS(AK,R,NEQ,NLO,NR,DET,1)
        NLO MAY BE 0
C
30     FOR RECOVERY GAUSS(AK,R,NEQ,NLO,-NR,DET,2)
        *****
C
        IF(NR.LT.0) GO TO 15
        NE=NEQ-NR
        DET=1.
        DO 500 M=1,NE
        MAX=NEQ-M
        N=MAX+1
        L=(N*(N+1))/2
40     LN=L-N
        IF(AK(L).GT.1.E-20) GO TO 600
        PRINT 1,N
        GO TO 500
        600 PIVOT=1./AK(L)
        IF(NCODE.GT.1) GO TO 400
        DO 300 J=1,MAX
        T=AK(LN+J)*PIVOT
        IF(T.EQ.0.) GO TO 300
        DO 200 I=J,MAX
        K=(I*(I-1))/2+J
50     KN=LN+I
        200 AK(K)=AK(K)-AK(KN)*T
        300 CONTINUE
        IF(NLO.NE.0) GO TO 400
        IF(NR.NE.1) GO TO 500
        DET=DET*AK(L)
55     400 DO 360 J=1,NLO

```


SUBROUTINE GAUSS

73/172 OPT=1.

FTN 4.6+446

78/01.

```
60 T=R(N,J)*PIVOT
    IF(T.EQ.0) GO TO 360
    DO 350 I=1,MAX
    K=LN+I
350 R(I,J)=R(I,J)-AK(K)*T
360 CONTINUE
500 CONTINUE
65 IF(NR.GT.1) RETURN
    DO 10 L=1,NLO
10 R(1,L)=R(1,L)/AK(1)
    M=2
70 IF(NR.LT.0) M=1-NR
    DO 20 I=M,NEQ
    K=I-1
    KI=(I+K)/2
    KN=KI+I
    DO 30 L=1,NLO
    DO 25 J=1,K
75 KJ=KI+J
25 R(I,L)=R(I,L)-R(J,L)*AK(KJ)
30 R(I,L)=R(I,L)/AK(KN)
80 20 CONTINUE
    1 FORMAT(* ZERO DIAGONAL AT ROW *,I5)
    RETURN
    END
```

SUBROUTINE ASHPL2 73/172 OPT=1

FTN 4.6+446

78/01.

```

1      SUBROUTINE ASHBL2(NL,NEQ,AMAX,AK,NF,NSHAPE,NSSYM)
      COMMON/P2/NVEL,NVEL,NMAT,NTYPE,NEQF,LMAX,NSYM,NPR,NBAY,NSTOR,
      1EX(6),EY(6),GXY(6),TH(6),EC(8),EL(6),LEL(9),
5      2ET(12,2),ETH(12),ETN(90),OK(9,9),IEH(12),IEH(12)
      COMMON/P3/T(3,5),K(3,3),S(5,5),B(3,5)
      DIMENSION AK(6105)
      INTEGER FP,EC,EL,ETH,ETN
      INTEGER AMAX

10     C *****
      C
      C THIS SUBROUTINE RETRIEVES THE SUB STIFF. MATRICES S
      C TRANSFORMED TO THE GLOBAL SYSTEM AND THEN ASSEMBLES
15     C THEM ONE BY ONE TO FORM THE OVERALL STRUCTURE
      C STIFF. MATRIX AK.
      C *****
      C
20     C REWIND 2
      C INITIALIZE AK
      C
      C LLL=AMAX
      C DO 100 I=1,LLL
25     C AK(I)=0.0
      C 100 CONTINUE
      C IF(NSSYM.NE.0) GO TO 101
      C LIM=5
      C GO TO 102
30     C 101 CONTINUE
      C LIM=3
      C 102 CONTINUE
      C ND=NEQ/NL
      C
35     C RETRIEVE EACH SUB MATRIX S
      C DO 9999 N=1,NF
      C READ(2) NSYM
      C DO 9999 I=1,NL
      C DO 9999 J=1,NL
40     C IF(I.GT.J) GO TO 9999
      C READ(2) ((S(I,J),JJ=1,LIM),II=1,LIM)
      C
      C ASSEMBEL S TO FORM AK
      C
45     C
      C ND=NO. OF DOF PER LEVEL
      C 3 CENTRAL DOF(U,V,ROT.) AND 1 VERTICAL DOF(W) PER CORNER
      C
      C IF(NSYM.NE.0) GO TO 777
50     C
      C 1..... ASSEMBEL FOR CENTRAL DOF(U,V,ROT.)
      C
      C NS=LIM-2
      C DO 5 IL=1,NS
      C DO 5 IIK=1,NS
55     C II=I*ND-ND+IL
      C JJ=J*ND-ND+IIK

```

SUBROUTINE ASMBL2

73/172 OPT=1

FTN 4.6+446

7

```

        IF (II.GT.JJ) GO TO 5
        LOC=((JJ-1)*JJ)/2+II
60      AK(LOC)=AK(LOC)+S(IL,IJK)
        5 CONTINUE
C
C
C      2.1.. ASSEMBEL FOR VERTICAL DOF OF CORNERS(W)
        EXCEPT LAST FACADE
65
        IF ((N.EQ.NF).AND.(NSHAPE.EQ.0)) GO TO 60
        N1=N+LIM-2
        N2=N+LIM-1
        DO 6 L=N1,N2
70      LL=L+1-N
        DO 6 IK=N1,N2
        KK=IK+1-N
        II=I*ND-ND+L
        JJ=J*ND-ND+IK
75      IF (II.GT.JJ) GO TO 6
        LOC=((JJ-1)*JJ)/2+II
        AK(LOC)=AK(LOC)+S(LL,KK)
        6 CONTINUE
        GO TO 99
80
C
C
C      2.2.. ASSEMBEL FOR VERTICAL DOF (W) OF LAST FACADE
60 CONTINUE
85      DO 7 L=1,2
        IF (L.NE.1) GO TO 8
        L1=N+3
        LL=4
        GO TO 9
90      L1=4
        LL=5
        9 DO 7 IK=1,2
        IF (IK.NE.1) GO TO 10
        K1=N+3
        KK=4
        GO TO 11
100     K1=4
        KK=5
        11 II=I*ND-ND+L1
        JJ=J*ND-ND+K1
        IF (II.GT.JJ) GO TO 7
        LOC=((JJ-1)*JJ)/2+II
        AK(LOC)=AK(LOC)+S(LL,KK)
105     7 CONTINUE
        GO TO 88
C
C
C      3.1.. ASSEMBEL FOR INTERACTING(CENTRE,CORNER) DOF *EXCEPT
        LAST FACADE
110     99 CONTINUE
C
        NCC=LIM-2
        DO 16 IL=1,NCC
        DO 16 IJK=N1,N2

```

SUBROUTINE ASMBLZ 73/172 OPT=I

FTN 4.6+446

7

```

115      KK=IIK+1-N
        II=I*ND-ND+IL
        JJ=J*ND-ND+IIK
        LOC=((JJ-1)*JJ)/2+II
        AK(LOC)=AK(LOC)+S(IL, KK)
120      16 CONTINUE
        GO TO 999

C
C
C      3.2.. ASSEMBEL FOR INTERACTING(CENTRE,CORNER) DOF *LAST FACADE*
125      88 CONTINUE
        DO 17 IL=1,3
        DO 17 IIK=1,2
        IF(IIK.NE.1) GO TO 20
130      NI=N+3
        NN=4
        GO TO 21
        20 CONTINUE
        NI=4
        NN=5
135      21 CONTINUE
        II=I*ND-ND+IL
        JJ=J*ND-ND+NI
        LOC=((JJ-1)*JJ)/2+II
        AK(LOC)=AK(LOC)+S(IL, NN)
140      17 CONTINUE
        GO TO 888

C
C
C      *..... ONLY FOR NON DIAGONAL SUB MATRICES S
        INTERACTING (CORNER,CENTRE) DOF
145      999 CONTINUE
        IF(I.EG.J) GO TO 9999

C
150      DO 50 L=N1,N2
        LL=L+1-N
        DO 50 KK=1,NCC
        II=I*ND-ND+L
        JJ=J*ND-ND+KK
155      LOC=((JJ-1)*JJ)/2+II
        AK(LOC)=AK(LOC)+S(LL, KK)
        50 CONTINUE

C
160      GO TO 9999
        4.2.. LAST FACADE

C
C
165      888 CONTINUE
        IF(I.EQ.J) GO TO 9999
        DO 41 L=1,2
        IF(L.NE.1) GO TO 42
        L1=N+3
        LL=4
        GO TO 43
170      42 CONTINUE
        L1=4

```

SUBROUTINE ASHRL2 73/172 OPT=1

FTN 4.6+446

7

```
LL=5
43 CONTINUE
175 DO 41 KK=1,3
II=I*ND-ND+L1
JJ=J*ND-ND+KK
LOC=((JJ-1)*JJ)/2+II
AK(LOC)=AK(LOC)+S(LL, KK)
41 CONTINUE
180 GO TO 9999
777 CONTINUE
DO 77 L=1,3
EC(L)=0
EL(L)=0
185 77 CONTINUE
CALL LABS(N,I,J,ND)
DO 70 LL=1,3
II=EC(LL)
DO 70 KK=1,3
190 JJ=EL(KK)
IF(II.GT.JJ) GO TO 70
LOC=((JJ-1)*JJ)/2+II
AK(LOC)=AK(LOC)+S(LL, KK)
70 CONTINUE
195 9999 CONTINUE
RETURN
END
```

SUBROUTINE LABS

73/172 OPT=1

FTN 4.6+446

7

```

1      SUBROUTINE LABS(N,I,J,ND)
      C
      C *****
      C *
      C * THIS SUBROUTINE FORMS LABEL FOR THE (S) MATRICES..
      C *
      C *****
      C
10     COMMON/P2/NHEL,NVEL,NHAT,NTYPE,NEOF,LMAX,NSYM,NPR,NBAY,NSIOR,
      1EX(6),EY(6),GXY(6),TH(6),EC(8),EL(6),LEL(9),
      2ET(12,2),ETM(12),ETN(90),OK(9,9),IEH(12),IEH(12)
      INTEGER FP,EC,EL,ETM,ETN
      C
15     EC(1)=NO*I-ND+1
      EL(1)=NO*J-ND+1
      IF(NSYM.EQ.1) GO TO 10
      IF(NSYM.EQ.2) GO TO 20
      EC(2)=0
      EC(3)=EC(1)+1
      EL(2)=0
      EL(3)=EL(1)+1
      GO TO 999
20     CONTINUE
      EC(2)=EC(1)+N-1
      EC(3)=EC(2)+1
      EL(2)=EL(1)+N-1
      EL(3)=EL(2)+1
      GO TO 999
30     CONTINUE
      EC(2)=EC(1)+N-1
      EC(3)=0
      EL(2)=EL(1)+N-1
      EL(3)=0
35     CONTINUE
      RETURN
      END

```

SUBROUTINE STRESS

73/172 OPT=1

FTN 4.6+446

7

```

1      SUBROUTINE STRESS(NL,NF,NDOF,NSHAPE,NSSYM,NOUT)
      COMMON/P1/ FP(4,4),RFP(4),X(4),Y(4),NPRINT(10)
      COMMON/P2/NHEL,NVEL,NMAT,NTYPE,NEOF,LMAX,NSYM,NPR,NBAY,NSTOR,
5      1EX(6),EY(6),GXY(6),TH(6),EC(8),EL(6),LEL(9),
      2ET(12,2),ETM(12),ETN(90),OK(9,9),IEH(12),IEH(12)
      COMMON/P3/ T(3,5),K(3,3),S(5,5),B(3,5)
      COMMON/P4/NEQ,R(70),AK(6105)
      DIMENSION FD(5),FLD(3),BB(3,9),C(3,3),BBC(3,9),Q(9),SIG(3)
      INTEGER FP,EC,EL,ETH,ETN
      *****
10     C
      C THIS SUBROUTINE EVALUATES STRESSES
      C IN EACH ELEMENT IN EACH FACADE
      C *****
15     C
      C EXTRACT THE 5 DISP. COMPONENTS(U,V,ROT,W1,W2)
      C FOR EACH LEVEL IN EACH FACADE FROM THE GENERALIZED
      C DISP. VECTOR R
20     C
      DO 1 I=1,NEQ
      R(I)=0.
      1 CONTINUE
      ND=NEQ/NL
      IF(NOUT.NE.0) GO TO 6.
      PRINT 500
      GO TO 7
      6 CONTINUE
      PRINT 100
      7 CONTINUE
      REWIND 1
      REWIND 5
      REWIND 6
      DO 9999 N=1,NF
      REWIND 3
      READ(3)(R(I),I=1,NEQ)
      REWIND 4
      IF(NOUT.NE.0) GO TO 8
      PRINT 600,N
      GO TO 9
      8 CONTINUE
      PRINT 200,N
      9 CONTINUE
      DO 2 I=1,3
      DO 2 J=1,5
      T(I,J)=0.
      2 CONTINUE
      READ(5) T
35     C
50     C RETREIVE THE CONDENSED FACADE STIFF. MATRIX
      C
      READ (1) NSYM,NEQF,LMAX,NEL,NMAT,NTYPE
      READ (1) (AK(I),I=1,LMAX),(ETN(J),J=1,NEL)
      READ (1) (SX(I),EY(I),GXY(I),TH(I),I=1,NMAT)
      READ (1) (ETM(I),IEH(I),IEH(I),(ET(I,J),J=1,2),I=1,NTYPE)
55     C
      DO 99 M=1,NL

```

SUBROUTINE STRESS

73/172 OPT=1

FTN 4.6+446

7

```

        DO 5 I=1,5
          FD(I)=0.
60      5 CONTINUE
          L=ND*M
          J=L-ND+1
          FD(1)=R(J)
          IF(NSSYM.EQ.0) GO TO 3
65      LIM=3
          FD(3)=R(J+N)
          IF(NSYM.NE.1) GO TO 4
          FD(2)=R(J+N-1)
          GO TO 11
70      4 CONTINUE
          IF(NSYM.NE.2) GO TO 11
          FD(2)=FD(3)
          FD(3)=0.0
          GO TO 11
75      3 CONTINUE
          LIM=5
          FD(2)=R(J+1)
          FD(3)=R(J+2)
          KK=J+2
80      LL=KK+N
          IF((N.EQ.NF).AND.(NSHAPE.EQ.0)) GO TO 10
          FD(4)=R(LL)
          FD(5)=R(LL+1)
          GO TO 11
85      10 CONTINUE
          FD(4)=R(LL)
          FD(5)=R(KK+1)
C
C TRANSFER THE PREVIOUS 5 DISP. COMPONENTS TO THE
C CORRESPONDING LOCAL 3 DISP. TA EACH LEVEL IN EACH FACADE
C I.E., TO U, V1, V2
C BY MULTIPLYING T TIMES FD
C
95      11 CONTINUE
          DO 12 J=1,3
            FLD(J)=0.0
            DO 12 I=1,LIM
              FLD(J)=FLD(J)+T(J,I)*FD(I)
100     12 CONTINUE
          WRITE(4) (FLD(I),I=1,3)
          99 CONTINUE
C
C
C FLD= FACADE LOCAL DISP. (ONLY THE REMAINED DOF)
105 C RETREIVE MATRICES FLD, INITIALIZE R, AND ASSEMBEL FLD IN R
C
C
C INITIALIZE LOCAL FACADE DISPL. VECTOR
C
110     DO 44 I=1,NEQF
          R(I)=0.
          44 CONTINUE
          NHEL=FP(N,3)
          NVEL=FP(N,4)

```


SUBROUTINE STRESS 73/172 CPT=1

FTN 4.6+446

75.

```

115     REWIND 4
        IF(NSYM.NE. 0) GO TO 90
        NP=3*NL
        DO 999 M=1,NL
120     READ(4) (FLD(I),I=1,3)
        I=M
        J=I+NVEL
        IK=J+NVEL
C
        R(I)=R(I)+FLD(1)
125     R(J)=R(J)+FLD(2)
        R(IK)=R(IK)+FLD(3)
        999 CONTINUE
        GO TO 105
        90 CONTINUE
        NR=2*NL
130     IF(NSYM.EQ.1) GO TO 91
        IF(NSYM.EQ.2) GO TO 92
        DO 93 M=1,NL
        READ(4) (FLD(I),I=1,3)
135     I=M
        J=I+NVEL
        IK=J+NVEL
        R(I)=R(I)+FLD(1)
        R(J)=R(J)+FLD(2)
140     93 CONTINUE
        GO TO 105
        91 CONTINUE
        DO 94 M=1,NL
        READ(4) (FLD(I),I=1,3)
145     I=M
        J=I+NVEL
        IK=J+NVEL
        R(I)=R(I)+FLD(1)
        R(J)=R(J)+FLD(2)
150     94 CONTINUE
        GO TO 105
        92 CONTINUE
        DO 95 M=1,NL
        READ(4) (FLD(I),I=1,3)
155     I=M
        J=I+NVEL
        IK=J+NVEL
        R(I)=R(I)+FLD(1)
        R(J)=R(J)+FLD(2)
160     95 CONTINUE
        105 CONTINUE
C
C RECOVER THE CONDENSED FACADE DOF
C
165     CALL GAUSS(AK,R,NEQF,NLO,-NR,DET,2)
C
C EXTRACT EACH ELEMENT NODAL DISP. FROM THE COMPLETE FACADE
C DISP. VECTOR..
C
170     NEL=NHEL*NVEL
        DO 9999 M=1,NEL

```

SUBROUTINE STRESS 73/172 OPT=1

FTN 4.6+446

78.

```

C
C ELEMENT PROPERTIES
C
175      IT=ETN(M)
        A=ET(IT,1)
        D=ET(IT,2)
C NOTE.... D=B=HEIGHT, OF ELEMENT
180      IM=ETH(IT)
        E1=EX(IM)
        E2=EY(IM)
        G12=GXY(IM)
        TT=TH(IM)
        NBAY=IEW(IT)
185      NSTOR=IEH(IT)
        BW=A/NBAY
        SH=D/NSTOR
C
        IF(NDOF.NE.0) GO TO 70
190      READ(6) EL,NPR
        IPPRT=NPRINT(NPR)
        IF(IPRNT.EQ.0) GO TO 9999
        ISTRS=1
        JSTRS=1
195      RB=1./NBAY
        RS=1./NSTOR
        LIM=6
C INITIALIZE STRAIN -DISP. MATRIX  BB 3X6
C
200      DO 20 I=1,3
        DO 20 J=1,6
        BB(I,J)=0.
        20 CONTINUE
C
C C EXTRACT EACH ELEMENT NODAL DISP.
205      C
C
        DO 40 I=1,LIM
        Q(I)=0.
        J=EL(I)
210      Q(I)=Q(I)+R(J)
        40 CONTINUE
C
        GO TO 71
215      70 CONTINUE
        READ(6) LEL,NPR
        IPRNT=NPRINT(NPR)
        IF(IPRNT.EQ.0) GO TO 9999
        ISTRS=1
        JSTRS=2
220      LIM=9
        D=D/2.
        A=A/2.
        RB=2./NBAY
        RS=2./NSTOR
225      C
C INITIALIZE STRAIN - DISPL. MATRIX BB 3X9
C
        DO 72 I=1,3

```

SUBROUTINE STRESS 73/172 OPT=1

FTN 4.6+446

78,

```

230      DO 72 J=1,9
          BB(I,J)=0.0
          72 CONTINUE
C
C EXTRACT EACH ELEMENT NODAL DISPLACEMENTS
235      DO 80 I=1,LIM
          Q(I)=0.0
          J=LEL(I)
          Q(I)=Q(I)+R(J)
          80 CONTINUE
          71 CONTINUE
240      C
          C FORM STRESS-STRAIN MATRIX C 3X3
          C
          DO 25 I=1,3
            DO 25 J=1,3
              C(I,J)=0.
            25 CONTINUE
            C(1,1)=E1
            C(2,2)=E2
            C(3,3)=G12
250      C
          IF(NOUT.NE.0) GO TO 75
          ISTRS=2*NSTOR
          75 CONTINUE
          DO 888 II=1,ISTRS
            IF(NOUT.EQ.2) GO TO 88
            ISIGN=(-1)**II
            IF(ISIGN.LT.1) GO TO 81
            JSTRS=NBAY
            IZ=1
            GO TO 88
          81 CONTINUE
            JSTRS=NBAY+1
            IZ=0
          88 CONTINUE
            DO 888 JJ=1,JSTRS
              E=.5
              IF(NDOF.NE.0) GO TO 73
              IF(NOUT.EQ.0) GO TO 82
              GO TO 83
            82 CONTINUE
            E=II*RS*0.5
            83 CONTINUE
275      C
          C FORM THE BB MATRIX >
          C
          IF(NOUT.EQ.2) GO TO 65
          Z=(JJ-1)*RB+IZ*RB*0.5
          GO TO 66
          65 CONTINUE
          Z=.5
          66 CONTINUE
          BB(2,3)=-Z/D
          BB(2,4)=-Z/D
          BB(2,5)=Z/D
          BB(2,6)=(1.-Z)/D
285

```

SUBROUTINE STRESS

73/172 OPT=1

FTN 4.6+446

78/

```

C
  BB(3,1)=-1/D
  BB(3,2)=1/D
  BB(3,3)=-((1-E)/A
290  BB(3,4)=(1.-E)/A
  BB(3,5)=E/A
  BB(3,6)=-E/A
C
  GO TO 74
295 73 CONTINUE
  IF(NOUT.EQ.0) GO TO 84
  GO TO 85
  84 CONTINUE
  E=II*RS*0.5-1.0
300 85 CONTINUE
C
C FORM THE BB MATRIX
C
C
305 C NOTE THAT BOTH D AND A REPRESENT ONLY ONE HALF THE
C HEIGHT AND THE LENGTH OF THE ELEMENT RESPECTIVELY
C
  IF(NOUT.EQ.2) GO TO 76
  Z=(JJ-1)*RB+IZ*RS*0.5-1.0
310 GO TO 77
  76 CONTINUE
  Z=JJ*1.-1.5
  77 CONTINUE
  BB(2,4)=Z*(1.-Z)/(4.*D)
315 BB(2,5)=-((1.-Z)*Z)/(2.*D)
  BB(2,6)=-((1.+Z)*Z)/(4.*D)
  BB(2,7)=-BB(2,6)
  BB(2,8)=-BB(2,5)
  BB(2,9)=-BB(2,4)
320 C
  BB(3,1)=-((1.-2.*E)/(2.*D)
  BB(3,2)=-2.*E/D
  BB(3,3)=(1.+2.*E)/(2.*D)
  BB(3,4)=-((1.-2.*Z-E+2.*Z*E)/(4.*A)
325 BB(3,5)=-Z*(1.-E)/A
  BB(3,6)=(1.+2.*Z-E-2.*Z*E)/(4.*A)
  BB(3,7)=(1.+2.*Z+E+2.*Z*E)/(4.*A)
  BB(3,8)=-Z*(1.+E)/A
  BB(3,9)=-((1.-2.*Z+E-2.*Z*E)/(4.*A)
330 74 CONTINUE
C
C MULTIPLY C TIMES BB AND STORE IN BBC
C
  DO 30 I=1,3
335 DO 30 J=1,LIM
  BBC(I,J)=0.
  DO 30 L=1,3
  BBC(I,J)=BBC(I,J)+C(I,L)*BB(L,J)
  30 CONTINUE
340 C
C CALCULATE STRESSES, SIG=(BBC)*X(IQ)
C

```

SUBROUTINE STRESS

73/172 CPT=1

FTN 4.6+446

75/

```

      DO 50 I=1,3
      SIG(I)=0.
345     DO 50 J=1,LIM
      SIG(I)=SIG(I)+BBC(I,J)*Q(J)
50     CONTINUE
C
      IF(NOUT.NE.0) GO TO 55
350     CALL FORCE(SIG,II,JJ,M,JSTPS,TT,BW,SH,IZ)
      GO TO 888
55     CONTINUE
C
      PRINT STRESSES , 50 LINES PER PAGE
355     NLINE=47
      IF(NLINE.GT.0) GO TO 60
      PRINT 1000
      NLINE=49
360     60 NLINE=NLINE-1
      PRINT 1010,M,(SIG(I),I=1,3)
      888 CONTINUE
      9999 CONTINUE
C
      100 FORMAT(47H10OUTPUT TABLE 2.. STRESSES AT ELEMENT CENTROIDS )
365     200 FORMAT(/// 20X,15HFACADE NUMBER ,I5///
      1       3X,7HELEMENT,7X,8HSIGMA(X),7X,8HSIGMA(Y),
      2       7X,8HTAU(X,Y))
      500 FORMAT(53H10OUTPUT TABLE..2 INTERNAL FORCES IN COLUMNS AND BEAMS )
370     600 FORMAT(//34X,*FACADE NUMBER *, I5///
      1 *     ELEMENT NO.     COL. AXIAL F.     COL. SHEAR     COL. MOMENT
      2 BEAM SHEAR     BEAM MOMENT */)
      1000 FORMAT(1H1, 7HELEMENT,7X,8HSIGMA(X),7X,8HSIGMA(Y),
      1       7X,8HTAU(X,Y))
375     1010 FORMAT(I10,1P3E15.4)
C
      RETURN
      END

```

SUBROUTINE FORCE

73/172 CPT=1

FTN 4.6+446

787

```

1      SUBROUTINE FORCE(SIG,II,JJ,M,JSTRS,TT,BH,SH,IZ)
      C
      C *****
      C *
      C *   THIS SUBROUTINE EVALUATES INTERNAL FORCES IN
      C *   BEAMS AND COLUMNS
      C *
      C *****
      C
10     DIMENSION SIG(3)
      C
      C   IF (IZ.EQ.0) GO TO 10
15     C
      C EVALUATE BEAM INTERNAL FORCES
      C
      SF=SIG(3)*TT*SH
      BH=SF*BH/2.
20     PRINT 100, M, II, JJ, SF, BH
      GO TO 999
10    CONTINUE
      C
      C EVALUATE COLUMN INTERNAL FORCES
25     C
      C   IF ((JJ.EQ.1).OR.(JJ.EQ.JSTRS)) GO TO 20
      AF=SIG(2)*TT*BH
      SF=SIG(3)*TT*BH
      GO TO 30
30     20 CONTINUE
      AF=SIG(2)*TT*BH/2.
      SF=SIG(3)*TT*BH/2.
      30 CONTINUE
      BH=SF*SH/2.
35     PRINT 200, M, II, JJ, AF, SF, BH
      999 CONTINUE
      100 FORMAT( 3I5 ,4X,2(4X,E10.3))
      200 FORMAT( 3I5 ,4X,E13.3,2(4X,E10.3))
      RETURN
40     END

```